Mathematica Montisnigri

At the front page there is a detail from the first known text in astronomy-mathematics that appeared in Montenegro. It was published in the book Psaltir in 1495. Psaltir was printed on September 22, 1495 in the printing shop of Djurdje Crnojević which was the first printing shop of South Slavs. In the book six, volume 23, Djurdje Crnojević, the sovereign of Montenegro, adapted the Tables of Jovan Damaskin and wrote the Paschalia with lunar calendar. He worked out a series of rules regarding the counting of days of Easter celebrations. Djurdje's Paschalia Tables can be found in numerous written and printed books of later period.

CONTENTS

Mathematics

Mathematical modeling

Computer science applications

Academic life

Person

A BREAF SURVEY ON ARMENDARIZ AND CENTRAL ARMENDARIZ RINGS

DUŠAN JOKANOVIĆ*

University of East Sarajevo, Production and Management Faculty Trebinje
*Corresponding author. E-mail: dusan.jokanovic@fpm.ues.rs.ba

Summary. In this paper R is a ring with unity, and σ is endomorphism of the ring. We deal with central Armendariz rings as a natural generalization of Armendariz rings. We investigate a posibility of extending central Armendariz property from a ring to coresponding polynomial or matrix extension. At the end of this paper we consider an interesting note on reduced rings.

1 INTRODUCTION

Throughout this article R denotes a ring with unity, $R[x]$ is coresponding polynomial ring, σ denotes an endomorphism of R, $R[x;\sigma]$ denotes skew polynomial ring with the ordinary addition and the multiplication subject to the relation $xr = \sigma(r)x$, and $R[[x;\sigma]]$ denotes power series ring. The notion of Armendariz ring is introduced by Rege and Chhawchharia (see [2]). They defined a ring R to be Armendariz if $f(x)g(x) = 0$ implies $a_i b_j = 0$, for all polynomials $f(x) = \sum_{i=0}^{n} a_i x^i$ and $g(x) = \sum_{j=0}^{m} b_j x^j$ from $R[x]$. The motivation for those rings comes from the fact that Armendariz had shown that the above reesult can be extended to a class of reduced rings, i.e., rings without non-zero nilpotent elements. In [1] authors introduced a class of central Armendariz rings. A ring R is called central Armendariz ring if $f(x)g(x) = 0$ implies $a_i b_j \in C(R)$, for all polynomials $f(x) = \sum_{i=0}^{n} a_i x^i$ and $g(x) = \sum_{j=0}^{m} b_j x^j$ from $R[x]$, where $C(R)$ is center of a ring R. Clearly Armendariz rings are central Armendariz rings. It is known from [1] that a class of central Armendariz rings is closed for polynomial extensions and localizations, and that the central hhArmendariz rings are strictly between Armendariz rings and abelian rings. As a generalization of σ-skew Armendariz rings, Onyang (see [4]) introduced a notion of weak σ-skew Armendariz ring (see [3],[4].[5]). A weak σ-skew Armendariz ring R is a ring in which $f(x)g(x) = 0$ implies $a_i \sigma^i(b_j)$ is the nilpotent element of R for all $f(x) = \sum_{i=0}^{n} a_i x^i$ and $g(x) = \sum_{j=0}^{m} b_j x^j$ from $R[x;\sigma]$. Chain and Tong (see [5]) have proved that if R and S are rings and σ is and isomorphism of rings R and S and R is α-skew Armendariz ring, then S is $\sigma\alpha\sigma^{-1}$-skew Armendariz ring. In this paper we give (see [3]) a variant of this theorem for weak skew-Armendariz rings. In our main result we give an example of central Armendariz matrix ring $T(n, R)$, for reduced ring R.

2 EXTENDING OF ARMENDARIZ PROPERTY

In this section we deal with posibility of extending the Armendariz property under ring isomorphism (see [3]). From universal algebra we know that every homomorphism σ of rings R and S can be extended to the homomorphism of the corresponding rings of polynomials $R[x]$ and $S[x]$ by $\sum_{i=0}^{m} a_i x^i \mapsto \sum_{i=0}^{m} \sigma(a_i)x^i$, which we also denote by σ. Chain and Tong in

[5] prove that if σ is ring isomorphism of rings R and S and R is α-skew Armendariz, then S is $\sigma\alpha\sigma^{-1}$ skew Armendariz ring. We prove the weak skew Armendariz variant of this theorem.

Theorem 2.1 ([3]) *Let R and S be rings with a ring isomorphism $\sigma: R \to S$. If R is weak $\alpha-$skew Armendariz then S is weak $\sigma\alpha\sigma^{-1} -$skew Armendariz.*

Proof. Let $f(x) = \sum_{i=0}^{m} a_i x^i$ and $g(x) = \sum_{j=0}^{n} b_j x^j$ be polynomials from the ring $S[x; \sigma\alpha\sigma^{-1}]$. We have to prove that $f(x)g(x) = 0$ implies $a_i(\sigma\alpha\sigma^{-1})^i b_j \in nil(S)$, for all i and j.

As we noted, σ extends to the isomorphism of corresponding polynomial rings, so that there exist polynomials $f_1(x) = \sum_{i=0}^{m} a_i' x^i$ and $g_1(x) = \sum_{j=0}^{m} b_j' x^j$ from $R[x]$ such that $f(x) = \sigma(f_1(x)) = \sum_{i=0}^{m} \sigma(a_i')x^{i,}$ and $g(x) = \sigma(g_1(x)) = \sum_{j=0}^{m} \sigma(b_j')x^j$.

First, we shall show that $f(x)g(x) = 0$ implies $f_1(x)g_1(x) = 0$. If $f(x)g(x) = 0$, we have

$$a_0 b_k + a_1(\sigma\alpha\sigma^{-1})(b_{k-1})+\ldots+a_k(\sigma\alpha\sigma^{-1})^k(b_0) = 0,$$

for any $0 \le k \le m$. From the definition of $f_1(x)$ and $g_1(x)$, we have

$$\sigma(a_0')\sigma(b_k') + \sigma(a_1')(\sigma\alpha\sigma^{-1})\sigma(b_{k-1}')+\ldots+\sigma(a_k')(\sigma\alpha\sigma^{-1})^k\sigma(b_0') = 0,$$

and using $(\sigma\alpha\sigma^{-1})^t = \sigma\alpha^t\sigma^{-1}$ we obtain

$$a_0' b_k' + a_1'\alpha(b_{k-1}')+\ldots+a_k'\alpha^k(b_0') = 0,$$

which means that $f_1(x)g_1(x) = 0$ in the ring $R[x; \alpha]$.

It remains to prove that $f_1(x)g_1(x) = 0$ implies $a_i(\sigma\alpha\sigma^{-1})^i(b_j) \in nil(S)$. From the fact that R is weak α-skew Armendariz we have $a_i'\alpha^i(b_j') \in nil(R)$, and since

$$a_i' = \sigma^{-1}(a_i), b_j' = \sigma^{-1}(b_j), \text{ we have } \sigma^{-1}(a_i)\alpha^i\sigma^{-1}(b_j) \in nil(R).$$

This implies

$$\sigma^{-1}(a_i)\sigma^{-1}\sigma\alpha^i\sigma^{-1}(b_j) = \sigma^{-1}(a_i(\sigma\alpha\sigma^{-1})^i(b_j)) \in nil(R)$$

and finally we obtain

$$a_i(\sigma\alpha\sigma^{-1})^i(b_j) \in nil(S), \ 0 \le i \le m, 0 \le j \le n.$$

Hence S is weak $\sigma\alpha\sigma^{-1}$-skew Armendariz.

3 MATRIX CENTRAL ARMENDARIZ RING $T(R, n)$

In this section we give an example of matrix central Armendariz ring. For a ring R consider a following set of triangular matrices

$$T_n(R) = \left\{ \begin{bmatrix} a_{11} & a_{12} & a_{13} & \dots & a_{1n} \\ 0 & a_{22} & a_{23} & \dots & a_{2n} \\ 0 & 0 & a_{33} & \dots & a_{3n} \\ \vdots & \vdots & \vdots & \ddots & \vdots \\ 0 & 0 & 0 & \dots & a_{nn} \end{bmatrix} \mid a_{ij} \in R \right\}.$$

We also consider the following set of triangular matrices over ring R

$$T(R,n) = \left\{ \begin{bmatrix} a_0 & a_1 & a_2 & \dots & a_{n-1} \\ 0 & a_0 & a_1 & \dots & a_{n-2} \\ 0 & 0 & a_0 & \dots & a_{3n} \\ \vdots & \vdots & \vdots & \ddots & \vdots \\ 0 & 0 & 0 & \dots & a_0 \end{bmatrix} \mid a_i \in R \right\},$$

which is subring of $T_n(R)$. It is well known that $T_n(R)$ and $T(R,n)$ are subrings of the triangular matrix rings with matrix addition and multiplication. Let α be endomorphism of ring R. It is well known that endomorphism α can be naturally extended to an endomorphism

$$\overline{\alpha}: T_n(R) \to T_n(R),$$

and

$$\overline{\alpha}: T(R,n) \to T(R,n),$$

with:

$$\overline{\alpha}\left(\begin{bmatrix} a_{11} & a_{12} & a_{13} & \dots & a_{1n} \\ 0 & a_{22} & a_{23} & \dots & a_{2n} \\ 0 & 0 & a_{33} & \dots & a_{3n} \\ \vdots & \vdots & \vdots & \ddots & \vdots \\ 0 & 0 & 0 & \dots & a_{nn} \end{bmatrix} \right) = \begin{bmatrix} \alpha(a_{11}) & \alpha(a_{12}) & \alpha(a_{13}) & \dots & \alpha(a_{1n}) \\ 0 & \alpha(a_{22}) & \alpha(a_{23}) & \dots & \alpha(a_{2n}) \\ 0 & 0 & \alpha(a_{33}) & \dots & \alpha(a_{3n}) \\ \vdots & \vdots & \vdots & \ddots & \vdots \\ 0 & 0 & 0 & \dots & \alpha(a_{nn}) \end{bmatrix},$$

and

$$\overline{\alpha}\left(\begin{bmatrix} a_0 & a_1 & a_{13} & \dots & a_{n-1} \\ 0 & a_0 & a_1 & \dots & a_{n-2} \\ 0 & 0 & a_{33} & \dots & a_{3n} \\ \vdots & \vdots & \vdots & \ddots & \vdots \\ 0 & 0 & 0 & \dots & a_0 \end{bmatrix} \right) = \begin{bmatrix} \alpha(a_0) & \alpha(a_1) & \alpha(a_2) & \dots & \alpha(a_{n-1}) \\ 0 & \alpha(a_0) & \alpha(a_1) & \dots & \alpha(a_{n-2}) \\ 0 & 0 & \alpha(a_{33}) & \dots & \alpha(a_{3n}) \\ \vdots & \vdots & \vdots & \ddots & \vdots \\ 0 & 0 & 0 & \dots & \alpha(a_0) \end{bmatrix}.$$

Theorem 3.1 *If R is reduced ring then $T(R,n)$ is central Armendariz ring.*

Proof. From [1] we obtain that for reduced ring R, the factor ring $R[x]/(x^n)$ is central Armendariz, for all $n \geq 2$. We use the ring isomorphism $f: R[x]/(x^n) \to T(R,n)$ given by

$$f(a_0 + a_1 x + \dots + a_{n-1} x^{n-1} + (x^n)) = (a_0, a_1, \dots, a_{n-1}),$$

where (x^n) is ideal in $R[x]$ generated with x^n, and $(a_0, a_1, \dots, a_{n-1})$ is a breaf representation for a matrix from $T(R,n)$. Therefore $T(R,n)$ is central Armendariz ring.

We end this section with our result from [3], in which we give sufficient condition for the power series ring $R[[x;\sigma]]$ to be reduced.

Theorem 3.2 *If an endomorphism σ of a reduced ring R satisfies so called compatibi-lity condition: $a\sigma(b) = 0 \Leftrightarrow ab = 0$, then the power series ring $R[[x;\sigma]]$ is reduced.*

Proof. Let $f(x) = \sum_{i=0}^{\infty} a_i x^i$ and $(f(x))^2 = 0$. It is clear that $a_0^2 = 0$, so that $a_0 = 0$. Now from the compatibility condition $a_1\sigma(a_1) = 0$ implies $a_1^2 = 0$, but since R is reduced we have $a_1 = 0$. By induction argument we have $a_i = 0$ for all i. This means that $f(x) = 0$ and so $R[[x;\sigma]]$ is reduced.

Without compatibility condition the previous theorem is not true. Since for the ring $R = Z_2 \oplus Z_2$ and σ defined by $\sigma(a,b) = (b,a)$, it is easy to check that $R[[x;\sigma]]$ is not reduced. Observe that $(1,0)(0,1) = (0,0)$ but $(1,0)\sigma(0,1) \neq (0,0)$.

REFERENCES

[1] N. Agayev, G. Gungoroglu, A. Harmanci and S. Halicioglu, "Central Armendariz Ring*s"*, *Bull. Malays. Math. Sci. Soc.*, **2**(34(1)), 137-145 (2011).

[2] M. Rege, and S. Chhawchharia, "Armendariz rings*", Proc. Japan Acad. Ser. A. Math. Sci.*, **73**, 14-17 (1997).

[3] D. Jokanović, "Properties of Armendariz rings and weak Armendariz rings", *Pubications de l'Institute Mathematique, Nouvelle serie*, **85**(99), 131-137 (2009).

[4] L. Ouyang, "Extensions of generalized α-rigid rings", *International Journal of Algebra*, **3**, 105-116 (2008).

[5] W. Chen and W. Tong, "On skew Armendariz and rigid rings", *Houston Journal of Mathematics*, **22**, (2007).

DOSS ALMOST PERIODIC FUNCTIONS, BESICOVITCH-DOSS ALMOST PERIODIC FUNCTIONS AND CONVOLUTION PRODUCTS

MARKO KOSTIĆ[*]

University of Novi Sad. Novi Sad, Serbia.
Faculty of Technical Sciences, Trg D. Obradovića 6, 21125 Novi Sad, Serbia
*Corresponding author. E-mail: marco.s@verat.net

Summary. The theory of almost periodic functions and almost automorphic functions in Banach spaces is a rapidly growing field of research. Concerning applications to the abstract partial differential equations in Banach spaces, one of the fundamental questions is the invariance of almost periodicity and almost automorphy under the action of convolution products. In the paper under review, we analyze the invariance of Doss almost periodicity and Besicovitch-Doss almost periodicity under the actions of convolution products. We thus continue our recent research studies by investigating the case in which the solution operator family under our consideration has special growth rates at zero and infinity. The results obtained in this paper can be incorporated in the qualitative analysis of solutions to abstract (degenerate) inhomogeneous fractional differential equations in Banach spaces.

1   INTRODUCTION

Let $(X, \|\cdot\|)$ and $(Y, \|\cdot\|)_Y$ be two non-trivial complex Banach spaces, and let $L(X,Y)$ be the space consisting of all linear continuous operators from X into Y; $L(X) \equiv L(X,X)$. By $\|\cdot\|_{L(X,Y)}$ we denote the norm in $L(X,Y)$.

The results obtained in [10], concerning the invariance of Besicovitch-Doss almost periodicity under the actions of convolution products, are applicable in the case that the solution operator family $(R(t))_{t>0} \subseteq L(X,Y)$ satisfies the estimate

$$\int_0^\infty (1+t) \| R(t) \|_{L(X,Y)} dt < \infty. \tag{1.1}$$

This, in particular, holds if there exists a finite constant $M > 0$ such that the following holds:

$$\| R(t) \|_{L(X,Y)} \le M e^{-ct} t^{\beta-1}, t > 0 \text{ for some finite constants } c > 0, \beta \in (0,1].$$

Therefore, the results from [10] can be applied to a large class of abstract (degenerate) inhomogeneous differential equations of first order in Banach spaces.

On the other hand, in the theory of abstract (degenerate) fractional differential equations in Banach spaces, the estimate

$$\parallel R(t) \parallel_{L(X,Y)} \le M \frac{t^{\beta-1}}{1+t^{\gamma}}, t > 0 \text{ for some finite constants } \gamma > 1, \beta \in (0,1], M > 0 \qquad (1.2)$$

plays a crucial role. In the case that $\beta - \gamma \ge -1,$ which naturally appears in applications, the estimate (1.1) does not hold so that the results of [10] cannot be applied; see [6], [9]-[11] and references cited therein for more details about the subject.

The main purpose of this paper is to analyze the invariance of Doss p -almost periodicity and Besicovitch-Doss p -almost periodicity under the actions of infinite convolution product

$$G(t) \equiv t \mapsto \int_{-\infty}^{t} R(t-s)g(s)ds, t \in \mathbb{R} \qquad (1.3)$$

and finite convolution product

$$H(t) \equiv \int_{0}^{t} R(t-s)[g(s)+q(s)]ds, t \ge 0 \qquad (1.4)$$

where $1 \le p < \infty$, $(R(t))_{t>0}$ satisfies the estimate (1.1), $g(\cdot)$ is Doss p -almost periodic or Besicovitch-Doss p -almost periodic, and $q(\cdot)$ is vanishing in time, in a certain sense.

The organization of paper is briefly described as follows. After giving some necessary facts about fractional calculus and types of fractional derivatives used in the paper, we analyze Doss almost periodic functions and Besicovitch-Doss almost periodic functions in Subsection 1.1. Our main contributions are given in Section 2 (Theorem 2.1, Theorem 2.4 and Proposition 2.2, Proposition 2.5); in Subsection 2.1, we present some applications of our abstract theoretical results established.

Fractional calculus and fractional differential equations are rapidly growing fields of research, due to their invaluable importance in modeling real world phenomena appearing in many fields of science and engineering, such as astrophysics, electronics, diffusion, chemistry, biology, aerodynamics and thermodynamics. For more details, see [7]-[9] and references cited therein. In this paper, we use the Weyl-Liouville fractional derivatives and Caputo fractional derivatives. The Weyl-Liouville fractional derivative $D_{t,+}^{\gamma}u(t)$ of order $\gamma \in (0,1)$ is defined for those continuous functions $u : \mathbb{R} \to X$ such that $t \mapsto \int_{-\infty}^{t} g_{1-\gamma}(t-s)u(s)ds, t \in \mathbb{R}$ is a well-defined continuously differentiable mapping, by

$$D_{t,+}^{\gamma}u(t) := \frac{d}{dt}\int_{-\infty}^{t} g_{1-\gamma}(t-s)u(s)ds, \quad t \in \mathbb{R}.$$

For further information about Weyl-Liouville fractional derivatives, we refer the reader to [12].

If $\alpha > 0$ and $m = \lceil \alpha \rceil$, then the Caputo fractional derivative $\mathbf{D}_t^\alpha u(t)$ is defined for those functions $u \in C^{m-1}([0,\infty) : X)$ such that $g_{m-\alpha} * (u - \sum_{k=0}^{m-1} u_k g_{k+1}) \in C^m([0,\infty) : X)$, by

$$\mathbf{D}_t^\alpha u(t) = \frac{d^m}{dt^m}\Big[g_{m-\alpha} * \big(u - \sum_{k=0}^{m-1} u_k g_{k+1}\big)\Big].$$

For further information about Caputo fractional derivatives, we refer the reader to [9]. Here, $g_\zeta(t) := t^{\zeta-1}/\Gamma(\zeta)$, where $\Gamma(\cdot)$ denotes the Euler Gamma function ($\zeta > 0$).

Set $(+\infty)^a := +\infty$ for any number $a > 0$. We will use the following elementary lemma:

Lemma 1.1. *Suppose that $1 \le p < \infty$ and $\varphi : \mathbb{R} \to [0,\infty)$ is a non-negative function. Then we have*

$$\limsup_{s \to +\infty}\big[\varphi(s)^{1/p}\big] = \big[\limsup_{s \to +\infty} \varphi(s)\big]^{1/p}.$$

Proof. Clearly, with the common consent introduced above, we have

$$\limsup_{s \to +\infty}\big[\varphi(s)^{1/p}\big] = \lim_{s \to +\infty} \sup_{y \ge s}\big[\varphi(y)^{1/p}\big] = \lim_{s \to +\infty}\big[\sup_{y \ge s} \varphi(y)\big]^{1/p}$$
$$= \big[\lim_{s \to +\infty} \sup_{y \ge s} \varphi(y)\big]^{1/p} = \big[\limsup_{s \to +\infty} \varphi(s)\big]^{1/p}.$$

1.1 Doss almost periodic functions and Besicovitch-Doss almost periodic functions

Let $1 \le p < \infty$, and let $I = \mathbb{R}$ or $I = [0,\infty)$. Let us recall that the set $D \subseteq I$ is relatively dense iff for each $\epsilon > 0$ there exists $l > 0$ such that any subinterval of I of length l contains at least one element of set D. Following A. S. Besicovitch [2], for every function $f \in L_{loc}^p(\mathbb{R} : X)$, we set

$$\| f \|_{\mathcal{M}^p} := \limsup_{t \to +\infty}\Big[\frac{1}{2t}\int_{-t}^t \| f(s) \|^p\, ds\Big]^{1/p};$$

if $f \in L_{loc}^p([0,\infty) : X)$, then we set

$$\| f \|_{\mathcal{M}^p} := \limsup_{t \to +\infty}\Big[\frac{1}{t}\int_0^t \| f(s) \|^p\, ds\Big]^{1/p}.$$

It is well known that $\| \cdot \|_{\mathcal{M}^p}$ is a seminorm on the space $\mathcal{M}^p(I : X)$ consisting of those $L_{loc}^p(I : X)$-functions $f(\cdot)$ for which $\| f \|_{\mathcal{M}^p} < \infty$. Put

$$K_p(I : X) := \{f \in \mathcal{M}^p(I : X) : \| f \|_{\mathcal{M}^p} = 0\}$$

and

$$M_p(I : X) := \mathcal{M}^p(I : X) / K_p(I : X).$$

The seminorm $\|\cdot\|_{\mathcal{M}^p}$ on $\mathcal{M}^p(I:X)$ induces the norm $\|\cdot\|_{M^p}$ on $M^p(I:X)$, under which $M^p(I:X)$ becomes a Banach space.

A function $f \in L^p_{loc}(I:X)$ is said to be Besicovitch p-almost periodic iff there exists a sequence of X-valued trigonometric polynomials converging to $f(\cdot)$ in $(M^p(I:X), \|\cdot\|_{M^p})$. By $B^p(I:X)$ we denote the vector space consisting of all Besicovitch p-almost periodic functions $I \to X$.

We will use the following lemma (see [10, Proposition 2.4] for the case that $I = [0,\infty)$ and the analysis of R. Doss [3, p. 478] for the case that $I = \mathbb{R}$):

Lemma 1.2. *Let* $1 \le p < \infty,$ *and let* $q \in L^p_{loc}(I:X).$ *Then* $\|q(t+\cdot)\|_{\mathcal{M}^p} = \|q\|_{\mathcal{M}^p}$ *for all* $t \in I.$

A function $q \in L^p_{loc}(I:X)$ is said to be Besicovitch p-vanishing iff $\|q\|_{\mathcal{M}^p} = 0$ (see [10, Definition 2.3, Proposition 2.4, Corollary 2.5] for the case that $I = [0,\infty)$).

Following the fundamental researches of R. Doss [3]-[4], established for scalar-valued functions, we have recently introduced the following notion in [10]:

Definition 1.3. Let $1 \le p < \infty,$ and let $f \in L^p_{loc}(I:X).$
Then it is said that $f(\cdot)$ is:
(i) B^p- bounded iff $\|f\|_{\mathcal{M}^p} < \infty.$
(ii) B^p- continuous iff

$$\lim_{\tau \to 0} \limsup_{t \to +\infty} \Big[\frac{1}{2t} \int_{-t}^{t} \|f(s+\tau) - f(s)\|^p\, ds\Big]^{1/p} = 0,$$

in the case that $I = \mathbb{R},$ resp.,

$$\lim_{\tau \to 0+} \limsup_{t \to +\infty} \Big[\frac{1}{t} \int_{0}^{t} \|f(s+\tau) - f(s)\|^p\, ds\Big]^{1/p} = 0$$

in the case that $I = [0,\infty).$

(iii) Doss $p-$ almost periodic iff, for every $\epsilon > 0$, the set of numbers $\tau \in I$ for which

$$\limsup_{t \to +\infty} \Big[\frac{1}{2t} \int_{-t}^{t} \|f(s+\tau) - f(s)\|^p\, ds\Big]^{1/p} < \epsilon, \tag{1.5}$$

in the case that $I = \mathbb{R},$ resp.,

$$\limsup_{t\to+\infty}\Big[\frac{1}{t}\int_0^t\|f(s+\tau)-f(s)\|^p\,ds\Big]^{1/p}<\epsilon,$$

in the case that $I=[0,\infty)$, is relatively dense in I.

(iv) Besicovitch-Doss p-almost periodic iff (i)-(iii) hold as well as, for every $\lambda\in\mathbb{R}$, we have that

$$\lim_{l\to+\infty}\limsup_{t\to+\infty}\frac{1}{l}\Big[\frac{1}{2t}\int_{-t}^t\|\Big(\int_x^{x+l}-\int_0^l\Big)e^{i\lambda s}f(s)\,ds\|^p\,dx\Big]^{1/p}=0,\tag{1.6}$$

in the case that $I=\mathbb{R}$, resp.,

$$\lim_{l\to+\infty}\limsup_{t\to+\infty}\frac{1}{l}\Big[\frac{1}{t}\int_0^t\|\Big(\int_x^{x+l}-\int_0^l\Big)e^{i\lambda s}f(s)\,ds\|^p\,dx\Big]^{1/p}=0$$

in the case that $I=[0,\infty)$.

By $\mathrm{B}^p(I:X)$ we denote the class consisting of all Besicovitch-Doss p-almost periodic functions $I\to X$. Before proceeding further, we would like to note that, in scalar-valued case $X=\mathbb{C}$, R. Doss has proved that $\mathrm{B}^p(I:X)=B^p(I:X)$. It is still unknown whether this equality holds in vector-valued case (see [10] for the problem raised). By $\mathrm{D}^p(I:X)$ we de-note the class consisting of all Doss p-almost periodic functions $I\to X$.

For more details about these classes of generalized almost periodic functions, we refer the reader to the monograph [2] by A. S. Besicovitch, the survey article [1] by J. Andres, A. M. Bersani, R. F. Grande, and the forthcoming monograph [11] by M. Kostić.

We also need the notion of Stepanov p-boundedness. A function $f\in L^p_{loc}(I:X)$ is said to be Stepanov p-bounded iff

$$\|f\|_{S^p}:=\sup_{t\in I}\Big(\int_t^{t+1}\|f(s)\|^p\,ds\Big)^{1/p}<\infty.$$

2   DOSS ALMOST PERIODIC PROPERTIES AND BESICOVITCH-DOSS ALMOST PERIODIC PROPERTIES OF CINVOLUTIONS PRODUCTS

We start this section by stating the following result:

Theorem 2.1. *Let* $1/p+1/q=1$ *and let* $(R(t))_{t>0}\subseteq L(X,Y)$ *satisfy* (1.2). *Let a function* $g:\mathbb{R}\to X$ *be Doss p-almost periodic and Stepanov p-bounded, and let* $q(\beta-1)>-1$ *provided that* $p>1$, *resp.* $\beta=1$, *provided that* $p=1$. *Then the function* $G:\mathbb{R}\to Y$, *defined*

through (1.3), *is bounded continuous and Doss p-almost periodic. Furthermore, if* $g(\cdot)$ *is* B^p *– continuous, then* $G(\cdot)$ *is* B^p *– continuous, as well.*

Proof. We primarily analyze the case that $g(\cdot)$ is Doss p-almost periodic with $p > 1$ and explain certain differences in the proof provided that $p = 1$; the assumption $X=Y$ can be made. Since $g(\cdot)$ is Stepanov p-bounded and $q(\beta - 1) > -1$, a similar line of reasoning as in the proof of [6, Theorem 2.1] shows that $G(\cdot)$ is bounded and continuous on the real line.

Now we will prove that $G(\cdot)$ is Doss p-almost periodic.

Let a number $\epsilon > 0$ be fixed. By definition, we can find a real number $l > 0$ such that any interval $I \subseteq \mathbb{R}$ of length l contains a point $\tau \in I$ such that (1.5) holds with $f = g$ therein. Further on, there exists of a positive real number $\zeta > 0$ satisfying

$$\frac{1}{p} < \zeta < \frac{1}{p} + \gamma - \beta \text{ (in the case that } p=1, \text{ take any number } \zeta \in (1, \gamma) \text{ and repeat the procedure).}$$

As in the proof of [6, Theorem 2.1], we may conclude that the integral

$$\int_{-\infty}^{0} \| g(s+t+\tau) - g(s+t) \|^p /(1+|s|^\zeta)^p \, ds$$

converges for any $t \in \mathbb{R}$ as well as that there exists an absolute constant $C>0$ such that

$$\| G(s+\tau) - G(s) \| \le C \Big[\int_{-\infty}^{0} \| g(v+s+\tau) - g(v+s) \|^p /(1+|v|^\zeta)^p \, dv\Big]^{1/p}, \, s \in \mathbb{R}.$$

Using this estimate, the Fubini theorem and Lemma 1.1, we get that

$$\limsup_{t\to+\infty} \Big[\frac{1}{2t}\int_{-t}^{t} \| G(s+\tau) - G(s) \|^p \, ds\Big]^{1/p} \le$$

$$C\limsup_{t\to+\infty} \Big[\frac{1}{2t}\int_{-t}^{t}\int_{-\infty}^{0} \| g(v+s+\tau) - g(v+s) \|^p /(1+|v|^\zeta)^p \, dv ds\Big]^{1/p} =$$

$$= C\limsup_{t\to+\infty} \Big[\int_{-\infty}^{0}\frac{1}{2t}\int_{-t}^{t} \| g(v+s+\tau) - g(v+s) \|^p /(1+|v|^\zeta)^p \, ds dv\Big]^{1/p} =$$

$$= C\Big[\limsup_{t\to+\infty}\int_{-\infty}^{0}\frac{1}{2t}\int_{-t}^{t} \| g(v+s+\tau) - g(v+s) \|^p /(1+|v|^\zeta)^p \, ds dv\Big]^{1/p}.$$

$$\limsup_{t\to+\infty} \Big[\frac{1}{2t}\int_{-t}^{t} \| G(s+\tau) - G(s) \|^p \, ds\Big]^{1/p} \le$$

$$C\limsup_{t\to+\infty} \Big[\frac{1}{2t}\int_{-t}^{t}\int_{-\infty}^{0} \| g(v+s+\tau) - g(v+s) \|^p /(1+|v|^\zeta)^p \, dv ds\Big]^{1/p} =$$

$$C\limsup_{t\to+\infty} \Big[\int_{-\infty}^{0}\frac{1}{2t}\int_{-t}^{t} \| g(v+s+\tau) - g(v+s) \|^p /(1+|v|^\zeta)^p \, ds dv\Big]^{1/p} =$$

$$C\Big[\limsup_{t\to+\infty}\int_{-\infty}^{0}\frac{1}{2t}\int_{-t}^{t}\|\,g(v+s+\tau)-g(v+s)\,\|^{p}\,/(1+|\,v\,|^{\varsigma})^{p}\,ds\,dv\Big]^{1/p}.$$

By the reverse Fatou lemma, the above implies

$$\limsup_{t\to+\infty}\Big[\frac{1}{2t}\int_{-t}^{t}\|\,G(s+\tau)-G(s)\,\|^{p}\,ds\Big]^{1/p}\le$$
$$C\Big[\int_{-\infty}^{0}\frac{1}{(1+|\,v\,|^{\varsigma})^{p}}\limsup_{t\to+\infty}\Big\{\frac{1}{2t}\int_{-t}^{t}\|\,g(v+s+\tau)-g(v+s)\,\|^{p}\,ds\Big\}dv\Big]^{1/p}.$$

Keeping in mind Lemma 1.2, we get that, for every $v\le 0$,

$$\limsup_{t\to+\infty}\frac{1}{2t}\int_{-t}^{t}\|\,g(v+s+\tau)-g(v+s)\,\|^{p}\,ds=\limsup_{t\to+\infty}\frac{1}{2t}\int_{-t}^{t}\|\,g(s+\tau)-g(s)\,\|^{p}\,ds,$$

so that

$$\limsup_{t\to+\infty}\Big[\frac{1}{2t}\int_{-t}^{t}\|\,G(s+\tau)-G(s)\,\|^{p}\,ds\Big]^{1/p}\le$$
$$C\Big[\int_{-\infty}^{0}\frac{1}{(1+|\,v\,|^{\varsigma})^{p}}\limsup_{t\to+\infty}\Big\{\frac{1}{2t}\int_{-t}^{t}\|\,g(s+\tau)-g(s)\,\|^{p}\,ds\Big\}dv\Big]^{1/p}=$$
$$C\Big[\limsup_{t\to+\infty}\frac{1}{2t}\int_{-t}^{t}\|\,g(s+\tau)-g(s)\,\|^{p}\,ds\Big]^{1/p}\Big[\int_{-\infty}^{0}\frac{dv}{(1+|\,v\,|^{\varsigma})^{p}}\Big]^{1/p}.$$

Applying again Lemma 1.1, we finally get

$$\limsup_{t\to+\infty}\Big[\frac{1}{2t}\int_{-t}^{t}\|\,G(s+\tau)-G(s)\,\|^{p}\,ds\Big]^{1/p}\le$$
$$C\limsup_{t\to+\infty}\Big[\frac{1}{2t}\int_{-t}^{t}\|\,g(s+\tau)-g(s)\,\|^{p}\,ds\Big]^{1/p}\Big[\int_{-\infty}^{0}\frac{dv}{(1+|\,v\,|^{\varsigma})^{p}}\Big]^{1/p}\le\quad C\epsilon\Big[\int_{-\infty}^{0}\frac{dv}{(1+|\,v\,|^{\varsigma})^{p}}\Big]^{1/p}.$$

This shows that $G(\cdot)$ is Doss p-almost periodic. Since the above computations holds for each $\tau\in\mathbb{R}$, it is clear that the $B^{p}-$continuity of function $g(\cdot)$ implies that of $G(\cdot)$, as well. The proof of the theorem is thereby complete.

Concerning the finite convolution product, we can state the following result which immediately follows from Theorem 2.1 and the proof of [6, Proposition 2.3]:

Proposition 2.2. *Let $q \in L_{loc}^p([0,\infty) : X)$, $1/p + 1/q = 1$ and let $(R(t))_{t>0} \subseteq L(X,Y)$ satisfy (1.2). Let a function $g : \mathbb{R} \to X$ be Doss p-almost periodic and Stepanov p-bounded, and let $q(\beta - 1) > -1$ provided that $p > 1$, resp. $\beta = 1$, provided that $p = 1$. Suppose that the function*

$$t \mapsto Q(t) \equiv \int_0^t R(t-s)q(s)ds, t \geq 0 \tag{2.1}$$

belongs to some space $\mathcal{F}_Y$ of functions $[0,\infty) \to Y$, satisfying that

$$\mathcal{F}_Y + C_0([0,\infty) : Y) = \mathcal{F}_Y. \tag{2.2}$$

Then the function $H(\cdot)$, defined through (1.4), is continuous and belongs t o the class $\mathrm{D}^{[0,\infty),p}(Y) + \mathcal{F}_Y$, where $\mathrm{D}^{[0,\infty),p}(Y)$ stands for the space of all restictions of Y-valued Doss p-almost periodic functions from the real line to the interval $[0,\infty)$.

Remark 2.3. Suppose that $\mathcal{F}_Y = B_0^p([0,\infty) : Y)$. Since the sum of spaces $\mathrm{D}^p(I : Y)$ and $B_0^p(I : Y)$ is $\mathrm{D}^p(I : Y)$ (see the proof of [10, Proposition 2.6] for the case that $I = [0,\infty)$), the extension of a function from $B_0^p([0,\infty) : Y)$ by zero outside the interval $[0,\infty)$ belongs to the space $B_0^p(\mathbb{R} : Y)$, and (2.2) holds, we get that the resulting function $H(\cdot)$ belongs to the space $\mathrm{D}^{[0,\infty),p}(Y)$, as well. It is also worth noting that it is not clear whether a Doss p-almost periodic function defined on $[0,\infty)$ can be extended to a Doss p-almost periodic function defined on the interval $\mathbb{R}$.

Concerning the Besicovitch-Doss p-almost periodic functions, the situation is a little bit delicate. It seems that the estimate (1.2) alone is not sufficiently enough to ensure the validity of condition (1.6) for the function $G(\cdot)$ defined through (1.3). In the following theorem, we impose the additional condition (2.3) for the inhomogeneity $g(\cdot)$ under our consideration:

Theorem 2.4. *Let 1/p+1/q=1 and let $(R(t))_{t>0} \subseteq L(X,Y)$ satisfy (1.2). Let a function $g : \mathbb{R} \to X$ be Besicovitch-Doss p-almost periodic and Stepanov p-bounded, and let $q(\beta - 1) > -1$ provided that p>1, resp. $\beta = 1$, provided that p=1. Suppose, additionally, that for every $\lambda \in \mathbb{R}$ and $\epsilon > 0$ there exists a number $l_0 > 0$ such that*

$$\frac{1}{l} \left\| \left(\int_0^l - \int_{-v}^{l-v} \right) e^{i\lambda s} g(s)ds \right\|^p < \epsilon, \quad l \geq l_0, v \geq 0. \tag{2.3}$$

Then the function $G : \mathbb{R} \to Y$, defined through (1.3), is bounded continuous and Besicovitch-Doss p-almost periodic.

Proof. Let $\lambda \in \mathbb{R}$. By Theorem 2.1, we only need to show that the function $G(\cdot)$ satisfies (1.6). In order to that, choose a positive real number $\zeta > 0$ satisfying

$\dfrac{1}{p} < \zeta < \dfrac{1}{p} + \gamma - \beta$ (in the case that $p=1$, we can take any number $\zeta \in (1, \gamma)$ and repeat the same procedure, again). Arguing similarly as in the proof of Theorem 2.1, we obtain that:

$$\frac{1}{l}\Big[\frac{1}{2t}\int_{-t}^{t}\|(\int_{x}^{x+l}-\int_{0}^{l})e^{i\lambda s}G(s)ds\|^p dx\Big]^{1/p}$$

$$\leq \frac{M}{l}\Big[\frac{1}{2t}\int_{-t}^{t}\|\int_{0}^{\infty}(\int_{x}^{x+l}-\int_{0}^{l})e^{i\lambda s}g(s-v)ds\frac{v^{\beta-1}dv}{1+v^{\gamma}}\|^p dx\Big]^{1/p}$$

$$\leq \frac{M}{l}\Big[\frac{1}{2t}\int_{-t}^{t}\Big\{\|\frac{1}{1+\cdot^{\zeta}}(\int_{x}^{x+l}-\int_{0}^{l})e^{i\lambda s}g(s-\cdot)ds\|_{L^p[0,\infty)}\times\|\frac{\cdot^{\beta-1}(1+\cdot^{\zeta})}{1+\cdot^{\gamma}}\|_{L^q[0,\infty)}\Big\}^p dx\Big]^{1/p}$$

$$\leq \frac{M}{l}\Big[\frac{1}{2t}\int_{-t}^{t}\int_{0}^{\infty}\frac{1}{(1+v^{\zeta})^p}\|(\int_{x}^{x+l}-\int_{0}^{l})e^{i\lambda s}g(s-v)ds\|^p dvdx\Big]^{1/p}$$

$$= \frac{M}{l}\Big[\frac{1}{2t}\int_{0}^{\infty}\int_{-t}^{t}\frac{1}{(1+v^{\zeta})^p}\|(\int_{x}^{x+l}-\int_{0}^{l})e^{i\lambda s}g(s-v)ds\|^p dxdv\Big]^{1/p};$$

here, M denotes the constant from (1.2). Applying the reverse Fatou lemma and Lemma 1.1, the above implies:

$$\limsup_{t\to+\infty}\frac{1}{l}\Big[\frac{1}{2t}\int_{-t}^{t}\|(\int_{x}^{x+l}-\int_{0}^{l})e^{i\lambda s}G(s)ds\|^p dx\Big]^{1/p}$$

$$\leq \frac{M}{l}\Big[\frac{1}{2t}\int_{0}^{\infty}\int_{-t}^{t}\limsup_{t\to+\infty}\Big\{\frac{1}{2t}\int_{-t}^{t}\|(\int_{x}^{x+l}-\int_{0}^{l})e^{i\lambda s}g(s-v)ds\|^p dx\Big\}\frac{dv}{(1+v^{\zeta})^p}\Big]^{1/p}$$

$$= \frac{M}{l}\Big[\frac{1}{2t}\int_{0}^{\infty}\int_{-t}^{t}\limsup_{t\to+\infty}\Big\{\frac{1}{2t}\int_{-t}^{t}\|(\int_{x-v}^{x+l-v}-\int_{-v}^{l-v})e^{i\lambda s}g(s)ds\|^p dx\Big\}\frac{dv}{(1+v^{\zeta})^p}\Big]^{1/p}.$$

Taking into account Lemma 1.2, we get from the above:

$$\limsup_{t\to+\infty}\frac{1}{l}\Big[\frac{1}{2t}\int_{-t}^{t}\|(\int_{x}^{x+l}-\int_{0}^{l})e^{i\lambda s}G(s)ds\|^p dx\Big]^{1/p}$$

$$\leq \frac{M}{l}\Big[\frac{1}{2t}\int_{0}^{\infty}\int_{-t}^{t}\limsup_{t\to+\infty}\Big\{\frac{1}{2t}\int_{-t}^{t}\|(\int_{x}^{x+l}-\int_{-v}^{l-v})e^{i\lambda s}g(s)ds\|^p dx\Big\}\frac{dv}{(1+v^{\zeta})^p}\Big]^{1/p}$$

$$\leq \frac{2^{\frac{p-1}{p}}M}{l}\Big[\frac{1}{2t}\int_{0}^{\infty}\int_{-t}^{t}\limsup_{t\to+\infty}\Big\{\frac{1}{2t}\int_{-t}^{t}\|(\int_{x}^{x+l}-\int_{0}^{l})e^{i\lambda s}g(s)ds\|^p dx\Big\}\frac{dv}{(1+v^{\zeta})^p}\Big]^{1/p}$$

$$+ \frac{2^{\frac{p-1}{p}}M}{l}\Big[\frac{1}{2t}\int_{0}^{\infty}\int_{-t}^{t}\limsup_{t\to+\infty}\Big\{\frac{1}{2t}\int_{-t}^{t}\|(\int_{0}^{l}-\int_{-v}^{l-v})e^{i\lambda s}g(s)ds\|^p dx\Big\}\frac{dv}{(1+v^{\zeta})^p}\Big]^{1/p}.$$

Take now any $\epsilon > 0$; then there exists $l_0 > 0$ such that (2.3) holds. Furthermore, the equation (1.6) holds with $f=g$ so that there exists $l_1 > 0$ such that

$$\frac{1}{l}\Big[\frac{1}{2t}\int_0^\infty\int_{-t}^t\limsup_{t\to+\infty}\Big\{\frac{1}{2t}\int_{-t}^t\big\|\big(\int_x^{x+l}-\int_0^l\big)e^{i\lambda s}g(s)ds\big\|^p dx\Big\}\frac{dv}{(1+v^\zeta)^p}\Big]^{1/p} < \epsilon$$

for all $l \geq l_1$. For $l \geq l_0$, the estimate (2.3) yields that

$$\frac{1}{l}\Big[\frac{1}{2t}\int_0^\infty\int_{-t}^t\limsup_{t\to+\infty}\Big\{\frac{1}{2t}\int_{-t}^t\big\|\big(\int_0^l-\int_{-v}^{l-v}\big)e^{i\lambda s}g(s)ds\big\|^p dx\Big\}\frac{dv}{(1+v^\zeta)^p}\Big]^{1/p} < \epsilon,$$

finishing the proof.

Now it is quite simple to state the following analogue of Proposition 2.2 and Remark 2.3:

Proposition 2.5. *Let $q \in L^p_{loc}([0,\infty):X)$, $1/p+1/q=1$ and let $(R(t))_{t>0} \subseteq L(X,Y)$ satisfy (1.2). Let a function $g : \mathbb{R} \to X$ be Besicovitch-Doss p-almost periodic and Stepanov p-bounded, and let $q(\beta-1) > -1$ provided that p>1, resp. $\beta=1$, provided that p=1. Suppose, additionally, that for every $\lambda \in \mathbb{R}$ and $\epsilon > 0$ there exists a number $l_0 > 0$ such that (2.3) holds as well as that the function $Q(\cdot)$ defined through (2.1) belongs to some space $\mathcal{F}_Y$ of functions $[0,\infty) \to Y$, satisfying that (2.2) holds. Then the function $H(\cdot)$, defined through (1.4), is continuous and belongs to the class $\mathrm{B}^{[0,\infty),p}(Y) + \mathcal{F}_Y$, where $\mathrm{B}^{[0,\infty),p}(Y)$ stands for the space of all restictions of Y-valued Besicovitch-Doss p-almost periodic functions from the real line to the interval $[0,\infty)$.*

Remark 2.6. Suppose that $\mathcal{F}_Y = B_0^p([0,\infty):Y)$. Then the resulting function $H(\cdot)$ belongs to the space $\mathrm{B}^{[0,\infty),p}(Y)$. It is not clear whether a Besicovitch-Doss p-almost periodic function defined on $[0,\infty)$ can be extended to a Besicovitch-Doss p-almost periodic function defined on $\mathbb{R}$, as well.

2.1 Some applications

Basically, our results can be applied at any place where the variation of parameters formula or some of its generalizations can be applied. For example, we can incorporate our results in the analysis of abstract fractional inclusions with multivalued linear operators $\mathcal{A}$ satisfying the condition (P) introduced by A. Favini and A. Yagi [5, p. 47]. Define the resolvent operator families $(S_\gamma(t))_{t>0}$ and $(R_\gamma(t))_{t>0}$ generated by $\mathcal{A}$ as in [11] and [6]. Let x_0 be a point of continuity of $(S_\gamma(t))_{t>0}$, i.e., $\lim_{t\to 0+} S_\gamma(t)x_0 = x_0$. Then there exist two finite constants $M_1 > 0$ and $M_2 > 0$ such that

$$\| R_\gamma(t) \| \le M_1 t^{\gamma\beta-1}, t \in (0,1] \quad \text{and} \quad \| R_\gamma(t) \| \le M_2 t^{-1-\gamma}, t \ge 1.$$

Let $\gamma \in (0,1)$. A continuous function $u : \mathbb{R} \to X$ is said to be a mild solution of the abstract fractional relaxation inclusion $D^\gamma_{t,+} u(t) \in -\mathcal{A}u(t) + f(t), t \in \mathbb{R}$ iff

$$u(t) = \int_{-\infty}^{t} R_\gamma(t-s)f(s)ds, t \in \mathbb{R}. \text{ A mild solution of the abstract fractional relaxation inclusion}$$

$$(\mathrm{DFP})_{f,\gamma} : \begin{cases} \mathbf{D}^\gamma_t u(t) \in \mathcal{A}u(t) + f(t), t > 0, \\ u(0) = x_0, \end{cases}$$

is any function $u \in C([0,\infty) : X)$ satisfying that $u(t) = S_\gamma(t)x_0 + \int_0^t R_\gamma(t-s)f(s)ds, \quad t \ge 0.$

Keeping in mind the estimate (2.4) and the fact that $\lim_{t \to +\infty} \| S_\gamma(t) \| = 0$, it is clear how we can apply Theorem 2.1 and Proposition 2.2 in the analysis of existence and uniqueness of Doss p-almost periodic solutions (Besicovitch-Doss p-almost periodic solutions) of the abstract fractional inclusions (2.5) and $(DFP)_{f,\gamma}$. These results can be simply incorporated in the study of qualitative properties of solutions of the fractional Poisson heat type equations with the Dirichlet Laplacian Δ in $L^p(\Omega)$, where Ω is an open bounded region in $\mathbb{R}^n$ (see [11] and [6] for more details). Concerning applications of C-regularized semigroups (see [8] and references cited therein for more details on the subject), it should be emphasized that we are in a position to analyze the existence and uniqueness of Doss p-almost periodic solutions (Besicovitch-Doss p-almost periodic solutions) of the initial value problems with constant coefficients

$$D^\gamma_{t,+} u(t,x) = \sum_{|\alpha| \le k} a_\alpha f^{(\alpha)}(t,x) + f(t,x), t \in \mathbb{R}, x \in \mathbb{R}^n$$

and

$$\begin{cases} \mathbf{D}^\gamma_t u(t,x) = \sum_{|\alpha| \le k} a_\alpha f^{(\alpha)}(t,x) + f(t,x), t \ge 0, x \in \mathbb{R}^n, \\ u(0,x) = u_0(x), \quad x \in \mathbb{R}^n \end{cases}$$

in the space $L^p(\mathbb{R}^n)$, where $1 \le p < \infty$ and some extra assumptions are satisfied.

3   CONCLUSIONS

The main purpose of this paper is to analyze the invariance of Doss almost periodicity and Besicovitch-Doss almost periodicity under the actions of finite convolution product and infinite convolution product. We briefly explain how our results can be employed in

the qualitative analysis of solutions to abstract (degenerate) inhomogeneous fractional differe-ntial equations in Banach spaces.

REFERENCES

[1]   J. Andres, A. M. Bersani, R. F. Grande, ``Hierarchy of almost-periodic function spaces'', *Rend. Mat. Appl.,* **26**(7), 121-188 (2006).

[2]   A. S. Besicovitch, *Almost Periodic Functions*, Dover Publications Inc., New York, (1954).

[3] R. Doss, ``On generalized almost periodic functions'', *Annals of Math.,* **59**(3), 477-489, 477-489 (1954).

[4] R. Doss, ``On generalized almost periodic functions-II,'' *J. London Math. Soc.,* **37**(1), 133-140 (1962).

[5] A. Favini, A. Yagi, *Degenerate Differential Equations in Banach Spaces,* Chapman and Hall/ CRC Pure and Applied Mathematics, New York, (1998).

[6] V. Fedorov, M. Kostić, ``A note on (asymptotically) Weyl-almost periodic properties of convolution products'', *Chelyabinsk Phy. Math. J.,* **4**(2), 195-206 (2019).

[7]   A. A. Kilbas, H. M. Srivastava, J. J. Trujillo, *Theory and Applications of Fractional Differential Equations*, Elsevier Science B.V., Amsterdam, (2006).

[8]   M. Kostić, *Generalized Semigroups and Cosine Functions,* Mathematical Institute SANU, Belgrade, (2011).

[9] M. Kostić, *Abstract Volterra Integro-Differential Equations*, Taylor and Francis Gro-up/CRC Press, Boca Raton, Fl., (2015).

[10] M. Kostić, ``On Besicovitch-Doss almost periodic solutions of abstract Volterra integro-differential equations'', *Novi Sad J. Math.,* **47**(2), 187-200 (2017).

[11] M. Kostić, *Almost Periodic and Almost Automorphic Solutions to Integro-Differential Equations,* W. De Gruyter, Berlin, (2019).

[12] J. Mu, Y. Zhoa, L. Peng, ``Periodic solutions and S-asymptotically periodic solutions to fractional evolution equations'', *Discrete Dyn. Nat. Soc.,* 1-12 (2017), https://doi.org/10.1155/2017/1364532.

EXTREMAL PROPERTIES OF THE FUNCTIONALS CONNECTED WITH THE SYSTEMS OF CONSERVATION LAWS

YU. G. RYKOV[*]

Keldysh Institute of Applied Mathematics, RAS. Moscow, Russia
*Corresponding author. E-mail: yu-rykov@yandex.ru

Summary. The paper contains a further concretization of the variational approach to the theory of systems of conservation laws described in the earlier author's work. This approach involves the development of methods for proving the existence and uniqueness theorems for generalized solutions that are based on the search for critical points of functionals in Banach spaces. A new definition of the generalized solution is proposed and its equivalence to the traditional one for the functions of a simple structure is proved. A new strategy for proving existence and uniqueness theorems is proposed. A number of illustrative theorems outlining the implementation of this strategy are proved.

1 INTRODUCTION

The paper is devoted to further assessment of new approach to the theory of systems of conservation laws, which was proposed in [1]. In order to give brief impression why any new approach in the field of conservation laws seems to be necessary, we give below several guidelines, these guidelines in no way pretend to reflect even a main topics in an extensive literature on the conservation laws theory. As is known, the state of the art in the field of quasilinear hyperbolic conservation laws systems is far from completeness. Still a sufficiently complete theory has been constructed only for a single conservation law by S.N.Kruzhkov in 1970, [2]. In the case of systems, fairly general results have been obtained only for one spatial variable and, as a rule, under the assumption that the variation range of the unknown functions is small, see basic research [3] and later interpretation in, for example, [4]. In the framework of present paper we set aside much more complex issues connected with the multidimensional case and do not mention the corresponding researches and results. For one dimensional systems, in order to remove smallness constraints, the vanishing viscosity method was used. This method leads to excellent results in the case of one conservation law (Kruzhkov theory) and in the case of systems it leads to the notion of measure-valued solutions [5]. Further the general existence theorems for generalized solutions to systems of two hyperbolic conservation laws (one spatial variable) with the aid of compensated compactness principle were obtained. But then the vanishing viscosity method seems to become the stumbling block for the theory because of the lack of necessary apriori estimates when the number of equations equals or more than three.

Moreover there are the facts that can be interpreted in the sense that the vanishing viscosity method, may be, is not very relevant to study the quasilinear systems of hyperbolic conservation laws. First, certain systems of two conservation laws, which are strictly hyperbolic, genuinely nonlinear have no classical solutions to Riemann problem and the application of viscosity method gives the emergence of delta-functions along the shock lines [6]. This seems inappropriate because there is no satisfactory interpretation how to deal with

delta-functions in nonlinear problems. The example of such systems considered in [6] is shown below

$$u_t + \left(u^2 - v\right)_x = 0$$

$$v_t + \left(u^3 / 3 - u\right)_x = 0,$$

(1)

here $u = u(t,x), v = v(t,x)$ and $(t,x) \in \mathbb{R}^+ \times \mathbb{R}$, the subscripts t and x denote the corresponding partial derivatives. Moreover, the system (1) can be obtained from the system of isothermal gas dynamics via certain nonlinear transformation.

In addition the recent paper by D.Serr [7] studies the so-called divergence-free positive symmetric tensors (DPT) and their connection with the fluid dynamics. The DPT is locally integrable tensor $T(y), y = (y_1,...,y_m), T = \{T_{ij}, i = 1,...,n; j = 1,...,m\}$, which is positive definite or positive semi-definite and $DivT \equiv \left(\sum_{j=1}^{m} \partial T_{ij} / \partial y_j\right)_{1 \le i \le n} = 0$. The divergence is understood in the weak sense. Many physical systems can be put in such a form including Euler and Navier-Stokes systems. The main result of [7] is the discovery of new apriori estimate for DPT, namely the finiteness of integral

$$\int \left(\det T(y)\right)^{1/(m-1)} dy \le \left(\det \int T(y) dy\right)^{1/(m-1)}.$$

(2)

In case of multidimensional gas dynamics which is considered as the one of most important examples of conservation laws systems the estimate (2) yields the following estimate

$$\int_0^T dt \int_{\mathbb{R}^m} \rho^{1/m} P dy \le const,$$

(3)

where ρ is the density and P is the pressure. The estimates like (3) rule out the possibility of delta-shocks as in [6], which are obtained via vanishing viscosity method. Moreover, as it is highlighted in [7] though the Navier-Stokes system has the form of divergent-free tensor it lacks positivity and thus in general cannot provide estimates like (3). So [7] asserts that vanishing viscosity method seems not suitable but the construction of a generalized solution should involve an approximation process which is consistent with the estimate (3), i.e. for the Euler equation the Boltzmann equation approximation or numerical schemes are proposed in [7].

Taking into account the fact that abovementioned methods are known for a long time but their application still seems does not lead to satisfactory constructions, in the present paper we discus another possibility (see [1]) of approaching the notion of generalized solutions, which is different from traditional approaches. Namely, we strive developing the notion of generalized solution, which is based on the existence of critical points of functionals in Banach space. As it can be seen below this task in fact requires much investigation and therefore here we only establish the general framework for this new approach.

The paper is organized as follows. In section 2 we recall the very basic known definitions and facts on the quasilinear conservation laws theory and introduce variational interpretation

of these concepts in lines with [1]. Also we give certain new interpretation of some results from [1] that are relevant to the topic of the present paper. In section 3 a new strategy for proving existence and uniqueness theorems is proposed. A number of illustrative theorems outlining the implementation of this strategy are proved though these theorems at the moment are still far from the proof of any existence and uniqueness theorem. Finally in section 4 several concluding remarks are made.

2 A VARIATIONAL VIEW ON THE SYSTEMS OF CONSERVATION LAWS

Consider the Cauchy problem for the system of quasilinear conservation laws, which is assumed to be strictly hyperbolic

$$\boldsymbol{U}_t + \boldsymbol{F}(\boldsymbol{U})_x = 0 \quad , \quad \boldsymbol{U}(0,x) = \boldsymbol{U}_0(x), \tag{4}$$

where $(t,x) \in \Pi_T \equiv \{(t,x) : (t,x) \in [0,T] \times \mathbb{R}\}$, $\boldsymbol{U}(t,x) = (u_1(t,x),...,u_n(t,x))$ and $\boldsymbol{F} = (f_1,...,f_n)$ is a sufficiently smooth (at least of class $C^1(\mathbb{R}^n)$) vector function of variables $(u_1,...,u_n)$. The solutions to system (4) that take given initial values are understood in the generalized sense with respect to the following conventional definition.

DEFINITION 1. Let $\boldsymbol{U}_0(x) \in \mathbb{R}^n$ be a bounded measurable function. A bounded and measurable function $\boldsymbol{U}(t,x)$ in Π_T is called a generalized solution to the problem (4) if, for every test function $\varphi \in C^\infty([0,T) \times \mathbb{R})$ such that $\varphi \in C_0^\infty(\mathbb{R})$ for fixed $t \in [0,T]$ and $\varphi \equiv 0$ for $T_1 \le t \le T$, $T_1 < T$, the following integral identity holds:

$$\iint_{\Pi_T} \left[\boldsymbol{U} \varphi_t + \boldsymbol{F}(\boldsymbol{U}) \varphi_x \right] dx dt + \int_{\mathbb{R}} \boldsymbol{U}_0 \varphi(0,x) dx = 0. \tag{5}$$

It is well known that the relations (5) do not guarantee the uniqueness of a solution to the problem (4). Thus an additional conditions are required for the function $\boldsymbol{U}(t,x)$. In the modern literature it is believed that such conditions should have the form of entropy inequalities (and this is true at least for the unknown functions with apriori small variation range).

DEFINITION 2. Let us call convex positive function $\eta(\boldsymbol{U}) \in C^1(\mathbb{R}^n)$ an entropy for the system in (4) if for the classical solutions an additional conservation law holds

$$\eta(\boldsymbol{U}(t,\boldsymbol{x}))_t + \left(q(\boldsymbol{U}(t,\boldsymbol{x})) \right)_x = 0, \tag{6}$$

providing certain smooth enough flow function $q(u_1,...,u_n)$.

DEFINITION 3. The function $\boldsymbol{U}(t,x)$, which is the generalized solution to (4) in the sense of Definition 1, will be called an entropy solution to the problem (4) if for every entropy $\eta(\boldsymbol{U})$ from the Definition 2 and test function $\varphi(t,x) \ge 0$ from the Definition 1 the following inequality holds

$$\iint\limits_{\Pi_T}\left[\eta(\boldsymbol{U})\varphi_t+q(\boldsymbol{U})\varphi_x\right]dxdt+\int\limits_{\mathbb{R}}\eta(\boldsymbol{U}_0)\varphi(0,x)dx\geq0. \tag{7}$$

In the present paper we will not touch the questions of uniqueness, certain interpretation of the notion of entropy solution from the variational point of view (see just below) can be found in [1]. Here we are interested in the non-conventional procedure of seeking any weak solution to system (4).

The main idea of variational approach that has been developed to a certain degree in [1] is as follows. Let us consider instead of function $\boldsymbol{U}(t,x)$ the functional $\boldsymbol{J}:\chi(\tau)\in C^1\left([0,T],\mathbb{R}\right)\to\mathbb{R}^n$,

$$\boldsymbol{J}\equiv\int\limits_0^T\boldsymbol{L}(\dot{\chi},\boldsymbol{U})d\tau\;;\;\boldsymbol{L}(\dot{\chi},\boldsymbol{U})\equiv\boldsymbol{U}\left(\tau,\chi(\tau)\right)\dot{\chi}(\tau)-\boldsymbol{F}\circ\boldsymbol{U}\left(\tau,\chi(\tau)\right). \tag{8}$$

It is shown in [1] that under certain regularity restrictions to $\boldsymbol{U}(t,x)$ the condition $\delta\boldsymbol{J}=0$ along some trajectory $x=\chi_{extr}(t)$ implies that $\boldsymbol{U}(t,x)$ satisfies (4) in classical sense along $x=\chi_{extr}(t)$ where $\boldsymbol{U}(t,x)$ is smooth and at the points of intersection of $x=\chi_{extr}(t)$ with discontinuities of $\boldsymbol{U}(t,x)$ the Hugoniot relations hold. This means that having the aim of seeking the generalized solutions to (4) it could be useful to consider instead of functions $\boldsymbol{U}(t,x)$ the functionals $\boldsymbol{J}$, and study the extremal properties of such functionals.

In order to further assess this idea we assume that $\boldsymbol{U}(t,x)$ belongs to the class K of piecewise continuously differential functions with finite number of discontinuities. Such a class was used by O.Oleinik in [8] and it is useful for the initial stages of construction of theories connected with the systems of conservation laws (see also [1]). More precisely in [1], in particular, the following theorem was proved.

THEOREM 4. Let $\boldsymbol{U}(t,x)\in K$, and suppose that there exists a trajectory $\chi_{extr}(t)\in C^1\left([0,T],\mathbb{R}\right)$ such that $\delta\boldsymbol{J}=0$ for this trajectory. Then, at the points $x=\chi_{extr}(t)$ where $\boldsymbol{U}(t,x)$ is smooth, equations (4) hold in the classical sense, and at the points of intersection of $\chi_{extr}(t)$ with the discontinuity lines of the function $\boldsymbol{U}(t,x)$, the Hugoniot relations

$$\frac{ds}{dt}\cdot\left(\boldsymbol{U}^+-\boldsymbol{U}^-\right)=\boldsymbol{F}\left(\boldsymbol{U}^+\right)-\boldsymbol{F}\left(\boldsymbol{U}^-\right) \tag{9}$$

are satisfied; here $x=s(t)$ is the discontinuity curve and $\boldsymbol{U}^{\pm}\equiv\boldsymbol{U}\left(t,s(t)\pm0\right)$. Moreover, the expression for $\delta^2\boldsymbol{J}$ on the trajectory $x=\chi_{extr}(t)$ contains only terms depending on $\left(\delta\chi\right)^2$ (i.e. the quadratic form does not contain terms with $\delta\dot{\chi}$).

The Theorem 4 shows that the system (4) is 'fulfilled in generalized sense' along the extremal trajectories of $\boldsymbol{J}$ and locally in (t,x) the extremum in general is either maximum or

minimum with respect to C-metrics. This means that the functional J, which corresponds to the generalized solution of (4), is the functional, for which any trajectory is extremal. Thus we can consider the set of all functionals of type (8) and try to find the one or ones with the property just described. This view constitutes a variational approach and potential strategy for finding the generalized solution to (4).

In the present paper we extend such a view as follows. Introduce the function $V(t,x) \equiv \int U(t,p)dp$ and consider the functional $I : \chi(\tau) \in C([0,T],\mathbb{R}) \to \mathbb{R}^n$ instead of J

$$I \equiv \int_0^T M(U)(\tau, \chi(\tau))d\tau \equiv \int_0^T \left[\frac{\partial V}{\partial \tau}(\tau, \chi(\tau)) + F \circ U(\tau, \chi(\tau)) \right] d\tau. \qquad (10)$$

With the provisions of functional (10) we can notice that it, in general, acts on the space of only continuous functions $\chi(\tau)$.

THEOREM 5. Let $U(t,x) \in K$, and suppose that there exists a trajectory $\chi_{extr}(t) \in C([0,T],\mathbb{R})$, $\chi_{extr}(0) = y$, $\chi_{extr}(T) = X$ such that δI is defined at $\chi_{extr}(t)$ (i.e., in particular, $\chi_{extr}(t) \in C^1([0,T],\mathbb{R})$) and $\delta I = 0$ for this trajectory. Then, at the points $x = \chi_{extr}(t)$ where $U(t,x)$ is smooth, equations (4) hold in the classical sense, and at the points of intersection of $\chi_{extr}(t)$ with the discontinuity lines of the function $U(t,x)$, the Hugoniot relations (9) are satisfied. Moreover, the property $\delta I = 0$ means that the function $M(U)$ is continuous along discontinuities of $U(t,x)$ and value of $\delta^2 I$ changes by the jump of $M(U)_\tau$.

PROOF. Because of the structure of class K for the proof of the theorem 5 it is enough to consider the situation when function $U(t,x)$ has the single discontinuity line $x = s(t) \in C^1([0,T])$ and there exists only one point of intersection of $x = s(t)$ and $x = \chi_{extr}(t)$. Let us note that in this case, as it is shown below, δI is defined if $\dot\chi_{extr}(t) \neq \dot s(t)$ at the intersection point of $x = s(t)$ and $x = \chi_{extr}(t)$. Further the subscript 'extr' will be omitted for notations' simplicity. We have

$$\delta I = \frac{d}{d\alpha}\bigg|_{\alpha=0} \int_0^T M(U)_{\chi+\alpha h} d\tau \equiv \frac{d}{d\alpha}\bigg|_{\alpha=0} \int_0^T \left[\frac{\partial V}{\partial \tau} + F \circ U \right](\tau, \chi(\tau)+\alpha h(\tau))d\tau, \qquad (11)$$

and

$$\delta^2 I = \frac{d^2}{d\alpha^2}\bigg|_{\alpha=0} \int_0^T M(U)\big|_{\chi+\alpha h} d\tau \equiv \frac{d^2}{d\alpha^2}\bigg|_{\alpha=0} \int_0^T \left[\frac{\partial V}{\partial \tau} + F \circ U \right](\tau, \chi(\tau)+\alpha h(\tau))d\tau, \qquad (12)$$

where $h(0) = h(T) = 0$.

Suppose that τ_0 is such moment of time that $\chi(\tau_0) = s(\tau_0)$ and consequently $\tau^*(\alpha)$ is the time moment where $\chi(\tau^*) + \alpha h(\tau^*) = s(\tau^*)$. Thus as $0 \leq \tau \leq \tau^*(\alpha)$ the function

$M(U)(\tau, \chi(\tau))$ is smooth and will be denoted as $M(U^-)$; at $\tau = \tau^*(\alpha)$ the function $M(U)$ has the discontinuity; and as $\tau^*(\alpha) \le \tau \le T$ the function $M(U)(\tau, \chi(\tau))$ is also sooth and will be denoted by $M(U^+)$. Now we split the integrals in (11), (12) by the integrals with respect to the segments $\left[0, \tau^*(\alpha)\right], \left[\tau^*(\alpha), T\right]$, perform the differentiation as in (11), (12) and obtain for δI

$$
\begin{aligned}
\delta I = & \int_0^{\tau_0} M(U^-)_x (\tau, \chi(\tau)) h(\tau) d\tau + \int_{\tau_0}^{T} M(U^+)_x (\tau, \chi(\tau)) h(\tau) d\tau + \\
& \tau_\alpha^*(0) \left[M(U^-) - M(U^+) \right]\Big\|_{\tau=\tau_0},
\end{aligned}
\tag{13}
$$

and for $\delta^2 I$

$$
\begin{aligned}
\delta^2 I = & \int_0^{\tau_0} M(U^-)_{xx} (\tau, \chi(\tau)) h^2(\tau) d\tau + \int_{\tau_0}^{T} M(U^+)_{xx} (\tau, \chi(\tau)) h^2(\tau) d\tau + \\
& \tau_{\alpha\alpha}^*(0) \left[M(U^-) - M(U^+) \right]\Big\|_{\tau=\tau_0} + 2\tau_\alpha^*(0) h(\tau_0) \left[M(U^-)_x - M(U^+)_x \right]\Big\|_{\tau=\tau_0} + \\
& \tau_\alpha^*(0)^2 \left[M(U^-)_\tau - M(U^+)_\tau + \dot{\chi}(\tau_0)\left(M(U^-)_x - M(U^+)_x \right) \right]\Big\|_{\tau=\tau_0}.
\end{aligned}
\tag{14}
$$

It is also easy to check that $\tau_\alpha^*(0) = \dfrac{h}{\dot{s} - \dot{\chi}}\bigg|_{\tau=\tau_0}$ and $\tau_{\alpha\alpha}^*(0) = \dfrac{(\ddot{\chi} - \ddot{s})\tau_\alpha^*(0)^2 + 2\dot{h}\tau_\alpha^*(0)}{\dot{s} - \dot{\chi}}\bigg|_{\tau=\tau_0}$.

From (13) it follows that if $\delta I = 0$ then

$$
M(U^\pm)_x = 0, \left[M(U^-) - M(U^+) \right]\Big\|_{\tau=\tau_0} = 0
\tag{15}
$$

because the $h(\tau)$ is arbitrary. Let us note that if $U(t,x) \in K$ then $V(t,x)$ is continuous and $V^-(\tau, s(\tau)) = V^+(\tau, s(\tau))$ for any $\tau \in [0,T]$ where $x = s(\tau)$ exists. Thus $V_\tau^- - V_\tau^+ = \dot{s}(V_x^+ - V_x^-) = \dot{s}(U^+ - U^-)$. Therefore from (15) we obtain

$$
\begin{aligned}
0 = & M(U^\pm)_x = \left[\frac{\partial V^\pm}{\partial \tau} + F \circ U^\pm \right]_x (\tau, \chi(\tau)) = U_\tau^\pm + F \circ U_x^\pm (\tau, \chi(\tau)), \\
0 = & \left[M(U^-) - M(U^+) \right]\Big\|_{\tau=\tau_0} = \left[V_\tau^- - V_\tau^+ + F \circ U^- - F \circ U^+ \right]\Big\|_{\tau=\tau_0} = \\
& \left[\dot{s}(U^+ - U^-) + F \circ U^- - F \circ U^+ \right]\Big\|_{\tau=\tau_0},
\end{aligned}
\tag{16}
$$

and we've got the assertion of Theorem 5 concerning the $\delta I = 0$ property.

Finally, substituting expressions (15) into the formula (16) for $\delta^2 I$ it can be seen that if $\delta I = 0$ then

$$\delta^2 \boldsymbol{I} = \int_0^{\tau_0} \boldsymbol{M}\left(\boldsymbol{U}^-\right)_{xx}(\tau, \chi(\tau)) h^2(\tau) d\tau + \int_{\tau_0}^T \boldsymbol{M}\left(\boldsymbol{U}^+\right)_{xx}(\tau, \chi(\tau)) h^2(\tau) d\tau +$$
$$\tau_\alpha^*(0)^2 \left[\boldsymbol{M}\left(\boldsymbol{U}^-\right)_\tau - \boldsymbol{M}\left(\boldsymbol{U}^+\right)_\tau \right]\Big|_{\tau=\tau_0}.$$
(17)

Thus the theorem 5 is proved.

It is easy to check that the following relation is true $\boldsymbol{I} + \boldsymbol{J} = \int^X \boldsymbol{U}(T, p) dp - \int^y \boldsymbol{U}(0, p) dp$.

Thus the results of theorem 5 clarifies the variational properties of $\boldsymbol{J}$ and demonstrates the equivalence of introducing $\boldsymbol{J}$ or $\boldsymbol{I}$ for the functions $\boldsymbol{U}(t, x) \in K$. Further, it is possible to lay into the basis of the definition of generalized solution the variational properties of functional $\boldsymbol{J}$ (but also use $\boldsymbol{I}$ for technical reasons), i.e the function $\boldsymbol{U}(t, x)$ belonging to one or the other functional space will be the generalized solution if any C^1 trajectory for corresponding $\boldsymbol{J}$ is its critical point. In the next section this approach will be put in more rigorous frame.

3 A NEW STRATEGY FOR FINDING THE GENERALIZED SOLUTION

Let us start with the variational definition of generalized solution to the system of conservation laws (4). We remind that in the present paper we do not touch the question of satisfaction with the initial conditions and the question of uniqueness.

Consider the vector function $\boldsymbol{U}(t, x) \in B$, where B is some functional Banach space (for example, $BV, L_1, L_{1,loc}, L^\infty$, etc.). Also consider the set X of all trajectories $\chi(t) \in C^1\left([0, T], \mathbb{R}\right)$. Let $\Gamma_U \subset X$ be the set of trajectories (depending on considered function $\boldsymbol{U}$) where the integral $\boldsymbol{J}$, see (8), is well defined. Denote by $\Delta_U \subset \Gamma_U$ the set of trajectories where $\delta \boldsymbol{J}$ exists.

DEFINITION 6. Consider the vector function $\boldsymbol{U}(t, x) \in B$, where B is some functional Banach space. Consider the functional $\boldsymbol{J} : \chi(\tau) \in C^1\left([0, T], \mathbb{R}\right) \cap \Gamma_U \to \mathbb{R}^n$ with respect to expression (8). The function $\boldsymbol{U}(t, x)$ will be called the generalized solution to conservation laws system (4) if any trajectory $\chi(\tau) \in C^1\left([0, T], \mathbb{R}\right) \cap \Gamma_U \cap \Delta_U$ is critical for $\boldsymbol{J}$ (i.e. $\delta \boldsymbol{J} = 0$).

Let us first show that there are sufficiently many trajectories where $\boldsymbol{J}$ is defined for locally integrable function $\boldsymbol{U}(t, x)$.

THEOREM 7. Consider any diffeomorphism of $\mathbb{R}^+ \times \mathbb{R}$ having the form: $t' = t$, $x' = \xi(t, x)$, $\xi_x \neq 0$. Suppose $\boldsymbol{U}(t, x) \in L_{1,loc}\left(\mathbb{R}^+ \times \mathbb{R}\right)$ with respect to Lebesgue measure. Then for a.e. x the function $\boldsymbol{U}(t, \xi(t, x))$ is locally integrable with respect to t and the functional $\boldsymbol{J}$ is defined provided the following estimate holds $\left|\boldsymbol{F}(\boldsymbol{U})\right| \leq |\boldsymbol{U}|$, $\boldsymbol{U} \in \mathbb{R}^n$.

PROOF. Let us take the diffeomorphism $(t', x') = \boldsymbol{\psi}(t, x)$ in the form pointed out in the conditions of theorem 7. For any measurable set A the set $\boldsymbol{\psi}(A)$ is also measurable and the change of variables formula is true

$$\iint\limits_{\boldsymbol{\psi}(A)} \boldsymbol{U}(t', x')\, dt'dx' = \iint\limits_A \boldsymbol{U} \circ \boldsymbol{\psi}(t, x) \frac{\partial(t', x')}{\partial(t, x)}\, dtdx. \tag{18}$$

At this, the function under the right hand side integral in (18) is integrable. By the Fubini theorem for a.e. x the function $\boldsymbol{U}(t, \xi(t, x))\xi_x$ is locally integrable with respect to t and so does the function $\boldsymbol{U}(t, \xi(t, x))$ because $\xi_x \neq 0$. Taking into account the estimate on $\boldsymbol{F}(\boldsymbol{U})$ from the conditions of theorem 7 we get the definiteness of functional $\boldsymbol{J}$. The theorem is proved.

The next theorem demonstrates another way of investigation the relevance of definition 6.

THEOREM 8. Suppose $\boldsymbol{U}(t, x) \in BV(\mathbb{R}^+ \times \mathbb{R})$ and is a generalized solution of system (4) in the sense of definition 6. Suppose there exists the following set of trajectories $\Omega_U : x = \xi(t, \alpha, \varepsilon) \equiv \alpha\chi_1(t) + (1 - \alpha)\chi_2(t, \varepsilon)$, $\alpha \in [0,1]$, $\chi_1(t) < \chi_2(t, \varepsilon) \in C^1([0,T], \mathbb{R})$ and $\chi_2(t) = \chi_1(t) + \varepsilon$ for $t \in [0, \tau_1] \cup [\tau_2, T]$, $\tau_2 > \tau_1 > 0$; $\varepsilon > 0$ is small. At this let $\boldsymbol{J}$ and $\delta\boldsymbol{J}$ are defined for the trajectories from Ω_U and $\delta\boldsymbol{J} = 0$ for any trajectory. Then $\iint\limits_E (\boldsymbol{U}_t + \boldsymbol{F}(\boldsymbol{U})_x)\, dtdx = 0$ in the sense of measures, $E: \tau_1 \leq t \leq \tau_2$, $\chi_1(t) \leq x \leq \chi_2(t, 0)$.

PROOF. Consider $\boldsymbol{J}$ along the trajectories from Ω_U as the function of α with fixed ε. Thus we have

$$\boldsymbol{J}(\alpha)_\varepsilon = \int\limits_0^T \left[\boldsymbol{U}(\tau, \xi(\tau, \alpha, \varepsilon))\xi_\tau(\tau, \alpha, \varepsilon) - \boldsymbol{F} \circ \boldsymbol{U}(\tau, \xi(\tau, \alpha, \varepsilon)) \right] d\tau. \tag{19}$$

Further, according to the conditions of the theorem $\delta\boldsymbol{J}$ exists for trajectories from Ω_U and therefore $\boldsymbol{J}_\varepsilon(\alpha)$ is differentiable for any small $\varepsilon > 0$. By mean value theorem $\boldsymbol{J}_\varepsilon(1) - \boldsymbol{J}_\varepsilon(0) = \delta\boldsymbol{J}_\varepsilon(\bar{\alpha})$, $0 < \bar{\alpha} < 1$. But $\delta\boldsymbol{J}$ vanishes for all trajectories from Ω_U, hence $\boldsymbol{J}_\varepsilon(1) = \boldsymbol{J}_\varepsilon(0)$ for any small $\varepsilon > 0$. Passing to the limit as $\varepsilon \to 0$ we immediately have from (19)

$$\int\limits_{\partial E} \left[\boldsymbol{U}(t, x)\, dx - \boldsymbol{F} \circ \boldsymbol{U}(t, x)\, dt \right] = 0. \tag{20}$$

For BV functions Green formula is valid and the assertion of the theorem follows from (20), see also [9]. The theorem is proved.

REMARK 9. In case when there exist sufficiently many domains E the solution in a sense of definition 6 will be also a weak solution in the sense of definition 1.

Definition 6 in fact assumes the strategy for proving the existence theorems for conservation laws, which seems different from the method of apriori estimates. Let us

associate with any function $U(t,x)$ from certain Banach functional space the functional $\boldsymbol{J}$ with respect to formula (8). Consider the set of such functionals. According to definition 6 in order to find the solution to system (4) we need to find $\boldsymbol{J}$ with a lot of critical points. Thus the strategy is as follows: let us start from any function $U(t,x)$ such that corresponding functional $\boldsymbol{J}$ has some critical trajectory, than it is necessary to find the gradual perturbation of $U(t,x)$ (and hence of $\boldsymbol{J}$) in order to move to the situation with more critical points of $\boldsymbol{J}$. It can be formulated as the following problem.

PROBLEM: To find the sequential deformation $\delta U(t,x)$ of the function $U(t,x)$ from the suitable Banach space B in order that the corresponding functional $\boldsymbol{J}$ has more and more critical points.

At present there is no any solution of the posed problem. One possible way to achieve this could be using the various forms of mountain pass theorem, which states the existence of saddle critical points, see [10], for example. At this important requirement is the fulfillment of one or another form of so called Palais-Smale condition. Palais-Smale condition in its form from [10] says that if $E(u)$ is some continuously differentiable functional on some Banach space B and there exists such sequence $u_m \in B$ that $\left|E(u_m)\right| \leq const, \forall m$, while $\left\|\delta E(u_m)\right\|_{B^*} \to 0$ as $m \to \infty$, then $\{u_m\}$ has strongly convergent subsequence.

In order to demonstrate the ways to prove assertions similar to this condition we will prove easier result for functional $\boldsymbol{I}$ (10). First, consider the function $\boldsymbol{M}(U)(t,x)$, see (10), and denote by $\boldsymbol{M}(U)_t(t,x)$ the partial derivative of this function in its areas of smoothness.

THEOREM 10. Suppose $U(t,x) \in K$ and suppose the functional $\boldsymbol{I}$ is coercive on some subset $A \in C([0,T],\mathbb{R})$. Also we assume that $\boldsymbol{M}(U)_t$ is bounded while $|x|$ is bounded. Then the set of critical points $\{\chi_i \in A\}, i = 1,2...$ of $\boldsymbol{I}$ such that $\left|\boldsymbol{I}(\chi_i)\right| \leq const$ for any i has the weakly convergent subsequence in the space $C([0,T],\mathbb{R})$ and $\boldsymbol{M}(U)\left(t,\lim \chi_{i_n}(t)\right)$ is continuous.

PROOF. The estimate $\left|\boldsymbol{I}(\chi_i)\right| \leq const$ and the coerciveness of $\boldsymbol{I}$ lead to the estimate $\left\|\chi_i\right\|_C \leq const$ uniformly with respect to i. Then some subsequence χ_{i_n} converges weakly in C, i.e. everywhere to some function χ. From (13) the criticality of χ_{i_n} means that $\boldsymbol{M}(U)_{i_n} \equiv \boldsymbol{M}(U)\left(\tau,\chi_{i_n}(\tau)\right)$ is continuous and $\boldsymbol{M}(U)\left(\tau,\chi_{i_n}(\tau)\right)_\chi = 0$ where $\boldsymbol{M}(U)_{i_n}$ is smooth. In the domains of smoothness

$$\dot{\boldsymbol{M}}(U)_{i_n} = \boldsymbol{M}(U)_\tau\left(\tau,\chi_{i_n}(\tau)\right) + \boldsymbol{M}(U)\left(\tau,\chi_{i_n}(\tau)\right)_\chi \dot{\chi}_{i_n}(\tau) = \boldsymbol{M}(U)_\tau\left(\tau,\chi_{i_n}(\tau)\right). \quad (21)$$

Hence $\dot{\boldsymbol{M}}(U)_{i_n}$ is uniformly bounded in the smoothness areas because of our assumptions and boundedness of χ_{i_n}. Passing to another subsequence if necessary and keeping the same

notation i_n we conclude that $M(U)_{i_n}$ converge to some continuous function $M(\tau)$. Because of everywhere convergence of χ_{i_n} we have $M(U)(\tau, \chi(\tau)) = M(\tau)$. The theorem is proved.

4 CONCLUSIONS

We present the consistent variational point of view to the theory of 1D systems of conservation laws, which seems to be new in this area. The approach implies the alternative methods for the proof of existence and uniqueness theorems. Such methods are based on the methods of seeking critical points of nonlinear functionals in Banach spaces and differ from conventional methods of apriori estimates or vanishing viscosity. Here we describe only the framework, main problems of the theory remain open. The established theorems only illustrate the validity of the approach. The author expects the development of the highlighted theory in the forthcoming publications.

REFERENCES

[1] Yu.G. Rykov, "On the variational approach to systems of quasilinear conservation laws", *Proceedings of the Steklov Institute of Mathematics*, **301**, 213-227 (2018).

[2] S.N. Kruzhkov, "Kvazilinejny`e uravneniya pervogo poryadka so mnogimi nezavisimy`mi peremenny`mi", *Mat. USSR Sb.*, **10**, 217-243 (1970).

[3] J. Glimm, "Solutions in the large for nonlinear hyperbolic systems of equations", *Commun. Pure Appl. Math.*, **18**, 697-715 (1965).

[4] A. Bressan, *Hyperbolic systems of Conservation Laws: the One-Dimensional Cauchy Problem*, Oxford Univ. Press, (2000).

[5] R.J. DiPerna, "Measure-valued solutions to conservation laws", *Arch. Ration. Mech. Anal.*, **88**, 223-270 (1985).

[6] B.L. Keyfitz, "Singular shocks, retrospective and prospective", *Confluentes Math.*, **3**, 445-470 (2011).

[7] D. Serre, "Divergence-free positive symmetric tensors and fluid dynamics", *Annales de l'Institut Henri Poincare*, **35**, 1209-1234 (2018).

[8] O. A. Oleinik, "Razry`vny`e resheniya nelinejny`x differencial`ny`x uravnenij", *Uspekhi Mat. Nauk*, **12**:3(75), 3–73 (1957).

[9] A.I. Volpert, "Prostranstva BV i kvazilinejny`e uravneniya", *Mat. USSR Sb.*, **2**, 225-267 (1967).

[10] M. Struwe, *Variational methods. Applications to nonlinear PDEs and Hamiltonian systems*, Springer, Berlin, Heidelberg, (1990).

FRAGMENTS OF DYNAMICS OF MÖBIOUS MAPPINGS AND SOME APPLICATIONS. PART I

Ž. PAVIĆEVIĆ[*1,2], J. ŠUŠIĆ[1]

[1]Faculty of Sciences and Mathematics, University of Montenegro, Podgorica, Montenegro;
[2]National Research Nuclear University MEPhI (Moscow Engineering Physics Institute),
Moscow, Russia
*Corresponding author. E-mail: zarkop@ucg.ac.me

Summary. In this article we prove that a continuous mapping on a simply-connected domain of the extended complex plane, which is normal with respect to the cycle group of all conformal automorphisms of the domain with a fixed attractive point, which belongs to the domain is a constant function. Applying this result we obtain new proofs of the classical Theorem of Liouville and little Picard Theorem for holomorphic, meromorphic and harmonic functions in complex plane. We also prove some results from the dynamic of Möbius mappings.

1   INTRODUCTION

A problem of Ch. Pommerenke, formulated in [1, p. 169], is if there exists a non-constant meromorphic mapping on the unit disc of the complex plane, which is automorphic and normal with respect to any non-continuous group Γ of Möbius mappings of the unit disc. The same problem was considered by D. Mind in [2, p. 119].

In [3] P. Järvi solved this problem by constructing an open Riemann surface which does not allow non-constant normal analytic mappings.

The question of connection between normality and constancy of functions was also considered by J. Väisälä in the article [4]. In this article it is shown (Theorem 2, p. 17) that styding the normal continuous functions on the complex plane and the extended complex plane does not make sense, since the family of all continuous functions on a simply connected elliptic (parabolic) domain in the complex plane, that are normal with respect to the group of all conformal automorphisms of such kind of domains, reduce to the family of constant functions. However, in this paper a more general result is proved. We prove that if for a simply connected domain of the extended complex plane there exists conformal automorphism g which has at least one attractive fixed point in that domain which is not ∞, then any function f which is continuous in that domain and which maps that domain in the Riemann sphere $\overline{\mathbb{C}}$ or extended set of real numbers $\mathbb{R}\cup\{-\infty,+\infty\}$, for which the family $\{f\circ g^{n}\,|\,n\in Z\}$ is a normal family of functions, is a constant function in that domain (*Theorem 3.2 and Theorem 5.2*).

From this result it follows that if a domain is of the parabolic type (complex plane) or the elliptic type (extended complex plane) then a continuous mapping on that domains will be a constant, if the family of all compositions of that function with all elements of cyclic group with generating element of the hyperbolic or parabolic Möbius mapping, is a normal family on the domain. We emphasize that the position of fixed points of a conformal automorphism plays the main role in obtaining these results.

These results are later used for obtaining the simple proof of the classical Liouville Theorem and little Picard Theorem for holomorphic, meromorphic and harmonic functions. Namely, in the theory of functions of complex argument the Liouville's Theorem on constancy of entire functions and little Picard Theorem on values of holomorphic and meromorphic functions have a special place. Proofs of these Theorems often use the classical results in the theory of analytic functions such as: Cauchy integral formula, the expansion of an analytic function in Taylor series and properties of elliptic modular function (see for example [5, 6, 7, 10]). The analogies of these Theorems for harmonic functions on the complex plane are also known (see [6, 11, 12]). We would like to highlight the reference [11], where the authors give six proofs of the Liouville Theorem for harmonic functions in the complex plane. The proof of Liouville's Theorem for harmonic functions on $R^n, n \geq 2,$ from [12], is interesting, as it has not used any single mathematical symbol. Our article gives a new approach in proving these results.

As a direct consequence of considering of constancy of continuous functions, we also obtain the known results which say that fixed points of parabolic and hyperbolic Möbius transforms, which are automorphisms of the unit disc, must be on the boundary of the unit disk, and that the fixed points of elliptic automorphisms of the unit disk cannot be attraction points as well as they cannot be on the boundary of the unit disc. We find a connection between the notion of normality and discontinuity of subgroups of Möbius group of all conformal automorphisms of the Riemann sphere $\overline{\mathbb{C}}$ (see [7, 8, 10]).

2. PRELIMINARY NOTATIONS AND DEFINITIONS

With $\mathbb{R}$ we denote the set of all real numbers, $\mathbb{Z}$ will denote the set of all integers, $\mathbb{N}$ the set of all natural numbers, and $\mathbb{C} = \{z | z = x + iy, \ x, y \in R\mathbb{R}\}$ will be the set of all complex numbers, i.e., the complex plane, $|z| = \sqrt{z\overline{z}}$ and $\overline{\mathbb{C}} = \mathbb{C} \cup \{\infty\}$ is Riemann sphere.

For z_1 and z_2 we denote by $d(z_1, z_2) = |z_1 - z_2|$ the Euclidean metric on $\mathbb{C}$, and

$$d_s(\omega_1, \omega_2) = \frac{2|\omega_1 - \omega_2|}{\sqrt{1 + |\omega_1|} \cdot \sqrt{1 + |\omega_2|}}, \omega_1, \omega_2 \in \mathbb{C}; \quad d_s(\omega_1, \omega_2) = \frac{2}{\sqrt{1 + |\omega_1|^2}}, \ \omega_1 \in \mathbb{C}, \ \omega_2 = \infty, \quad \text{is the}$$

spherical Riemann distance on $\overline{\mathbb{C}}$.

The set $\mathbb{C}$ with the metric $d(z_1, z_2)$ is Hausdorff and complete metric space, but it is not compact.

However, $\overline{\mathbb{C}} = \mathbb{C} \cup \{\infty\}$ with the metric $d_s(\omega_1, \omega_2)$ is a compact metric space. On the compact subset of $\mathbb{C}$ these metrics are equivalent.

The convergences are meant in these metrics.

The group $G\left(\overline{\mathbb{C}}\right)=\left\{\dfrac{az-b}{cz-d}\,\Big|\,a,b,c,d\in\mathbb{C},\ ad-cd=1\right\}$ is the group of all conformal automorphisms of the Riemann sphere $\overline{\mathbb{C}}$, and the group $G(\mathbb{C})=\left\{az+b\,|\,a,b\in C, a\neq 0\right\}$ is the group of all conformal automorphisms of the complex plane $\mathbb{C}$. The group $G(\mathbb{C})$ is a subgroup of the group $G\left(\overline{\mathbb{C}}\right)$. We use notation: $G(\mathbb{C})\Delta G\left(\overline{\mathbb{C}}\right)$. Groups, $G\left(\overline{\mathbb{C}}\right)$, i $G(\mathbb{C})$ are Möbius groups for the Riemann sphere $\overline{\mathbb{C}}$ and the complex plane $\mathbb{C}$, respectively, and their elements are referred to as Möbius mappings.

The Möbius mappings g_1 i g_2 are equivalent if there exists a Möbius mapping $h\in G\left(\overline{\mathbb{C}}\right)$ such that $g_1(z)=\left(h\circ g_2\circ h^{-1}\right)(z)$, $z\in\overline{\mathbb{C}}$.

For every $g(z)=\dfrac{az+b}{cz+d}\in G\left(\overline{\mathbb{C}}\right)$ there exists a matrix $A=\begin{pmatrix} a & b \\ c & d \end{pmatrix}$ in the group

$$GL(2,\mathbb{C})=\left\{A\,\Big|\,A=\begin{pmatrix} a & b \\ c & d \end{pmatrix},\ a,b,c,d\in\mathbb{C},\ ad-bc\neq 0\right\}.$$

It may be shown that the group $G\left(\overline{\mathbb{C}}\right)$ is isomorphic to the group $SL(2,\mathbb{C})/\{I,-I\}$, where l is the identity matrix, and $SL(2,\mathbb{C})$ is the set of all matrices A such that $\det A=1$. On the group $G\left(\overline{\mathbb{C}}\right)$ one may introduce the norm $\|g\|=\left(|a|^2+|b|^2+|c|^2+|d|^2\right)$, which generates the metric on $G\left(\overline{\mathbb{C}}\right)$, which defines the topology on it. With respect to that topology, $G\left(\overline{\mathbb{C}}\right)$ is a topological group.

For $g(z)=\dfrac{az+b}{cz+d}\in G\left(\overline{\mathbb{C}}\right)$ we have: $M=\begin{pmatrix} a & b \\ c & d \end{pmatrix}$ and $tr(g)=\dfrac{(a+d)^2}{\det M}$.

With the symbol O we will always denote a simply connected domain of the Riemann sphere $\overline{\mathbb{C}}$, i.e., $O\subset\overline{\mathbb{C}}$.

Let $G(O)$ be the group of all conformal automorphisms of the domain O. A point $z_0\in O$ is *fixed point* of $g\in G(O)$ if $g(z_0)=z_0$. Then we have $g^{-1}(z_0)=z_0$, and therefore z_0 is also a fixed point for g^{-1}.

For $g\in G(O)$ we use notation $g^n(z)=\underbrace{g\ \big(g\big(...\big(g(z)...\big)\ \big)}_{n\ \text{times}}$ and

$$g^{-n}(z) = \left(g^{-1}\right)^n (z) = \underbrace{g^{-1}\left(g^{-1}\left(...\left(g^{-1}(z)...\right)\right)\right)}_{n \text{ times}}, \ n \in \mathbb{N}.$$

For a fixed point z_0 of g in the group $G(O)$ the equality $g^n(z_0) = z_0$, $n \in \mathbb{Z}$ holds.

A fixed point $z_0 \in O$ of $g \in G(O)$, $g \neq i = g^0$, where i is the identity mapping, is an *attractive point of an automorphism g*, if for every $z \in O$ we have $\lim\limits_{n \to \infty} g^n(z) = z_0$.

3. FRAGMENTS OF DYNAMIC OF MÖBIUS MAPPINGS

Further, we need to analyse the fixed points of Möbius mappings of the group $G(\overline{\mathbb{C}})$.

In [8], on p. 67, a classification of Möbius mappings in $G(\overline{\mathbb{C}})$ based on description of fixed points of their Poincare extensions on $\mathbb{R}^3 \cup \{\infty\}$ is given.

Namely, if $g \in G(\overline{\mathbb{C}})$, $g \neq i$, has one fixed point in $\mathbb{C}$, then it is called the *parabolic element of the group* $G(\overline{\mathbb{C}})$, or *parabolic Möbius mapping*.

If the Poincare extension of an element $g \in G(\overline{\mathbb{C}})$ on $\mathbb{R}^3 = \{(x, y, z) | x, y, z \in \mathbb{R}\}$ has only two fixed points in $\mathbb{R}^3$, then it is called the *loxodromic Möbius mapping*.

If for a loxodromic Möbius mapping g there exists an open circle or an open half plane in the complex plane $\overline{\mathbb{C}}$ which are invariant with respect to g, then we call g the hyperbolic element of the group $G(\overline{\mathbb{C}})$, or hyperbolic Möbius mapping. In opposite case it is called the *strictly loxodromic mapping*.

If the Poincare extension of $g \in G(\overline{\mathbb{C}})$ on $\mathbb{R}^3 \cup \{\infty\}$ has infinitely many fixed points on $\mathbb{R}^3 \cup \{\infty\}$, then it is called the *elliptic element of the group* $G(\overline{\mathbb{C}})$, or *elliptical Möbius mapping*.

Theorem 3.1 ([8], see Theorem 4.3.4, p. 67). *For $g \in G(\overline{\mathbb{C}})$, $g \neq i$ we have: g is a parabolic element if and only if we have $tr^2(g) = 4$, g is an elliptic element if and only if $tr^2(g) \in [0, 4)$, g is the hyperbolic element if and only if $tr^2(g) \in (4, \infty)$ and g is strictly loxodromic element if and only if $tr^2(g) \notin (4, \infty)$.*

Any element of $G(\overline{\mathbb{C}})$, different from the identity, has one or two fixed points in $\overline{\mathbb{C}}$.

Theorem 3.2 ([8], p. 73). (i) *If $g \in G(\overline{\mathbb{C}})$, $g \neq i$, is a parabolic element with a fixed point $z_0 \in \mathbb{C}$, then for every $z \in \overline{\mathbb{C}}$ we have $\lim\limits_{n \to \infty} g^n(z) = z_0$.*

(ii) If g is a loxodromic element with fixed points z_0 and z_1, then for one of these points, without loss of generality z_0, that for every $z \in \overline{\mathbb{C}} \setminus \{z_1\}$ the equality $\lim_{n \to \infty} g^n(z) = z_0$ holds, but then for every $z \in \overline{\mathbb{C}} \setminus \{z_0\}$ $\lim_{n \to \infty} g^{-n}(z) = z_1$.

(iii) If g is an elliptic element with fixed points z_0 and z_1, then g remains invariant for every circle with respect to which the points z_0 z_1 are invertible.

For elements of $G(\mathbb{C})$ we will use the following Lemma in the proof of Theorems in sections 5, 6 i 7.

Lemma 3.3. For $g \in G(\mathbb{C}) = \{g(z) = az + c \mid a \in \mathbb{C},\ a \neq 0,\ c \in \mathbb{C}\}$, $g \neq i$ the following holds:

(i) g is a parabolic Möbius mapping if and only if $a = 1$, ant it's fixed attractive point is ∞;

(ii) g is an elliptic Möbius mapping if and only if $|a| = 1$, $a \neq 1$, and it's fixed points are $\dfrac{c}{1-a}$ and ∞;

(iii) g is a hyperbolic Möbius mapping with fixed attractive points $\dfrac{c}{1-a}$ if and only if $a \in \mathbb{R}$, $0 < a < 1$, and ∞ is its repulsive fixed point;

(iv) g is a hyperbolic Möbius mapping with repulsive fixed point $\dfrac{c}{1-a}$ if and only if $a \in \mathbb{R}$, $1 < a$, and its attractive point is ∞;

(v) in other cases g is strictly loxodromic Möbius mapping.

Proof of Lemma 3.3. For $g(z) = az + c \in G(\mathbb{C})$, $g \neq i$, $a \in \mathbb{C}$, $a \neq 0$, $b \in \mathbb{C}$, we have $tr^2(g) = a + \dfrac{1}{a} + 2$. Since $g(z)$ is parabolic, elliptic or hyperbolic Möbius mapping we have that

$tr^2(g) \in \mathbb{R}$. If $a = \alpha + i\beta$, $\alpha, \beta \in \mathbb{R}$, then we have $tr^2(g) = \alpha + \dfrac{\alpha}{|a|^2} + 2 + \beta\left(1 - \dfrac{1}{|a|^2}\right)i$, so we obtain $tr^2(g) \in \mathbb{R}$ if $1 - \dfrac{1}{|\alpha|^2} = 0$ or $\beta = 0$.

I case. Assume that $1 - \dfrac{1}{|\alpha|^2} = 0$, then $|a| = 1$. It follows $a = e^{i\theta}, \theta \in [0, 2\pi),$ so

$\alpha = \cos\theta$ i $\beta = \sin\theta$. Since $tr^2(g) = 2\alpha + 2 = 2\cos\theta + 2$, from Theorem 3.1 we have that g is a parabolic Möbius mapping if and only if $2\cos\theta + 2 = 4$. Therefore, g is a parabolic Möbius mapping if and only if $\cos\theta = 1$, i.e., for $\theta = 0$. It follows that $\beta = \sin 0 = 0$ and $a = \alpha = 1$. It is easy to see that ∞ is its attraction fixed point. We have proved the part i).

From Theorem 3.1 it follows that g is an elliptic Möbius mapping if and only if $0 \le tr^2(g) < 4$. We conclude that $0 \le 2\cos\theta + 2 < 4$, which is equivalent to $-1 \le \cos\theta < 1$. Since $0 < \theta < 2\pi$, we have $-1 \le \sin\theta < 1$. This yields $a = \alpha + i\beta = \cos\theta + i\sin\theta = e^{i\theta}, 0 < \theta < 2\pi$. Therefore, g is an elliptic Moebius mapping if and only if $|a| = 1$, $a \ne 1$. It is easy to see that all fixed points of it are

$\dfrac{c}{1-a}$ and ∞. Thus, statement *ii)* is proved.

From Theorem 3.1 it follows that g is a hyperbolic Möbius mapping if and only if $4 < tr^2(g)$. This means that $4 < 2\cos\theta + 2$, which is equivalent to $1 < \cos\theta$, but this is impossible, this case excludes the hyperbolic Möbius mappings.
We have finished the case **I**.

II case. Let $\beta = 0$. Then $a = \alpha \in \mathbb{R} \setminus \{0\}$, and therefore $tr^2(g) = \alpha + \dfrac{1}{\alpha} + 2$.

If $tr^2(g) = \alpha + \dfrac{1}{\alpha} + 2 = 4$, then g is a parabolic Möbius mapping. The preceding equality is equivalent to $(\alpha - 1)^2 = 0$, and this is equivalent to $\alpha = 1$, thus in this case we also have *i)*.

The mapping g is an elliptic Möbius mapping if $0 \le tr^2(g) < 4$, from which it follows that $0 \le \alpha + \dfrac{1}{\alpha} + 2 < 4$, or $-2 \le \alpha + \dfrac{1}{\alpha} < 2$, which is equivalent to $-2 \le \alpha + \dfrac{1}{\alpha}$ and $\alpha + \dfrac{1}{\alpha} < 2$.

If we would have $\alpha < 0$, then we will derive $-2\alpha \ge \alpha^2 + 1$ and $\alpha^2 + 1 > 2\alpha$, i.e., $0 \ge (\alpha + 1)^2$ and $(\alpha - 1)^2 > 0$, but this is impossible.

If we would have $\alpha > 0$, then we will derive $-2\alpha \le \alpha^2 + 1$ and $\alpha^2 + 1 < 2\alpha$, i.e., $0 \le (\alpha + 1)^2$ and $(\alpha - 1)^2 < 0$, which is also impossible.

Therefore, the case $\beta = 0$. excludes the elliptic Möbius mappings. Therefore we have proved *ii)*.

The condition that g is an hyperbolic Möbius mapping is that $4 < tr^2(g)$. From this we obtain that $4 < \alpha + \dfrac{1}{\alpha} + 2$, or $2 < \alpha + \dfrac{1}{\alpha}$.

If we would have $\alpha < 0$, this would imply $2\alpha > \alpha^2 + 1$, i.e., $0 > (\alpha - 1)^2$, which is not true.

If $\alpha > 0$, $2\alpha < \alpha^2 + 1$, i.e., $0 < (\alpha - 1)^2$, which is true for every $\alpha \in (0,1) \cup (1, +\infty)$.

Therefore, $\alpha \in (0,1) \cup (1, +\infty)$ is necessary and sufficient for g to be a hyperbolic Moebius mapping.

If $\alpha \in (0,1)$, then form $\alpha z + c = z$ we obtain that $\dfrac{c}{1-a}$ is a fixed point for g. Since we have

$$g^n(z) = \alpha^n z + \alpha^{n-1}c + \alpha^{n-2}c + ... + \alpha c + c = \alpha^n z + \frac{c(1-\alpha^n)}{1-\alpha}, \text{ we obtain } \lim_{n \to \infty} g^n(z) = \frac{c}{1-a}, \text{ from this it}$$

follows that $\dfrac{c}{1-a}$ is a fixed attractive point for the hyperbolic Möbius mapping g, and ∞ is its *repulsive fixed point.*. This is the statement of the part *iii)*.

If $\alpha \in (1, +\infty)$ then $\dfrac{c}{1-a}$ and ∞ are fixed points for the *hyperbolic Möbius mapping g*. Since

$$g^n(z) = \alpha^n z + \alpha^{n-1}c + \alpha^{n-2}c + ... + \alpha c + c = \alpha^n z + \frac{c(1-\alpha^n)}{1-\alpha}, \text{ we conclude } \lim_{n \to \infty} g^n(z) = \infty. \text{ From this}$$

we conclude that ∞ is fixed attractive point for the hyperbolic Moebius mapping *g,* so $\dfrac{c}{1-a}$ is its *repulsive fixed point*, and we have finished the part *vi)*.

If g isn't parabolic, elliptic, or hyperbolic Möbius mapping, then it is strictly loxodromic Moebius mapping. Therefore we have *v)*. □

4. THE MAIN RESULTS

We say that a family of functions $\Im = \left\{ f \mid f : O \to \overline{\mathbb{C}} \right\}$ is *normal family on the domain O*, $O \subset \mathbb{C}$, if any sequence (f_n) of $\Im$ has a subsequence (f_{n_k}) which is uniformly convergent to a function $f : O \to \overline{\mathbb{C}}$ on compacts of *O. For this type of normality of the family $\Im$ we say that it is normal in the sense of Montel*. The family of functions $\Im = \left\{ f \mid f : O \to \overline{\mathbb{C}} \right\}$ is normal in $z \in O$ if it is a normal family in a domain which contains *z*.

It is known (see for example [5, 9, 10,14]) that the family of functions $\Im = \left\{ f \middle| f : O \to \overline{\mathbb{C}} \right\}$ is a normal family on a domain O if and only if it is normal in every point of the domain O.

If $O \subset \overline{\mathbb{C}}$, i.e., if $\infty \in O$, then the family of functions $\Im = \left\{ f \middle| f : O \to \overline{\mathbb{C}} \right\}$ is normal in ∞ if the family $\Im' = \left\{ f\left(\dfrac{1}{z}\right) \middle| f \in \Im \right\}$ is normal in 0, and the function $\Im = \left\{ f \middle| f : O \to \overline{\mathbb{C}} \right\}$ is normal on O if it is normal in every point of the domain O.

A family $\Im$ of functions is *equicontinuous in a point* $z_0 \in O$, $O \subset \overline{\mathbb{C}}$, if for every $\varepsilon > 0$ there exists $\delta = \delta(z_0, \varepsilon) > 0$ such that for every $f \in \Im$ and every z for which $d_1(z, z_0) < \delta$ there holds $d_2(f(z), f(z_0)) < \varepsilon$, where d_1 and d_2 are previously defined metrics on $\mathbb{C}$ i $\overline{\mathbb{C}}$. We can take $d_1 = d_2 = d_s$, if we consider a domain $O \subset \overline{\mathbb{C}}$ which contains the point ∞. A family $\Im$ of functions is equicontinuous family of functions on a domain O if it is equicontinuous in every point of the domain.

Let $G(O)$ be the group of all conformal authomorphisms of the domain O. For a function $f : O \to \overline{\mathbb{C}}$ we say that it is a *normal function* on the domain O with respect to the group G if the family $\Im = \left\{ f \circ \varphi \middle| \varphi \in G \right\}$ is normal family on O, i.e., if any sequence of this family has a subsequence which is uniformly convergent on compact subsets of O.

We will need the following Theorem for the proof of our main result which is given in Theorem 3.2:

Theorem 4.1. ([5], p. 12, or [10]). *A family $\Im$ of continuous functions on a domain O is a normal family on that domain if and only if the family $\Im$ is equicontinuous in O.*

The main result in this paper is the following Theorem:

Theorem 4.2. *Let g be a conformal automorphism of simply connected domain $O \subset \overline{\mathbb{C}}$ which has a attractive fixed point $z_0 \in O$, $z_0 \neq \infty$, and let $f : O \to \overline{\mathbb{C}}$ be a continuous function on O. If the function f is normal on the domain O with respect to the cyclic group $G_g = \left\{ g^n \middle| n \in \mathbb{Z} \right\}$, which is determined by the conformal automorphism g, then f is a constant function on O.*

Proof of Theorem 4.2. Assume the contrary, i.e., that there exists a continuous function f on O which is not constant on O but is normal with respect to the group $G_g = \{g^n \mid n \in \mathbb{Z}\}$. Then there exists a point $z_1 \in O$ such that $f(z_1) \neq f(z_0)$, so $d_2(f(z_1), f(z_0)) > 0$. Denote

$$\varepsilon = \frac{d_2(f(z_1), f(z_0))}{2} > 0. \tag{1}$$

From the condition that f is normal on the domain O with respect to the cyclic group $G_g = \{g^n \mid n \in \mathbb{Z}\}$ and Theorem 4.1 it follows that the family $\{f \circ g^n \mid n \in \mathbb{Z}\}$ is equicontinuous on the domain O, so it is equicontinuous *in* $z_0 \in O$. It follows that for $\varepsilon = \dfrac{d_2(f(z_1), f(z_0))}{2}$ there exists $\delta > 0$, such that for every z for which $d_1(z, z_0) < \delta$ there holds

$$d_2(f \circ g^n(z), f \circ g^n(z_0)) < \varepsilon, \; n \in \mathbb{Z}, \tag{2}$$

where d_1 i d_2 are metrics defined before.

Let us consider the sequence (w_n), $w_n = g^n(z_1)$, $n \in \mathbb{N}$. Since z_0 is an attractive fixed point for g, we have $\lim\limits_{n \to \infty} g^n(z_1) = \lim\limits_{n \to \infty} w_n = z_0$, so for δ there exists a natural number N such that for every $n \geq N$ there holds that $d(w_n, z_0) < \delta$. From this and (2) it follows that $d_2(f \circ g^{-n}(w_n), f \circ g^{-n}(z_0)) < \varepsilon$ for every $n \geq N$, i.e., $d_2(f \circ g^{-n}(g^n(z_1)), f \circ g^{-n}(g^n(z_0))) < \varepsilon$ for every $n \geq N$, from this and from (1) it follows that $d_2(f(z_1), f(z_0)) < \dfrac{d_2(f(z_1), f(z_0))}{2}$. Which is contradiction and the Theorem follows. $\square$

For $g \in G(\mathbb{C})$, $g \neq i$, with G_g we will denote in the further exposition the cyclic group $G_g = \{g^n \mid n \in \mathbb{Z}\}$. The group G_g is a group of all conformal automorphisms of the complex plane $\mathbb{C}$, as well as the Riemanin sphere $\overline{\mathbb{C}}$. Therefore $G_g \, \Delta \, G(\mathbb{C}) \, \Delta \, G(\overline{\mathbb{C}})$.

Remark 4.3. If we take the complex plane $\mathbb{C}$ or the Riemann sphere $\overline{\mathbb{C}}$ for the domain O in Theorem 4.2, and the group G_g for the group of conformal automorphisms, where g is a hyperbolic element from part *iii)* of Lemma 3.3, then from Theorem 4.2 we have the statement of Theorem 2 from [5], on page 17. Therefore, Theorem 4.2 is a generalization of Theorem 2 in [5].

5. APPLICATIONS ON HOLOMORPHIC AND MEROMORPHIC FUNCTIONS

In this section we prove that Liouville and little Picard Theorem may be obtained as a direct consequences of the Montel Theorem on normality of family of holomorphic and meromorphic functions.

For the following considerations we will need the local boundedness of the family of functions. A family of functions $\mathfrak{I} = \{f \mid f : O \to \mathbb{C}\}$ is locally bounded on a domain O if for every $z_0 \in O$ there exists a constant $M = M(z_0) > 0$ and a disc $D(z_0, r) = \{z \mid z \in \mathbb{C}, |z - z_0| < r\} \subset O, r > 0$, such that for every $z \in D(z_0, r)$ and every $f \in \mathfrak{I}$ there holds $|f(z)| < M$.

Theorem 5.1 ([10], Montel's Theorem, p. 35)**.** *If $\mathfrak{I}$ is a family of locally bounded holomorphic functions on a domain O, then $\mathfrak{I}$ is a normal family on the domain O.*

Theorem 5.2 ([7], Theorem 1.3 (Liouville's Theorem), p. 3)**.** *A holomorphic function $f : \mathbb{C} \to \mathbb{C}$ which is bounded on $\mathbb{C}$, must be a constant on $\mathbb{C}$.*

Proof of Theorem 5.2. Let $g \in G(\mathbb{C})$, $g(z) = az + c, 0 < a < 1, c \in \mathbb{C}$. From the boundedness of an holomorphic function on $\mathbb{C}$, the function f and from Theorem 5.1 it follows that the family $\mathfrak{I}_f = \{f \circ g^n \mid n \in \mathbb{Z}\}$ is a normal family on $\mathbb{C}$ with respect to the group G_g. The statement of Theorem 5.2 now follows straightforwardly from *iii)* of Lemma 3.3 and Theorem 4.2. $\square$

Theorem 5.3 (see [11], p. 112, or Lemma 2.5, [7], p. 17)**.** *A holomorphic function $f : \overline{\mathbb{C}} \to \mathbb{C}$ must be constant on $\overline{\mathbb{C}}$.*

Proof of Theorem 5.3. From the Theorem of maximum of modulus of an holomorphic function it follows that f is a bounded holomorphic function on $\overline{\mathbb{C}}$. Now from Theorem 5.1 it follows that f is normal function on $\overline{\mathbb{C}}$ with respect to the group G_g, $g(z) = az + c, 0 < a < 1, c \in \mathbb{C}$. Since G_g is a group of all conformal automorphisms of $\overline{\mathbb{C}}$, from *iii)* in Lemma 3.3 and Theorem 4.2 it follows that f a constant function on $\overline{\mathbb{C}}$. $\square$

Theorem 5.4 ([10], Fundamental Normality Test, p. 54) *If $\mathfrak{I}$ is a family of holomorphic functios on a domain O that do not take two fixed values a and b in $\mathbb{C}$, then $\mathfrak{I}$ is normal family on O.*

Theorem 5.5 ([7], Theorem 2.6 (Picard's Theorem), p. 17)**.** *An holomorphic function $f : \mathbb{C} \to \mathbb{C}$, which is not constant on $\mathbb{C}$, takes all values in $\mathbb{C}$, with at most one exception.*

Proof of Theorem 5.5. Assume that the statement of Theorem 5.5 is not correct, i.e., that there exists an holomorphic function $f : \mathbb{C} \to \mathbb{C}$, which is not constant on $\mathbb{C}$, which achieves all values in $\mathbb{C}$, except two or more fixed values in $\mathbb{C}$. Let us consider the family $\mathfrak{I}_f = \left\{ f \circ g^n \,\middle|\, n \in \mathbb{Z} \right\}$, where $g(z) = az + c, 0 < a < 1, c \in \mathbb{C}$, is a hyperbolic element of the group $G(\mathbb{C})$. Then functions from the family $\mathfrak{I}_f = \left\{ f \circ g^n \,\middle|\, n \in \mathbb{Z} \right\}$ does not assume two fixed values in $\mathbb{C}$, therefore from Theorem 5.4 it follows that the family $\mathfrak{I}_f = \left\{ f \circ g^n \,\middle|\, n \in \mathbb{Z} \right\}$ is a normal family in $\mathbb{C}$. Therefore the function f is normal on $\mathbb{C}$ with respect to the cyclic group $G_g = \left\{ g^n \,\middle|\, n \in \mathbb{Z} \right\}$. Since from *iii)* of Lemma 3.3 it follows that the element g has an attractive fixed point in $\mathbb{C}$, Theorem 4.2 yields that f is constant on $\mathbb{C}$, which is contrary to our assumption. This proves Theorem 5.5. $\square$

Theorem 5.6 ([10], Fundamental Normality Test, p. 74)**.** *Let $\mathfrak{I}$ be a family of meromorphic functions on a domain O such that any function in the family does not take any of three fixed values a, b and c in $\mathbb{C}$. Then $\mathfrak{I}$ is a normal family on O.*

Theorem 5.7 (Picard's Theorem for meromorphic functions)**.** *A meromorphic functions $f : \mathbb{C} \to \overline{\mathbb{C}}$, which is not constant, achieves all values in $\mathbb{C}$, with possible exception of at most two values.*

Theorem 5.7 may be proved in the same fashion as Theorem 5.5 using the cyclic group $G_g = \left\{ g^n \,\middle|\, n \in \mathbb{Z} \right\}$, which is generated by a hyperbolic Möbius mapping $g(z) = \alpha z + c, 0 < \alpha < 1$, $c \in \mathbb{C}$, which by *iii)* of Lemma 3.3 has an attractive fixed point in $\mathbb{C} \subset \overline{\mathbb{C}}$, but in the proof we should use Theorem 5.6 instead of Theorem 5.4.

Theorem 4.2 shows that in given proofs of Theorems of Liouville and Picard, instead of hyperbolic Möbius mapping $g(z) = az + c, 0 < a < 1$, in $G(\mathbb{C})$ we could take any hyperbolic or parabolic Möbius mapping in $G(\overline{\mathbb{C}})$, which has an attractive fixed point in $\mathbb{C}$.

Remark 5.8. The results of this section are proved in [13] using Theorem 2 from [5], p. 17. In this section for the proof of Theorem Liouville and Picard we use the weaker result which is given in Theorem 4.2, and which shows that for constancy of functions on a *simply connected domain O, $O \subset \overline{\mathbb{C}}$*, the existence of *conformal automorphism of the domain O, which has a fixed attractive point $z_0 \in O$*, $z_0 \neq \infty$ is important.

6. APPLICATIONS ON MÖBIUS MAPPINGS

Here we consider some properties of elements and subgroups of the Möbius group $G(\overline{\mathbb{C}})$.

In the sequel we denote by D the unit disc, H a half plane $\overline{\mathbb{C}}$, i.e., $D = \{z \mid z \in \mathbb{C}, \ |z| < 1\}$, and $H = \{z \mid z = x + iy, \ x \in \mathbb{R}, \ y \geq 0\}$, and with ∂D and ∂H we denote the boundary of D and H, respectively.

The next Theorem follows from the proof of Theorem 5.2.1 in [7], p. 93, which will be shown:

Theorem 6.1. *A parabolic or hyperbolic Möbius mapping in group $G(\overline{\mathbb{C}})$ with invariant disc D or half plane H, has fixed points that must be on the boundary ∂D, or on the boundary ∂H, but fixed points of elliptic Möbius mappings cannot be attractive fixed points.*

The statement of 6.1 may be derived directly from Theorem *4.2*. This is shown below:

Proof of Theorem 6.1. Assume the contrary i.e., that there exists a hyperbolic element $g \in G(\overline{\mathbb{C}})$, such that at least one of its fixed points is in *D*. Then by Theorem 4.2 *g is a constant function*, but this is not so.

Therefore, a fixed point of g cannot be in *D*.

In the same way one can show that a fixed point of *g* cannot be in $\mathbb{C} \backslash D$.

In the same way it is possible to prove a statement in the case of half plane *H,* and when ∞ is a fixed point, it is clear that it belongs to the boundary ∂H.

The statement for fixed points of parabolic Möbius mappings can be proved analogously.
Since fixed points of elliptic mappings belong to *D* or *H*, it follows from Theorem 4.2 that they cannot be attractive points, otherwise then it would follow that bounded analytic functions on *D* or *H* are constants, which is impossible. This statement follows from the property that an elliptic Möbius mapping is equivalent to the Möbius mapping $g(z) = |k|z, \ |k| = 1,$ which are rotations with respect to 0. This follows from *(iii)*, of Theorem 3.2. □

Subgroup G of group $G(\overline{\mathbb{C}})$ is *discrete* if and only if for every $k > 0$ the set $\{g \in \mathcal{G} \mid \|g\| < k\}$ is finite.

The subgroup G of the group $G(\overline{\mathbb{C}})$ is *discontinuous in the point z_0* if z_0 is not in the closure of the set $\mathcal{G}(z) = \{g(z) \mid g \in \mathcal{G}\}$, for every $z \in \overline{\mathbb{C}}$. In other words, the subgroup G of the group

$G(\overline{\mathbb{C}})$ is *discontinuous in* the point z_0 if there does not exist a sequence of mutually different elements $g_n \in G$ such that for every $z \in \overline{\mathbb{C}}$ we have $g_n(z) \to z_0$, if $n \to \infty$. The group G is *discontinuous* on the set S if it is *discontinuous* in every point of the set S. The group G is *discontinuous* if it is *discontinuous* on an nonempty set.

If a subgroup G of the group $G(\overline{\mathbb{C}})$ *is discontinuous, then it is a discrete group.* The converse statement does not hold. Namely, there exists a subgroup G of the group $G(\overline{\mathbb{C}})$ which is discrete but not discontinuous. The example is the group of Picard (see [8], p. 95-103, or [10], p. 200-201).

The next Theorem shows conditions under which a discrete subgroup G of the group $G(\overline{\mathbb{C}})$ *is discontinuous* group on a domain.

Theorem 6.2. ([10], Theorem 5.5.10, p. 205). *A subgroup* G *of* $G(\overline{\mathbb{C}})$ *is discontinuous in a point* α *if and only if* G *is discrete and makes a normal family of functions in* α.

Theorem 6.2 shows that it is important to answer under which conditions a *subgroup* G of the group $G(\overline{\mathbb{C}})$ is normal, or is not normal in a point. One answer is given by the following Theorem:

Theorem 6.3. *Let a subgroup* G *of group* $G(\overline{\mathbb{C}})$ *contain a loxodromic (parabolic) element of the group* $G(\overline{\mathbb{C}})$. *Then:*

  i) *the subgroup* G *is a not normal family of functions in the fixed point of that loxodromic (parabolic) element,*

  ii) G *is not normal on any domain which contains a fixed point of a loxodromic (parabolic) element of subgroup* G. *In particular,* G *is not normal on* $\overline{\mathbb{C}}$.

Proof of Theorem 6.3. Assume that g a is loxodromic element of the group G and let z_0 be a fixed point of g. Then $G_g = \{ g^n \mid n \in \mathbb{Z} \}$ is a cyclic subgroup of the group G, and z_0 is an attractive point of g or g^{-1}. Let z_0 be an attractive point for g, without loss of generality.

For every fixed $z_1 \neq z_0$ we have

$$(1) \qquad \lim_{n \to \infty} g^n(z_1) = \lim_{n \to \infty} w_n = z_0,$$

where $w_n = g^n(z_1)$, $n \in \mathbb{N}$ (see Theorem 3.2).

Assume that the family G is a normal family of functions in the point z_0.

From the normality of family G in z_0, the normality of family $G_g = \{g^n \,|\, n \in \mathbb{Z}\}$ in z_0 follows. Since g^n, $n \in \mathbb{Z}$, is continuous on $\overline{\mathbb{C}}$, the family $G_g = \{g^n \,|\, n \in \mathbb{Z}\}$ is a normal family in z_0 if and only if there exists an neighbourhood O of z_0 on which the family $G_g = \{g^n \,|\, n \in \mathbb{Z}\}$ is equicontinuous (Theorem 4.1). It follows that for every $\varepsilon > 0$ there exists $\delta = \delta(z_0, \varepsilon) > 0$, such that for every g^n, $n \in \mathbb{Z}$, and every z for which $d(z - z_0) < \delta$ the inequality

$$\varepsilon = d(z_1 - z_0) > 0. \tag{3}$$

Then for ε given in (3) there exists $\delta > 0$ such that for every z which satisfies $d(z - z_0) < \delta$ it holds

$$d\big(g^n(z), g^n(z_0)\big) < \varepsilon, \qquad n \in \mathbb{Z}. \tag{4}$$

Since $z_1 \neq z_0$, (1) yields $\lim_{n \to \infty} g^n(z_1) = z_0$. Then there exists $N \in \mathbb{N}$ such that for every $n \geq N$ we have $d\big(g^n(z_1) - z_0\big) = d\big(g^n(z_1) - g^n(z_0)\big) < \delta$. Now having in mind (4) we obtain

$$d\big(g^{-n}\big(g^n(z_1)\big), g^{-n}\big(g^n(z_0)\big)\big) < \varepsilon, \qquad n \geq N. \tag{5}$$

From (5) we obtain $d(z_1 - z_0) < \varepsilon$, and from (3) we conclude that $\varepsilon < \varepsilon$. This is a contradiction so the subgroup G in z_0 is not a normal family of functions in z_0, so we finish the proof of part *i*).

The part *ii*) follows directly from the part *i*).

If the above proof for g we take an parabolic element of subgroup G we derive a proof for elements of parabolic type.

Theorem *4.2* yields that G is not normal on $\overline{\mathbb{C}}$. $\square$

From Theorems 6.2 and 6.3 we obtain the following:

Theorem 6.4. ([8], Lemma 5.3.3, p. 96). *Let G be a subgroup of group $G(\overline{\mathbb{C}})$ and let O be an open set on Riemann sphere $\overline{\mathbb{C}}$ which contains a fixed point of a parabolic or loxodromic element g in G. Then G does not acts discontinuously on O.*

7. Apendix: APPLICATIONS ON HARMONIC FUNCTIONS

Further, we will need the set $\overline{\mathbb{R}} = \mathbb{R} \cup \{-\infty, +\infty\}$, i.e., the extended set of real numbers which is compactified by the two points $-\infty$ and $+\infty$. For x_1, $x_2 \in \mathbb{R}$ we will denote $d_{\mathbb{R}}(x_1, x_2) = |x_1 - x_2|$ the distance on $\mathbb{R}$, but for $x_1, x_2 \in \overline{\mathbb{R}}$ we have $d_{\overline{\mathbb{R}}}(x_1, x_2) = |arctg\ x_1 - arctg\ x_2|$, $arctg\ (+\infty) = \dfrac{\pi}{2}$, $arctg\ (-\infty) = -\dfrac{\pi}{2}$, a metric on $\overline{\mathbb{R}}$. On compact subsets of $\mathbb{R}$ the metrics $d_{\mathbb{R}}(x_1, x_2)$ and $d_{\overline{\mathbb{R}}}(x_1, x_2)$ are equivalent. The extended set of real numbers $\overline{\mathbb{R}}$ with the distance $d_{\overline{\mathbb{R}}}(x_1, x_2)$ is a Hausdorff compact and complete metric space.

In the sequel we will also need the extended Arzela-Ascoli Theorem. Assume that X and Y are two compact metric spaces, let $C_{X,Y}$ be the set of all continuous functions f which map X in Y and let for $f, g \in C_{X,Y}$ $d_{X,Y}(f, g) = \sup\limits_{x \in X} d_Y(f(x), g(x))$. With d_{XY} we have the distance functions on set $C_{X,Y}$. From the convergence of the sequence (f_n) in $C_{X,Y}$ in the metric $d_{X,Y}$ follows the uniform convergence of that sequence on compact sets in X.

In the sequel we will also need the definition of equicontinuous family of functions $\Im$, $\Im \subset C_{XY}$. Namely, a family $\Im$ is equicontinuous *on* X, if for every $\varepsilon > 0$ there exists $\delta = \delta(\varepsilon) > 0$ such that for every $f \in \Im$ and all $x, y \in X$, for which $d_X(x, y) < \delta$, we have $d_Y(f(x), f(y)) < \varepsilon$.

Theorem 7.1 ([14], *a general Arzela-Ascoli Theorem*, p. 114). A set $\Im$, $\Im \subset C_{X,Y}$, is precompact, *(compact, since we have compact metric spaces X and Y), i.e., $\Im$ is a normal family of functions in $C_{X,Y}$, if and only if $\Im$ is equicontinuous set of functions on X.*

Using Theorem 6.1, and statement *iii) of* Lemma 3.3, one can show in a similar way as Theorem 4.2, the following Theorem:

Theorem 7.2. *Let g be a conformal automorphism of a simply connected domain $O \subset \mathbb{C}$ which has a fixed attractive point $z_0 \in O$, $z_0 \neq \infty$, and let $f : \mathbb{C} \to \overline{\mathbb{R}}$ be a continuous function on O. If the function f is normal on the domain O with respect to the cyclic group $G_g = \{g^n | n \in \mathbb{Z}\}$, generated by the conformal automorphism g, then f is a constant function on O.*

We will consider a harmonic function in a domain of the complex plane. A function $f : O \to \mathbb{R} \subset \overline{\mathbb{R}}$ is harmonic on a domain O, $O \subset \mathbb{C}$, if $f \in C^2(O)$ and f satisfies the Laplace

equation $\dfrac{\partial^2 f}{\partial x^2} + \dfrac{\partial^2 f}{\partial y^2} = 0$ on O. If f is harmonic on a domain O and if $\varphi : O' \to O$ is a conformal mapping of O', $O' \subset \mathbb{C}$, onto O, then a $f \circ \varphi$ is harmonic on O' (see [6]. or the [11]) .

Let $\mathcal{H} = \left\{ f \, \middle| \, f : O \to \mathbb{R} \subset \overline{\mathbb{R}} \right\}$ denote a family of harmonic functions on a domain O .

Theorema 7.3 ([10], Theorem 5.4.2, p. 185). *A locally bounded family H of harmonic functions on a domain O is a normal family on that domain.*

Theorem 7.4 (Liouville's Theorem for bounded harmonic functions). *A harmonic and bounded function on the complex plane $\mathbb{C}$ is constant on $\mathbb{C}$.*

Proof of Theorem 7.4. Let $g \in G(\mathbb{C})$, $g(z) = az + c, 0 < a < 1, c \in \mathbb{C}$. From the boundedness of the harmonic function f on $\mathbb{C}$ and Theorem 6.3 it follows that the family $\Im_f = \left\{ f \circ g^n \, \middle| \, n \in \mathbb{Z} \right\}$, is normal on $\mathbb{C}$ with respect to the group G_g . Since a harmonic function f on $\mathbb{C}$ is continuous on $\mathbb{C}$, the statement of Theorem 7.4 now follows directly from part *iii)* of Lemma 3.3 and Theorem 7.2. □

Theorem 7.5 ([10], Theorem 5.4.3, p. 185). *The family* H$^+$ *of positive harmonic functions on a domain O is normal.*

Theorem 7.6 (Liouville's Theorem for positive harmonic functions). *A positive harmonic function on the complex plane $\mathbb{C}$ is constant on $\mathbb{C}$.*

Proof of Theorem 7.6. From the conditions of Theorem 6.6 and Theorem 6.5 it follows that $\Im_f = \left\{ f \circ g^n \, \middle| \, n \in \mathbb{Z} \right\}$, $g(z) = az + c, 0 < a < 1, c \in \mathbb{C}$, is a normal family of harmonic functions on $\mathbb{C}$. Since the harmonic function f on $\mathbb{C}$ is also continuous on $\mathbb{C}$, from the part *iii)* of Lemma 3.3 and Theorem 7.2 it follows that f is a constant function on $\mathbb{C}$.□

Corollary 7.7. *If a harmonic function f in the complex plane $\mathbb{C}$ is bounded above or below then f is a constant function on $\mathbb{C}$.*

Proof of Corollary 7.7. From the condition that a function f is bounded above it follows that there exists a constant M>0 such that for every $z \in \mathbb{C}$ we have $f(z) < M$. Now the function

$\varphi(z) = M - f(z)$, $z \in \mathbb{C}$, is positive and harmonic on $\mathbb{C}$. From Theorem 7.6 it follows that φ is a constant on $\mathbb{C}$, then it follows that f is also constant on $\mathbb{C}$.

Similarly one can show that if f is bounded below on $\mathbb{C}$ then it is a constant. □

Theorem 7.8 ([10], Corollary 5.4.5, p. 186). *A family* H *of harmonic functions in a domain O which omit one specific real value* α *is normal.*

Theorem 7.9. (Picard's Theorem for harmonic functions). *A nonconstant harmonic function on the complex plane* $\mathbb{C}$ *takes every value in the set of real numbers* $\mathbb{R}$.

Proof of Theorem 7.9. Assume contrary, i.e., that there exists a nonconstant harmonic function f on the complex plane $\mathbb{C}$ which does not take all values in the set of real numbers $\mathbb{R}$. Then there exists $a \in \mathbb{R}$ such that for every $z \in \mathbb{C}$ the inequality $f(z) \neq a$ holds. Now, Theorem 7.8 yields that $\Im = \left\{ (f \circ g)(z) \mid g \in G(\mathbb{C}) \right\}$ is a normal family of harmonic functions on $\mathbb{C}$. From part *iii)* of Lemma 3.3 and Theorem 7.2 follows that the function f is constant on $\mathbb{C}$. We have reached a contradiction, therefore our Theorem is proved. □

8. CONCLUSION

In this article we show that using theory of normal family of functions and properties of fixed points of Moebius mappings one can prove classical Theorems of Liouville and little Picard Theorem for holomorphic, meromorphic and harmonic functions in a simple way. Our proofs show why in some domains of Riemann sphere one can study properties of classes of functions (for example: class of bounded holomorphic functions). Applying our result some properties of elements and subgroups of Möbius group $G(\overline{\mathbb{C}})$ can be easily verified.

It would be of interest to further investigate if the approach given in this paper concerning the Montel normality of family of functions and properties of Möbius mappings is helpful in proving some results for holomorphic, meromorphic or harmonic functions and compare the results that are known for the Bloch principle (see [10, 13,15]).

Also it would be of interest to try to apply some of our approach in the study of functions on $\mathbb{R}^2$ and functions with a domain in $\mathbb{R}^n$, $n > 2$.

Acknowledgements

REFERENCES

[1] J. Clunie and W.K. Hayman, *Symposium on Complex Analysi*s, Canterbury, (1973), London Mathematical Society Lecture Note Series 12, Cambridge University Press, Cambridge (1974).

[2] C. D. Minda, "Marden constants for Bloch and normal functions", *J. Anal. Math*. **42**, 117-127 (1982/83).

[3] P. Järvi, "On the existence of normal analytic functions", *Ann. Acad. Sci. Fenn. Ser.A I Math*., **11**, 203-206 (1986).

[4] J. Väisälä, "On normal quasiconformal functions", *Ann. Acad. Sci. Fenn. Ser. A. I.*, **266**, 33 (1959).

[5] V.L. Ahlfors, *Complex Analysis: an Introduction to the Theory of Analytic Functions of One Complex Variable*, McGraw-Hill, Inc. (1979).

[6] B.V. Shabat, *Vvedenie v kompleksnyi analiz. Chast 1*, M.: Nauka, (1985)

[7] J. Milnor, *Dynamics in One Complex Variable*, Princeton University Press, Princeton and Oxford (2006).

[8] A.F. Beardon, *The Geometry of Discrete Groups*, Springer (1995).

[9] P. Montel, *Lecons sur les Familles Normales de Functons Analytiques et leurs applica tions*, Paris, Gautnier-Villars (1927).

[10] L.J. Schiff, *Normal Families*, Springer Science + Business Media, LLC (1993).

[11] S. Axler, P. Bourdon, W. Ramey, *Harmonic Function Theory*, Springer-Verlag, New York (2001).

[12] E. Nelson, "A Proof of Liouville's Theorem", *Proc. Amer. Math. Soc*, **12**(6), 995 (1961).

[13] Ž. Pavićević, "Normal Families, Theorems of Liouville and Picard and Bloch Principle", *Math. Montis.*, **43**, 5-9 (2018).

[14] A.N. Kolmogorov, S.V. Fomin, *Elementy teorii funktsiy i funktsional'nogo analiza*, Fizmatlit (2019).

[15] Walter Bergweiler, "Bloch's Principle", *Computational Methods and Function Theory*, **6** (1), 77–108 (2006).

MONTE CARLO MODELING OF THE PHOTON-ELECTRON CASCADE IN HETEROGENEOUS MATTER

MIKHAIL B. MARKOV, ROMAN V. USKOV[*], MIKHAIL E. ZHUKOVSKIY

Keldysh Institute of Applied Mathematics of RAS (KIAM),
Miusskaya sq. 4, 125047, Moscow, Russia

*Corresponding author. E-mail: roman.uskov@gmail.com, web page: http://keldysh.ru

Summary. Algorithms of statistical simulating the processes of the photon-electron cascade transport in objects using heterogeneous computers is worked out. The processes include the generation of electron fluxes resulting in photon collisions, the appearance of photons due to bremsstrahlung and pair production. The cascade tree processing method is developed. It considers significant difference in physical properties of different particles and allows constructing the particle trajectories economically. Random photon trajectories are constructed by use of ray-tracing the whole irradiated object. Electron trajectories are created in "quasi-homogeneous" region of electron stopping path size. A weight algorithm for registration of events of low probability is constructed. The algorithm is based on the splitting the photon trajectories. Modern technologies of calculation parallelization MPI and NVidia CUDA are used. Some results of the model calculations on the hybrid calculating cluster (HCC) K100 (http://www.kiam.ru/MVS/resourses/k100.html) are represented.

1 INTRODUCTION

Mathematical modeling is an effective and powerful means for investigating the properties of modern materials of the complex structure. It is useful for developing complex experimental methods [1 - 6], as well as investigation of effectiveness and reliability of technical equipment [7]. Investigating the process of transformation of X-ray radiation into electron flux and vice versa are of interest when creating amplifier screens or developing new X-ray equipment.

Radiation transport is a cascade process involving particles of different types. Compton scattering of gamma-radiation as well as photoelectric absorption and pair production leads to emergence of rapid electrons. Rapid electrons can generate additional electrons as the result of impact ionization and photons as the result of bremsstrahlung or electron-positron annihilation. The cascade modelling is complicated by the huge number of the particles. It is mainly the result of secondary electrons generation during impart ionisation process. Another difficulty is significant difference in physical properties of different particles like penetrating ability of the photons and electrons. These abilities may differ thousand times. The number of collisions along trajectory varies greatly for the photon and electron as well.

Hybrid computing clusters (HCC) development brings new possibilities of the cascade radiation transport modelling. One is the development of the fundamental model of electrons transport [8,9] allowing detail research of electrons exposure to microstructure elements of the object being under radiation. The use of the hybrid architecture however requires specific approach to organising the calculations to achieve maximum GPU performance and proper

simultaneous CPU/GPU load [10]. Approaches for modelling of cascade processes of radiation propagation in complex objects are developed to perform calculations on heterogeneous computational equipment.

Some results of the model calculations on the hybrid calculating cluster HCC K100 (http://www.kiam.ru/MVS/resourses/k100.html) are represented.

2 MODEL OF THE RADIATION INTERACTION WITH MATTER

We consider processes of the interaction between radiation and matter when the time of changing the source strength is considerably longer than the lifetime of the particles in dense matter of the object being under radiation. In this case, the quasi-stationary integral-differential equation of the photon and electron transport are true. Time is considered as a parameter. The description of the particle state uses variables $x = (\mathrm{r}, \Omega, E)$, where r, Ω, E are coordinates, direction of motion and energy, respectively. The integro-differential equation for the density of the flow of particles $\Phi(x)$ is reduced to the Fredholm integral equation of the 2nd kind [9]:

$$\Phi(x) = \Phi_0(x) + \int_0^\infty d\xi \exp\{-\tau(\mathrm{r} - \xi\Omega)\} \int d\Omega' \int dE' \mu_s(\mathrm{r} - \xi\Omega, \Omega', E') \Phi(\mathrm{r} - \xi\Omega, \Omega', E'), \qquad (1)$$

$$\Phi_0(\mathbf{r}, \mathbf{\Omega}, E) = \int_0^\infty d\xi \exp\{-\tau(\mathbf{r} - \xi\mathbf{\Omega}, \mathbf{r}, E)\} S(\mathbf{r} - \xi\mathbf{\Omega}, \mathbf{\Omega}, E). \qquad (2)$$

Formula (2) describes the flux of undistracted particles from external and internal sources of radiation; $S(x)$ is the radiation source; $\tau(\mathbf{r}', \mathbf{r}) = \int_0^\xi \mu(\mathbf{r} - \xi'\mathbf{\Omega}) d\xi'$ is the optical distance (depth) between points $\mathbf{r}$ and $\mathbf{r}' = \mathbf{r} - \xi\mathbf{\Omega}$; μ, μ_s are the full and differential macroscopic scattering cross sections respectively.

The complicated process of particle transport through the matter can be represented by a sequence of elementary processes of the interaction between the particle and the atoms of matter (particle trajectory). These processes include the scattering, braking or disappearance of the particle due to absorption or escape from the considered system (from the object). This representation is convenient for modelling the radiation transport by the Monte-Carlo method. In doing this, the considered transport equation is converted to the form:

$$Q(x) = Q_1(x) + \int_0^\infty d\xi \cdot \exp\{-\tau(\mathbf{r} - \xi\mathbf{\Omega}, \mathbf{r}, E)\} \int d\mathbf{\Omega}' \int dE' \mu_s(\mathbf{r}, \mathbf{\Omega}', \mathbf{\Omega}, E', E) \frac{\mu(x)}{\mu(x')} Q(x'). \qquad (3)$$

In formula (3) variable $Q(x) = \mu(x)\Phi(x)$ is the density of collisions and $Q_1(x) = \mu(x)\Phi_0(x)$ is the density of the first collisions. The kernel of the integral operator $k = \exp\{-\tau(\mathbf{r} - \xi\mathbf{\Omega}, \mathbf{r}, E)\} \mu_s(\mathbf{r}, \mathbf{\Omega}', \mathbf{\Omega}, E', E) \frac{\mu(x)}{\mu(x')}$ has the meaning of probability density of $x' \to x$ transition.

The transport of the particles accompanied by the birth of secondary particles in cascade processes of the interaction of radiation with matter (for example, the birth of electrons during Compton scattering, photo-absorption of X-ray or gamma radiation, pair production) is described by a system of integral equations. The following chain can be an example of such a process: gamma-radiation–Compton and photo electrons–electrons deceleration–X-ray radiation (bremsstrahlung).

The objective of the radiation transport theory is to compute the readings of detector J located in the field of radiation. The desired (measured) values are presented as the readings of some detector and are written as functional on the space of the transport equation solutions.

$$J = \int Q(x)D(x)dx,$$

$D(x)$ is determined by the type of the desired (measured) value. We consider such registering facilities (detectors) whose readings J are equal to the sum of the contributions of some particle's collisions in a sensitive volume of the detector (additive detectors). To evaluate the desired measured value by the Monte Carlo method, the random trajectories of the particles are simulated. The contributions of these trajectories to the detector's measurable value are summed up. The particle trajectory construction is performed according to the chosen physical model of the interaction between the radiation and matter.

The basic quantitative data of the transport model are the probability distributions of the particle's interactions with matter. These distributions are built by processing the cross sections (differential cross sections) of the corresponding interaction processes [8]. The main source of these data is the database of the National Centre of Nucleic Data (http://www.nndc.bnl.gov/sigma/).

2.1 Model of the interaction of electrons with matter

The following processes of the interaction of electrons with matter are considered:
- elastic scattering on atoms of matter leading to the deviation of an electron from its initial direction of motion;
- excitation of atoms accompanied by small losses of electron energy;
- ionization collisions or collision ionization (electro ionization) with the appearance of the secondary electron;
- electron slowing down in the Coulomb field of an atom results in generating the bremsstrahlung photon;
- electron-positron annihilation.

The generally accepted schemes of transport modelling are based on various modifications of the imbedded trajectories model (ETRAN [11], ITS3 [12], EGS4 [13], GEANT4 [14]). The electron scattering of electrons is usually described within the Goudsmit-Saunderson theory of multiple scattering [15]. Inelastic interactions of electrons with matter are described by various modifications of the approximation of continuous slowing down in most works. Fluctuations of the energy losses are accounted for by the Landau theory [16] using the Blunck and S. Leisegang corrections [17].

The implementation of these schemes for modelling electron transport on hybrid computing equipment is inefficient due to the complex internal logic of the schemes and the need to use iterative procedures in some cases.

Simulating the trajectories of electrons carried out using the probability distributions of the characteristics of electrons [8] without the use of the mentioned widespread approximations in this work.

2.2 Model of the interaction of photon radiation with matter

Interaction model of gamma rays and x-rays includes the following processes:
- coherent (Rayleigh) scattering;
- incoherent (Compton) scattering;
- photo absorption of quanta (photoionization of atoms);
- pair production.

Coherent scattering is the interaction process with a bound atomic electron without energy loss. The scattering results in the direction of the photon's movement changes. The cross section of this process is described by the Thompson formula subject to the relativistic form factor [18].

The Compton scattering of the photon on the free quiescent electron is described by the differential Klein-Nishina cross section and the electron connectedness in the atom is taken into consideration by the introduction of the scattering function [18].

The process of photoionization is the ionization of an atom by knocking the electron out of the atomic shell. An electron absorbs a photon and acquires its kinetic energy after subtracting the binding energy of an electron in an atom.

The interaction of a gamma-quant with an atom may lead to electron-positron pair production. The total cross section of this process is tabulated for instance, in [18]. Differential cross sections of the pair production are taken from [14, 19, 20].

3 THE PHOTON-ELECTRON CASCADE TRANSPORT MODELING

An efficient algorithm for simulation of the cascade and its implementation require the solution of several problems:
- constructing the effective discrete geometrical model to minimize the cost of approximating complex objects;
- using the individual computational algorithms for each type of particle considering their physical properties;
- maximizing the statistical value of every trajectory for decreasing the computational cost.

3.1 Geometrical model

Modelling of radiation transport by use of the Monte Carlo method requires building huge number of particles random trajectories. Segments of intersection with different homogeneous parts of an object are all the information needed to construct trajectory chain from geometrical point of view. The interaction point and the type of the interaction are played along constructed set of the intervals by use of the probability distributions associated. The process keeps going until the particle "dies". Quasi-stationary gives possibility to get rid of grids of any kind. The most minimalistic and unified approach setting up geometrical model is to describe everything by surfaces. Parts of an object are described by closed bounding surfaces. The detection areas are either closed surfaces for volume-based measurements (density of energy deposit) or general surfaces for surface-based measurements (particles flux density).

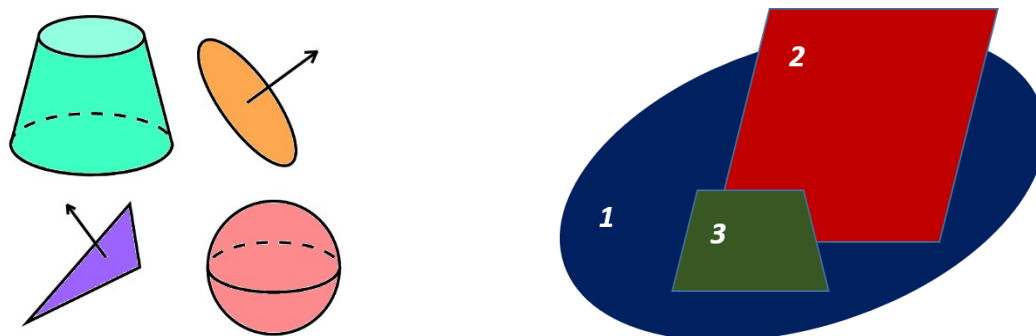Areas of interest (see below) are described by its bounding surfaces as well.

Fig. 1. Supported primitives – left; layers displacement – right

Surfaces consist of various types of "primitives". Currently supported are triangle, circle, sphere and frustum (Fig.1, left). The operation on the primitives are:
- getting coordinates of intersection between given ray along the particle motion direction and primitive;
- determining the distance from given point to primitive;
- testing the intersection between given line segment and the primitive.

Every surface is associated numbered "layer". It determines the molecular composition and density of a matter. The layers with larger numbers displace ones with smaller numbers if they occupy the same space (Fig. 1, right).

3.2 Photons trajectories simulation

Photons are characterized by relatively small number of collisions along trajectory and high penetrating ability. The construction of its trajectory includes object tracing and playing the interaction. The whole scheme is shown on fig. 2. It consists of the following steps:
- Intersections with the surfaces bounding the homogeneous components of the object are found. This is done by GPU;
- Intersection segments are formed using the points of the surface intersections;
- Interaction point is played on a set of intersection intervals (segments). The probability distributions of processes in corresponding material are loaded;
- Type of the interaction is played basing on loaded probability distributions. Photon properties are adjusted basing on played interaction. Additional particles that may appear due to interaction are stored for later simulation.
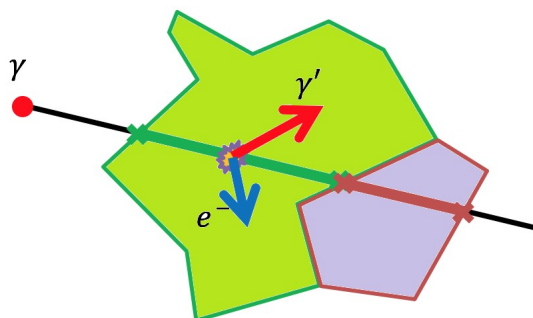
Fig. 2. Photon trajectory chain construction

The process repeats until trajectory ends. The approach is pretty much straightforward and efficient for this type of particle.

3.3 Electron trajectories simulation

Interactions between electron and matter are much different to photons. The number of collisions along trajectory is huge while penetrating ability is very low. The whole trajectory usually lays in small area inside an object. Straightforward approach used for photons is very excessive as full object tracing is barely needed at every step of the electron trajectory. Therefore, quasihomogeneous approach is used for electrons. Electron trajectory is built by large segments laying in homogeneous parts of an object. Those segments can contain hundreds to thousands of interactions. Even the whole trajectory. General scheme of electron trajectory segment construction is described below. Process starts with determining the layer in which the electron is located. Continuous slowdown approximation (CSDA) range of the electron in a current layer is calculated. CSDA range is a value showing the average length of electron trajectory until thermalization. The big circle on fig. 3 limits the area inside CSDA range of a particle. This is the area that particle will unlikely to leave. Defining the area that particle will likely to stay in allows ignoring the geometrical model outside this area for this electron. Surface elements outside CSDA range of a particle are filtered out – grayed out elements shown on fig. 3. Distance to the element from the original electron location is kept for elements that are inside of CSDA range. Elements are also sorted by this value ascending.
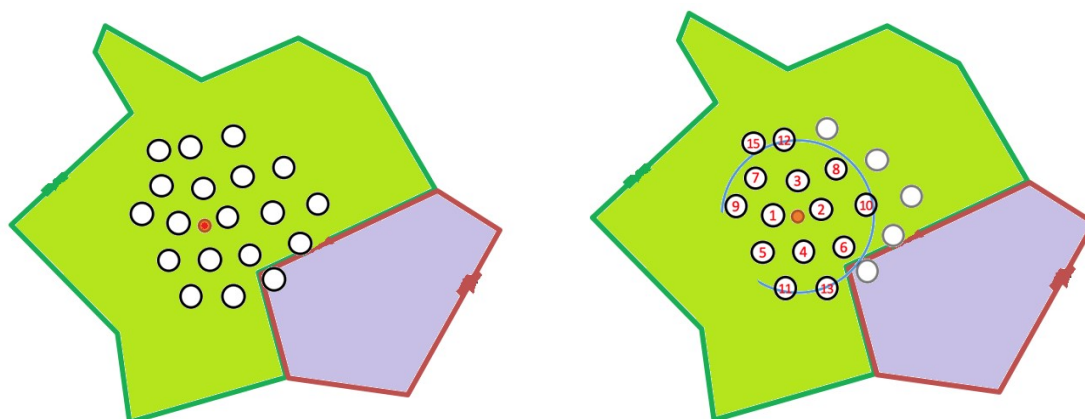
Fig. 3. Filtering out nearby primitives and sorting by distance

Trajectory segment construction is done very fast on GPU. Current distance L to the original point where trajectory segment started is calculated every time particle position changes. Intersection checks are performed starting from closest elements to farthest and stops when distance to the next elements exceeds L. This keeps geometry checks minimal. On the right-side fig. 4 shows how determining the distance L during trajectory construction allows to ignore even more of filtered (on the left side) elements.

Setting up very complex geometries and very high radiation energies may lead to situations when the number of the elements inside of CSDA range exceeds maximum. Filtering range is then decreased from CSDA range to something smaller that fits required number of elements. Decreasing filtering range increases the probability for particle to leave filtered area but keeps number of filtered elements relatively small.

The way trajectory intersection with an element is handled depends on the type of surface being intersected. Intersection with detector is simply recorded (position, direction, energy, weight etc.) to be processed on CPU later. Crossing the boundary of an object means that an electron can move to another layer. The CSDA range will change in this case. The trajectory segment construction ends at this point. Another stop-criteria for trajectory segment construction is reaching minimal energy supported by the software. Electron reaching this energy is considered thermalized. Last stop-criteria is electron leaving the area limited by CSDA range.
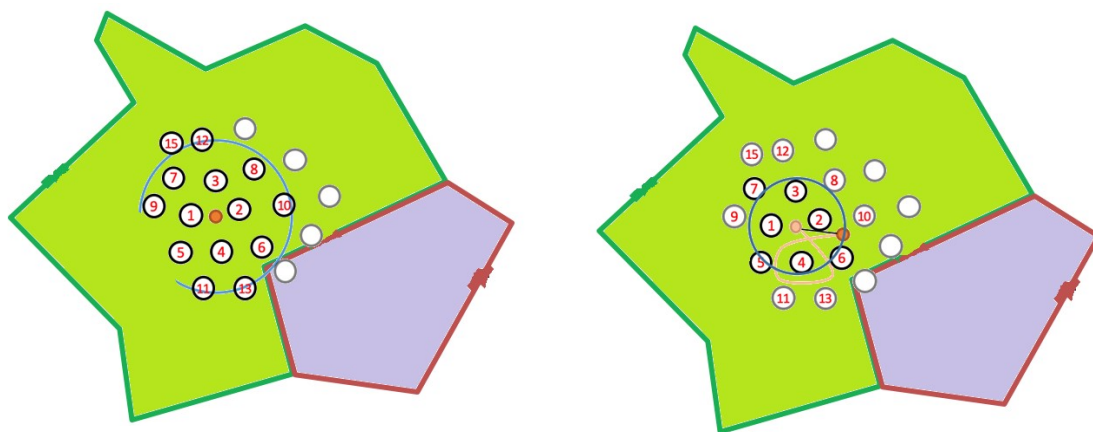

Fig. 4. Geometrical checks during electron trajectory simulation

Once trajectory segment construction ends all accumulated data is sent back to CPU. Data includes changed particle properties (position, direction, energy, weight etc.), detectors intersection history and newly born particles (impact ionization electrons and bremsstrahlung photons). These particles are saved for later modelling. Detector intersections are properly registered and whole process repeats for the electron.

3.4 Algorithm for registration of improbable events

Maximizing statistical value of the particle trajectory is very important when desired value

is contributed by improbable events. Statistical evaluating the flux of emitting electrons from the surface of a plate irradiated by X-ray or evaluating the energy deposit in lightweight bremsstrahlung detector behind heavy target irradiated by electrons are both good examples of the problem.

Some portion of photons fly through the plate leaving no contribution in desired value at all in first example. The number of such photons depends on radiation energy, material and thickness of the plate. Problems of such a kind are usually solved by letting photon always interact with an object correspondingly decreasing its statistical weight. Unfortunately, only photons interacting in close proximity to surface can generate electron being able to emit. So, the most of modelled photon interactions will have zero statistical value.

In second example photon must interact with detector to contribute to energy deposit. Most of generated bremsstrahlung interacts with target rather than detector and gives no statistical contribution in detector.

General approach to solving the problems is developed. The main idea is introducing special "areas of interest" – volumes around detectors involving the electron registration (energy deposit, electron flux, current, charge). These volumes are described by bounding surfaces and naturally fit in developed geometrical model. Photon intersecting such area is split into several parts having corresponding statistical weights. Some of these parts interacts explicitly within area of interest. This allows electrons being explicitly born within proximity to detector significantly increasing statistical value of photon trajectory.
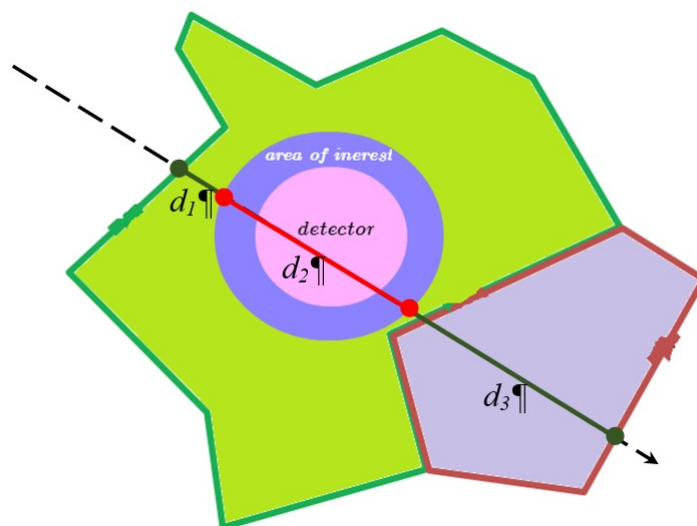

Fig. 5. Photons trajectory split

Fig. 5 shows an example of the photon trajectory intersecting area of interest inside an object. The photon trajectory inside the object consists of three intervals. First and third intervals are the outside the area of interest. Second one is intersection interval lays in the area of interest. The probabilities of photon to interact on these intervals are:

$$P_1 = 1 - e^{-\mu d_1}; \quad P_2 = e^{-\mu d_1} \cdot (1 - e^{-\mu d_2}); \quad P_3 = e^{-\mu(d_1 + d_2)} \cdot (1 - e^{-\mu d_3}),$$

where d_1, d_2 and d_3 are lengths of intervals, μ full macroscopic cross section. In this case the trajectory is split in three parts (Fig. 5). Statistical weights are:

$$w_1 = w_0 \cdot P_1; \quad w_2 = w_0 \cdot P_2; \quad w_3 = w_0 \cdot P_3,$$

where w_0 is initial weight of the photon. Thus, splitting trajectory allows electron to explicitly appear within area of interest. This electron will likely intersect detector contributing the statistical value. Trajectory splitting works the same way in case of intersections with multiple areas of interest.

4 AN EXAMPLE OF COMPUTATION

Interaction of radiation with matter is a cascade process. Radiation transport is accompanied by radiation-induced effects. Supercomputer simulation of radiation-induced charge effects in heterogeneous polydisperse materials is of interest in the investigation of their properties.

Some results of the modeling of the charge effects generated by X-ray radiation presented in this section.

Let us consider a fragment of a dispersed structure in the form of a cubic object with a side of 30 microns, in which polybutadiene is used as a binder, and an aluminum or dielectric ball with a diameter of 20 microns is an inclusion.

The fragment irradiated by photons of 20 keV energy is depicted in Fig. 6. Red and blue balls are detectors for evaluating the charge density during simulation by Monte Carlo method.
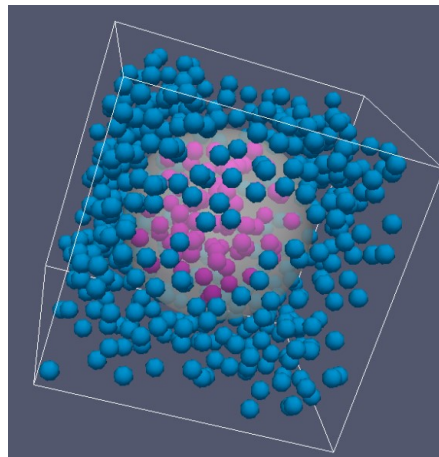

Fig. 6. Fragment of a dispersed structure with a detector system. Red balls are in the inclusion

The results of the calculation of the spatial distribution of the charge are presented below.

We note the common for both the inclusion regularities of the formation of radiation-induced charge effects.
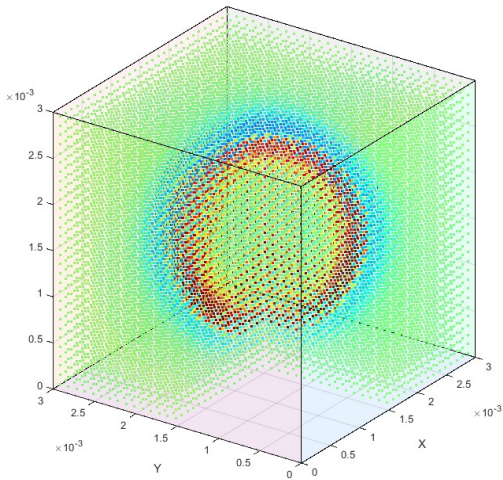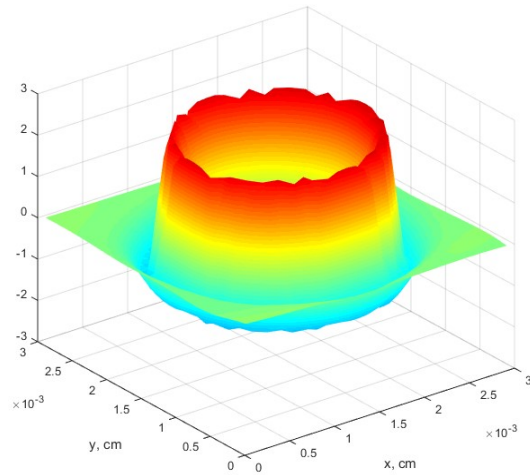
Fig. 7. 3D image of charge density distribution

Fig. 8. Charge distribution in the plane perpendicular to the z axis through the center of inclusion

The Central inner part of the inclusion and the periphery of the binder are weakly charged due to the small path of electrons and, therefore, the local electronic equilibrium in these areas (Fig. 7, 8, green color).

A positive charge (red color) is formed in the inner boundary region of the inclusion due to the predominance of the electron departure from the inclusion to the binder over the reverse process. A negative charge (blue color) is formed in the binder near the inclusion due to the transfer of electrons from the inclusion into the binder.

The charge distribution along the straight line $x=y=15\ mkm$ is presented in Fig. 9,10. The boundaries of inclusions are marked with black dashed lines.
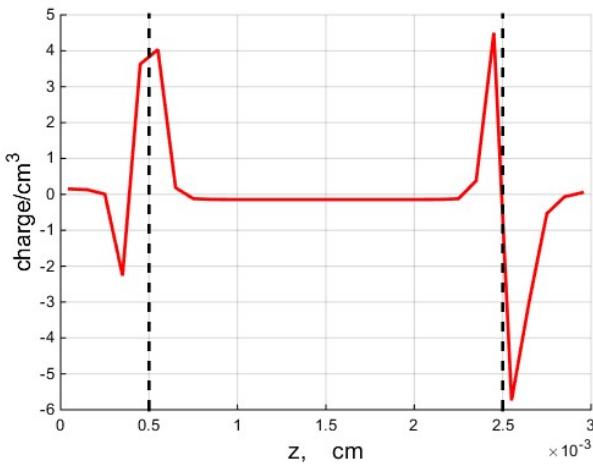

Fig. 9. The charge distribution in the fragment with aluminum inclusion
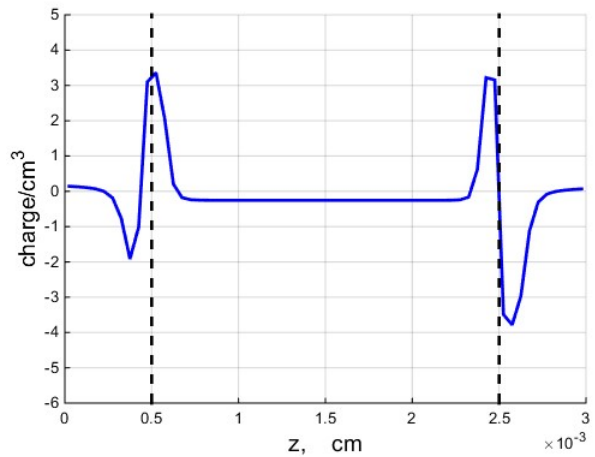
Fig. 10. The charge distribution in the fragment with dielectric inclusion

The graphs in Fig. 9,10 show sharply inhomogeneous spatial structure of the charge distribution generated by the interaction between radiation and dispersed structures. The

inhomogeneities occur near the boundary surfaces of the binder and inclusions.

5   CONCLUSION

Effective statistical algorithms of the mathematical simulating the cascade processes of radiation transport have been developed by hybrid calculation procedures. These algorithms consider significant difference in physical properties of different particles and propose effective approaches to trajectory construction. Weight modifications of Monte-Carlo method significantly increasing the statistical value of random particle trajectories are built. Software is developed considering the features of the performed calculations on heterogeneous super-computers by use of graphic accelerators as arithmetic co-processor. The performed model calculations illustrate the efficiency of the proposed method of modelling of cascade processes on computation facilities with a hybrid architecture.

REFERENCES

[1] *Nerazrushaiushchii kontrol. Rossiia*. 1990-2000, Spravochnik, V.V.Kliuev (Ed.), Mashinostroenie (2001).

[2] V.I. Mazhukin, V.V. Nosov. U. Semmler, "Issledovanie teplovykh i termouprugikh polei v poluprovodnikakh pri impulsnoi obrabotke", *Matematicheskoe modelirovanie*, **12** (2), 75–83 (2000).

[3] K.K. Inozemtseva, M.B. Markov, F.N. Voronin, "The electromagnetic and thermomechanical effects of electron beam on the solid barrier", *Mathematica Montisnigri*, **39**, 79-100 (2017).

[4] *Ionizing radiation effects in MOS devices & circuit*, T.P. Ma and P.V. Dressendorfer (Eds.), John Wiley and Sons (1989).

[5] M.A. Trapeznikova, N.G. Churbanova and A.A. Lyupa, "Simulation of three-phase fluid flow in a porous medium with account of thermal effects", *Mathematica Montisnigri*, **33**, 105-115 (2015).

[6] A.V. Utkin, "Analysis of parallelmolecular dynamics for MPI, CUDA and CUDA-MPI implementation", *Mathematica Montisnigri*, **39**, 101-109 (2017).

[7] D.M. Ivashchenko, A.A. Fedorov, "Rossiiskie uskoriteli elektronov, ispolzuiushchiesia v kachestve modeliruiushchikh ustanovok", *Voprosy atomnoi nauki i tekhniki, seriia «Fizika radiatsionnogo vozdeistviia na radioelektronnuiu apparaturu»*, **3**, 120-128 (2002).

[8] M. E. Zhukovskiy, S. V. Podolyako, and R. V. Uskov, "Model of individual collisions for description of electron transport in matter," *Math. Models Comput. Simul*., **4** (1), 101–109 (2012).

[9] M. E. Zhukovskiy and R. V. Uskov, "Modelirovanie vzaimodeistviia gamma-izlucheniia s veshchestvom na gibridnykh kompiuterakh", *Matematicheskoe modelirovanie*, **23** (7), 20–32 (2011).

[10] M. E. Zhukovskiy and R. V. Uskov, "Matematicheskoe modelirovanie radiatsionnoi elektronnoi emissii na gibridnykh superkompiuterakh", *Vychislitelnye Metody i Programmirovanie*, **13** (1), 271–279 (2012).

[11] https://link.springer.com/chapter/10.1007/978-1-4613-1059-4_7 (accessed October 22, 2019).

[12] J. A. Halbleib, R. P. Kensek, T. A. Mehlhom, G. D. Valdez, S. M. Seltzer and M. J. Berger, "ITS version 3.0: the integrated TIGER series of coupled electron/photon Monte Carlo transport codes", *Report SAND91–1634*, Sandia National Laboratories, Albuquerque, NM (1992).

[13] W. R. Nelson, Í. Hirayama and D. W. O. Rogers, "The EGS4 Code System", *Report SLAC_265*, Stanford Linear Accelerator Center, Stanford, CA (1985).

[14] http://geant4-userdoc.web.cern.ch/geant4-userdoc/UsersGuides/PhysicsReferenceManual/html/index.html (accessed October 22, 2019).

[15] S. Goudsmit and J. L. Saunderson, "Multiple scattering of electrons", *Phys. Rev.*, **57**, 24–29 (1940).

[16] L.D. Landau, "On the Energy Loss of Fast Particles by Ionization", *J. Phys.*, **8** (4), 201-205 (1944).

[17] O. Blunck and S. Leisegang, "Zum Energieverlust schneller Elektronen in duennen Schichten", *Zeitschrift für Physik,* **128** (4), 500–505 (1950).

[18] https://www.nndc.bnl.gov/sigma/index.jsp?as=28&lib=endfb7.1&nsub=10010 (accessed October 22, 2019).

[19] https://oecd-nea.org/science/docs/2011/nsc-doc2011-5 (accessed October 22, 2019).

[20] https://mcnp.lanl.gov/ (accessed October 22, 2019).

[21] M. E. Zhukovskiy, S. V. Podolyako, and R. V. Uskov, "Modelirovanie perenosa elektronov v veshchestve na gibridnykh vychislitelnykh sistemakh", *Vychislitelnye Metody i Programmirovanie,* **12** (1), 152–159 (2011).

ATOMISTIC MODELING OF THE CRITICAL REGION OF COPPER USING A LIQUID-VAPOR COEXISTENCE CURVE

M.M. DEMIN, O.N. KOROLEVA[*], A.V. SHAPRANOV, A.A. ALEKSASHKINA

Keldysh Institute of Applied Mathematics of RAS, Russia, Moscow

* Corresponding author. E-mail: koroleva.on@mail.ru

Summary. A liquid – vapor coexistence curve was obtained for copper by the method of molecular dynamics modeling (MDM), and the corresponding critical parameters were determined: temperature, density, and pressure. The interaction potential of particles was of the "embedded atom" type (EAM). The critical temperature T_{cr} was determined from the MDM results using the average cluster size method in the critical region. To clarify the critical density value, the empirical rule of rectilinear diameter was used. The results of modeling of this work were compared with the results of evaluating of the critical parameters of copper by other authors using different approaches.

1 INTRODUCTION

Studying the properties of metals in the vicinity of a critical point is a very important but difficult task. The critical point parameters are the most important characteristics of a substance [1], which in a generalized quantitative form express the effect of the action of intermolecular forces. Of particular interest is the boundary curve (binodal), which is the line of phase equilibrium of the liquid and gaseous phases and separates the homogeneous states of matter from two-phase metastable states. The metastable states of superheated liquid and saturated vapor have been studied relatively little [2]. Meanwhile, knowledge of the properties of superheated liquid and saturated vapor is required to calculate many practical problems [3]. In particular, the properties of the superheated liquid significantly affect the nature of the boiling of the liquid, and the properties of the supersaturated vapor determine the condensation process [4]. At the critical point, unlike other points of the boundary curve, the properties of both phases (liquid, vapor) are identical, that is, the critical state is the same limiting physical state of the substance for the both phases.

When approaching the critical point, the properties of a substance change, as new phenomena and mechanisms of interaction of particles of the substance appear, such as the fluctuations in the parameters of the substance (primarily density), the value of which grows very rapidly when approaching the critical point and tends to infinity at the critical point itself. In such a situation, consideration of the critical state on the basis of a theoretical approach using thermodynamic functions is applicable only in the region where fluctuations are relatively small [5].

The possibilities of experimental research are also limited. Due to the difficulty of conducting experiments at high temperatures, the critical point and binodal parameters were obtained only for a small amount of substances, which include alkali metals and mercury, which have relatively low temperature characteristics [6-11]. For other materials, there are

only theoretical estimates within the framework of various models, among which phenomenological methods [12-24] and atomistic modeling methods [25-31] stand out.

The empirical relations connecting the parameters of the critical point with various characteristics of the substance in the liquid and gas state are widely used. These include the methods based on similarity laws connecting characteristic lines (for example, Zeno-line — the unit compressibility line) of gases and liquids with critical parameters have also gained widespread popularity [14–17, 21,24] and the method of rectilinear diameter [5], estimates of critical parameters based on the relationship of metal vapors with the ionization potential of atoms [12], among these relations there is also the Kopp-Lang rule [13], which relates the critical temperature to the energy of evaporation. Estimates obtained from semiempirical equations of state are also widely used [20,22, 23]. In [18], a method was proposed for calculating the parameters of critical points and the binodal of a vapor – liquid (dielectric – metal) transition in metal vapors. The model is based on the assumption that cohesion, which determines the basic characteristics of metals under normal conditions, is also responsible for the properties of metals in the vicinity of the critical point.

An important tool in the modeling of the properties of substances and physical processes inaccessible to direct measurement was mathematical modeling based on atomistic models. The atomistic approach is represented by Monte Carlo [19,29,30,31] and molecular dynamics [25-28] methods. Within the framework of the Monte Carlo method, to determine the critical parameters of metals and nonmetallic substances, the Wang – Landau (EWL) approach [29].

Mathematical modeling based on the molecular dynamics method over the past two decades has become a powerful tool for fundamental research of properties [25-27] and processes [28] in materials.

Despite the large number of estimated theoretical approaches, the obtained values of the critical parameters and binodal of copper have large differences. For example, in [29, 30] the critical parameters of copper were obtained from molecular dynamics simulations with the same potential (EAM), but using different techniques. The results obtained in these works for the critical temperature differ by 1.27 times. Despite the complexity of both theoretical and experimental approaches, interest in research in this area persists.

The aim of this work is to obtain a liquid – vapor coexistence curve for copper and determine the corresponding critical parameters: temperature, density, and pressure using molecular dynamics simulations with the EAM interaction potential [32]. This potential was previously tested and used to describe the processes in solid and liquid copper in the melting region in [33]. The calculations were performed using the LAMMPS package [34]

2 STATEMENT OF THE PROBLEM

2.1 Mathematical formulation of the problem

The molecular dynamics method is based on the representation of the considered object as a set of particles for which the Newton's equations are written. For each particle, the mass m_i, velocity v_i, and radius vector r_i are considered. This results in a system of 2N ordinary differential equations (ODE)

$$\begin{cases} m_i \dfrac{d\vec{v}_i}{dt} = \vec{F}_i + F_i^{ext} \\ \dfrac{d\vec{r}_i}{dt} = \vec{v}_i \end{cases} \quad , \ i = 1..N \quad (1)$$

where $\vec{F}_i = -\dfrac{\partial U(\vec{r}_1..\vec{r}_N)}{\partial \vec{r}_i}$ is the force of the interaction between the particles, $\vec{F}_i^{ext}$ is the force of interaction with the external fields, $U(\vec{r}_1,..., \vec{r}_N)$ is the potential energy of the system of N particles.

2.2 Initial and boundary conditions

At the initial moment of time, the object under consideration is a crystal at the temperature T. The particle velocities at the initial moment are set as random variables corresponding to the Maxwell distribution at twice the temperature $2T$. Before the simulation starts, such an object is equilibrated with the thermostat [35] and barostat [36] turned on, and quite quickly part of the kinetic energy goes into potential one, and the temperature becomes T, and the pressure is set to $P = 0$.

As boundary conditions, the periodic conditions are used. Under the periodic boundary conditions with respect to Ox, it is believed that a particle exiting through the right boundary is replaced by a particle having the same velocity but entering through the left boundary.

Subsequently, the ODE system (1) is solved using the Verlet finite-difference scheme [37]. In this method, the coordinates of the particles are calculated on the integer time layers, and the velocity on half-integer ones.

2.3 Particle interaction potential

The accuracy of the results of molecular dynamics modeling substantially depends on the used particle interaction potential. Since the 1980s, the potentials of the "embedded atom" family (EAM) have become widespread for metals. To determine the branches of the liquid – vapor coexistence curve and critical parameters of copper in this work, we used the EAM1 potential, which is a modification of the potential from this family, developed and tested on copper in [32]. The potential of EAM1 is based on both experimental and ab initio data. The results of testing of the potential on copper showed its reliability and good agreement with the experimental data.

3   RESULTS AND DISCUSSION

The computational domain was chosen in the form of a parallelepiped with sizes of $32\times15\times15$ unit cells of copper, which corresponds to a size of $11.568\times5.4225\times5.4225$ nm^3. This domain contains 29,250 particles. Periodic boundary conditions were set along all three axes. The dimensions of the region in which the sample is located are larger along the x axis than the dimensions of the sample. On this axis, the size occupied by the atoms of the sample were 11 nm, and the size of the entire region was assumed to be 55 nm. The selection of the size of the region was given special attention. Through some preliminary calculations, the

sizes were determined so that the liquid – vapor boundary did not disappear as a result of evaporation before the time it reached the critical temperature. And vice versa, so that the entire area is not prematurely filled with an expanded fluid.

3.1 Formation of the binodal branches

The sample was heated using a thermostat by changing the current temperature T by $\varDelta T$. Relatively fast heating to a temperature of 4500 K in 100 ps using a thermostat was carried out at zero pressure, supported by the switched-on barostat. This heating mode was maintained up to 5000K. After reaching 5000K, the barostat was turned off, since in the near-critical region it can no longer maintain zero pressure. For this reason, the heating of the sample, by decreasing $\varDelta T$, was slowed down, compared with heating with the barostat turned on, in order to avoid rupture of the liquid region. So, if, using the Berendsen thermostat, heating, starting from the temperature $T = 4500$ K, was carried out with $\varDelta T = 500$ K, with $T = 5000$ K the $\varDelta T$ value decreased to 250 K, and with $T = 6000$ K $\varDelta T$ decreased to 100 K.

The binodal branches were formed according to the results of MDM by averaging the density over time and space. In all calculations, after each temperature change, the system remained unchanged for a time $t = 1$ ns. During this time, the density was averaged over time. Density was also averaged over space. We represent this procedure in the following example. Figure 1 shows the spatial density distributions of copper at two temperatures averaged at 6100K and 6600K.
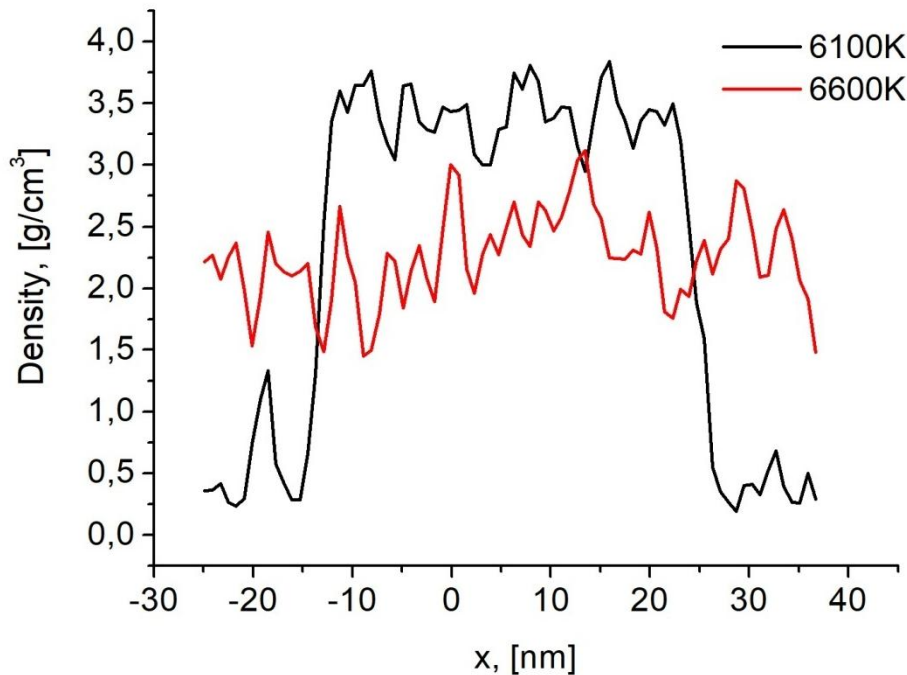

Fig. 1. The spatial distribution of the density of copper averaged over time.

The graph shows that for the temperature of 6100 K, two spatial ranges $x_1 \in \left(-25, -15\right)$ nm and $x_2 \in \left(-10, 25\right)$ nm are clearly distinguished, in which fluctuations around two different density values are noted. In each of these ranges, the coordinate x was chosen in the middle

where density was averaged over time. In the first range $x1$, the average density $\bar{\rho}_1 = 0.397$ g/cm^3 was obtained, and in the second range x_2, the average density $\bar{\rho}_2 = 3.5$ g/cm^3. Both density values correspond to the same temperature. The first value belongs to the liquid branch, and the second to the vapor branch of the binodal at the temperature of 6100K. On the curve corresponding to the density of copper at the temperature of 6600 K (Fig. 1), the oscillations occur around one average value of $\bar{\rho} \approx 2.25$ g/cm3, which indicates an approximate equality of the density of the liquid and vapor of copper in this region, as well as the proximity of the indicated temperature of the substance ($T = 6600$K) to the critical temperature.

3.2 Critical density ρ_{cr}

The branches of the liquid-vapor phase equilibrium curve obtained by similar averaging were deposited on the ρ - T plane (Fig. 2.). However, due to fluctuations, determining the exact value of the critical density is difficult. To clarify the value of the critical density, the rule of the rectilinear diameter is usually used [5]

$$\rho_L + \rho_v = 2\rho_{cr} + \lambda(T_{cr} - T) \qquad (2)$$

where ρ_L in the density of liquid at the temperature T, ρ_v is the density of saturated vapor in equilibrium with the liquid phase at the same temperature. The coefficient λ is different for different substances and is close to 1. At $T \approx T_{cr}$ the rule of the rectilinear diameter has the form:

$$\rho_{cr} \approx \frac{\rho_L + \rho_v}{2} \qquad (3)$$

The name "rectilinear diameter", is determined by the fact that in the coordinates ρ - T the diameter of the curve $\rho(T)$ is a straight line. To draw the straight line, two points $D_1(T_1, \rho_{Lv1})$ and $D_2(T2, \rho_{Lv2})$ are enough, the ordinates of which are the values calculated by formula (3) at a certain temperature. As the first point, the binodal values are selected, at a maximum temperature $T_1 = 6400$ K, which still allows the determination of density. For the temperature $T_1 = 6400$K, the ordinate is calculated by formula (3) using the values of $\rho_L(6400)$ and $\rho_v(6400)$. To determine the second point $D_2(T_2, \rho_{Lv2})$ of the rectilinear diameter, one can choose any of the values $T < T_1$ and a pair of densities of the liquid and vapor branches of the binodal corresponding to this temperature. In total, five options were calculated for determining the coordinates of the second point, and five options were constructed for lines of rectilinear diameter passing through the point $D_1(6400; \rho (6400))$ and, therefore, five density values $\rho_{cr,i}$ (i = 0, ..4) can be obtained at the temperature T_{cr}, which has not yet been determined.

In fig. 2 rectilinear diameter options are shown with colored dashed lines.

The density value at the known value of $T = T_{cr}$ can be determined as the average

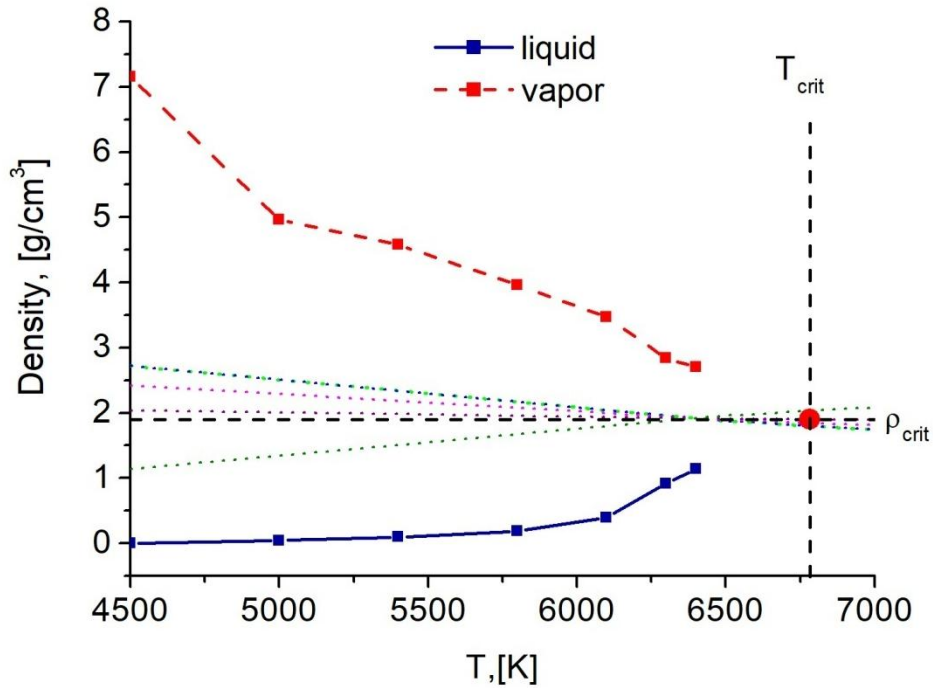$$\rho_{cr} = \sum_i \rho_{cr,i} \Big/ 5 . \qquad (4)$$

Fig.2. Binodal of copper.

3.3 Critical temperature T_{cr}

To obtain the critical density, it was necessary to determine the critical temperature T_{cr}, for which we used the method of the average cluster size in the critical region [38]. The essence of the method is as follows. In the subcritical region, with increasing temperature, the density and pressure of saturated vapor increase. In the near-critical region, atomic vapor particles begin to unite into clusters, which reach maximum sizes just at the critical point. With a further increase in temperature, the density no longer grows. Moreover, due to an increase in the kinetic energy of chaotic motion, the clusters begin to break up into smaller ones. Thus, the average cluster size must have a singularity at the critical point. This fact is used in this method to determine the critical temperature.

The average number of atomic particles forming a cluster can be estimated by the formula

$$\langle N \rangle = \frac{n(T) k_B T}{P_v(T)} , \qquad (5)$$

where $P_v(T)$ is the pressure of the saturated vapor at the given temperature T, $n(T)$ is the concentration of atomic particles in saturated vapor.

The temperature dependence of the average cluster size is shown in Fig. 3. The temperature plot has a characteristic kink at a critical point. Thus, using the average cluster size method, the critical temperature $T_{cr} \approx 6550$ K was found. After that, the critical density $\rho_{cr} \approx 1.895$ g/cm^3 was determined from (4).
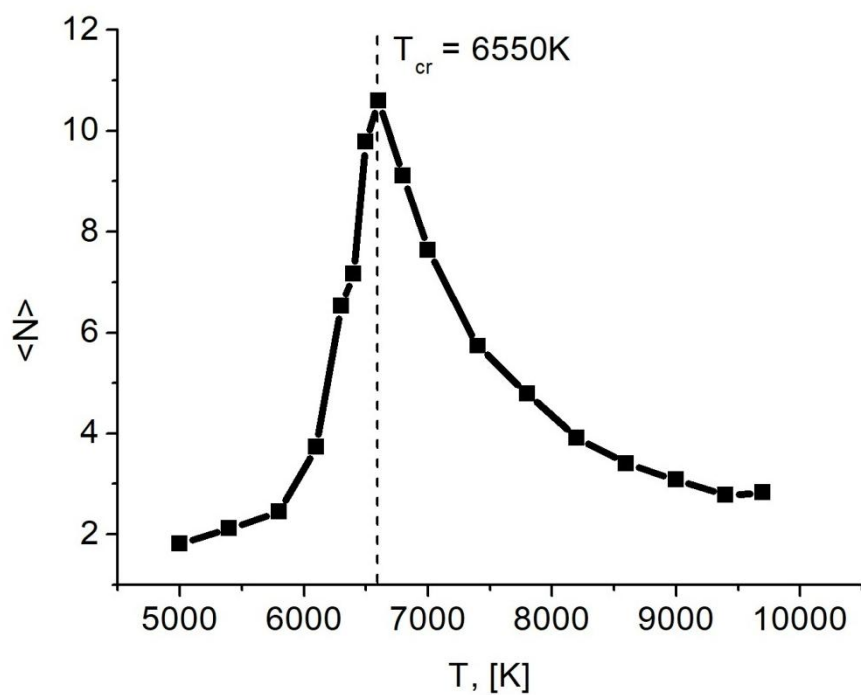
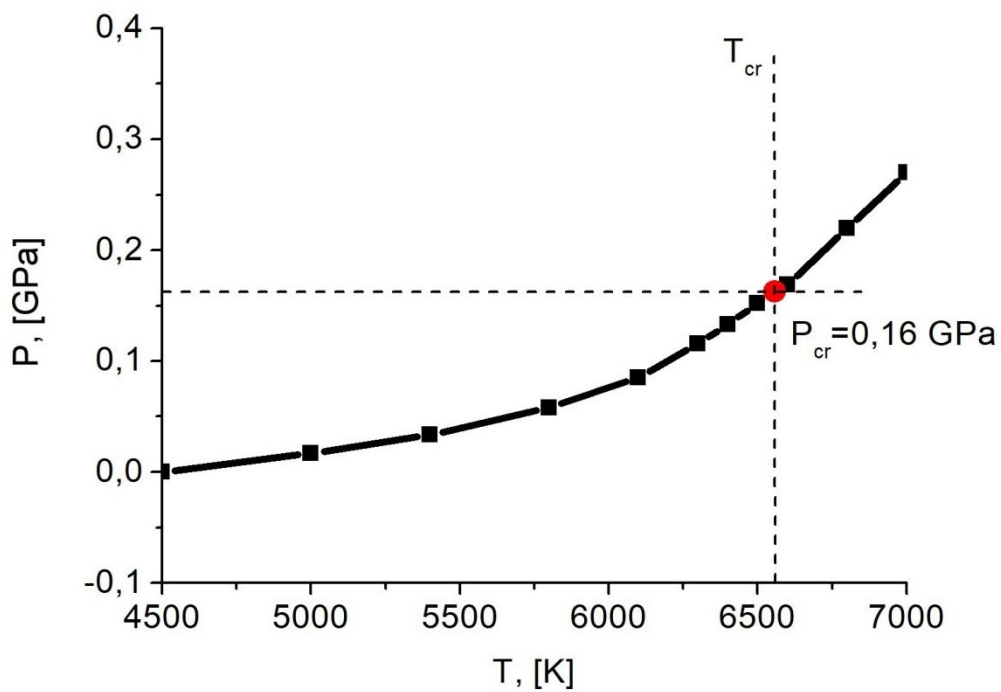Fig.3. Temperature dependence of the cluster size.

Fig. 4. Temperature dependence of saturated vapor pressure.

The temperature dependence of the saturated vapor pressure P_v was also obtained from the MDM results by averaging the results over time and space (Fig. 4). At the critical temperature T_{cr} and density ρ_{cr}, the saturated vapor pressure $P_v \approx 0.16$ GPa.

3.4 Comparison of the results with the theoretical predictions

Due to the lack of experimental information on the values of the critical parameters of copper, a comparison of the results was carried out with theoretical predictions of other studies. Table 1 shows the results of evaluating of the critical parameters of copper from this work and papers [17, 18, 20-24, 29,31]. The critical parameter values in the table are shown in decreasing order of Tcr. Among them are estimates obtained: on the basis of similarity relations [17,21, 24]; derived from the semi-empirical equation of state [20,22,23]; using the concept of "cohesive energy" [18]; as a result of numerical simulation with Morse potential [31]; the potential of an embedded atom method [29]. The table also presents the results of calculating the relative deviation of the critical parameters obtained in this work from these results

$$\sigma_{Tcr} = \frac{T_{cr,N} - T_{cr,10}}{T_{cr,N}} \qquad \sigma_{\rho cr} = \frac{\rho_{cr,N} - \rho_{cr,10}}{\rho_{cr,N}} \qquad \sigma_{Pcr} = \frac{P_{cr,N} - P_{cr,10}}{P_{cr,N}}$$

where $N=1,\ldots9$ is the number of critical parameter values in the table 1, $T_{cr,N}$, $\rho_{cr,N}$, $P_{cr,N}$ – are the critical parameters by other authors, for the present work $N = 10$. The comparison results are shown at Figs. 5-7.

N	T_{cr},K	σ_{Tcr} %	ρ_{cr}, г/см³	$\sigma_{\rho cr}$ %	Pcr, ГПа	σ_{Pcr} %	References
1	8650	24,28	2.631	27,974	0.9543	83,234	[31]
2	8440	22,39	1.94	2,32	0.651	75,422	[20]
3	8390	21,93	2.39	20,71	0.746	78,552	[21]
4	7850	16,56	2,63	0	0.905	82,32	[22]
5	7625	14,10	1.058	-79,11	0.83	80,72	[23]
6	7620	14,04	1.4	-35,357	0.577	72,27	[24]
7	7580	13,59	1.58	-19,937	0.7976	79,94	[17]
8	7250	9,66	2.3	17,609	1.35	88,148	[18]
9	5696	-14,99	1.8	-5,278	0.1141	-40,23	[29]
10	6550		1.895		0.16		This work

Table 1. The values of the parameters of copper at the critical point.

As can be seen from Table 1, the critical temperature and density obtained in this work are in good agreement with the results of other studies (Fig. 5, 6). The maximum deviation (less than 25%) of the critical temperature obtained in this work from the results of [31] using the grandcanonical transition-matrix Monte Carlo method with the Morse potential. The smallest deviation (9.66%) from the results of [18] (Fig. 5). The scatter of the deviation of the critical density values, as well as the T_{cr} values, is small and amounts to $\approx 25\%$. The exception is the results of [23] ($\approx 80\%$) and [24] ($\approx 35\%$) (Fig. 6). The critical pressure estimates differ quite significantly (Fig. 7).
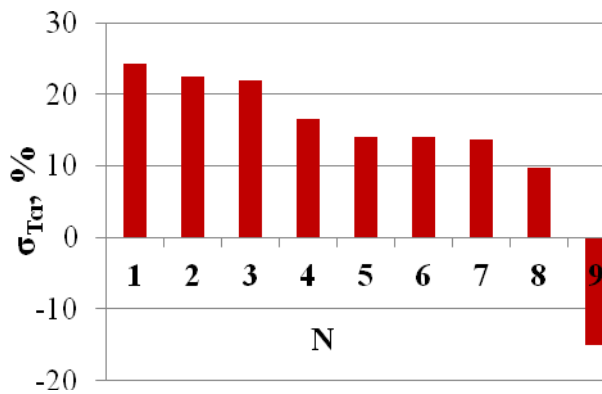
Fig. 5. Comparison results of T_{cr} with other authors
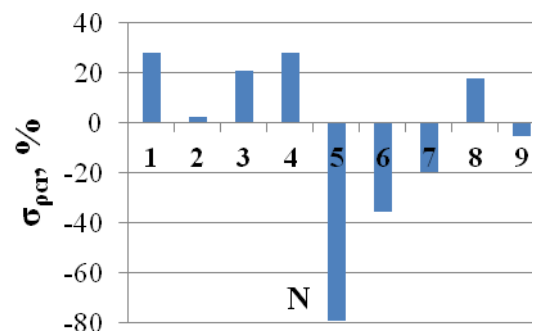
Рис. 6. Comparison results of ρ_{cr} with other authors
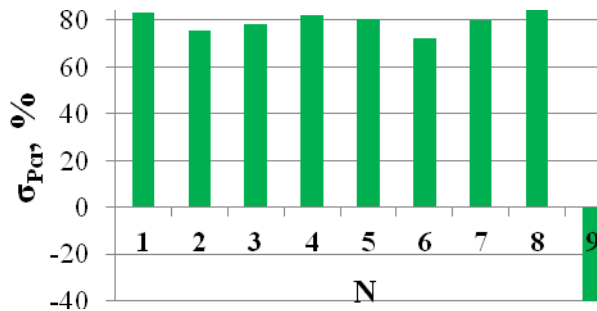
Рис. 7. Comparison results of P_{cr} with other authors

In addition to [29], the deviation of the obtained P_{cr} from other works is ≈ 80%. This can be explained by the fact that pressure is the most sensitive characteristic of a substance that responds to any changes in the system.

The comparison of the obtained critical parameters with the results of [29], in which the interaction potential of particles from the family of the "embedded atom" (EAM) was used for modeling, showed the minimum differences of all critical parameters. Critical temperature differs by 15%, critical density by 5%, critical pressure by 40%. Of all those shown in table 1, these results are the closest. Obviously, this similarity of results is associated with the use of potentials of one family.

4. CONCLUSION

1. Based on a series of calculations using molecular dynamics modeling, a liquid – vapor coexistence curve was obtained and critical parameters of copper were determined: temperature, density, and pressure using the interaction potential of particles EAM1 [32].
2. The determination of the critical density value (according to the results of MDM) from the binodal curve due to strong density fluctuations near the critical temperature was carried out using the empirical rectilinear diameter procedure.
3. Значение критической температуры T_{cr} определялось по результатам МДМ с использованием метода среднего размера кластеров в критической области. The critical temperature T_{cr} was determined from the MDM results using the method of the average cluster size in the critical region.
4. A comparison of the simulation results of this work with the results of evaluations of the critical parameters of copper obtained by other researchers using different approaches showed a good coincidence.

REFERENCES

[1] Shang-Keng Ma, *Modern Theory of Critical Phenomena*, Routledge, Taylor & Francis Group, New York, (2018).

[2] V.P. Skripov. *Metastabil`naia zhidkost`*, M., Nauka, (1972).

[3] V.A. Kirilillin, V.V. Sychev, A.E. Sheindlin, *Tekhnicheskaia termodinamika*. M.: Izdatel`stvo ME`I, (2008).

[4] F. Hensel, "35 years Liquid Metals conferences: what do we and what do we not yet understand about liquid metals", *J. Non-Cryst. Solids*, **312–314,** 1–7 (2002).

[5] M.P. Vukalovich, I.I. Novikov, *Termodinamika*, M.: Mashinostroenie, (1972).

[6] G. Franz, W. Freyland et F. Hensel, "Thermodynamic and electric transport properties of fluid cesium and rubidium in the M-NM transition region", *J. Phys. Colloques*, **41**, C8-70 – C8-73 (1980). DOI: 10.1051/jphyscol:1980819

[7] R. Winter, F. Hensel, T. Bodensteiner, W. Gläser, "The static structure factor of cesium over the whole liquid range up to the critical point", *Ber. Bunsenges. Phys. Chem.*, **91**(12), 1327-1330 (1987).

[8] R. Winter, C. Pilgrim, F. Hensel, C. Morkel, W. Gläser, "Structure and dynamics of expanded liquid alkali metals", *J. Non-Crystalhne Sohds*, **156-158**, 9-14, (1993)

[9] F. Hensel, E. Marceca, W.C. Pilgrim, "The metal-non-metal transition in compressed metal vapours", *J. Physics: Condensed Matter*, **10**(49), 11395-11404 (1998). doi: 10.1088/0953-8984/10/49/026

[10] F. Hensel, G.F. Hohl, D. Schaumloffel,W.C. Pilgrim, E.U. Franck, "Empirical regularities in behaviour of the critical constants of fluid alkali metals", *Z. Phys. Chem.*, **214**(6), 823–831 (2000).

[11] J. Jüngst, B. Knuth, F. Hensel, "Observation of singular diameter in the coexistence curve of metals", *Phys. Rev. Lett.*, **55,** 2160–2163 (1985).

[12] A.A. Likalter, "On the critical parameters of metals", *High Temperature*, **23**(3), 371–377 (1985).

[13] G. Lang, "Critical temperatures and temperature coefficients of the surface tension of liquid metals", *Zeitschrift fuer Metallkunde,* **68**(3), 213-218 (1977)

[14] V.L. Kulinskii, "Simple Geometrical Interpretation of the Linear Character for the Zeno-Line and the Rectilinear Diameter", *J. Phys. Chem. B*, **114**, 2852 (2010).

[15] V.L. Kulinskii, "The Critical Compressibility Factor Value: Associative Fluids and Liquid Alkali Metals", *J. Chem. Phys.,* **141**, 054503 (2014).

[16] E.M. Apfelbaum, V.S. Vorob'ev, "The similarity relations set on the basis of symmetrization of the liquid − vapor phase diagram", *J. Phys. Chem. B*, **119**, 8419 (2015).

[17] E.M. Apfelbaum and V.S. Vorob'ev, "The Wide-Range Method to Construct the Entire Coexistence Liquid−Gas Curve and to Determine the Critical Parameters of Metals", *J. Phys. Chem. B*, **119** (35), 11825–11832 (2015)

[18] A.L. Khomkin, A.S. Shumikhin, "Critical points of metal vapors". *JETP*, **121**(3), 521- 528 (2015)

[19] C. Desgranges, J. Delhommelle, "Evaluation of the grand-canonical partition function using expanded Wang-Landau simulations. I. Thermodynamic properties in the bulk and at the liquid-vapor phase boundary", *J. Chem. Phys.*, **136**, 184107(1-12) (2012)

[20] A.A. Likalter, "Critical points of metals of three main groups and selected transition metals", *Physica A: Statistical Mechanics and its Applications*, **311**,137-149 (2002)

[21] V.E Fortov, AN Dremin, AA Leont'ev, "Evaluation of the parameters of the critical point", *High Temperature*, **13**(5), 984–992 (1975)

[22]   L.V. Al`tshuler, A.V. Bushman, M.V. Zhernocletov i dr., "Ize`ntropy` razgruzki i uravneniia sostoianiia metallov pri vy`sokikh plotnostiakh e`nergii", *ZHETF*, **78**(2), 741-760 (1980)

[23]   D.A. Young, B.J. Alder, "Critial point of metals from the van der Waals model", *Phys. Rev. A*, **3**(1), 364-371 (1971)

[24]   A. A. Likalter, "Equation of state of metallic fluids near the critical point of phase transition", *Phys. Rev. B*, **53**, 4386 (1996)

[25]   V.I. Mazhukin, A.A. Samokhin, M.M. Demin, A.V. Shapranov, "Explosive boiling of metals upon irradiation by a nanosecond laser pulse", *Quantum Electronics*, , **44**(4), 283–285 (2014)

[26]   V.I. Mazhukin, A.A. Samokhin, A.V.Shapranov, M.M.Demin, "Modeling of thin film explosive boiling - surface evaporation and electron thermal conductivity effect", *Mater. Res. Express*, **2** (1), 016402 (1-9) (2015).

[27]   Q.-L. Cao, P.-P. Wang, D.-H. Huang, Q. Li, F.-H. Wang, L. Cang Cai, "Pressure Dependence of Fusion Entropy and Fusion Volume of Six Metals", *J. Chem. Eng. Data*, **58**(1), 64–70 (2013)

[28]   M.V. Shugaev, C.Y. Shih, E.T. Karim, C. Wu, L.V.Zhigilei, "Generation of nanocrystalline surface layer in short pulse laser processing of metal targets under conditions of spatial confinement by solid or liquid overlayer", *Applied Surface Science*, **417**, 54-63 (2017).

[29]   T. Aleksandrov, C. Desgranges, J. Delhommelle, "Vapor–liquid equilibria of copper using hybrid Monte Carlo Wang—Landau simulations", *Fluid Phase Equilib.*, **287**, 79–83 (2010)

[30]   E.M. Apfelbaum, V. S. Vorob'ev, "The Zeno line for Al, Cu, and U", *J. Phys. Chem. B*, **120**, 4828−4833 (2016).

[31]   J.K. Singh, J. Adhikari, S.K. Kwak, "Vapor−liquid phase coexistence curves for Morse fluids", *Fluid Phase Equilib.*, **248**, 1-6 (2006).

[32]   Y. Mishin, M. J. Mehl and D. A. Papaconstantopoulos, A. F. Voter, J. D. Kress, "Structural stability and lattice defects in copper: Ab initio, tight-binding, and embedded-atom calculations", *Phys. Rev. B*, **63**, 224106 (2001).

[33]   V.I. Mazhukin, M.M Demin, A.A Aleksashkina, "Atomistic modeling of thermophysical properties of copper in the region of the melting point", *Mathematica Montisnigri*, **41**, 99-111 (2018)

[34]   S. Plimpton, "Fast parallel algorithms for short-range molecular dynamics", *J. Comput. Phys.*, **117**(1), 1-19 (1995).

[35]   H.J.C. Berendsen, J.P.M Postma., W.F. van Gunsteren, A. DiNola, J.R. Haak, "Molecular dynamics with coupling to an external bath", *J. Chem. Phys.*, **81**, 3684 - 3690 (1984)

[36]   M.P.Allen and D.J.Tildesley, *Computer Simulation of Liquids*, Oxford: Clarendon Press (2002)

[37]   L. Verlet, "Computer "Experiments" on Classical Fluids. I. Thermodynamical Properties of Lennard-Jones Molecules", *Phys. Rev.*, **159**, 98-103 (1967).

[38]   V.I. Mazhukin, A.V. Shapranov, O.N. Koroleva, A.V. Rudenko, "Molecular dynamics simulation of critical point parameters for silicon", *Mathematica Montisnigri*, **31**, 56-76 (2014).

SIMULATION OF TRAFFIC FLOWS ON ROAD SEGMENTS USING CELLULAR AUTOMATA THEORY AND QUASIGASDYNAMIC APPROACH

N.G. CHURBANOVA[1,2*], A.A. CHECHINA[1], M.A. TRAPEZNIKOVA[1,2], P.A. SOKOLOV[2]

[1] Keldysh Institute of Applied Mathematics RAS, Moscow, Russia

[2] Moscow Automobile and Road Construction State Technical University (MADI), Moscow, Russia

* Corresponding author. E-mail: nataimamod@mail.ru

Summary. The research deals with the creation of mathematical tools for the simulation of vehicular traffic flows on complex urban transport networks using modern supercomputers. The goal of the present paper is further development of micro- and macroscopic models created by the authors earlier. The proposed 2D microscopic model is based on the cellular automata theory. In this work algorithms taking into account various driving strategies have been incorporated into the model. The model is implemented as a program package that includes User interface and Visualization module. The macroscopic model uses the continuous medium approximation: it is constructed by analogy with the quasigasdynamic system of equations. The one dimensional version is proposed in the paper, nevertheless, it allows reproducing changes in the number of lanes as well as possible road entrances and exits. Parallel algorithms adapted to high-performance computing systems have been created for both models, ensuring rapid computations on city road networks.

1 INTRODUCTION

Mathematical modeling of traffic flows is a topic of increasing interest for lots of scientists all over the world. Due to the permanent growth of the number of vehicles, modern cities require solutions to support traffic management, both short-term and long-term, and the rising capacity of modern supercomputer systems allows using more detailed and precise models for computations. At the same time, for different types of models different tasks are to be fulfilled. The microscopic models (these include cellular automata models) consider various aspects of real life driver behaviour, resulting in more fluctuations inside the flow that consequently leads to reproducing experimentally observed features of traffic. The macroscopic (gasdynamic) models are means for providing a general picture for traffic situation on a network while avoiding excessive computational cost.

The first approach under consideration is the microscopic approach. As in atomic models describing the interaction of atoms and molecules [1-5], here we consider the interaction of individual particles represented in the form of cars with their drivers. Cellular automata (CA) models are a special type of microscopic models. The CA theory, first proposed by John von Neumann in the mid-twentieth century, has got applications in many fields of science. It helps to predict economic, social, technical, biological and other processes. The first application of the theory of cellular automata to the traffic flow simulation was proposed in [6]. But

especially rapidly this trend began to develop since 1992, when Kai Nagel and Michael Schreckenberg applied the CA theory to transport modeling [7]. Scientists from around the world have created many variants of traffic flow models based on it. One of the most interesting reviews on cellular automata models is given in [8]. It is noted that the main goal of CA models is to describe the macroscopic characteristics of traffic flows using a simple description of microscopic interactions.

One can trace the further development of this direction, for example, in the following works. Article [9] suggests stochastic version of the CA model. Article [10] discusses the simulation of dynamic systems on toroidal structures. In [11, 12] on the basis of the CA model investigations are carried out to illustrate the three-phase Kerner theory [13]. Article [14] is devoted to the same issues. In [15] the effect of the difference in driver psychology on flow stability on a two-lane highway is estimated using the CA model. The article also shows the influence of safety parameters on the volume of traffic. Some works [16-21] deal with the adaptation of the CA model to various real transport situations, such as the impact of the distribution of lanes and turn signals at the intersection on the total traffic capacity, accounting for interaction with neighboring vehicles, accounting for pedestrian crossings, traffic on a U-shaped turn, the interaction of cars with buses and bicycles, addresses traffic safety issues. Some of these transport situations are considered by the authors in the present paper.

Previously, the CA approach seemed to be the most promising for a detailed description of local road situations at short distances, since the models are quite flexible due to the ability to implement any driver strategy without significant algorithmic costs. However, the capacity of modern ultra-high-performance computing equipment allows models of this type to be successfully used to simulate traffic on large road networks.

The second approach discussed in this paper uses the continuous medium approximation. An approach of this kind is widely used in different branches of science, such as gas dynamics [22-25], flows in porous media [26] and many others. To clarify the basic regularities of dense traffic flow, it is convenient to use the continuous medium approximation in traffic simulations, i.e. to use macroscopic models (see [27]). In contrast to microscopic models, the main objects of study in such models are fields of the average vehicle speed and the density of vehicular flow. Recently, the number of works devoted to macroscopic models has slightly decreased, however, there are some cases when the macroscopic description is more computationally advantageous and gives more clear representation of the average characteristics of the traffic flow.

A significant amount of works is devoted to models such as Lattice Boltzmann hydrodynamic models. The following articles can be listed here. A theoretical analysis of these types of models is presented in [28]. In [29] such characteristics of drivers as "timidity" or "aggression" are taken into account. In [30, 31] the influence of the human factor on the stability of a two-way flow is investigated. The authors of article [32] propose a new lattice model, which helps to study how the driver's memory volume affects the dynamics of the traffic flow. Analysis of the linear stability demonstrates that the temporary length of the driver's memory has an important effect on the stability of the traffic flow. And in article [33] the same authors propose an extended one-dimensional hydrodynamic lattice model to study flow dynamics when driving along a curved road. They obtain the stability condition via the linear stability analysis. The result of the analysis indicates that the radian of a curved road plays an important role in influencing the flow stability. In addition, compared with other

segments of the curved road, the flow easily becomes unstable at the road entrance and exit. Article [34] also explores movement along a curved road. On the basis of the lattice model it is confirmed that a curved road negatively affects the stability of the traffic flow.

As follows from the above review, traffic flow simulation has been actively developed in previous decades. Nevertheless an adequate description of the interaction of traffic flows in the network nodes under conditions of congested traffic requires further modernization of existing models and methods for their computer implementation. In view of the significantly increased loading of city transport networks in recent years, a separate independent task is to create software for the efficient use of parallel computer technologies.

The aim of the present paper is the development of mathematical tools for modeling the dynamics of traffic flows on complex fragments of road networks that are structural elements of a branched transport system of a metropolis. For this purpose the paper discusses two possible ways of solving the given problem. Previously the authors created the original microscopic model based on the cellular automata theory and the macroscopic model using the ideology of the quasigasdynamic system of equations. In the current research these models undergo the needed modification.

In the field of micromodeling, the goal is the extension of the CA model by introducing new algorithms that describe a variety of traffic situations, as well as possible driver strategies. Improved algorithms of lane changing, crossroad overcoming, queue forming, moving on the road with complex geometry, driving around obstacles are to be created. Algorithms depicting different driving strategies are also to be included. Another goal is to create a so-called "slow-to-start" model for reproducing real fluctuations that occur in congested traffic.

In the field of macromodeling the main goal is the development of the gasdynamic type model with a simple enough structure but with possibility to describe the movement over crossroads, roads with the changing number of lanes and to account for the existence of on-ramps and off-ramps. In paper [35] a 2D macroscopic model was proposed by analogy with the quasigasdynamic (QGD) system of equations designed to predict a wide class of compressible gas flows including low Mach number flows (see [36]). However, when modeling traffic at complex junctions and interchanges, and especially in numerical implementation, such a description may cause additional difficulties. At the same time, in many practically important cases a one-dimensional description can be sufficient to study peculiarities of vehicular flow and to obtain qualitatively correct results.

A common task for models of both types is their adaptation to distributed memory multiprocessor systems to make the calculations most efficient.

The approaches are to be verified by various numerical experiments, including test predictions of traffic on signalized intersections at different traffic light regimes.

2 THE ORIGINAL 2D CA MODEL

The original cellular automata model created by the authors presents a generalization of the classic Nagel-Schreckenberg model [7] to the multilane case with various driver behaviour algorithms included.

The road is divided into equal cells. As is usual for traffic CA models, a cell is 7.5 meters long and one lane wide, the time step is 1 second. The cell can be either empty or occupied by a single vehicle (Fig.°1).
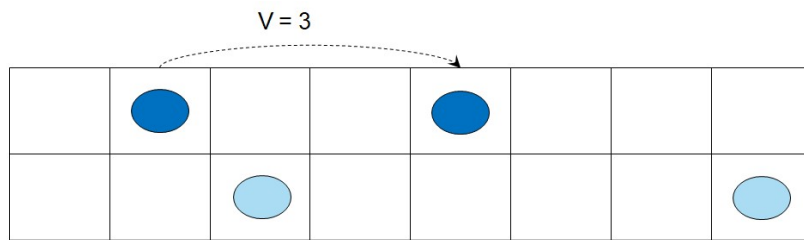
Figure 1. The computational domain for CA-model

Each car has a set of parameters: unique ID, maximum speed – V_{max}, current location (the road number, the lane number and the cell number), current speed – from 0 to V_{max} and final destination; its driver can be 'cautious' or 'aggressive', 'cooperative' or not. These parameters, especially location and speed can change at each time step, it depends on the situation around the car.

Each time step cell state update is carried out according to the following rules:

- a vehicle changes a lane if it is necessary (to reach the desired destination or to drive around an obstacle), it is advantageous for a driver (leads to speed increase and/or density decrease) and it is possible (i.e. if the lane change is allowed and the target cell is empty);
- a vehicle moves along the road according to the classic rules for the one-lane traffic [7].

These rules consist of the substeps represented as a block-scheme (Fig. 2) for each car, d – the distance between the current car and the next one in front of it.
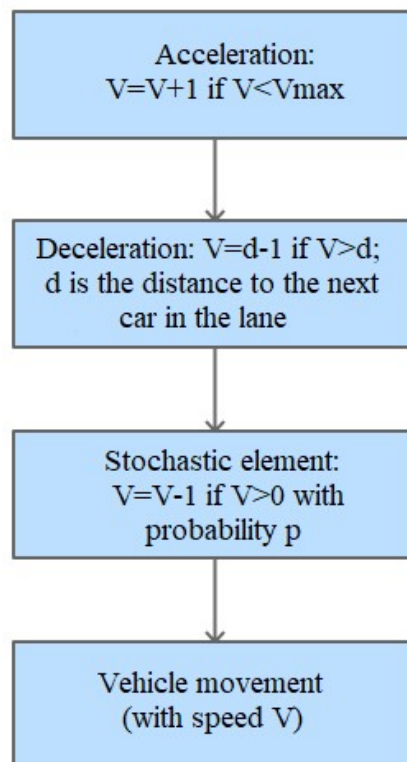
Figure 2. Block-scheme for the 1D Nagel-Schreckenberg model

The first step reflects the general desire of all drivers to drive as quickly as possible. The second guarantees no collisions with vehicles in front. An element of stochastics, taking into account randomness in the behaviour of drivers, is introduced in the third step. On the fourth, the state is finally updated for this movement participant.

3   ALGORITHMS INCLUDED IN THE CA MODEL

3.1 Changing lanes

The rules of changing lanes can depend on various conditions, i.e. road segment, road signs, driver behaviour.

Figure 3. Block-scheme for the lane change algorithm

The block-scheme for the basic algorithm of lane changing is presented in the Fig.°3:
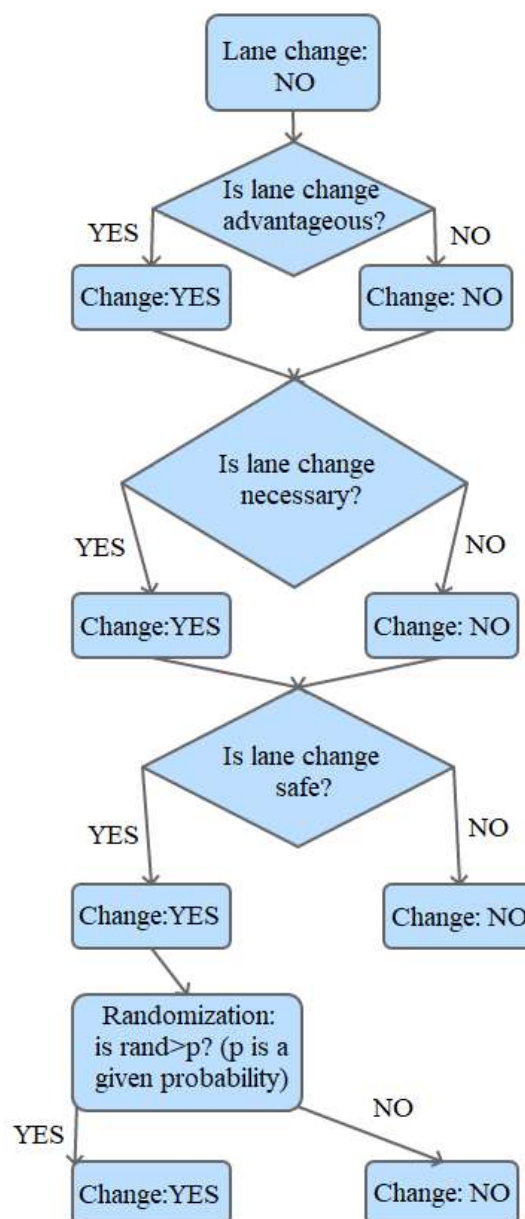Lane changing takes place under following conditions:
- a vehicle is located in a domain where lane change is allowed;
- lane change leads to the speed increase (density decrease) or is necessary to reach the destination;
- there is an obstacle not far away on the current lane;
- the target cell is empty;
- the safety condition is satisfied - on the target lane the distance behind is greater or equal to the maximal/current velocity of the previous car (cautious/aggressive drivers), the distance in front is greater or equal to the concerned vehicle velocity;
- lane change takes place with a given probability.

The described algorithm is basic and its variations are included as an integral part in all subsequent algorithms for the movement of cars on various elements of the transport network. The algorithms described below have a much more complex structure, so their graphical representation in the form of block-schemes is rather bulky for the article format.

3.2 The algorithm of crossroad overcoming

- Within 100 meters before traffic lights the vehicle changes lane under its purpose according to the road laws.
- A vehicle accelerates or decelerates according to the Nagel-Schreckenberg model.
- Additional speed decreasing takes place under the following conditions:
  - if a vehicle is located near the turning point (at the turning point it stops);
  - if a traffic light is red;
  - if there is the collision threat on the crossroad.
- A vehicle moves under the foregoing rules with randomization.
- A vehicle turns if it is located in the turning point and has got the corresponding target.

3.3 Forming the entrance queue

According to the entrance flow value for the given direction that is set by user before the calculation, time steps on which new vehicles should be added in the system are specified. At a given time step the vehicle appears in the entrance cell of the right lane if it is not occupied by another vehicle. If it happens to be occupied, other lanes are checked. If there is a traffic jam and all the entrance cells in the given direction contain vehicles already, the car can't enter and it is added into the queue. As soon as one of the entrance cells vacates, the car appears on the road.

3.4 Road narrowing/widening

Each driver is able to "see" if the road narrows down some distance ahead. In this case, the driver tries to change lane if his lane is going to disappear, even if the speed in the target lane is lower than the speed in his current lane and the traffic over there is denser. Some drivers in the target lane, if they are "cooperative", can stop to let the driver change his lane.

In case of the road widening, drivers react only when they reach it, following the general "lesser density/higher velocity" rule, i.e., seeing the empty lane, they move there for more comfortable driving.

3.5 Driving around an obstacle

If there is an obstacle in the middle of the road (for example, a broken car or cars after a road accident), a driver is able to "see" it before it reaches it, like in the case of a road narrowing. He also tries to drive around it, first determining which direction of lane changing is preferable, and then he changes lanes till he reaches a free one, with or without help of "cooperative" drivers.

3.6 Different driving strategies

Each driver has his own driving style: ones are more determined, change lanes more easily, others are more cautious, they wait for a larger gap to move to the neighbouring lane. Their behaviour influences the overall situation on the road. To reflect that, the following driver types were included in the model:

- "Cautious" drivers change lanes only if the gap between the target cell and the first occupied cell upstream is larger than the maximum speed;
- "Aggressive" drivers change lanes if the gap between the target cell and the first occupied cell upstream is larger than the actual speed of the vehicle which is situated in the first occupied cell;
- "Cooperative" drivers can be either cautious or aggressive. The percentage of cooperative drivers in the system can vary. These drivers:
  - slow down (V = V - 1; V ≥ 1), if they see a traffic jam before an obstacle or a road bottleneck on the neighbouring lane;
  - if there is a jam before the obstacle on the neighbouring lane, and there are drivers that want to change their lane, cooperative drivers stop and let them pass;
  - wait for several time steps if the car from the other lane can't move immediately, because the target cell is occupied by another car.

4   THE 'SLOW-TO-START' VERSION OF THE CA MODEL

According to the classic one-lane Nagel-Schreckenberg rules, the driver checks if the next cell is empty, and if it is, he starts moving. But there is another class of models – 'slow-to-start' – where vehicles begin their movement only on condition that there is more than one free cell in front of them (see [8]). This rule was included in the model so that cars did not disperse too quickly from the place of the traffic jam. It allows to reproduce the effect of hysteresis that is observed during the transition from the free flow phase to the synchronized flow phase, depending on random processes in the traffic flow.

According to the three phase theory by B. Kerner [13], there are three phases in the traffic flow: F is the phase of free flow, S is the phase of synchronized flow and J is the phase of wide moving jams. Due to the instability of the flow, for example, due to the effect of over-acceleration (see [7]), phase transitions can occur spontaneously. As experimental data show, models of the 'slow-to-start' class reproduce such phase transitions more successfully.

To satisfy the 'slow-to-start' rule, a set of appropriate conditions was added to the created model. The results obtained via this model can be found in paper [37].

5 NUMERICAL REALIZATION

The created program package consists of two modules: the Computational module that carries out calculations and the User Interface and Visualization module that serves the purpose of getting the initial data from a user, transferring it to the Computational module, getting results back and providing their visual interpretation.

The code is written in C/C++ and uses the MPI library for parallel calculations. Separate sub-programmes simulate traffic on different types of road elements in parallel, with data exchange on the boundaries.

The results of computations for some standard road elements are shown in Fig. 4. Different colours of cars represent different destinations attributed to them. Fig. 4(a) and Fig. 4(c) represent signalized intersections (T-cross and X cross respectively). In Fig. 4(b) an U-turn on a road with a wide median is shown. In Fig. 4(d), where the road with an accident is presented, the black circle represents an unmoving car that experienced the accident. In Fig. 4(e) an on-ramp is shown.

| 4(a) | 4(b) | 4(c) |

| 4(d) | 4(e) |
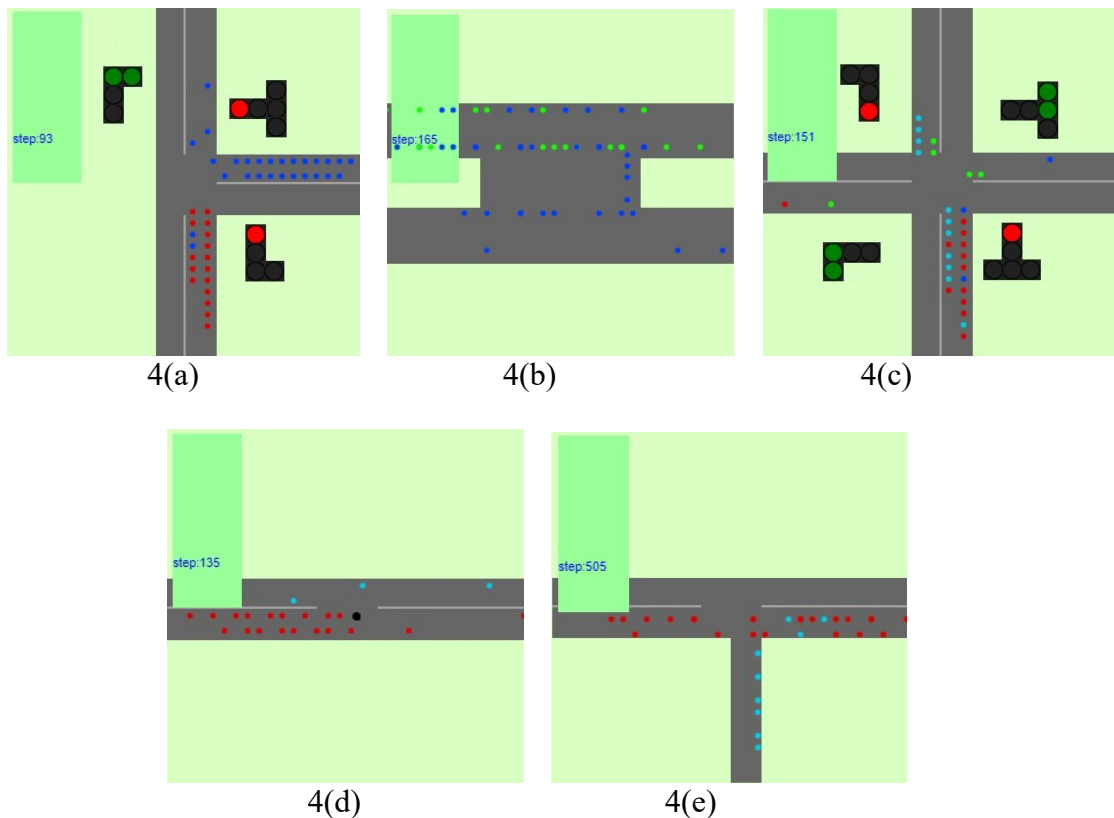
Figure 4. Basic road fragments

At each time step processors exchange information whether any vehicles are crossing the boundaries during this step. If the answer is positive, the data regarding those vehicles is packed and sent/received, and the cars appear on the next road fragment. In order to avoid the situation where the target cell is already occupied, the information about all vehicles that stopped near the beginning of the road fragment is collected. If there is a traffic jam on the road, the drivers from the previous (upstream) fragment that are nearing its end can "see" it

and slow down or stop if necessary.

6   TEST PREDICTIONS FOR THE CA MODEL

The models have been verified by various numerical experiments (see, for example, [38, 39]), including the comparison with experimental data [37].

For further comparison and verification of the created models a few test problems were researched. The first one is modelling traffic on a small road network of two neighbouring intersections (see Fig. 5). It consists of two elements: an U-turn on the road with a median wide enough to fit in a car, and a signalized X-crossroad, that are connected by data exchange on the boundaries via MPI. Once the car leaves its element, it appears on the next, obtaining a new destination (since its previous destination is considered to be reached).
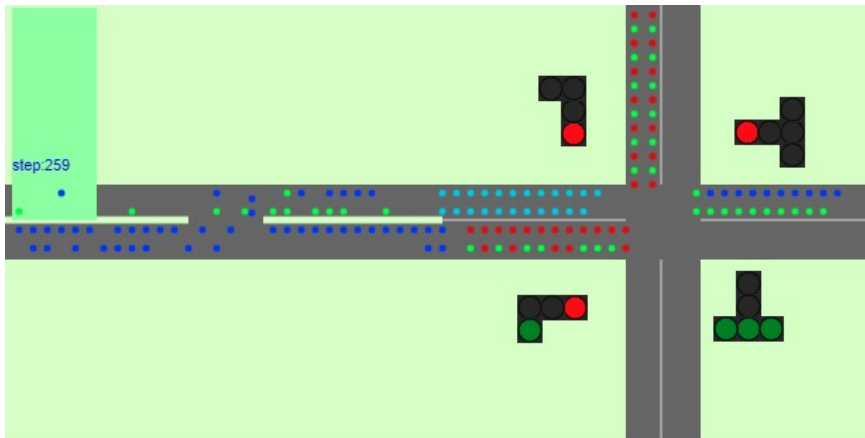
Figure 5. Simulating traffic on two neighbouring intersections: U-Turn +X-Crossroad

Another test problem is modeling traffic on a small network which consists of two signalized intersections (Fig. 6). When a car approaches the boundary with another element, the possibility of entering is checked. If the desired cells are occupied by other cars waiting for the green light on the target element, the car stops and waits until one of these cells is empty.
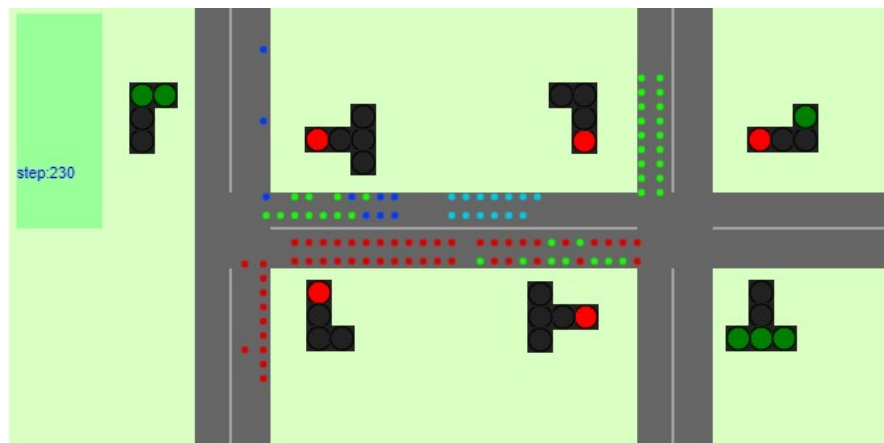
Figure 6. Simulating traffic on two neighbouring intersections: T-Crossroad + X-Crossroad

Along with the visual representation of what is happening with traffic on this part of the network, various average characteristics can be obtained [37].

7 THE QGD APPROACH TO TRAFFIC FLOW MODELING

7.1 The governing macroscopic model

In case of congested traffic when average quantities of traffic flow are of primary interest the continuous medium approximation is convenient to employ, i.e. to use macroscopic models. In contrast to microscopic models, the main objects of study in such models are fields of the average vehicle speed and the density of vehicular flow. The most popular models of this type are models like gas-dynamic ones.

For many practically important problems a one-dimensional description is sufficient to study peculiarities of vehicular flow and to obtain qualitatively correct results. The paper focuses on a 1D variant of the quasigasdynamic equations system for vehicular traffic flow. It can be written as follows:

$$\frac{\partial \rho}{\partial t} + \frac{\partial \rho V}{\partial x} = \frac{\partial}{\partial x} \frac{\tau}{2} \frac{\partial (\rho V^2 + P)}{\partial x} + F_\rho , \tag{1}$$

$$\frac{\partial \rho V}{\partial t} + \frac{\partial \rho V^2}{\partial x} = f - \mathrm{grad} P + \frac{\partial}{\partial x} \frac{\tau}{2} \frac{\partial (\rho V^3 + PV)}{\partial x} + F_V . \tag{2}$$

Here $\rho \left[\dfrac{\mathrm{veh}}{\mathrm{km} \cdot \mathrm{lane}} \right]$ is the traffic density, $V \left[\dfrac{\mathrm{km}}{\mathrm{h}} \right]$ is the spatial average speed of vehicles.

The above system belongs to macroscopic models of the second order [27]. It includes two equations in the form of conservation laws for obtaining the density (1) and the speed (2). Since the solution of the system can be occasionally discontinuous, i.e. so-called traffic shock-waves can take place, as a rule diffusion terms are introduced into the equations for solution smoothing. The QGD system possesses such a property initially. One of the basic assumptions for the QGD system is existence of additional mass flux that ensures a smooth solution at the reference scale of the medium (see [36]). The right-hand sides of equations (1) and (2) include such fluxes. By analogy with gas dynamics minimal reference time and space scales are introduced for traffic flows in order to satisfy the continuous medium approximation. The small parameter τ is interpreted as a reference time that means the time interval in which several vehicles cross a given point of the road. As a reference length the distance between vehicles for the given speed can be considered.

Equations (1)-(2) employ the listed below additional functions related specifically to transport problems.

The analogue of pressure: $P(\rho) = \dfrac{\alpha \rho^\beta}{\beta}$.

Phenomenological constants are taken from works by other authors as $\alpha = 60 \dfrac{\mathrm{km}^2}{\mathrm{h}^2}$, $\beta = 2$.

The accelerating/decelerating force: $f = a\rho$. Here a is the relaxation term reflecting adaptation of the speed to the equilibrium speed: $a = \dfrac{V_{eq}(\rho) - V}{T}$.

The involved equilibrium speed $V_{eq}(\rho)$ has the sense of the optimal speed under the given conditions. It is a function depending only on the density and obtaining from the fundamental diagram. In the current investigation the parabolic fundamental diagram is used:

$$Q_{eq}(\rho) = \rho V_0 \left(1 - \frac{\rho}{\rho_{jam}} \right). \tag{3}$$

Taking into account the relation $Q_{eq} = \rho V_{eq}$ we get the next dependence of the equilibrium speed on the density:

$$V_{eq}(\rho) = V_0 \left(1 - \frac{\rho}{\rho_{jam}} \right).$$

Here V_0 is the free traffic speed, ρ_{jam} is the density at which vehicles stop moving ("traffic jam"). In computations the next values are used: $V_0 = 90 \dfrac{\text{km}}{\text{h}}$, $\rho_{jam} = 120 \dfrac{\text{veh}}{\text{km} \cdot \text{lane}}$.

The function T depends on the density:

$$T(\rho) = t_0 \left(1 + \frac{r\rho}{\rho_{jam} - r\rho} \right), \text{ where } t_0 = 50 \text{ and } r = 0.95 \text{ are the model parameters.}$$

The source functions in the right-hand sides of equations (1)-(2) are equal to zero if the road is homogeneous, that is the number of lanes does not change and there are no entrances/exits. If there is a change in the number of lanes, then the concept of the real function I, which has the meaning of the number of lanes, is introduced [27]. It does not change abruptly, but is piecewise linear or may have a more complex form. When the number of lanes changes, it takes not integer (i.e. real) values on a certain distance before the narrowing/widening. The integer part of this value reflects the contribution of the continuing lanes, and the mantissa is the contribution of the closing/opening lane to the traffic movement as a whole.

In addition, if there are entries/exits, the corresponding source terms appear in the right-hand sides of the equations. If by analogy with [27] we introduce the concept of "the effective source density", denoting it v_{rmp}, the right-hand side of equation (1) takes the following form:

$$F_\rho(x,t) = -\frac{\rho V}{I} \frac{dI}{dx} + v_{rmp}(x) \tag{4}$$

where

$$v_{rmp}(x,t) = \begin{cases} \dfrac{Q_{rmp}(t)}{IL_{rmp}} & \text{if } x \text{ is inside the entry / exit zone,} \\ 0 & \text{otherwise.} \end{cases}$$

Here Q_{rmp} denotes the incoming (from the entry) or outgoing (from the exit) traffic flow, L_{rmp} is the acceleration band length – the length of the on-ramp or off-ramp. The source term for the momentum equation (2) can be also obtained after [27]. For the conservative form of the equation it will be as follows:

$$F_V(x,t) = -\frac{\rho V^2}{I}\frac{dI}{dx} + V v_{rmp}(x) + \rho A_{rmp} \tag{5}$$

where

$$A_{rmp} = \frac{(V_{rmp}-V)|Q_{rmp}|}{\rho I L_{rmp}},$$

V_{rmp} is the speed of on-ramp vehicles merging or diverging the main road, $V_{rmp} < V$.

Differential equations should be supplemented at boundary points of the computational domain by boundary conditions of the first or second kind for the density and velocity that depend on the specific formulation of the problem.

7.2 Numerical implementation

For numerical implementation of system (1)-(2) an explicit finite-difference method is used. The next two-level scheme is applied, convective terms are approximated by central differences [40]:

$$\frac{\hat{\rho}-\rho}{\Delta t} + (\rho V)_{\overset{\circ}{x}} = 0.5\tau(\rho V^2 + P)_{\bar{x}x} + F_\rho,$$

$$\frac{\hat{\rho}-\rho}{\Delta t} + (\rho V^2 + P)_{\overset{\circ}{x}} = f + 0.5\tau(\rho V^3 + PV)_{\bar{x}x} + F_V.$$

The conditional stability of schemes is ensured by the presence of diffusion terms in the right hand sides. As the numerical implementation is based on explicit schemes its parallelization can be performed with high efficiency. The parallel algorithm is focused on the use of distributed memory supercomputers.

For the interaction of parallel processes in the code the MPI (Message Passing Interface) technology is employed. Parallelization is based on the principle of geometrical parallelism. For macroscopic traffic flow computations the algorithm with partitioning of the computational domain (the road network) into subdomains was proposed. Each subdomain represents one segment of the network connecting two neighbouring nodes (intersections). In network nodes the data exchange between adjacent segments occurs. Splitting is carried out in such a way that two neighbouring sections have two common points for the correct implementation of boundary conditions at bordering points of subdomains. Thus, each section

of the road is calculated on a separate processor, transmitting and synchronizing data via MPI operations.

Further calculations were carried out at Keldysh Institute of Applied Mathematics RAS on the MVS-Express supercomputer, which has a distributed memory architecture (see [32]).

8   TEST PREDICTIONS FOR THE QGD TRAFFIC MODEL

As in case of the CA model the QGD traffic model verification was performed by test problems on signalized intersections. In test predictions the intersection is represented as a graph, at parallelization each subdomain corresponds to the graph edge.

In the signalized intersection test problem a traffic light is placed in the graph node, allowing one or another entrance flow alternately pass through the intersection in accordance with the traffic light phase.

For the flow for which the green light is on, conditions of matching are set on the boundary between neighboring subdomains — a simple exchange of the boundary values of densities and velocities takes place. For the flow for which the red light is on, the density and the velocity at the point of the traffic light location are discontinuous: on the left of the traffic light the velocity equals zero, the density increases up to the maximum. On the right of the traffic light the movement continues. Equations (1)-(2) in this point are simplified to the next ones (the acceleration and the pressure gradient become equal to zero):

$$\frac{\partial \rho}{\partial t} = -\frac{\partial \rho V}{\partial x},$$

$$\frac{\partial \rho V}{\partial t} = -\frac{\partial \rho V^2}{\partial x}.$$

For flow entering the node on the right boundary of the subdomain before the traffic light these conditions in the difference form with the first order of approximation are as follows:

$$\rho_N^{n+1} = \rho_N^n + \frac{\Delta t}{h}\left(\rho V\right)_{N-1}^n,$$

$$V_N^{n+1} = 0.$$

For flow exiting the node on the left boundary of the subdomain after the traffic light:

$$\rho_0^{n+1} = \rho_0^n - \frac{\Delta t}{h}\left(\rho V\right)_1^n,$$

$$\left(\rho V\right)_0^{n+1} = \left(\rho V\right)_0^n - \frac{\Delta t}{h}\left(\rho V^2\right)_1^n.$$

Here superscripts correspond to the time levels and subscripts correspond to the points of computational subdomains.

Figure 7 reflects the obtained results for T-type signalized intersection at different traffic light phases. The density values are presented. Black arrows show the direction of cars' movement. The traffic light phases are depicted by the traffic light colours near the roads. The picture at Time 1 demonstrates the initial statement of the problem. At Time 29 one can see the density increase before the red traffic lights. At Times 44 and 90 when the green traffic

light is on, the density jump in the corresponding section of the road in front of the traffic light begins to decrease.
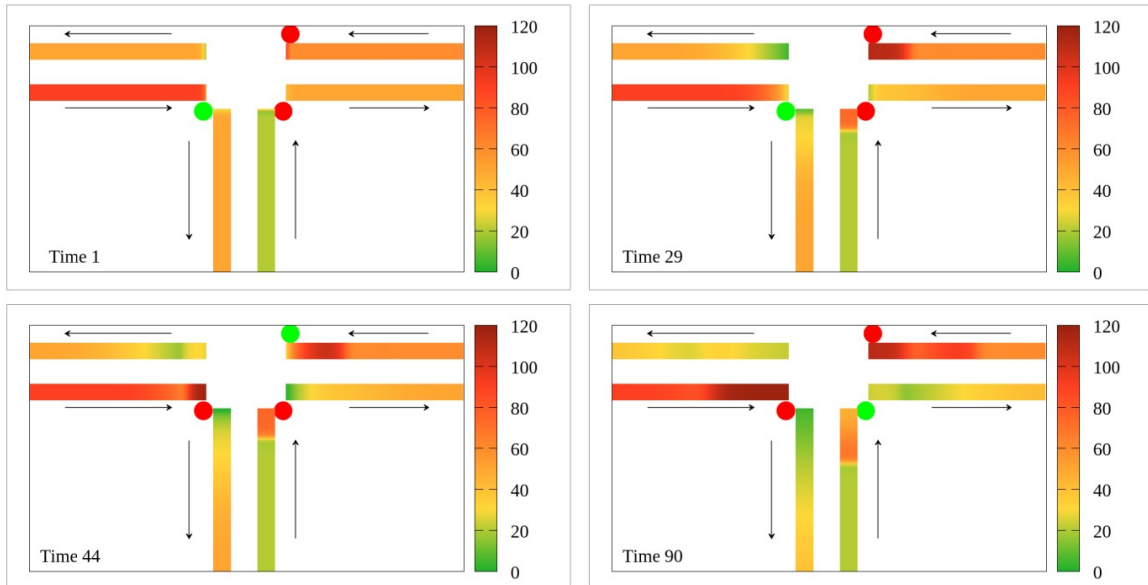

Figure 7. Simulating traffic on T-type signalized intersection at different traffic light phases
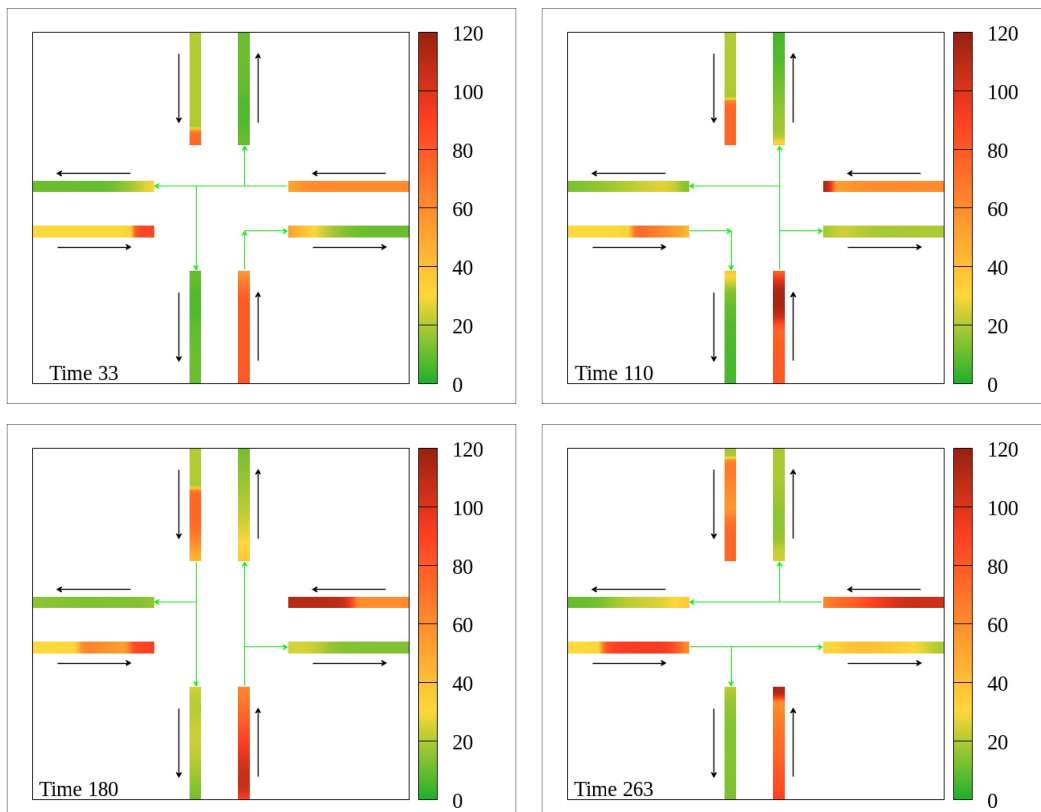

Figure 8. Simulating traffic on X-type signalized intersection at different traffic light phases

Figure 8 demonstrates the results for X-type signalized intersection. The traffic light phases are depicted by green arrows showing the allowed directions of movement at the intersection during the given phase. In the pictures one can observe the same dependence of the density on traffic signals as in the previous case.

One more test prediction is the simulation of traffic flow on the road with a preset geometry. It should be noted that the simplest test calculations of traffic on the road with an increase and decrease in the number of lanes, as well as a comparison of the results with the calculations from [27] are given in [41]. The following problem statement is considered in this article. The 20 km road section with the number of lanes I is under consideration. The computational domain is depicted in Fig. 9.
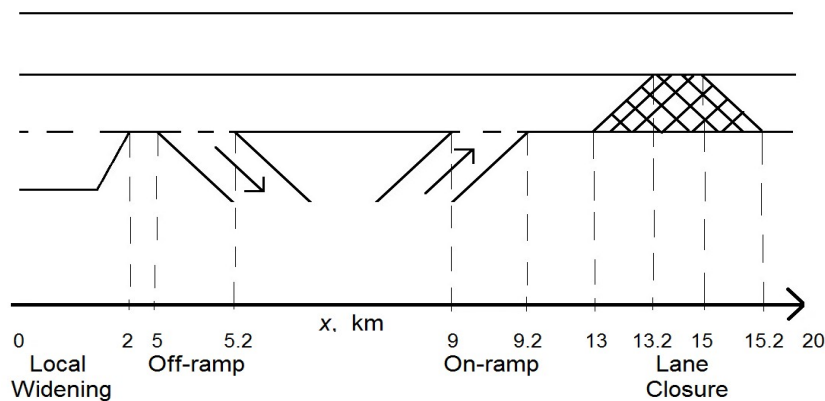
Figure 9. Geometry of the road section under consideration

This section contains:
- a local road widening of 2 km long,
- an exit (the off-ramp with length $L_{rmp\_out} = 0.02\ km$ starting at the point $x = 5$ km),
- an entry (the on-ramp with length $L_{rmp\_in} = 0.02\ km$ starting at $x = 9$ km),
- a lane closure starting at $x = 13.2$ km and lasting 1.8 km.

The volume of traffic (input flows of the entry, exit and main road) is constant and is set by values Q_{rmp_in}, Q_{rmp_out} and Q.

Results of calculations (the spatiotemporal pattern of the density) are presented in Fig. 10.

Figure 10. Density field on the road section under consideration

Obtained results show that significant degradation of the road situation occurs at the lane closure point. The bottleneck capacity can no longer keep up with the input flow and the traffic breakdown takes place at this point, the density jam propagates upstream.
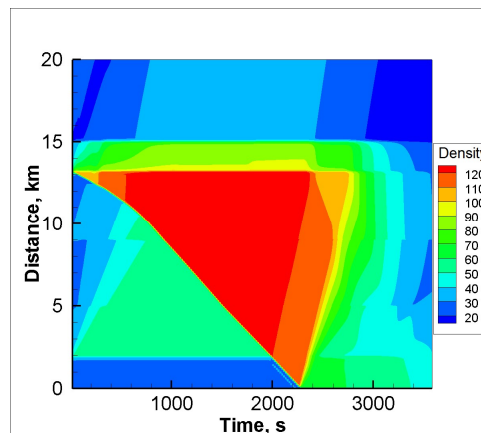
One can conclude that the numerical simulation with the use of the proposed QGD traffic model and the developed parallel software leads to correct results. In the calculations, parallelization efficiency of almost 100 percent was achieved.

Models created can be implemented as a part of Intelligent Transportation System (ITS) of a city, serving the purpose of informing drivers, rerouting if necessary, managing road infrastructure in order to use a transportation network safely and efficiently.

9   CONCLUSIONS

The following results obtained should be noted.

The microscopic CA model of traffic flows has been extended by improving the existing algorithms and adding new ones:

- lane changing;
- crossroad overcoming for different types of crossroads;
- forming the entrance queue;
- moving on the road with narrowing/widening;
- driving around an obstacle;
- implementing different driving strategies.

A new version of the CA model, namely the 'slow-to-start' model, has been proposed in order to reproduce the transition from the free flow phase to the synchronized flow phase more realistically.

The program package consisting of two modules – the Computational module and the User Interface and Visualization module – has been created and adapted for supercomputer calculations.

Several test problems have been solved to verify the developed models and algorithms. Vehicle movement on different road fragments, such as a T-cross, an X-cross, an U-turn, an on-ramp, has been predicted, the expected behaviour of movement has been observed. It was shown that traffic on more complex road networks can be simulated by various combinations of the listed road elements.

The one-dimensional variant of the QGD system of equations for the description of vehicular traffic flow on roads with T-cross and X-cross has been proposed. The model can take into account the changing number of lanes, on-ramps and off-ramps. The corresponding test predictions have demonstrated the adequacy of the proposed model. The parallel algorithm based on the principle of geometrical parallelism has been developed. Due to the implementation of the model by explicit difference schemes very high efficiency of parallelization was achieved. The approach can be successfully employed if the average quantities such as the density and the velocity of traffic flow are under consideration.

REFERENCES

[1] V.I. Mazhukin, A.V. Shapranov, A.V. Mazhukin, O.N. Koroleva. "Mathematical formulation of a kinetic version of Stefan problem for heterogeneous melting/crystallization of metals". *Mathematica Montisnigri*, **36**, 58-77 (2016).

[2] A.A. Samokhin, V.I. Mazhukin, A.V. Shapranov, M.M. Demin, A.E. Zubko, "Molecular dynamics modeling of nanosecond laser ablation: transcritical regime", *Mathematica Montisnigri*, **38**, 78-88 (2017).

[3] A.A. Samokhin, V.I. Mazhukin, M.M. Demin, A.V. Shapranov, A.E. Zubko, "Molecular dynamics simulation of al explosive boiling and transcritical regimes in nanosecond laser ablation", *Mathematica Montisnigri*, **41**, 55-72 (2018)

[4] T. Kudryashova, Yu. Karamzin, V. Podryga, S. Polyakov, "Two-Scale Computation of N2-H2 Jet Flow Based on QGD and MMD on Heterogeneous Multi-Core Hardware", *Advances in Engineering Software*, **120**, 79-87 (2018)

[5] V. Podryga, S. Polyakov, "Correction of the gas flow parameters by molecular dynamics", *Proceedings of IV Int. Conf. on Particle-Based Methods - Fundamentals and Application (PARTICLES 2015), Barcelona, Spain*, 779-788 (2015).

[6] M. Cremer, J. Ludwig, "A fast simulation model for traffic flow on the basis of Boolean operations", *Math. Comp. Simul.*, **28**, 297-303 (1986).

[7] K. Nagel, M. Schreckenberg, "A cellular automaton model for freeway traffic", *J. Phys. I France*, **2**, 2221–2229 (1992).

[8] S. Maerivoet, B. De Moor, "Cellular automata models of road traffic", *Physics Reports*, **419** (1), 1–64 (2005).

[9] Th. Chmura, B. Herz, F. Knorr, Th. Pitz, M. Schreckenberg, "A simple stochastic cellular automaton for synchronized traffic flow", *Physica A: Statistical Mechanics and its Applications*, **405** (1), 332-337 (2014).

[10] A.P. Buslaev, A.G. Tatashev M.V. Yashina, "On cellular automata, traffic and dynamical systems in graphs", *Int. J. of Eng. & Techn.*, **7** (2.28), 351–356 (2018).

[11] B. Kerner, S. Klenov, M. Schreckenberg, "Simple cellular automaton model for traffic breakdown, highway capacity, and synchronized flow", *Phys. Rev. E,* **84,** 046110 (2011).

[12] B. Kerner, S. Klenov, G. Hermanns, M. Schreckenberg, "Effect of driver over-acceleration on traffic breakdown in three-phase cellular automaton traffic flow models", *Physica A: Statistical Mechanics and its Applications*, **392** (18), 4083-4105 (2013).

[13] B. Kerner, *The Physics of Traffic*, Springer, Berlin, (2004).

[14] H. Yang, J. Lu, X. Hu, J. Jiang, "A cellular automaton model based on empirical observations of a driver's oscillation behavior reproducing the findings from Kerner's three-phase traffic theory", *Physica A: Statistical Mechanics and its Applications*, **392**, 4009-4018 (2013).

[15] H. Jiang, Zh. Zhang, Q. Huang, P. Xie, "Research of vehicle flow based on cellular automaton in different safety parameters", *Safety Science*, **82**, 182-189 (2016).

[16] X. Li, J.-Q. Sun, "Effects of turning and through lane sharing on traffic performance at intersections", *Physica A: Statistical Mechanics and its Applications*, **444**, 622-640 (2016).

[17] K. Gao, R. Jiang, B.-H. Wang, Q.-S. Wu, "Discontinuous transition from free flow to synchronized flow induced by short-range interaction between vehicles in a three-phase traffic flow model", *Physica A: Statistical Mechanics and its Applications*, **388**, (15–16), pp. 3233-3243 (2009).

[18] M.E. Lárraga, L. Alvarez-Icaza, "Cellular automaton model for traffic flow based on safe driving policies and human reactions", Physica A: *Statistical Mechanics and its Applications*, **389**, (23), 5425-5438 (2010).

[19] J.S.L. Combinido, M.T. Lim, "Modeling U-turn traffic flow", *Physica A: Statistical Mechanics and its Applications*, **389** (17), 3640-3647 (2010).

[20] H.B. Zhu, "Numerical study of urban traffic flow with dedicated bus lane and intermittent bus lane", *Physica A: Statistical Mechanics and its Applications*, **389** (16), 3134-3139 (2010).

[21] J. Vasic, J. Heather, H.J. Ruskin, "Cellular automata simulation of traffic including cars and bicycles", *Physica A: Statistical Mechanics and its Applications*, **391** (8), 2720-2729 (2012).

[22] S.V. Polyakov, "Exponential finite-difference schemes for diffusion-convection equation", *Mathematica Montisnigri,* **26**, 29-44 (2013).

[23] A. Galanina, A. Favorskiy, "Local two-dimensional perturbations evolution in small-conductivity gas flow in magnetic field", *Mathematica Montisnigri*, **27**, 53-63 (2013).

[24] A.G. Churbanov, O. Iliev, V.F. Strizhov, P.N. Vabishchevich, "Numerical simulation of oxidation processes in a cross-flow around tube bundles", *Applied Mathematical Modelling*, **59**, 251-271 (2018).

[25] A.E. Bondarev, "On the construction of the generalized numerical experiment in fluid dynamics", *Mathematica Montisnigri*, **42**, 52-64 (2018).

[26] M.A. Trapeznikova, N.G. Churbanova, A.A. Lyupa, "Simulation of three-phase fluid flow in a porous medium with account of thermal effects", *Mathematica Montisnigri*, **33**, 105-115 (2015).

[27] M. Treiber, A. Kesting, *Traffic Flow Dynamics. Data, Models and Simulation,* Springer, Berlin-Heidelberg, (2013).

[28] H. Ge, R.J. Cheng, L. Lei, "The theoretical analysis of the lattice hydrodynamic models for traffic flow theory", *Physica A: Statistical Mechanics and its Applications*, **389** (14), 2825-2834 (2010).

[29] G. Zhang, D. Sun, W. Liu, M. Zhao, S. Cheng, "Analysis of two-lane lattice hydrodynamic model with consideration of drivers' characteristics", *Physica A: Statistical Mechanics and its Applications*, **422**, 16-24 (2015).

[30] G. Peng, Ch. Liu, M. Tuo, "Influence of the traffic interruption probability on traffic stability in lattice model for two-lane freeway", *Physica A: Statistical Mechanics and its Applications*, **436**, 952- 959 (2015).

[31] J.-L. Cao, Zh.-K. Shi, "Analysis of a novel two-lane lattice model on a gradient road with the consideration of relative current", *Communications in Nonlinear Science and Numerical Simulation*, **33**, 1-18 (2016).

[32] J. Zhou, H.L. Zhang, C.P. Wang, Z.K. Shi, "A new lattice model for single-lane traffic flow with the consideration of driver's memory during a period of time", *Int. J. of Modern Physics C*, **28** (7), 1750086 (2017).

[33] D. Jin, J. Zhou., H.L. Zhang, C.P. Wang, Z.K. Shi, "Lattice hydrodynamic model for traffic flow on curved road with passing", *Nonlinear Dynamics*, **89** (1) 107-124 (2017).

[34] R. Kaur, S. Sharma, "Analysis of driver's characteristics on a curved road in lattice model", *Physica A: Statistical Mechanics and its Applications*, **471**, 59-67 (2017).

[35] A.B. Sukhinova, M.A. Trapeznikova, B.N. Chetverushkin, N.G. Churbanova, "Two-dimensional macroscopic model of traffic flows", *Mathematical Models and Computer Simulation*, **1** (6), 669–676 (2009).

[36] B.N. Chetverushkin, *Kinetic Schemes and Quasi-Gas Dynamic System of Equations,* CIMNE, Barcelona, (2008).

[37] A. Chechina, N. Churbanova, M. Trapeznikova, "Reproduction of experimental spatio-temporal structures in traffic flows using mathematical model based on cellular automata theory", *Periodicals of Engineering and Natural Sciences*, **7** (1), 76–81 (2019).

[38] A. Chechina, N. Churbanova, M. Trapeznikova, A. Ermakov, M. German, "Traffic flow modeling on road networks using cellular automata theory", *Int. J. of Engineering & Technology*, **7** (2.28) 225–227 (2018).

[39] A. Chechina, N. Churbanova, M. Trapeznikova, "Multilane traffic flow modeling using cellular automata theory", *EPJ Web of Conferences*, **173**, 06003 (2018).

[40] A.A. Samarskii, *The Theory of Difference Schemes,* CRC Press, (2001).

[41] P.A. Sokolov, I.V. Shkolina, M.A. Trapeznikova, A.A. Chechina, N.G. Churbanova, "Modelirovanie dvizheniya avtotransporta na osnove KGD sistemy` uravnenij s ispol`zovaniem superkomp`yuterov", *T-Comm*, **13** (6), 46-52 (2019).

[42] KIAM – The official site of Keldysh Institute of Applied Mathematics, "Hybrid computational cluster MVS-Express" available at: http://www.kiam.ru/MVS/resourses/mvse.html. (Accessed November 19, 2019)

[43] Aimsun Transport Simulation Systems https://www.aimsun.com/ (Accessed November 19, 2019)

FEATURES OF THE PROCESSES OF ELASTIC DEFORMATION IN CUBIC CRYSTALS

E. A. STREBKOVA[1,2*], M. N. KRIVOSHEINA[1,2] AND YA. V. MAYER[1,2]

[1]Institute of Strength Physics and Material Science of the Siberian Branch of RAS
Akademicheskii 2/4, 634021 Tomsk, Russia

[2]Tomsk State University, Lenina Avenue 36, 634050 Tomsk, Russia

*Corresponding author. E-mail: elenatuch@yandex.ru

Summary. The processes of elastoplastic deformation in single-crystal alloys characterized by cubic symmetry of properties are investigated. Using the heat-resistant single-crystal alloy VZhM8 used to create gas turbine engine blades by directional crystallization as an example, the dependences of deformation processes on the orientation of loading directions with respect to crystallographic axes are shown. Significant anisotropy of mechanical properties, including the presence of negative Poisson's ratios, in heat-resistant nickel alloys is maintained up to a temperature of 1150 °C. Therefore, over the entire range of operating temperatures, the propagation velocities of elastic and plastic waves in single-crystal heat-resistant nickel alloys depend on the propagation direction. On the example of a VZhM8 single-crystal alloy under dynamic loading in a three-dimensional formulation, the differences in the processes of deformation realized in a single crystal under loading along the [011], [111] and [001] axes are investigated.

1 INTRODUCTION

The mechanical properties of anisotropic materials, which include single crystals [1] with cubic symmetry properties, depend on the direction. When they are loaded in some directions, a common feature is auxeticity (deformation of the same sign in the direction perpendicular to the direction of loading). In single crystals with cubic symmetry of properties [2–9], elastic properties in the plane (011) are traditionally subject to investigation. This is due to the presence of negative values of Poisson's coefficients (auxeticity) in some planes, as well as values exceeding 0.5 and even 1.5 for some types of single crystals. Therefore, the processes of elastic deformation under loading of single crystals along the axis [011] have a number of features. The problems of single crystal deformation with cubic symmetry of properties under dynamic loading conditions [10] are considered, for example, single-crystal VZhM8 based on nickel, with face-centered lattice. In materials with cubic symmetry of properties in the (011) plane, the elastic properties coincide only when the axes are rotated by an angle of 90°; for any other angles of rotation in the (011) plane, the elastic properties are different. Therefore when the shock loading direction changes relative to the crystallographic axes of single crystals with cubic symmetry

of properties, as well as when the computational coordinate system rotates in any plane relative to the crystallographic axes, the wave pattern of deformation changes. Turbine blades of heat-resistant nickel alloys are made from such materials. VZhM8 V generation single-crystal alloy, created for use by gas turbine engine blades, is characterized by significant anisotropy of elastic properties, plasticity, creep, short-term and long-term strength, high-cycle and low-cycle fatigue, and crack resistance [11]. Alloy VZhM8 contains Cr—vol 3%, Mo—vol 3.5%, W—vol 4.2%, Re—vol 6.3%, Ta—vol 6%, Al—vol 5.7%, Co—vol 5.5%, Ru—vol 6%.

The single-crystal alloy VZhM8 has a dendritic structure. It has a heterophase structure. The rhenium-containing alloy is additionally alloyed with ruthenium to stabilize the phase composition. All mechanical characteristics have their own anisotropy [12], which significantly depends on temperature. Aircraft engine blades are grown in such a way that their longitudinal axis coincides with the crystallographic direction [001]. This is determined by the need to minimize the magnitude of the Young's modulus and, consequently, the magnitude of thermal stresses in the direction of the centrifugal forces. The azimuthal orientation of the single-crystal alloy with respect to the blade geometry is not controlled [13–15]. To study the mechanical properties in the [001], [011] and [111] directions in single crystal alloys, sample castings are obtained using seed single crystals of Ni–W alloy. The samples have a cylindrical shape; the longitudinal axis of the samples coincides with one of the directions: [001], [011] and [111]. Poisson's coefficients, Young's modulus under tensile conditions at different temperatures [16], as well as plasticity and strength characteristics are investigated in the obtained samples. The values of elastic and plastic properties of the VZhM8 alloy obtained in full-scale experiments in the directions [001], [011] and [111] in [17] were used in modeling the processes of elastic and plastic deformations.

Using the example of solving a test problem (Taylor test) with different orientations of the crystallographic axes of a single crystal with cubic symmetry properties relative to the cylinder axis in a three dimensional formulation, features of the deformation processes characteristic of auxetic materials are shown. These studies are needed to corrected the mathematical models used to process the results of field experiments used to study the dynamic properties of materials [18, 19]. The values of the propagation velocities of elastic waves depending on the direction in anisotropic and in particular auxetic materials play an important role in such field experiments.

The paper presents the results of numerical simulation of spall fracture of a target from a VZhM8 alloy for the case of coincidence of the direction of shock loading with the [011] axis and it is shown that in this case a non-axisymmetric deformation process occurs in the target. From the solution of the problem of shock loading of the cylinder along the [011] direction the reason of this asymmetry is clear. In the study of the deformation processes for the three cases of loading of the cylinders against a rigid wall and shock loading targets carried out nu-

merically by the dynamic finite element method using original programs [20, 21]. The aim of the work is to study the processes of elastic-plastic deformation in materials characterized by cubic symmetry of mechanical properties under dynamic loads. The influence of the presence of negative Poisson's coefficients in the elastic properties of cubic single crystals on the implementation of various processes of elastic-plastic deformation depending on the directions of shock loading relative to the crystallographic axes of single crystals is shown. A mathematical model of elastic-plastic modeling of anisotropic materials is applied, taking into account the correspondence of uniform bulk deformation to anisotropic stress.

2 MATHEMATICAL STATEMENT OF THE PROBLEM

Dynamic loading of an anisotropic solid is modeled within the framework of continuum mechanics using the continuity equation and equations of motion [22] in a three dimensional formulation: continuity equation

$$\frac{\mathrm{d}\rho}{\mathrm{d}t} + \rho \mathrm{div}\bar{v} = 0, \tag{1}$$

continuum motion equations

$$\rho \frac{\mathrm{d}v^k}{\mathrm{d}t} = \frac{\partial \sigma^{ki}}{\partial x_i} + F^k, \tag{2}$$

where ρ is the medium density; v is speed vector; F^k are the mass vector components; σ^{ij} are the contravariant components of the symmetric stress tensor. The components of the symmetric strain rate tensor (e_{ij}) were calculated as follows $e_{ij} = (\nabla_i v_j + \nabla_j v_i)/2$, where v_j are the velocity vector components; $i, j = x, y, z$. The elastic deformation of an anisotropic material is carried out using the values of total stresses and rates of total deformations and is described by the generalized Hook's law:

$$\mathrm{d}\sigma_{ij}/\mathrm{d}t = C_{ijkl}e_{kl}, \tag{3}$$

where C_{ijkl} are the components of the elastic constant tensor in the calculated coordinate system. The calculations were carried out using a mathematical model that includes the decomposition of the total stress tensor into the deviator part and the "anisotropic" hydrostatic stress [21]:

$$\sigma_{ij} = S_{ij} - P_e \lambda_{ij}, \tag{4}$$

where S_{ij} are the total stress deviator components, λ_{ij} is the generalized Kronecker symbol, P_e is the mean pressure. In the field of elastic deformations $S_{ij} = C_{ijkl}\varepsilon_{kl}$, $\lambda_{ij} = C_{ijkl}\delta_{kl}/(3K_a)$, $K_a = C_{ijkl}\delta_{ij}\delta_{kl}/9$, $P_e = \varepsilon_V C_{ijkl}\delta_{ij}\delta_{kl}/3$, where K_a is the generalized bulk strain modulus, δ_{kl} is the Kronecker symbol, ε_{kl} are the deformation deviator components, C_{ijkl} are the elastic constants defined in directions that coincide with the directions of the calculated coordinate system, ε_V is volumetric deformation of anisotropic medium. In the field of elastic deformations

$\varepsilon_V = \varepsilon_{11} + \varepsilon_{22} + \varepsilon_{33}$. In the field of plastic deformations $\varepsilon_V = (V - V_0)/V_0$. The volumetric deformation of the anisotropic medium does not change, when the direction of the deformation changes, but due to different compressibility factors of the material in different directions, it causes anisotropic hydrostatic stress in cases when λ_{ij} is not equal to one.

Using of numerical calculations in the field of elastic deformations of the decomposition of the total stress tensor in the form of (4) is equivalent to calculations in full stresses. The total stresses in the field of plastic deformations were also calculated by formula (4). Those in the present work, this approach is extended to the region of plastic deformations and it was assumed that the pressure anisotropy coincided in the region of elastic and plastic deformations. When modeling plastic deformation of anisotropic material, the average pressure P_e in the material was calculated using the Mie–Grüneisen equation as a function of specific internal energy E and current density:

$$P_e = \sum_{n=1}^{3} K_n \left(\frac{V}{V_0} - 1 \right)^n \left[1 - K_0 \frac{(V/V_0 - 1)}{2} \right], \tag{5}$$

where K_0, K_1, K_2, K_3 are the material constants, V, V_0 are the current and initial volumes. In the field of plastic deformations, P_e was also multiplied by the values of the coefficients λ_{ij}. The components of the total stress deviator were calculated using the flow theory. The associated law of flow is used to calculate the plastic deformation in the form

$$d\varepsilon_{ij}^p = d\lambda \frac{\partial F}{\partial \sigma_{ij}}, \tag{6}$$

the parameter $d\lambda = 0$ at elastic deformation, at plastic is always positive, is defined by means of a condition of plasticity, $d\varepsilon_{ij}^p$ are the components of plastic deformation, F is the plasticity function.

The Mises–Hill plasticity condition, written through stress deviators for transtropic material with regard to isotropic hardening, has the form [23]

$$F(S_{ij}, R) = \frac{S_{11}^2}{r_1^2} + \frac{S_{22}^2}{r_2^2} + \frac{S_{33}^2}{r_3^2} + \frac{S_{12}^2}{r_4^2} + \frac{S_{31}^2}{r_5^2} + \frac{S_{23}^2}{r_6^2} - R^2 = 0, \tag{7}$$

where r_i is determined through yield limits for tensile and shear transtropic material, R is the isotropic hardening function.

From the experimental studies presented in [23] it is known that the function R characterizing isotropic hardening is invariant to the type of stress state, is determined from experiments on simple loading and depends linearly on the accumulated plastic deformation ε^p: $R(\varepsilon^p) = 1 + \xi \varepsilon^p$, where $\varepsilon^p = \int \left| d\varepsilon_{kl}^p \right|$, $k, l = 1, 2, 3$.

The elastoplastic material deformation model is supplemented by a fracture criterion containing the ultimate porosity of the material. Spalling of the sample is considered as a process of merging micropores in a plastically deformed material under the action of tensile stresses. By averaging over the volume, we pass from the volume of the porous medium to the solid medium with the averaged density and the equation of state of the porous material.

Assuming that the change in pore volume depends on the plastic characteristics of the material and does not depend on the viscosity characteristics, an equation is solved that is the equality of the pressure increment obtained by the equation of state of the matrix material and due to the growth of the spherical pores. As a measure of damage, the porosity parameter α introduced by Herrmann. The porosity parameter in the Herrmann model is the ratio of the specific volume $(V = V_{\mathrm{m}} + V_{\mathrm{p}})$ of the porous medium to the specific volume of the solid matrix material (starting material):

$$\alpha = V/V_{\mathrm{m}}. \tag{8}$$

In modeling of the detachment fracture, an equation was used to determine the porosity parameter, obtained from the equilibrium condition of the spherical pore under the action of the applied pressure, in the following form:

$$\alpha P_e + \alpha_{\mathrm{s}} \ln(\alpha/(\alpha - 1)) = 0, \tag{9}$$

where $\alpha_{\mathrm{s}} = 2\sigma_{\mathrm{sm}}/3$. This equation is applied provided that

$$P_e < \alpha_{\mathrm{s}} \ln(\alpha/(\alpha - 1)), \tag{10}$$

otherwise the change in porosity does not occur in time, i.e.

$$\mathrm{d}\alpha/\mathrm{d}t = 0. \tag{11}$$

The moment of completion of the local macroscopic destruction of the material is the achievement of porosity of the critical value. The elastic-plastic deformation of the isotropic projectile material was carried out using the Prandtl–Reiss model. The stresses defined in the element, rigidly rotated in space, are recalculated using the Jaumann derivative

$$\frac{\mathrm{D}\sigma_{ij}}{\mathrm{D}t} = \mathrm{d}\sigma_{ij}/\mathrm{d}t - \sigma_{ik}\omega_{jk} - \sigma_{jk}\omega_{ik}, \tag{12}$$

where $\omega_{ij} = 0.5\left(\partial v_j/\partial x_i - \partial v_i/\partial x_j\right)$.

3 COMPUTATIONAL EXPERIMENT

The impact of a cylinder with a height of 50 mm and a radius of 5 mm from a single crystal alloy VZhM8 on a rigid target with an initial velocity of 50 m/s is considered. The axis of symmetry of the cylinder in each problem coincides with one of the three axes in which the elastic, plastic, and strength properties in cubic crystals are traditionally investigated: [111], [001], and [011]. In the first case, all three calculated axes coincide with the directions [111]. In the second case, the direction of the axis of symmetry of the cylinder and the other two coincides with the direction of the crystallographic axes [001], [010] and [100]. In the third case, the axis of symmetry of the cylinder coincides with the direction [011], and the other two axes of the calculated coordinate system with [100] and [0$\bar{1}$1]. Those, in the first and in the second cases, axisymmetric problems are solved, and in the third case, a three-dimensional stress state is realized in the cylinder. The differences in each case of the axes of symmetry of a single crystal alloy relative to the axis of symmetry of the cylinder leads to the fact that in all three problems the values of technical elastic constants and velocities of propagation of elastic waves in the direction of each coordinate axis have different values. Only elastic deformations are considered, in order to determine their contribution in cases of development of elastoplastic deformations. The ratios of the strain values are analyzed, as well as their sign in three cases of different orientations of the VZhM8 crystallographic axes with respect to the direction of impact.

In the first case, the values of technical elastic constants are: $E = 250.6$ GPa, $v = 0.28$, $G = 46.7$ GPa, longitudinal wave speeds $v_L = 6548$ m/s, shear wave speeds $v_S = 2646$ m/s.

In the second case, the values of technical elastic constants are: $E = 102.2$ GPa, $v = 0.426$, $G = 118.7$ GPa longitudinal wave speeds $v_L = 5539$ m/s, shear wave speeds $v_S = 3619$ m/s.

In the third case, the values of technical elastic constants differ in three mutually perpendicular directions: $E_x = 102.2$ GPa, $E_y = E_z = 193.2$ GPa, $G_{xy} = G_{zx} = 118.7$ GPa, $G_{yz} = 35.8$ GPa, $v_{xy} = 0.788$, $v_{yz} = -0.14$, $v_{zx} = 1.489$, longitudinal wave speeds $v_L = 6311$ m/s, shear wave speeds $v_{S1} = 3619$ m/s and $v_{S2} = 1989$ m/s [13]. In this case, the cylinder material is characterized by auxeticity; the other two Poisson ratios exceed the value of 0.5. Material density $\rho_0 = 9060$ kg/m^3. The axis of symmetry of the cylinder in all three cases coincides with the axis OZ. The shock loading of a cylindrical body made of VZhM8 alloy with a steel projectile with an initial velocity of 600 m/s is simulated. The elastoplastic deformation of the isotropic material of the projectile is determined using the Prandtl–Reuss model. Plastic deformation in the material of an target is determined using a flow model with isotropic hardening. The Mises–Hill function is used as a function of plasticity for anisotropic media. The yield strength at a temperature of 800 °C is 934 MPa in the [011] direction and 1050.8 MPa in the [001] direction. The spallation of a cylindrical body from a VZhM8-target alloy is modeled on the base of a mathe-
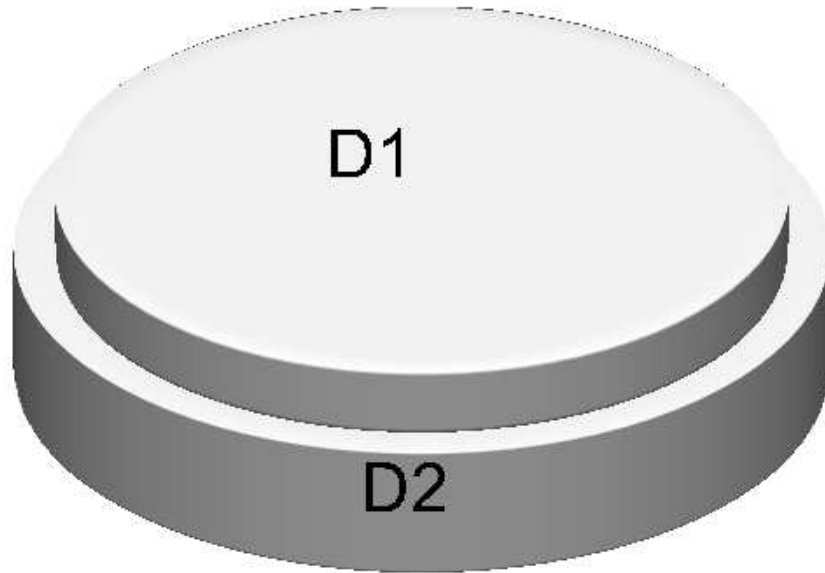
Figure 1: The initial configuration of the projectile and target.

matical model modified for anisotropic media [24]. The element is considered to be destroyed and all stress components in it are equated to zero when a local stretch of the grid element is more than 30%. This simulates the appearance of a spall crack in the material of a target with its shock loading. Consider the interaction of two bodies in the general, three-dimensional case in the Cartesian coordinate system XYZ (figure 1).

The calculation method used is the finite element method modified by G. R. Johnson for solving problems in dynamic formulation [20]. It has first order accuracy in time and in space. Discretization of the computational domains was carried out using simplex approximation. Boundary conditions of impact—loading of the cylinder on a rigid wall. Each body occupies an area D_i ($i = 1, 2$), bounded by the surface Q_i, respectively. The velocity vector of the striker at the initial moment of time has a value V_0 and its direction coincides with the longitudinal axis of the striker. Surfaces Q_1 and Q_2 are stress-free, Q_3—the contact surface between bodies. Each material is in a non-stressed undeformed homogeneous state. Initial conditions ($t = 0$): $u = V_0$, $\sigma_{ij} = E = w = v = 0$, with $x, y, z \in D_1(i = x, y, z)$, $\sigma_{ij} = E = w = v = u = 0$, with $x, y, z \in D_2(i = x, y, z)$, $\rho = \rho_i$, with $x, y, z \in D_i, i = 1, 2$, Where u, v, w are the components of the velocity vector along the axes XYZ are respectively. The boundary conditions are as follows: on free

surfaces the conditions are fulfilled $T_{nn} = T_{ns} = T_{nb} = 0$, friction-free sliding conditions are re-alized on the contact surfaces $T_{nn+} = T_{nn-}$, $T_{nb+} = T_{nb-} = T_{ns+} = T_{ns-} = 0$, $v_{n+} = v_{n-}$. Here, n is the unit vector of the normal to the surface at the point under consideration, b and s are the unit vectors tangent to the surface at this point, T_n is the force vector on the site with the normal n, v is the velocity vector. The lower indices of the vectors T_n and v mean projections on the corresponding vectors of the basis; the plus "+" characterizes the value of parameters in the material at the upper boundary of the contact surface, the minus "−"—at the bottom.

Discretization of computational domains. To construct a uniform numerical grid of nodes in the computational domain, an algorithm for constructing a grid in a Cartesian coordinate system is used [25]. Simplex elements—tetrahedra—were used to construct the grid in a three-dimensional coordinate system. The mass of the element was evenly distributed between the four nodes. In cases where a node belonged to several elements, the total mass, concentrated in the i-th node was equal to one-fourth of the mass of all elements containing this node.

4   THE DISCUSSION OF THE RESULTS

Figure 2 shows a decrease in the length of the cylinders, for three cases of orientation of the crystallographic axes relative to the axis of symmetry of the cylinder. Curve 1 shows that due to the maximum values of the elastic properties along the [111] direction, the oscillations of the cylinder length have a shorter period. For the considered ratio of the length of the cylinder to its diameter, the oscillations of the length of the cylinder are determined by the values of the rod ones, not the longitudinal speeds. Figure 2 shows that there is a clear relationship between the periods of oscillations of the lengths of the cylinders and the values of the velocities of propagation of longitudinal waves. In the case of orientation along the axis of symmetry of the cylinder, the direction of the [001] crystal changes the cylinder length to the maximum and have a maximum oscillation period (curve 2, figure 2). In all three cases, the times of arrival of the wave to the free surface of the cylinder are different due to differences in the velocities of propagation of longitudinal waves. In the case of orientation along the axis of symmetry of the cylinder, the direction of the crystal [011] (curve 3, figure 2) exceeds the maximum change in the length of the cylinder by 17% in the case of the direction [111] along the axis of the cylinder.

Auxeticity of anisotropic materials is manifested in directions perpendicular to the direction of loading. In figure 3, curve 3 shows the elastic variation of the cylinder radius along the *OY* axis at a height of 1 mm from the contact surface of the cylinder for the case of direction [011] along the axis of the cylinder with time. Until the cylinder is separated from the target, elastic oscillations of the magnitude of the cylinder radius demonstrate compressive deformation. After the cylinder is separated from the target, changes in the radius value occur around the original value. When the directions [111] or [001] coincide, the magnitudes of changes in the radiuses of
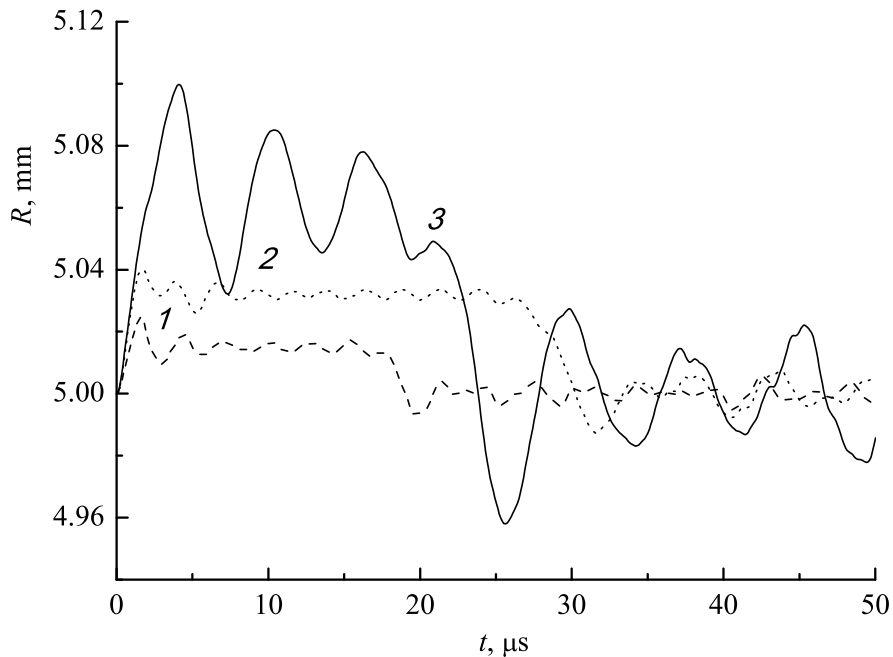
Figure 2: The change of the cylinder radius in time along the axis *OX*, for the cases: *1*—the axis of symmetry of the cylinder is directed along the [111] axis; *2*—along the [001] axis; *3*—along the [011] axis.

the cylinders at a height of 1 mm from the contact surface demonstrate only tensile deformation up to cylinder bounce. The periods and amplitudes of oscillations of the radiuses of the cylinders in these cases are much smaller. The presence of a negative value of the Poisson coefficient in the plane formed by the loading direction and the axis *OY* manifests itself in the compression of the cylinder along the axis *OY*, but only during the contact time of the cylinder and target.

The elastic change in the cylinder radius is also at a height of 1 mm from the contact surface of the cylinder, but in the perpendicular direction, shown in figure 4. Curve 3 shows the change in the cylinder radius over time, which significantly exceeds the change in the radiuses of the cylinders for the cases of curves 1 and 2. In the plane formed by the direction of loading and the axis *OX* for the material oriented in the cylinder along the direction [011] the Poisson's ratio is greater than 0.5, i.e. exceeds the maximum value for isotropic materials. Therefore up to a cylinder bounce from an target in the case of [011] along the *OX* axis, an increase in radius 2 times greater than in the case of orientation along the cylinder axis of the single crystal [001] is observed, with Poisson's ratio equal to 0.426 (curve 2, figure 4).

Such a ratio of changes in the radiuses of the cylinders for three cases of orientation of the crystallographic axes relative to the axes of symmetry of the cylinders is observed at any distance from the contact to the free surfaces of the cylinders. The obtained results explain the reason why a non-symmetric deformed state is realized in the target from single crystal
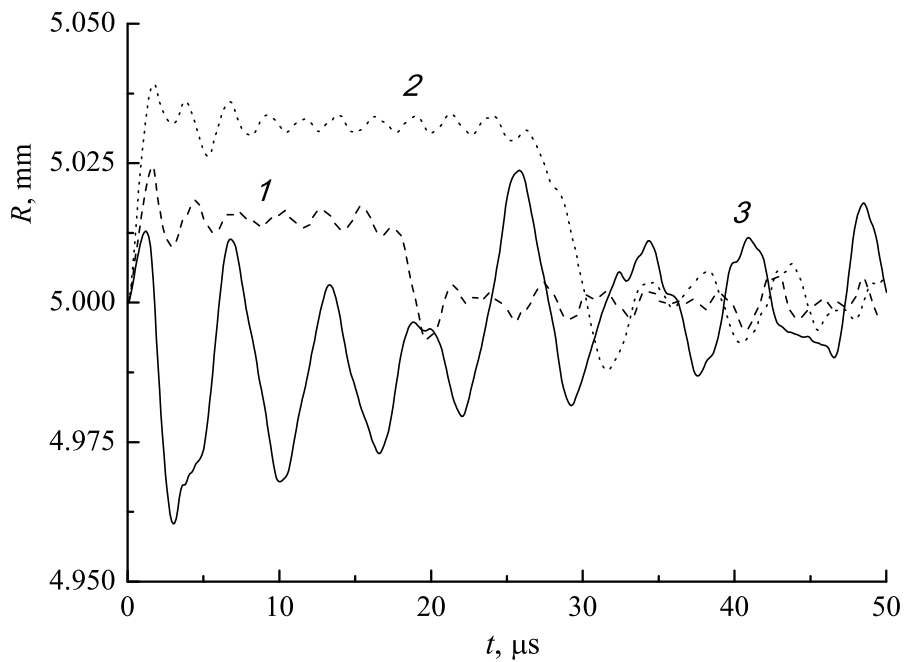
Figure 3: The change in the cylinder radius over time along the *OY* axis, for the cases: *1*—the axis of symmetry of the cylinder is directed along the [111] axis; *2*—along the [001] axis; *3*—along the [011] axis.

alloy VZhM8 with its shock loading in the direction [011]. Target from single crystal alloy VZhM8 has a cylindrical shape but its height is 2 mm and a radius of 7.5 mm. Its shock loading was carried out by a steel projectile with a height of 1 mm and a radius of 7.45 mm with an initial speed of 600 m/s. In this case a problem is numerically modeled in a three-dimensional statement. It is realized in field experiments in the study of dynamic characteristics. The process of deformation in the target includes elastic, plastic deformation as well as spall fracture. The degree of deviation from axisymmetric deformation in an target can be illustrated by changing the magnitude of the target radii on the lateral surfaces along the axis *OX* and *OY* (figure 5).

Since the yield strength of the VZhM8 alloy in the direction of the *OY* axis is less than in the direction of the *OX* axis it was logical to expect that a larger increase in radius would be observed in the direction of the *OY* axis. The figure shows that by the time point of 1 μs, when the spalling destruction has already occurred, the target radius in its middle part along the *OX* axis increased by 0.19 mm, and in the *OY* axis direction—only by 0.13 mm. As shown in the analysis of the process of elastic deformation under shock loading of the cylinder along the same direction [011], the missing part of the deformation in the direction of the *OY* axis is determined by the auxetism of the VZhM8. That is the missing part of the deformation in the direction of the *OY* axis is determined by the compressive elastic deformation due to the negative value of the Poisson's ratio. This calculation showed that in the study of the dynamic
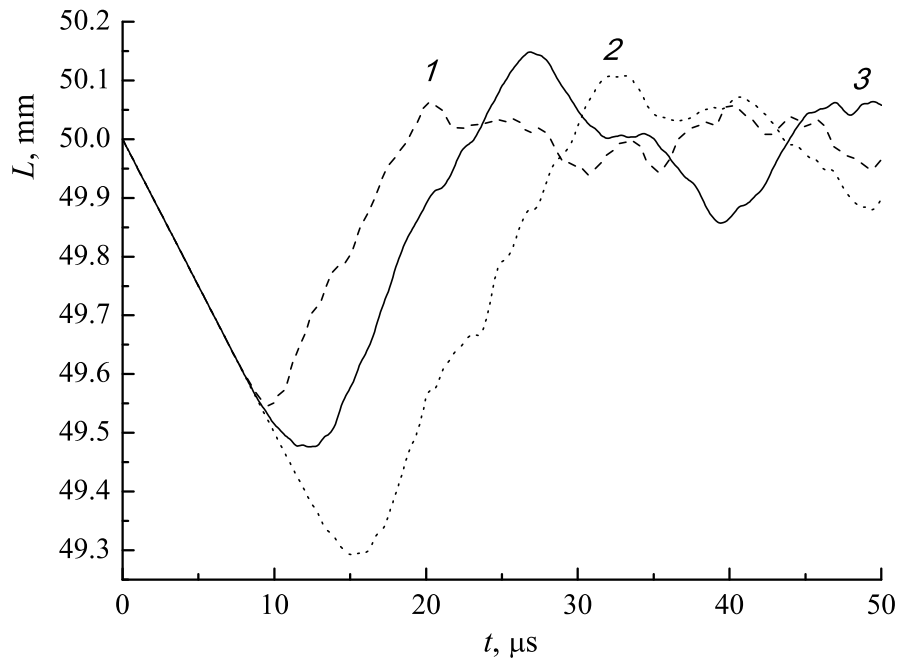
Figure 4: The change in the height of the cylinder, for the cases: *1*—the axis of symmetry of the cylinder is directed along the [111] axis; *2*—along the [001] axis; *3*—along the [011] axis.

properties of auxetic material with an initial shock loading speed of 600 m/s until the moment of spall fracture the elastic properties to a greater extent determine the process of elastoplastic deformation of the target. The type and location of the spall crack in the target is shown in figure 6.

The distribution of relative volumes ($V_v = V/V_0$) of elements is shown (the ratio of the current volume of the element of the computational grid to the initial one) in the section of the target. The figure shows that in the area where the crack was formed the volume of elements on average increased 1.5–1.75 times. The cross section of the projectile and target is made in the *OZY* plane: the *OZ* axis is directed upwards, the loading was simulated along it; *OY* axis is perpendicular to it. Dark blue targets areas are areas where is no stretch. In areas from blue to red there are stretch areas, where the relative volume is greater than 1.
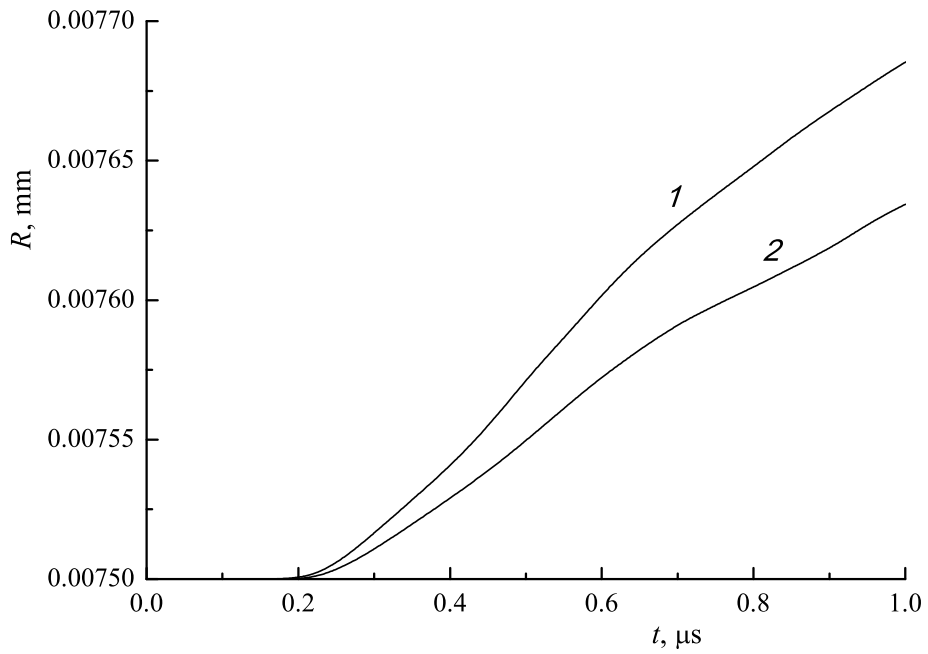
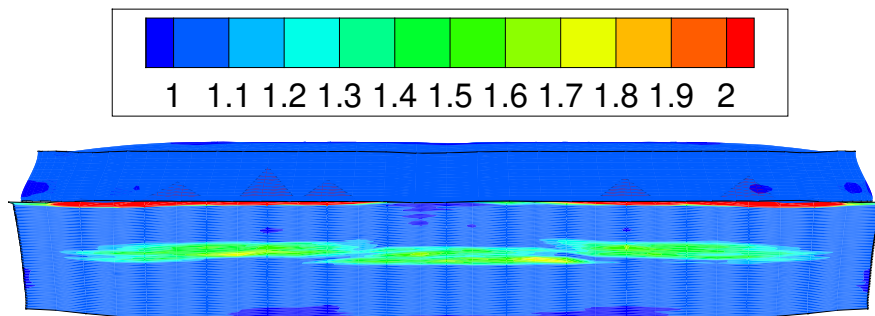Figure 5: The change in the radius of the target in time: *1*—along *OX* axis; *2*—along *OY* axis.

Figure 6: Distribution of the relative volume of the material in the cross section *OZY* of the projectile and target at the moment 0.85 μs.

5 CONCLUSIONS

On the example of a heat-resistant single-crystal alloy VZhM8, characterized by a significant anisotropy of mechanical properties, including auxeticity, significant differences in the processes of elastic-plastic deformation under loads along the axis [011], [111] and [001] are shown. To demonstrate the features of the elastic deformation processes for the VZhM8 alloy, the solutions of the Taylor test (cylinder impact on a non-deformable wall) obtained numerically in a three-dimensional formulation are shown. When modeling the shock loading of a thin cylindrical target made of a single-crystal alloy VZhM8 along the direction [011], it is shown that a three-dimensional elastic-plastic deformation is realized in the target, due to the auxeticity of the target material.

REFERENCES

[1] O. N. Koroleva, A. V. Mazhukin, and V. I. Mazhukin, "Modeling of silicon characteristics in the semiconductor-metal phase transition region", *Math. Montis.*, **41**, 73–90 (2018).

[2] T. C. T. Ting and D. M. Barnett, "Negative Poisson's ratios in anisotropic linear elastic media", *J. Appl. Mech.*, **72**, 929–931 (2005).

[3] T. P. Hughes, A. Marmier, and K. E. Evans, "Auxetic frameworks inspired by cubic crystals", *Int. J. Solids Struct.*, **47**, 1469–1476 (2010).

[4] G. N. Greaves, A. L. Greer, R. S. Lakes, and T. Rouxel, "Poisson's ratio and modern materials", *Nature Materials*, **10**, 823–837 (2011).

[5] A. C. Branka, D. M. Heyes, and K. W. Wojciechowski, "Auxeticity of cubic materials under pressure", *Phys. Stat. Sol. B*, **248**, 96–104 (2011).

[6] R. V. Goldstein, V. A. Gorodtsov, and D. S. Lisovenko, "Classification of cubic auxetics", *Phys. Stat. Sol. B*, **250**, 2038–2043 (2013).

[7] U. Scharer and P. Wachter, "Negative elastic constants in intermediate valent SmLaS", *Sol. St. Commun.*, **96**, 497–501 (1995).

[8] U. Scharer and P. Wachter, "Brillouin spectroscopy with surface acoustic waves on intermediate valent, doped SmS", *Phys. B*, **244**, 148–153 (1998).

[9] K. E. Evans, M. A. Nkansah, I. J. Hutchinson, and S. C. Rogers, "Molecular network design", *Nature*, **353**, 124–125 (1991).

[10] K. K. Maevskii, "Thermodynamic parameters of mixtures with silicon nitride under shock-wave loading", *Math. Montis.*, **45**, 52–59 (2019).

[11] A. I. Epishin and D. S. Lisovenco, "Ekstremal'nye znacheniya koefficienta Puassona kubicheskih kristallov", *Tech. Phys.*, **86**, 74–82 (2016).

[12] S. V. Ershov, A. A. Garbul, S. G. Pozdnyakov, V. G. Sokolov, and A. G. Voloboy, "Lighting simulation in anisitropic media", *Math. Montis.*, **39**, 42–56 (2017).

[13] A. E. Solovyov, S. A. Golinec, and K. K. Khvatskiy, "Anizotropiya harakteristik uprugosti pri rastyazhenii monokristallicheskih zharoprochnyh nikelevyh splavov", *Trudi VIAM*, **10**, 112–118 (2017).

[14] N. Djordjevic, R. Vignjevic, N. Djordjevic, R. Vignjevic, L. Kiely, S. Case, T. Vuyst, J. Campbell, and K. Hughes, "Modelling of shock waves in fcc and bcc metals using a combined continuum and dislocation kinetic approach", *Int. J. Plast.*, **105**, 211–224 (2018).

[15] E. A. Rodas and R. W. Neu, "Crystal viscoplasticity model for the creep-fatigue interactions in single-crystal ni-base superalloy CMSX-8", *Int. J. Plast.*, **100**, 14–33 (2018).

[16] N. V. Petrushin, O. G. Ospennikova, and E. S. Elutin, "Renij v monokristallicheskih zharoprochnyh nikelevyh splavah dlya lopatok gazoturbinnyh dvigatelej", *Aerospace Engineering and Technology*, **5**, 5–16 (2014).

[17] R. M. Nazarkin, V. G. Kolodochkina, O. G. Ospennikova, and M. R. Orlov, "Izmeneniya mikrostruktury monokristallov zharoprochnyh nikelevyh splavov v processe dlitel'noj ekspluatacii turbinnyh lopatok", *Aerospace Engineering and Technology*, **4**, 9–17 (2016).

[18] K. V. Khishchenko, "Equation of state for magnesium hydride under conditions of shock loading", *Math. Montis.*, **43**, 70–77 (2018).

[19] K. V. Khishchenko, "Equation of state of sodium for modeling of shock-wave processes at high pressures", *Math. Montis.*, **40**, 140–147 (2017).

[20] C. E. Anderson, P. A. Cox, G. R. Johnson, and P. J. Maudlin, "A constitutive formulation for anisotropic materials suitable for wave propagation computer programs", *Comput. Mech.*, **15**, 201–223 (1994).

[21] M. N. Krivosheina, S. V. Kobenko, E. V. Tuch, O. A. Kashin, A. I. Lotkov, and Yu. A. Khon, "Fracture features of anisotropic materials at different impact velocities", *Eur. J. Comput. Mech.*, **26**, 609–621 (2017).

[22] L. I. Sedov, *Mekhanika Sploshnoj Sredy*, Moscow: Nauka, (1976).

[23] V. V. Kosarchuk, B. I. Kovalchuk, and A. A. Lebedev, "Report 1. Opredelyayushchie sootnosheniya", *Problemy prochnosti*, **4**, 50–56 (1986).

[24] J. N. Johnson, "Calculation of plane wave propagation in anisotropic elastic plastic solids", *J. Appl. Phys.*, **43**, 2074 (1972).

[25] M. N. Krivosheina, A. V. Radchenko, and S. V. Kobenko, "Razrushenie ortotropnogo i izotropnogo sfericheskih tel pod dejstviem impul'sa vsestoronnego szhatiya", *Mekhanika kompozicionnyh materialov i konstrukcij*, **7**, 95–102 (2001).

MOLECULAR DYNAMIC CALCULATION OF LATTICE THERMAL CONDUCTIVITY OF GOLD IN THE MELTING-CRYSTALLIZATION REGION

M.M. DEMIN, V.I. MAZHUKIN, A.A. ALEKSASHKINA

Keldysh Institute of Applied Mathematics of RAS, Russia, Moscow.
*Corresponding author. E-mail: vim@modhef.ru

Summary. Of all the metals, gold is the most well-known and widely used material in scientific research, industrial production and, more recently, in biomedicine problems. In the temperature range $300 \leq T \leq 2000$ K, including the region of the melting – crystallization phase transition, the results of modeling the phonon thermal conductivity of gold are presented. Phonon thermal conductivity plays an important role in modeling the mechanisms of interaction of pulsed laser radiation with gold in the framework of the two-temperature continuum model. In the region of the phase transition, overheating-undercooling of the solid phase occurs, the substance changes its structure. These phenomena are associated with changes in the phonon subsystem of gold, therefore, for mathematical modeling of heating-cooling, it is necessary to know the characteristic of heat transfer as the thermal conductivity of the phonon subsystem of gold. Obtaining the temperature dependence of phonon thermal conductivity in such a wide temperature range from experiment is problematic. In this work, phonon thermal conductivity was obtained by the direct non-equilibrium method in the framework of molecular dynamics modeling using the EAM potential.

1 INTRODUCTION

Of all metals, gold is the most well-known and widely used material in scientific research [1], industrial production [2] and, more recently, in biomedicine problems [3,4]. Besides various applications, the specific features of gold are of great fundamental interest in connection with the rapid development of new nanoscale materials [5]. Gold nanoparticles have unique properties [6,7], which served as the basis for their possible use for theranostics in nanomedicine [8].

One of the promising directions in the generation of nanoparticles and nanoclusters is laser ablation of materials by ultrashort (femto-picosecond) pulses [9, 10]. Femto-picosecond ablation occurs under conditions of strong thermodynamic non-equilibrium, which is characterized, in particular, by the presence of two temperatures: electron T_e for the degenerate gas of free electrons and phonon T_{ph} for the crystal lattice. In the problems of mathematical modeling, the presence of two temperatures requires separation and quantitative determination of all thermodynamic and thermophysical characteristics of the material under study. Of all the thermophysical characteristics of metals, the separation and quantitative determination of phonon thermal conductivity was carried out less frequently than others. This was because it was believed that free electrons make the dominant contribution to thermal transfer in metals, while the phonon contribution to the total thermal conductivity was

considered negligible. Moreover, in most cases, knowledge of only the general thermal conductivity of metals was required; therefore, it was not necessary to separate the electronic and phonon thermal conductivity. The interest in quantifying phonon thermal conductivity in metals was stimulated primarily by the need for a deeper understanding of the mechanisms of thermal transfer during nonequilibrium energy transfer in a number of applications, for example, [10, 11].

Significant progress in recent years in the development of numerical methods and computational algorithms allows us to determine the phonon thermal conductivity for the most metals with a sufficient degree of accuracy. Two most common families of methods can be distinguished: classical molecular dynamics (MD) [12,13] and quantum ab-initio methods [14, 15]. In the MD methods, when modeling the properties and processes in metals, the empirical and semi-empirical potentials of the "embedded atom method" (EAM) [16, 17] were obtained using the methods that include ab-initio ones [18]. In EAM potentials, in addition to pair interactions, collective interaction is also taken into account. As a result, the potential energy of the metal is represented as the sum of two potentials: the embedding potential of the i-th atom, which depends on the effective electron density in the region of the center of the atom and the pair potential. The main disadvantages of EAM potentials are not taking into account the phonon-electron interaction and the large number of fitting parameters included in it (up to two dozen). The choice of shape and the selection of parameters in the EAM potential can be carried out using quantum mechanical methods. These methods, implemented in the form of Abinit, VASP, SIESTA, and other software codes, make it possible to calculate the forces acting on each metal particle in a wide temperature range. Not all EAM potentials used allow a good description of both the crystalline and liquid phases of a metal. Therefore, when choosing the potential for atomistic modeling, careful testing of the potential used is necessary.

The ab-initio methods have appeared recently. They are considered the most promising and can be applied to any material. The ab-initio method does not require specifying interparticle potential. Its advantage is the ability to calculate electronic wave functions and electronic spectra. However, the use of small models does not guarantee the receipt of thermodynamic, structural and thermophysical properties with a sufficient degree of accuracy. The increase in model size is associated with high computational costs. Until recently, this was the main limitation that restrained the development and application of the ab-initio method. With the advent of high-performance computing, this limitation is successfully overcome.

The use of ab-initio methods in calculating phonon thermal conductivity allows one to take into account the influence of both phonon-phonon (p-p) and phonon-electron (p-e) interactions, which can significantly increase the reliability of the results. However, the number of calculations of the phonon thermal conductivity of metals and, in particular, gold [19], [20], [21], is currently relatively small. As a rule, all calculations are limited to the solid phase in the temperature range $T \sim (300 - 1000)$ K. There are no systematic results of experimental-theoretical studies of the properties of liquid metals in a wide temperature range (from the beginning of melting to the critical region).

At the same time, the knowledge of the temperature dependences of thermal conductivity is relevant in many aspects of materials science, from the kinetics of fast phase transitions [22], [23] to nanomicro processing of metal samples [24], [25].

The aim of this work is to obtain a quantitative dependence of the phonon thermal conductivity of gold in the temperature range, including the melting region (T ~ 300–2000 K).

The goal was achieved by mathematical modeling, in which the atomistic model was numerically solved by the molecular dynamics method using a computational algorithm based on the finite-difference Verlet scheme [26]. The determination of phonon thermal conductivity in the framework of classical molecular dynamics is a complex problem. To solve it, the two most common approaches are used: the direct nonequilibrium method, which relies on spatial gradients of the type "heat source - sink" [27, 28, 29] and the equilibrium Green-Kubo method [27, 28, 30], associated with the calculation of time integrals of the correlation functions that specify the correlation in the systems with random processes.

In this work, to determine the phonon thermal conductivity of a metal (Au), we chose the direct nonequilibrium method as a more obvious one and requiring less time.

2 STATEMENT OF THE PROBLEM

Direct non-equilibrium method of determination of the phonon thermal conductivity coefficient κ_{lat} is based on the phenomenological relation of Fourier for the heat flux W [31]:

$$W = -\kappa_{lat} \frac{\partial T}{\partial x} \qquad (1)$$

The computational algorithm is constructed according to a scheme close to the experimental measurements of the coefficient κ_{lat} [29, 32]. First, with the help of external heating in the sample, a stationary spatial temperature profile is constructed using the heat source – sink scheme, which provides a stationary heat flux. The presence of a stationary heat flux allows using the phenomenological Fourier relation (1) to determine the coefficient κ_{lat}.

A specific feature of the atomistic representation of processes in a solid sample is the choice of the linear dimensions of the sample (modeling domain), which must satisfy the following requirements.

In the molecular-dynamic implementation of the direct method, it is necessary to monitor the 2 most critical factors.

It is important that a stationary spatial temperature profile is obtained between the heat source and the sink, which is equivalent to obtaining a constant heat flux, with minimal finite size effect on the phonon thermal conductivity. For this, the linear dimensions of the sample should far exceed the average mean free path of phonons. The fulfillment of this condition is hampered by the fact that the dimensions of the computational domain should be of the micrometer scale, which in the calculations corresponds to a large number of atoms, several hundred million [33]. Keeping the computational domain in the nanometer range and performing calculations with a relatively small number of atoms is usually achieved using the scaling procedure [27], [28]. Its essence is as follows. First, using nanoscale calculation regions (along the x direction) of various lengths L_n, a series of calculations of thermal conductivity is carried out for several fixed values of temperature T. Then, the reciprocal dependence of the thermal conductivity $1/\kappa_{lat}$ is constructed with respect to the reciprocal of the length of the simulation region, $1/L_n$, and the thermal conductivity is determined by extrapolating the data $1/L_n \rightarrow 0$ [27]. This procedure is justified by the expression for thermal conductivity obtained from the kinetic theory [27, 29].

In the direct method, large (10^9 - 10^{10} K / m) temperature gradients are used to reduce the temperature fluctuations. Too large temperature gradients can cause large nonlinear response

effects for which the Fourier relation (1) is not applicable. In these cases, it is necessary to control the supply of heat to the source region with a thermostat, in order to determine the allowable value of non-linear distortions.

The calculation of the phonon thermal conductivity of gold was carried out as part of the following computational experiment. A region in the form of a parallelepiped with sizes of 10 × 10 × 40 unit cells, corresponding to 16,000 particles, with periodic boundary conditions in all three directions was considered. For boundary conditions along the x axis, this means that a particle exiting through the upper boundary of the region is replaced by a particle having the same velocity but entering through the lower boundary and vice versa. Gold has a cubic face-centered lattice, the lattice constant is 0.406 nm. The interatomic interaction potential of EAM was used as the interaction potential [18].

The region along the x axis was divided into the number of intervals corresponding to the number of unit cells along this axis, which in turn corresponds to the number of particles. Heating was performed in the first interval of the computational domain, the sink interval was located in the middle of the domain. At each time step, a fixed amount of heat δQ_N was introduced into the heating region, and the same amount was taken from the sink region. The heat flux W was calculated as

$$W = dQ/(SNdt)/2, \tag{2}$$

where $dQ = N \times dt \times \delta Q_N$ is the total released energy, where δQ_N is the energy released during one timestep, N is the number of steps, dt is the timestep size, S is the cross-sectional area. The timestep dt was chosen to be 3fs at low temperature $300 \leq T \leq 1000$K, 2 fs for $1000 < T \leq T_m$, and 1fs for $T > T_m$. The division by 2 is used due to periodic boundary conditions, i.e. heat flow goes in two directions. Then, the resulting temperature gradient was calculated, and the Fourier law (1) was used to obtain thermal conductivity.

3   MODELING RESULTS

Fig. 1 (a), (b) show the time-averaged spatial temperature profiles used to calculate the thermal conductivity. The average temperature is 300 K (Fig. 1 (a)) and 2000 K (Fig. 1 (b)). In a small region (~ 2 nm) in the immediate vicinity of the source, a very strongly nonlinear temperature profile is observed. The same strongly nonlinear temperature profile is also observed near the sink. In the intermediate region, the behavior of the temperature profile is close to a linear dependence. This interval between the heat source and the heat sink is indicated by dashed lines in the graphs (Fig. 1 (a), (b)). This is where the temperature gradients were measured.

To overcome the effects of finite size, the heat flux was determined by a series of calculations. Calculations were carried out for various lengths of the computational domain L_n: 40, 80, 160, 240, and 320 unit cells with a constant cross section of 10 × 10 cells at the same temperature.

The heat flux (2) was determined from the temperature difference between the heating and heat sink areas, for which the instantaneous temperature difference was averaged over the entire calculation time after establishing the stationary distribution. To increase the accuracy of the calculations, the temperature difference was calculated not over the entire interval between the source and the sink, but in its central part with a length of 0.8 of the full length.

To calculate the thermal conductivity from the Fourier law (1), the scaling procedure described above was used. For each temperature value, an inverse dependence of the thermal conductivity $1/\kappa_{lat}$ was constructed with respect to the reciprocal of the length L_n of the calculation region, $1/L_n$, and the thermal conductivity was determined by extrapolating the data $1/L_n \to 0$. In Fig. 2 (a), (b) the dependences of the reciprocal of the thermal conductivity on the reciprocal of the size of the region for two temperatures 300K and 2000K are shown. MD simulation results are shown by a black line with markers.

We consider the scaling procedure using the example of obtaining thermal conductivity for a temperature $T = 300$ K (Fig. 2 (a)).
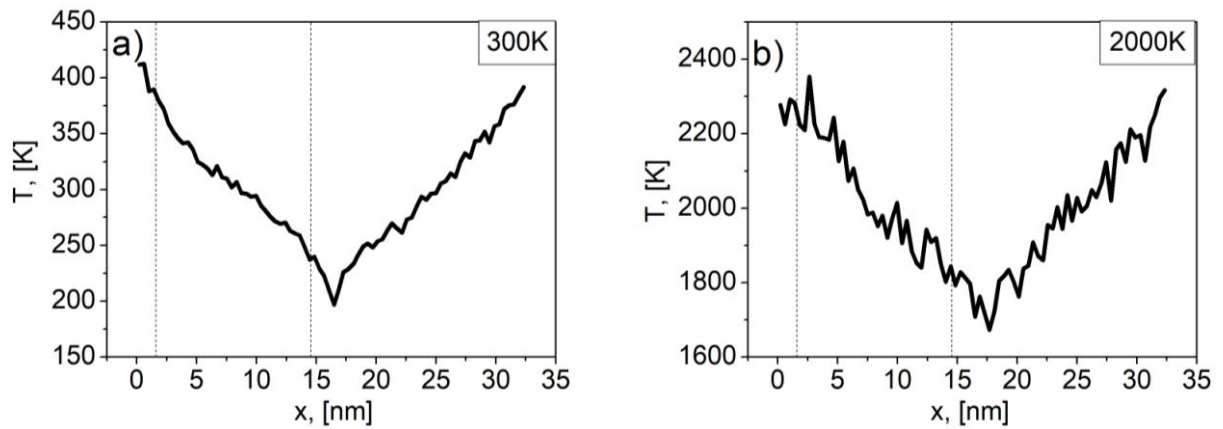

Fig.1 Spatial distribution of the temperature (a) at 300K (b) at 2000K
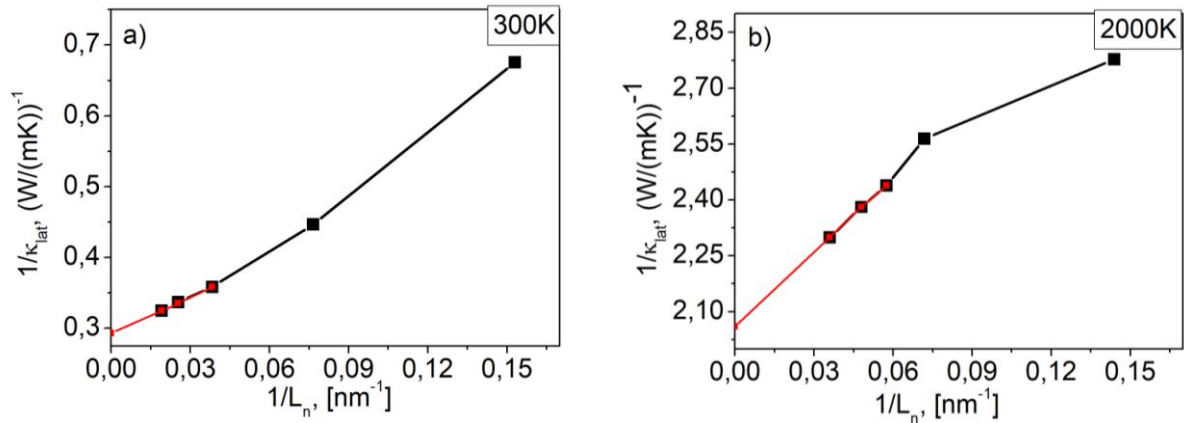

Fig.2. The dependence of the reciprocal of the thermal conductivity on the reciprocal of the length L_n of the computational domain at temperatures: (a) 300K, (b) 2000K.

Using the least squares method, a linear dependence was obtained for three values of $1/L_n$ (n = 1,2,3), corresponding to the lengths of the computational domain $L_1 = 40$, $L_2 = 80$ and $L_3 = 160$ cells (Fig. 2 (a)):

$$P(z) = 0.293 + 1.713z$$

109

In fig. 2 (a), the obtained dependence $P(z)$ is shown by a red line with markers. At $z = 1/L_n = 0$ we obtain the value corresponding to the infinite length of the computational domain. The reverse of this value is equal to the thermal conductivity at this temperature (300K). The procedure was repeated for all necessary temperatures in the range 300K ≤ T ≤ 2000K.
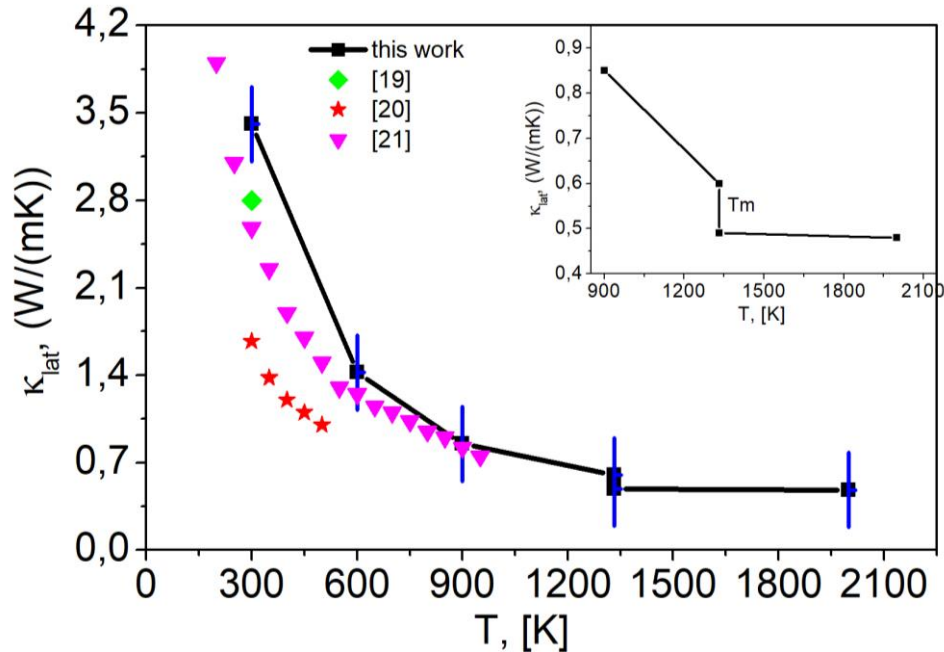

Fig.3. The temperature dependence of phonon themal conductivity of gold. The markers show the results of calculations by other authors.

Fig. 3 shows the temperature dependence of the phonon thermal conductivity of gold obtained as a result of the calculations. At the temperature of 300 K, the phonon thermal conductivity is κ_{lat} = 3.41 W / mK. With increasing temperature, the thermal conductivity of gold decreases. At the equilibrium melting temperature Tm = 1332 K, the thermal conductivity in the solid phase is κ_{lat} = 0.6 W / mK, and in the liquid phase at the same temperature the thermal conductivity is κ_{lat} = 0.49 W / mK. Thus, an abrupt decrease in thermal conductivity by 0.11 W / mK was obtained (inset in Fig. 3), which is 18%. The calculation was carried out up to a temperature T = 2000 K, at which the thermal conductivity is κ_{lat} = 0.48 W / mK. Such a change in the phonon thermal conductivity with increasing temperature does not contradict the ideas about the behavior of the phonon thermal conductivity of metals.

The comparison with alternative calculations [19-21] showed a good agreement. At low temperatures (300K≤T <600K), the largest difference with [19, 21] is Δκ ~ 32%. With increasing temperature, the difference in results becomes smaller. At T = 600 K [21], the difference is Δκ ~ 12%, and at T = 900 K almost completely coincides Δκ ~ 2%. The consistency with the results of [20] is lesser. In the temperature range T> 1000K, there is no data for comparison. In general, such comparison results suggest that the selected method and potential describe the model with good accuracy and are applicable for further studies.
The calculations were performed using the LAMMPS package [34]

4 CONCLUSIONS

In the course of molecular dynamics experiments using the direct nonequilibrium method with the EAM potential [18], the phonon thermal conductivity of gold was calculated in the temperature range from 300 K to 2000 K. The indicated interval includes a region of a first-order phase transition (melting). At the melting point, the phonon thermal conductivity is calculated for two states of matter: solid and liquid.

A comparison of the obtained temperature dependence of the phonon thermal conductivity coefficient with the results from [19, 20, 21] shows a good agreement.

REFERENCES

[1] G.A. Shafeev, I.I. Rakov, K.O. Ayyyzhy, G.N. Mikhailova, A.V. Troitskii, O.V. Uvarov, "Generation of Au nanorods by laser ablation in liquid and their further elongation in external magnetic field", *Applied Surface Science,* **466**, 477–482 (2019). doi:10.1016/j.apsusc.2018.10.062

[2] Sandra Jendrzej, Bilal Gökce, Matthias Epple, Stephan Barcikowski, "How Size Determines the Value of Gold - Economic Aspects of Wet Chemical and Laser-Based Metal Colloid Synthesis", ChemPhysChem., **18,** 1-9 (2017). DOI: 10.1002/cphc.201601139

[3] N. Elahi, M. Kamali, M. H. Baghersad, "Recent biomedical applications of gold nanoparticles: A review", *Talanta*, **184**, 537-556, (2018) https://doi.org/10.1016/j.talanta.2018.02.088

[4] X. Zhang, "Gold Nanoparticles: Recent Advances in the Biomedical Applications", *Springer*, **72** (3), 771–775 (2015).

[5] S. Barcikowski, A. Hahn, A.V. Kabashin, B.N. Chichkov, "Properties of nanoparticles generated during femtosecond laser machiningin air and water", *Appl. Phys. A,* **87**, 47–55 (2007). DOI: 10.1007/s00339-006-3852-1

[6] K. Maximova, A. Aristov, M. Sentis, A.V. Kabashin, "Size-controllable synthesis of bare gold nanoparticles by femtosecond laser fragmentation in water", *Nanotechnology,* **26,** 065601 (8pp) (2015).

[7] Paulina Abrica-González, J. A. Zamora-Justo, Blanca Estela Chavez-Sandoval, José Abraham Balderas-López, "Measurement of the Optical Properties of Gold Colloids by Photoacoustic Spectroscopy", *Int. J. Thermophysics*, **39**(8), 93 (2018) DOI: 10.1007/s10765-018-2412-1

[8] X. Xue, & X.-J. Liang, "Multifunctional Nanoparticles for Theranostics and Imaging. Nanostructure Science and Technology", Y. Ge et al. (Eds.) in *Nanomedicine, Nanostructure Science and Technology,* Springer Science+Business Media New York, *101–115* (2014). doi:10.1007/978-1-4614-2140-5_6

[9] E.G. Gamaly, "The physics of ultra-short laser interaction with solids at non-relativistic intensities", *Physics Reports,* **508**(4-5), 91–24*3* (2011). doi:10.1016/j.physrep.2011.07.002

[10] A.V. Mazhukin, V.I. Mazhukin, M.M. Demin, "Modeling of femtosecond laser ablation of Al film by laser pulses", *Applied Surface Science,* **257**, 5443–5446 (2011).

[11] R. Venkatasubramanian, E. Siivola, T. Colpitts and B. O. Quinn, "Thin Film Thermoelectric Devices with High Room Temperature Figures of Merit", *Nature*, **413,** 597-602 (2001). http://dx.doi.org/10.1038/35098012

[12] F.F. Abraham, "Computational statistical mechanics: methodology, applications and supercomputing", *Advances in Physics*, **35,** 1-111 (1986).

[13] A.F. Bakker, G.H. Gilmer, M.H. Grabow, and K. Thompson, "A special purpose computer for molecular dynamics calculations", *J. Comp. Phys.*, **90**, 313-335 (1990).

[14]   R. Car, M. Parrinello, "Unified approach for molecular dynamics and Density-Functional theory", *Phys. Rev. Lett.*, **55**, 2471 (1985).

[15]   D. Marx, J. Hutter, *Ab Initio Molecular Dynamics: Basic Theory and Advanced Methods*, Cambridge University Press, New York (2009). ISBN 978-0521898638

[16]   S.M. Foiles, M.I. Baskes, and M.S. Daw, "Embedded-atom-method functions for the fcc metals Cu, Ag, Au, Ni, Pd, Pt, and their alloys", *Physical Review B*, **33(12)**, 7983-7991 (1986). DOI: 10.1103/physrevb.33.7983.

[17]   S.V. Starikov, A.Y. Faenov, T.A. Pikuz, I.Y. Skobelev, V.E. Fortov, S. Tamotsu, M. Ishino, M. Tanaka, N. Hasegawa, M. Nishikino, T. Kaihori, T. Imazono, M. Kando, and T. Kawachi, "Soft picosecond X-ray laser nanomodification of gold and aluminum surfaces", *Applied Physics B*, **116(4)**, 1005-1016 (2014). DOI: 10.1007/s00340-014-5789-y.

[18]   V.V. Zhakhovskii, N.A. Inogamov, Yu.V. Petrov, S.I. Ashitkov, K. Nishihara, "Molecular dynamics simulation of femtosecond ablation and spallation with different interatomic potentials", *Appl. Surf. Sci.,* **255**, 9592-9596 (2009)

[19]   Z. Tong, S. Li, X. Ruan, and H. Bao*, "*Comprehensive first-principles analysis of phonon thermal conductivity and electron-phonon coupling in different metals", *Physical review B,* **100**, 144306 (2019)

[20]   A. Jain and A.J.H. McGaughey, "Thermal transport by phonons and electrons in aluminum, silver, and gold from first principles", *Physical review B,* **93**, 081206(R) (2016).

[21]   Y. Wang, Z. Lu, and X. Ruan, "First principles calculation of lattice thermal conductivity of metals considering phonon-phonon and phonon-electron scattering", *Journal of applied physics*, **119**, 225109 (2016)

[22]   V.I. Mazhukin, "Kinetics and Dynamics of Phase Transformations in Metals Under Action of Ultra-Short High-Power Laser Pulses", Chapter 8, I. Peshko (Ed.), in *Laser Pulses – Theory, Technology, and Applications, InTech, Croatia*, 219 -276 (2012).

[23]   V.I. Mazhukin, A.V. Shapranov, A.V. Mazhukin, O.N. Koroleva, "Mathematical formulation of a kinetic version of Stefan problem for heterogeneous melting/crystallization of metals", *Math. Montis.*, **36**, 58-77 (2016).

[24]   V.I. Mazhukin, A.V. Mazhukin, M.M. Demin, A.V. Shapranov, "Nanosecond laser ablation of target Al in a gaseous medium: explosive boiling", *Appl. Phys. A*, **124** (3), 237 (1-10) (2018). https://doi.org/10.1007/s00339-018-1663-9 .

[25]   V.I. Mazhukin, "Nanosecond Laser Ablation: Mathematical Models, Computational Algorithms, Modeling", Chapter 2, Tatiana E. Itina (Ed.) In *Laser Ablation - From Fundamentals to Applications, InTech, Croatia*, 31-55 (2017).

[26]   L. Verlet, "Computer "Experiments" on Classical Fluids. I. Thermodynamically Properties of Lennard-Jones Molecules", *Phys. Rev.*, **159**, 98-103 (1967).

[27]   P. K. Schelling, S. R. Phillpot, P. Keblinski, "Comparison of atomic-level simulation methods for computing thermal conductivity", *Phys. Rev. B*, **65**, 144306 (2002)

[28]   L. Hu, W. J. Evans, P. Keblinski, "One-dimensional phonon effects in direct molecular dynamics method for thermal conductivity determination", *J. Appl. Phys.*, **110**, 113511 (2011)

[29]   Florian Müller-Plathe, "A simple nonequilibrium molecular dynamics method for calculating the thermal conductivity", *J. Chem. Phys.*, **106**, 6082 (1997).

[30]   R. Zwanzig, "Time-correlation functions and transport coefficients in statistical mechanics", *Annu. Rev. Phys. Chem.*, **16,** 67-102 (1965).

[31]   W. Evans and P. Keblinski, "Thermal conductivity of carbon nanotube cross-bar structures", *Nanotechnology,* **21**(47), 475704, (2010) doi: 10.1088/0957-4484/21/47/475704

[32]   Shenghong Ju and Xingang Liang, "Thermal conductivity of nanocrystalline silicon by direct molecular dynamics simulation", *J. Appl. Phys.*, **112**, 064305 (2012)

[33]   Chaofeng Hou, Ji Xu, Wei Ge and Jinghai Li, **"Molecular dynamics simulation overcoming the finite size effects of thermal conductivity of bulk silicon and silicon nanowires",** *Modelling Simul. Mater. Sci. Eng*., **24,** 045005 (1-9) (2016)
[34]   S. Plimpton, "Fast parallel algorithms for short-range molecular dynamics", *J. Comput. Phys*., **117**(1), 1-19 (1995).

ON METAL-DIELECTRIC TRANSITION IN LASER ABLATION MODELING

A.A. SAMOKHIN[1*], A.E. ZUBKO[1]

[1]Prokhorov General Physics Institute of the Russian Academy of Sciences (GPI RAS)
Moscow, Russia
*Corresponding author. E-mail: asam40@mail.ru

Summary. Laser ablation modeling taking into account possibility of metal-dielectric transition in the irradiated metal targets is considered. In the framework of 1-D heat conduction approach it is shown that the steady-state vaporization regime with metal-dielectric transition in mercury can be observed only in very narrow laser intensity interval. From analysis of recent experimental results on mercury ablation with nanosecond laser pulses it follows that the results can not be described in the framework of 1-D approach.

1 INTRODUCTION

Laser-matter interaction gives possibility to obtain rather high temperature and pressure values which include values of liquid-vapor critical parameters for any element. However critical parameters of most metals remain badly known and this fact is mentioned in many papers [1-4]. From [1] it follows that the difference between critical pressure values for Al in scientific literature is about an order of magnitude. In ref. [4] one can read:

"Very old and not resolved yet problem of extreme uncertainty in our knowledge in location and critical point parameters for uranium and its compounds (UO_2, UN, UC…) is under discussion. The expected critical region for uranium is not presently achievable experimentally. The same is true for powerful, but laborious contemporary socalled first-principle approaches (QMD, QMC etc). At the same time traditional way of theoretical estimations for critical parameters on the base of far extrapolation of well-known low-temperature thermal and caloric properties for condense phase, lead to extreme dispersion in predicted values for uranium critical temperature and pressure. We discuss possible physical reasons, which could explain and justify mentioned above critical parameters discrepancy for uranium. In particular we discuss possible anomalies in falling of effective "ionization degree" on the expansion way from triple to critical point, as well as possibility for existing of hypothetical additional "entropic" phase transition, similar to that predicted by Landau and Zeldovich long ago."

For this reason, further theoretical and experimental investigations of intense laser-metal interaction are necessary including the possibility of metal-dielectric transition which is also discussed in many papers (see e.g. [4-11] and references therein).

In the present paper possible manifestations of this transition for mercury are analyzed in the framework of simplified one-dimensional approach using the previous results [7,8] and recent experimental investigation [11].

2 1-D HEAT CONDUCTION APPROACH

2.1 Steady-state regime of laser ablation

One dimensional temperature distribution in laser irradiated condensed matter located at $z \geq z_0 \geq 0$ is described with the heat conduction equation

$$\frac{\partial T}{\partial t} = \frac{\partial}{\partial z}\left(\chi \frac{\partial T}{\partial z}\right) + \frac{\alpha I}{C} e^{-\alpha(z-z_0)} \tag{1}$$

where T, χ, C, α, I, z_0 are temperature, thermal diffusivity, heat capacity, absorption coefficient, absorbed intensity and irradiated surface position respectively. In (1) hydrodynamic movement is not taken into account, the approximation being applicable to some extent for sufficiently short laser pulses and for the cases when heat expansion can be neglected.

At irradiated surface z_0 in vacuum vaporization boundary condition is formulated as

$$\chi \frac{\partial T}{\partial z} = \frac{LV}{C}, \qquad T(z_0) = T_s \qquad \text{at } z = z_0 \tag{2}$$

$$V = 0.82 \frac{P_b \, exp\big(A(1 - T_b/T_s)\big)}{\sqrt{2\pi m \, kT_s}} \tag{3}$$

where L, V, T_s, T_b, P_b, k are heat of vaporization, vaporization velocity, surface temperature, boiling temperature, boiling pressure and Boltzmann constant respectively; constant $A = 11.4$. Boundary condition (2) and vaporization velocity (3) does not change in the moving reference frame for the vacuum vaporization case.

In the reference frame moving together with evaporating surface (the change of reference system is $z = z' - \int V dt$) the irradiated surface position is fixed ($z_0 = 0$, used below everywhere) and instead of (1) one has

$$\frac{\partial T}{\partial t} - V \frac{\partial T}{\partial z} = \frac{\partial}{\partial z}\left(\chi \frac{\partial T}{\partial z}\right) + \frac{\alpha I}{C} e^{-\alpha z}$$

Under conditions $\partial T/\partial t = 0$ and $I = const$ this equation yields the steady-state form of the heat conduction equation

$$\frac{\partial}{\partial z}\left(\chi \frac{\partial T}{\partial z}\right) + V \frac{\partial T}{\partial z} + \frac{\alpha I}{C} e^{-\alpha z} = 0 \tag{4}$$

After space integration in (4) from $z_0 = 0$ to $z \to \infty$ it follows (see [12] and references therein)

$$I = V\,[L + C\,(T_s - T_\infty)] \tag{5}$$

where T_∞ is temperature of unperturbed medium at $z \gg \alpha^{-1}$, $z \gg \chi/V$. Relation (5) is an energy balance equation, and in conjunction with (3) it allows to find T_s and V at given I. Note that (5) remains valid also for the case of variables α and χ.

The relation (5) does not depend on α and χ, while it is not so for temperature distribution $T(z)$ which at constant α and χ values is given by the well-known expression (see e.g. [12] and references therein)

$$T(z) = T_\infty - \left(\frac{L}{C} + \frac{y}{1-y}\frac{I}{CV}\right)e^{-\frac{\alpha z}{y}} + \frac{1}{1-y}\frac{I}{CV}e^{-\alpha z} \qquad (6)$$

The curve $T(z)$ depends significantly on the dimensionless parameter $y = \alpha\chi/V$ as it is seen from Fig. 1 which describes two curves $T(z)$ at different y values ($y = 460$ for mercury and $y = 1.1$ for water) and constant $T_s/T_c \approx 0.6$ where T_c is a critical temperature of liquid-vapor transition.
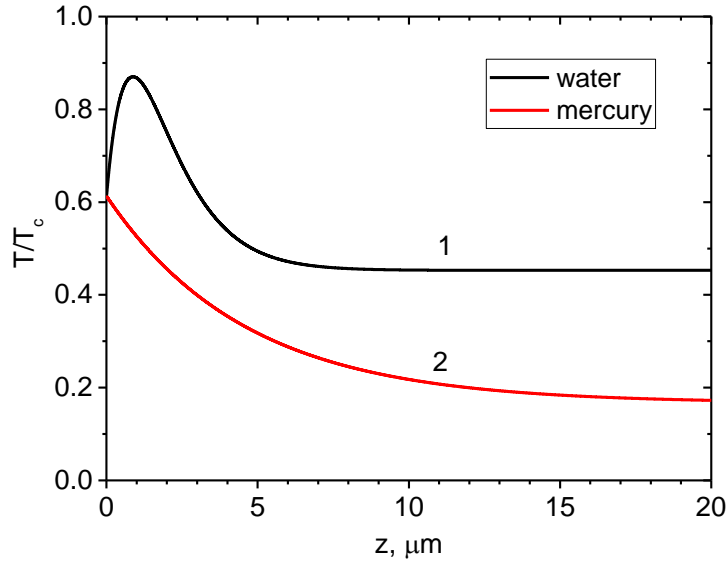

Figure 1: Steady-state temperature profiles normalized to critical temperature in water (curve 1) and in mercury (curve 2) at absorbed intensities of 40 and 660 kW/cm^2 respectively.
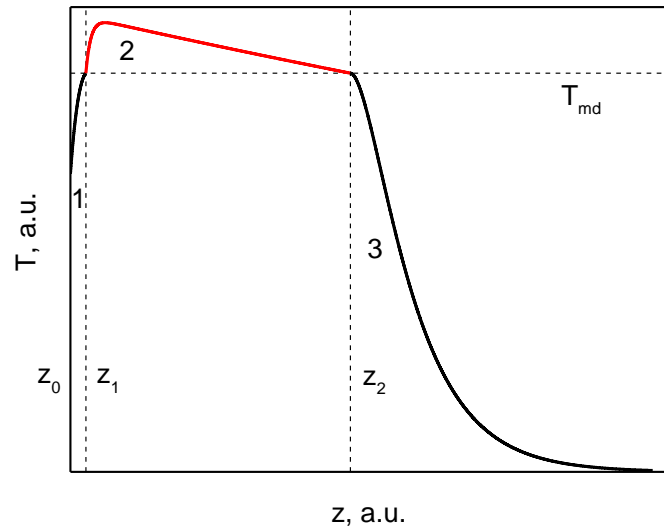

Figure 2: General form of steady-state temperature profile with a metal-dielectric transition in liquid metal: 1 – thin metal film on irradiated surface, 2 – dielectric layer, 3 – metal.

2.2 Steady-state regime of metal-dielectric transition in mercury

In the case of metal-dielectric transition parameter y is not constant in the steady-state regime and the temperature distribution has the form [7,8] which is shown schematically in Fig. 2. This not-in-scale representation of temperature distribution is necessary to mark explicitly boundaries between metal and dielectric layers which can have very different thickness in accordance with solution of equation (4). The solution has piecewise form including three different layers with thicknesses H_1, H_2, $H_3 >> H_1$, $H_3 >> H_2$.

In each layer i with constant α_i and χ_i the temperature distribution $T_i(z)$ can be expressed as follows

$$T_i(z) = a_i\exp[-\alpha_i(z-z_{i-1})] +b_i\exp[-\beta_i(z-z_{i-1})] +c_i \qquad \text{for} \quad z_{i-1} \leq z \leq z_i, \quad i = 1, 2, 3 \qquad (7)$$

$$a_i = I_{i-1}/[CV(1-y_i)], \qquad \beta_i = V/\chi_i, \qquad y_i = \alpha_i\chi_i/V, \qquad z_3 \to \infty$$

The constants α_i and χ_i in metal layers are $\alpha_1 = \alpha_3 = \alpha_m$, $\chi_1 = \chi_3 = \chi_m$, and in dielectric layer are $\alpha_2 = \alpha_d$, $\chi_2 = \chi_d$. The absorbed intensity in each layer is determined by the recurrence relation $I_i = I_{i-1} \exp(-\alpha_i H_i)$ where $I_0 = I$ and layer thickness is $H_i = z_i - z_{i-1}$. At point $z_0 = 0$ boundary conditions (2) are used, and at the points z_1 and z_2 the following boundary conditions are used [7,8].

$$T_1(z) = T_{md}, \qquad T_2(z) = T_{md}, \qquad \chi_2 \, \partial T_2/\partial z = \chi_1 \, \partial T_1/\partial z \qquad \text{at} \quad z = z_1 \qquad (8)$$

$$T_2(z) = T_{md}, \qquad T_3(z) = T_{md}, \qquad \chi_3 \, \partial T_3/\partial z = \chi_2 \, \partial T_2/\partial z \qquad \text{at} \quad z = z_2 \qquad (9)$$

$$T_3(z) = T_\infty, \qquad \partial T_3/\partial z = 0 \qquad \text{at} \quad z \to \infty \qquad (10)$$

where T_{md} is a metal-dielectric transition temperature. Note that the last equality in (10) is valid due to the exponential form of (7).

The coefficients b_i, c_i in (7) for the first (metal) layer is determined by the evaporative boundary conditions (2) and are given below

$$b_1 = -L/C -I_0y_1/[CV(1-y_1)], \qquad c_1 = T_s +L/C -I_0/(CV)$$

The whole solution is obtained after the sequential determination of unknown layer thicknesses and coefficients b_i, c_i in (7). The first parts of the conditions (8,9) determine the thicknesses of a thin subsurface metal film H_1 and a dielectric layer H_2 through the transcendental equation

$$a_j\exp(-\alpha_jH_j) +b_j\exp(-\beta_jH_j) +c_j = T_{md} \qquad \text{for } j = 1, 2$$

The equations for the temperature distribution coefficients in the second and third layers in (7) are obtained using the remaining conditions from (8,9)

$$a_{j+1}+b_{j+1}+c_{j+1} = T_{md}, \qquad \text{for } j = 1, 2$$

$$-\chi_{j+1}[\alpha_{j+1}a_{j+1}+\beta_{j+1}b_{j+1}] = -\chi_j[\alpha_ja_j\exp(-\alpha_jH_j)+\beta_jb_j\exp(-\beta_jH_j)] \equiv f_j \qquad \text{for } j = 1, 2$$

which give finally

$$b_{j+1} = -f_j/V-y_{j+1}a_{j+1}, \qquad c_{j+1} = T_{md}-a_{j+1}-b_{j+1} \qquad \text{for } j = 1, 2$$

It should be mentioned that $c_3 = T_\infty$ is not independent parameter when values of I, V and T_s are given. This is due to energy conservation relation (5) or its special case which follows after integrating $T_3(z)$ from z_2 to $z \to \infty$

$$I_2 = VC\,(T_{md} - T_\infty) + C f_2$$

It is useful to note also that the distribution $T_3(z)$ in metal is monotonous in contrast to (6) because boundary condition at $z = z_3$ differs from the vaporization case (2).
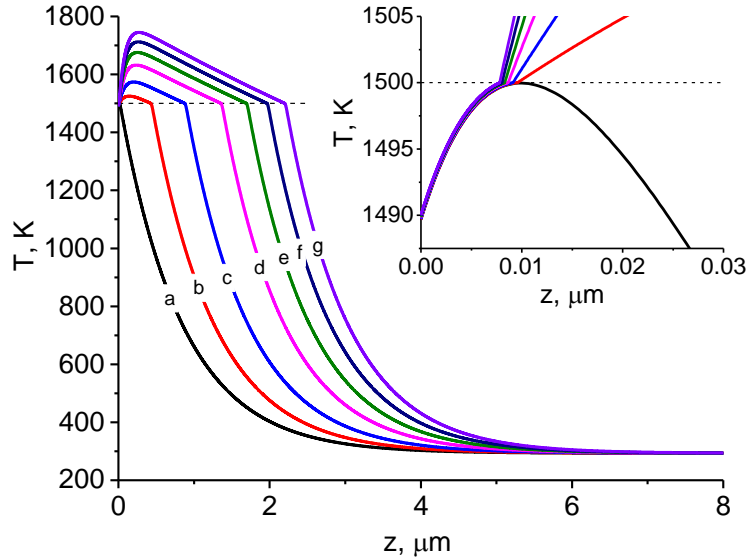

Figure 3: Steady-state temperature profiles in liquid mercury at various absorbed intensities (a-g) providing subcritical values of temperature maximum in dielectric layer for the case of $\alpha_d = 10^3$ cm^{-1} and $I = 4.221$ (a), 4.2215 (b), 4.222 (c), 4.223 (d), 4.224 (e), 4.225 (f), 4.226 (g) MW/cm^2.
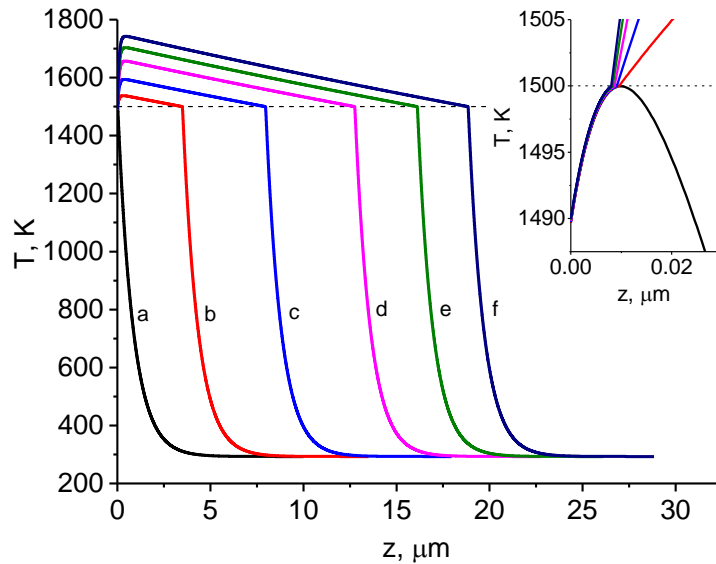

Figure 4: Steady-state temperature profiles in liquid mercury at various absorbed intensities (a-g) providing subcritical values of temperature maximum in dielectric layer for the case of $\alpha_d = 10^2$ cm^{-1} and $I = 4.221$ (a), 4.2215 (b), 4.222 (c), 4.223 (d), 4.224 (e), 4.225 (f) MW/cm^2.

In metal case $y \gg 1$ and maximum value T_{max} in the temperature distribution (6) differs from T_s but slightly. Temperature maximum T_{max} in dielectric layer can exceed T_{md} significantly as it is evident from curve 1 in Fig. 1. From $T_2(z)$ distribution and the equation $\partial T_2/\partial z = 0$ for $T_{max} = T_2(z_{max})$ one obtains

$$T_{max} = a_2\left(-\frac{b_2\alpha_2}{a_2\beta_2}\right)^{\frac{\beta_2}{\alpha_2-\beta_2}} + b_2\left(-\frac{b_2\alpha_2}{a_2\beta_2}\right)^{\frac{\alpha_2}{\alpha_2-\beta_2}} + c_2, \qquad z_{max} = z_1 - \frac{ln\left(-\frac{b_2\alpha_2}{a_2\beta_2}\right)}{\alpha_2-\beta_2}$$

It is clear that maximum distribution temperature T_{max} should not exceed the thermodynamic stability limit (spinodal line) T_l which is somewhat lower than the critical temperature T_c. One should keep in mind also that the difference $T_c - T_{md}$ is small compared with T_c.

This condition results in rather strong limits on possible realization of such vaporization regime. Due to this condition the intensity interval ΔI_{md} for realization of the steady-state vaporization regime with metal-dielectric transition is very narrow and its localization is close to the threshold intensity value I_{th}.

symbol	value
α_m	10^6 cm^{-1}
χ_m	5.8×10^{-2} cm^2/s
χ_d	5.8×10^{-3} cm^2/s
ρ	13.5 g/cm^3
C	1.9 J cm^{-3} K^{-1}
L	3.8 kJ cm^{-3}
T_{md}	1500 K

Table 1 : The constant mercury parameters used in the calculation of the metal-dielectric transition.
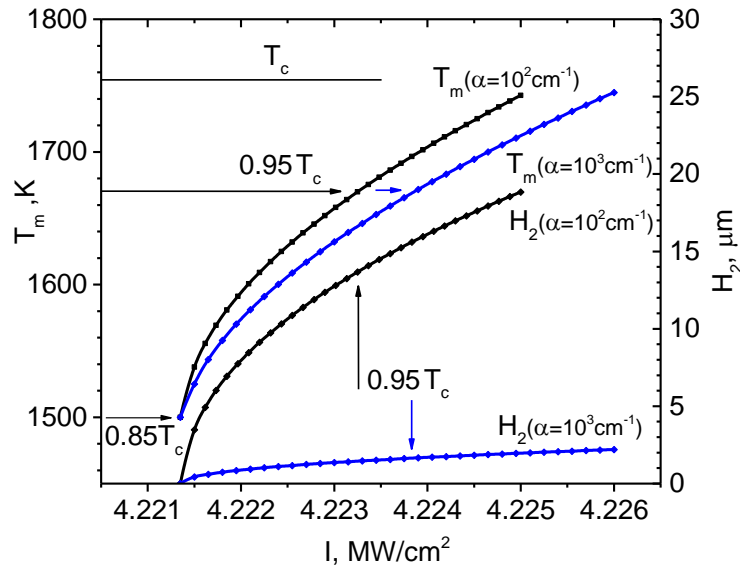

Figure 5: The dependences of steady-state dielectric layer thickness H_2 and temperature maximum T_m on absorbed intensity I in interval from dielectric layer threshold to critical temperature T_c.

Figure 6: The dependence of steady-state dielectric layer thickness H_2 on absorption coefficient α_d in this layer at constant absorbed intensity $I = 4.222$ MW/cm^2.

The calculated temperature distributions in mercury are shown in Fig. 3, 4. The threshold intensity value is $I_{th} = 4.2215$ MW/cm^2 while the intensity interval for realization of the steady-state vaporization regime with metal-dielectric transition $\Delta I_{md} = 4.5$ kW/cm^2 (at $\alpha_d = 10^3$ cm^{-1}) or $\Delta I_{md} = 3.5$ kW/cm^2 (at $\alpha_d = 10^2$ cm^{-1}) is rather small $\Delta I_{md} << I_{th}$.

Dependences of mercury dielectric layer thickness H_2 and temperature maximum T_m on absorbed intensity I in interval from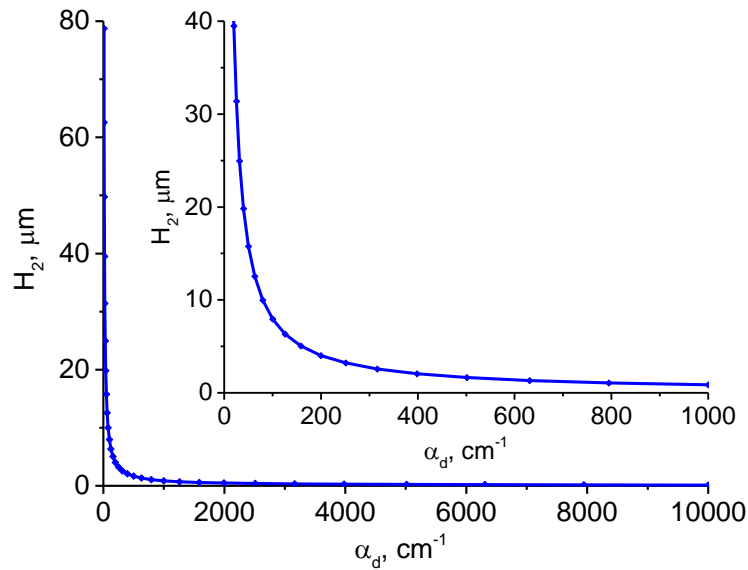 dielectric layer threshold to critical temperature T_c as well as dependence of dielectric layer thickness H_2 on absorption coefficient α_d at constant absorbed intensity $I = 4.222$ MW/cm^2 are shown in Fig. 5 and 6.

In experiments the metal-dielectric transition in transient regime can be realized at higher intensities than $I_{th} \sim 4.2$ MW/cm^2 for the steady-state case. In the transient regime the transition front velocity exceeds the vaporization front velocity and temperature maximum in the target attains the thermodynamic stability limit T_l. When this occurs the explosive boiling begins to develop in subnanosecond scale [13,14].

3   1-D ESTIMATIONS OF RECENT EXPERIMENTAL RESULTS

In ref. [11] pressure behavior in liquid mercury is investigated during irradiation with different laser pulses: a train of several subnanosecond laser peaks divided with 8 ns intervals and a single 30 ns relatively smooth laser pulse. Using intensity modulated laser pulses permits to obtain information about irradiated surface displacement as it was first demonstrated in [15] for the case of dielectric liquids irradiated with harmonically modulated laser pulses. For metals laser intensity modulation due to mode-locking is more preferable than harmonic modulation due to two mode beating [10,16].

It is shown in [11] that the pressure response detected with piezoelectric transducers as well as the surface displacement can not be explained in the framework of surface metal evaporation. In particular, significant diminishing δ of the acoustical arrival time is observed

which means that the laser absorption zone deepens into the target for far more distance $h = v_s\delta$, v_s – sound velocity, than it is the case for metal ablation where $h_m \sim \alpha_m^{-1}$.

Behavior of the kind may be related to the metal-dielectric transition [5-10] when its front moves deeply into the irradiated target. The transition modeling in [8] for supposed metal-dielectric transition in Al shows additional bump in the pressure curve which is visible also in [11] at intensities ≥ 50 MW/cm^2.

One can estimate the transition front velocity as $v_f \sim h/\tau = v_s\delta/\tau$ which exceeds sound velocity v_s if $\delta > \tau$. In experimental results [11] $\delta/\tau \sim 2$ which means supersonic movement of the transition front.

From energy balance equation it follows that to realize such movement it is necessary to have the absorbed laser intensity at the transition front determined approximately by the expression $I = v_f C (T_{md} - T_\infty)$. For $v_f \sim 2v_s = 2.8$ km/s, $C = 1.9$ J/cm^3, T_{md}–$T_\infty = 1200$ K this gives $I = 0.6$ GW/cm^2. This intensity value exceeds the value in experiment [10] which is lower than 0.1 GW/cm^2. The estimated pressure generated during such front movement also far exceeds the maximum pressure value observed in [11] which is about one kbar while the 1-D estimation gives about a hundred kbar.

A possible reason of such discrepancies is probably due to violation of 1-D approach in the considered case [11] where intensity distribution is not constant over the irradiation spot. The initial Gaussian distribution over the irradiation spot can transform itself to more sharp distribution during its propagation in the target where the metal-dielectric transition occurs.

4 CONCLUSIONS

In the framework of simplified 1-D heat conduction approach it is shown that the steady-state vaporization regime of mercury with supposed metal-dielectric transition can occur only in very narrow irradiation intensity interval. Analysis of the recent experimental results [11] of mercury laser ablation shows remarkable discrepancy between the 1-D theoretical estimation and experiment. The discrepancy can be probably due to violation of 1-D approach applicability in the considered case because possibility of significant transformation of initial Gaussian intensity distribution over the irradiation spot. For this reason, it is interesting to investigate laser ablation of mercury with constant laser intensity distribution over the irradiated spot as well as to study stability of this regime and to model the ablation process with metal-dielectric transition in the framework of continual 2-D approach or molecular dynamic calculations.

REFERENCES

[1] A.L. Khomkin and A.S. Shumikhin, "Critical Points of Metal Vapors", *JETP*, **121**, 521–528 (2015).

[2] V.S. Vorob'ev and E.M. Apfelbaum, "The Generalized Scaling Laws Based on Some Deductions from the van der Waals Equation", *High Temperature*, **54**, 175–185 (2016).

[3] Ch. Wu and L.V. Zhigilei, "Microscopic Mechanisms of Laser Spallation and Ablation of Metal Targets from Large-Scale Molecular Dynamics Simulations", *Appl. Phys. A.*, **114**, 11–32 (2014).

[4] I. Iosilevskiy, V. Gryaznov, "Uranium critical point location problem", *Zababakhin Scientific Talks, International Conference March 18–22*, 95 (2019).

[5] L.D. Landau, Ya.B. Zeldovich, "On the Relation between the Liquid and the Gaseous States of Metals", *Acta Physicochim. USSR*, **18**, 194–197 (1943).

[6] V.A. Batanov, F.V. Bunkin, A.M. Prokhorov, V.B. Fedorov, "Evaporation of Metallic Targets

Caused by Intense Optical Radiation", *JETP*, **36**(2), 311–322 (1973).

[7] R.V. Karapetyan and A.A. Samokhin, "Influence of an increase in the transparency on the intense evaporation of metals by optical radiation", *Sov. J. Quantum Electron.*, **4**, 1141–1142 (1975).

[8] S.N. Andreev, V.I. Mazhukin, N.M. Nikiforova, A.A. Samokhin, "On possible manifestations of the induced transparency during laser evaporation of metals", *Quantum Electronics*, **33**, 771–776 (2003).

[9] N.E. Bykovsky, S.M. Pershin, A.A. Samokhin and Yu.V. Senatsky, "Transmittance jump in a thin aluminium layer during laser ablation", *Quantum Electron.*, **46**(2), 128–132 (2016).

[10] A.A. Samokhin, S.I. Kudryashov, A.E. Zubko, and A.V. Sidorin, "Modelling of nanosecond laser ablation. Continual approach", *Math. Montis.*, **37**, 76–90 (2016).

[11] A.A. Samokhin, E.V. Shashkov, N.S. Vorobiev, A.E. Zubko, "On acoustical registration of irradiated surface displacement during nanosecond laser-metal interaction and metal–nonmetal transition effect", *Applied Surface Science*, (2020, in press), DOI: 10.1016/j.apsusc.2019.144261

[12] A.A. Samokhin, "First-order phase transitions induced by laser radiation in absorbing condensed matter", in *Effect of laser radiation on absorbing condensed matter*, V.B. Fedorov (Ed.), Nova Science Publishers, (1990).

[13] V.I. Mazhukin, A.A. Samokhin, A.V. Shapranov and M.M. Demin, "Modeling of thin film explosive boiling–surface evaporation and electron thermal conductivity effect", *Mater. Res. Express*, **2**, 016402 (2015), DOI: 10.1088/2053-1591/2/1/016402

[14] A.A. Samokhin, V.I. Mazhukin, M.M. Demin, A.V. Shapranov, A.E. Zubko, "Molecular dynamics simulation of al explosive boiling and transcritical regimes in nanosecond laser ablation", *Math. Montis.*, **41**, 55–72 (2016).

[15] A.A. Samokhin and N.N. Il'ichev, "On photoacoustic monitoring of laser evaporation front movement", *Quantum Electronics*, **40**(8), 659–660 (2010).

[16] A.E. Zubko and A.A. Samokhin, "Pressure pulses generated in metals under the action of nanosecond laser pulses with periodically modulated intensity", *Engineering Physics*, **3**, 47–52 (2017); (the main text is in Russian).

QUANTITATIVE EVALUATION OF SYNTAX SIMILARITY

E.S. KLYSHINSKY[1]*, O.V. KARPIK [2]

[1] National Research University «Higher School of Economics», Moscow, Russia
[2] Keldysh Institute of Applied Mathematics RAS, Moscow, Russia
*Corresponding author. E-mail: eklyshinsky@hse.ru

Summary. Machine learning systems are facing problem of incomparability of their results in case of different languages; one of the subarea here is quantitative analysis of syntax. In this paper, we introduce a new quantitative method based on statistics of words co-occurrence in syntactically tagged corpora. The method allows quantitatively evaluate difference and similarity among languages, select most influential phenomena. Experimental setup consists materials for more than 50 languages. Our experiments demonstrate that the introduced method correctly cluster languages among language families.

1   INTRODUCTION

An advance in the area of computational linguistics and natural language processing relies on results of mathematical formulation of linguistic phenomena. One of the examples here is the distributional semantics [1] that allows introducing of vector operations in semantics using Word2Vec [2] and Glove [3] technologies. These techniques are currently improved in different non-Euclidian spaces (see [4] and [5]). Such scientific domains as quantitative linguistics [6] and theory of language complexity [7] also numerically describe language phenomena. Using these theories, we are able to describe language processes quantitatively but not qualitatively; this makes us possible numerically evaluate and compare the results achieved. One of the subareas here is the quantitative analysis of natural language syntax. In spite of many studies in this area (e.g., see [8]), the results here are still more descriptive than quantitative. It is necessary to state that the quantitative analysis uniform scheme at the moment does not exist. Therefore, there are no common algorithms of machine word processing, on which basis it would be possible to develop methods of computer modeling of language processes. There is a lack of new methods for numerical evaluation of syntactic phenomena. Such method should allow formalizing and emphasizing similarities and dissimilarities among languages and language groups. It is obvious practical usefulness in information about the syntax similarities and differences of the native and studied language during learning foreign languages. The creation of an effective formal languages description promises great prospects in automated text processing, machine translation and the creation of artificial intelligence. In addition to the applied task of syntactic structures computer modeling and text processing, syntax formalization can also help to develop updated metalanguage of linguistic research. The development of flexible and universal language describing means, which should replace the approach based on purely qualitative descriptive methods, is impossible without parameters presented in a simple numerical form.

[9] have shown that co-occurrence networks of natural language are scale-free small world graphs (for the small world graph definition see [10], another applications of modeling on small world graph represented in [11]). The same is true for syntactic representation of a text.

In this paper we introduce a new method based on statistics of words co-occurrence in syntactically tagged corpora. The rest of the paper is organized as following. Section 2 briefly describes stages of natural language processing and the aim of the syntactic analysis. In section 3, we introduce a formal method for description of syntactic analysis and a new method for evaluation of the syntactic similarity of languages. Section 4 describes data used in our experiments, experimental results and evaluation of their correctness. In section 5, we are analyzing achieved results from the computational linguistics point of view. The conclusion sums up the results of this paper.

2 THEORETICAL BACKGROUND

Depending on a task statement, a natural text could be processed in several stages. The first one is tagging which divides text into sentences, word and non-word tokens. Non-word tokens are punctuation marks, numbers, IP-addresses etc. Such languages as Chinese or Japanese have their own peculiarities; the tagging accounts here for concatenating sole hieroglyphs into chunks. For example, Chinese hieroglyph 电 means *electricity*, 池 means *a tank*, while their combination 电池 means *accumulator*.

The next stage is the lexical analysis which defines a word's initial form, part of speech, and grammatical features (number, gender, grammatical case etc.). The complicity of this stage depends on a language in hand. This stage could be unnecessary for hieroglyphically languages like Chinese and Japanese; however, morphologically complicated languages need much more effort to define (disambiguate) correct initial form, part of speech, and set of grammatical features. For example, a token *text* in an English text could represent several parts of speech: verb (*to send messages*), noun (*set of characters*), and adjective (*something textual*). Thus, a correct choice depends on the context.

In this paper, we are analysing the results of the syntactic analysis, the third stage of the natural text analysis. The aim of syntactic analysis is to define connections between tokens and labelling these connections. We give a formal definition of this stage in the Section 3; here, we will just briefly discuss it in a very few words.

There are two main methods for representation of syntactic analysis results. The first one, dependencies trees [12], will be used in this paper; the second one, constituency trees [13], is not discussed here. In case of dependencies tree, words are connected by labelled edges representing a tree graph. A label represents a role which plays a word in the given context. The most common labels are a *subject* – the main actor, a *predicate* – the main action, an *object* – the object influenced by an action, etc. In order to keep uniformity of a graph representation, a fake node named *root* is introduced. The Fig. 1 represents an example of a dependencies tree for a sentence *A big black dog runs after a poor cat*. It is easy to see, that the subject here is the word *dog*, the predicate is *run*, and the object is *cat*.

A comprehensive survey of other graph representations of text could be find in [14].

Among others, there is such phenomenon as a branching. The left branching is a situation when a tail word precedes a head word; the other case is named the right branching. It is well known that different languages prefer different types of branching. For example, Germanic languages prefer left branching for adjective-noun connection, while Romance languages prefer right branching in the same situation.
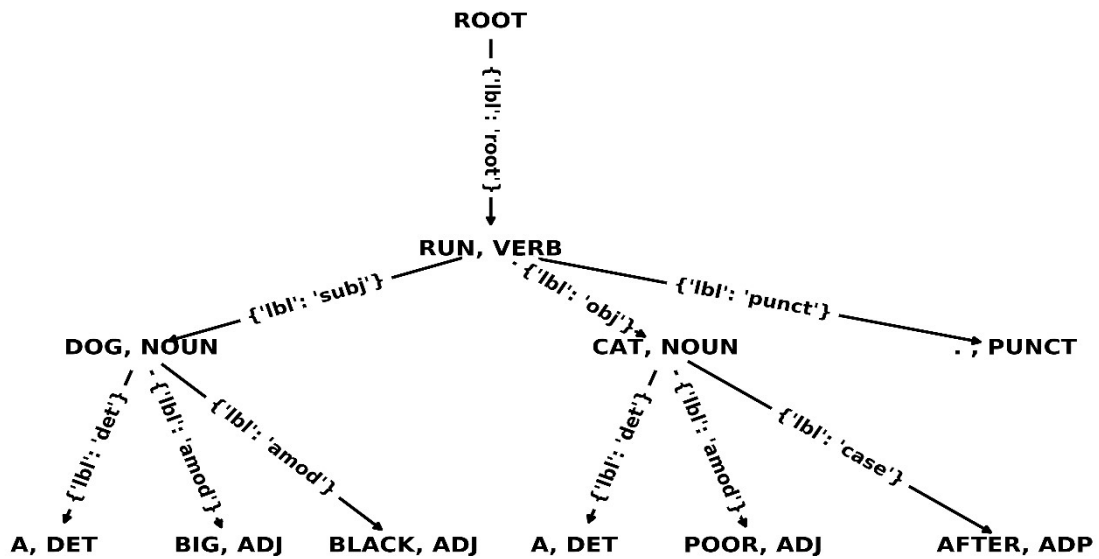
Figure 1. Dependency tree for a sentence *A big black dog runs after a poor cat*

Common sense definition of syntactical similarity of two languages means that the same ideas should be expressed in quite the same manner using quite the same parts of speech, labels, type of branching, etc. For example, Romance languages use auxiliary words for shaping tenses while Slavic languages create new word forms and new words. Thus, we can state the difference between language groups and the similarity among languages of the same group.

In this paper, we assume that similar syntactical constructions are used for expression of the similar ideas. It is not like that in common case, however we will use overall statistics that will eliminate biases. In case of serious deviance, we could state that languages use different constructions. However, such approach tends to have some disadvantages. We should guarantee that selected texts express quite the same ideas in the same style; either we should prove that language properties are hardly dependent on these features and texts could be compared with a reasonable mistake. The theoretical linguistics follows a tradition to describe a phenomenon using series of negative and positive examples. This is very convenient since a reader could draw his or her own conclusions. The quantitative linguistics gives numerical evaluation of such phenomena. In spite of numerous scientific studies discussing similarity and complexity of different phenomena in different languages (e.g., see [8]), there is a lack of overall comparison of the main world languages.

The aim of this paper is to introduce a new numerical method for a quantitative evaluation of syntactical similarity of main world languages. For this purposes, we give a formal description of dependencies trees and describe a formal method for such evaluation.

3 THE METHOD OF QUANTITATIVE EVALUATION

Following to [12] let us represent a sentence S as a sequence of words from the vocabulary W: S = <w_1, w_2, …, w_n>, where $w_i \in W$ and w_i = <id, l, π>, where id is a unique identifier and position of a word in a sentence, l is the lemma of this word, π is its part of speech. In this paper, we are not using lexical and grammatical features of words. We also consider that all words are disambiguated, therefore, there is only one tuple for every word and it is correct. Let us also define a relation set $R = \{r_1, r_2, …, r_m\}$. In this case, a dependency tree G = <V , A> for a

sentence S is a labeled directed tree consisting of nodes V and arcs A: V = {root, w_1, w_2, …, w_n}, A $\subseteq$ V × R × V, if <w_i, r, w_j> $\in$ A then <w_i, r', w_j> $\notin$ A for all r' ≠ r. 'Root' here is a fake word which is always a root of the tree G; let us take $id = 0$ for root. Let us also denote <w_i, r, w_j> as <i, r, j>, where w_i is a parent node and w_j is a child node.

To illustrate this definition let us consider a sentence *A big black dog runs after a poor cat* (Fig.1). Here V = <root, <1, A, DET>, <2, BIG, ADJ>, <3, BLACK, ADJ>, <4, DOG, NOUN>, <5, RUN, VERB>, <6, AFTER, ADP>, <7, A, DET>, <8, POOR, ADJ>, <9, CAT, NOUN>, <10, . , PUNCT> >, A={<0, root, 5>, <5, nsubj, 4>, <4, det, 1>, <4, amod, 2>, <4, amod, 3>, <5, obl, 9>, <9, det, 7>, <9, amod, 8>, <9, case, 6>, <5, punct, 10>}. This example also demonstrates the need of introduction of unique identifiers for words. This sentence has two determiners with lemma A; if we shall write <CAT, det, A> we could not understand if we mean the word on the first or the seventh position.

Let us consider a tuple <w_i, r, w_j>. In case of $i < j$, we can speak about the right branching; in case of $i > j$, we can speak about the left branching.

Let us consider a tuple <w_i, r, w_j>. We denote here the part of speech of *i*-th word as π_i, and define r_{ij} as a label of an arc connecting w_i and w_j. In this case, we could calculate frequency of occurrence for every tuple $g = <\pi_i, \pi_j, r_{ij}, b_j>$ where b_j is direction of connection of *j*-th word: $b = 0$ if i < j (right branching) and $b = 1$ otherwise (left branching).

Left and right branching are important features of a language. For example, the English language demands an adjective in preceding position before its governing noun; in Slavic languages, the preferred position is the same with some deviations; in Romance languages, preferred position is right side from the noun with some deviations. The degree of these deviations depends on the language. Calculating statistics for tuples like $<\pi_i, \pi_j, r_{ij}, b_j>$, we could find out the difference between the preferred word orders, investigate the words' aptitude for making connection with other words, and find out similarity among considered languages.

However, syntax could not be defined merely using connections between pairs of words and their order. In this paper, we are also going to investigate relations between triples of words: $h_1 = <\pi_i, \pi_j, \pi_*, r_{ij}, r_{jk}, b_j, b_k>$ and $h_2 = <\pi_i, \pi_j, \pi_*, r_{ij}, r_{ik}, b_j, b_k>$.

In this paper, we will understand a syntactic profile of a corpus as a statistics of occurrence for all pairs and triples occurred in this corpus: $Q = \{<g_i, f_i>\} \cup \{<h_j, f_j>\}$ where f_i and f_j are frequencies of occurrence for tuples g_i and h_j accordingly.

However, the syntactic label of a word could define its aptitude for making connection with other words. Thus, let us define extended tuples containing a label for a head word: $g = <\pi_i, \pi_j, r_{*i}, r_{ij}, b_j>$, $h_1 = <\pi_i, \pi_j, \pi_k, r_{*i}, r_{ij}, r_{jk}, b_j, b_k>$, and $h_2 = <\pi_i, \pi_j, \pi_k, r_{*i}, r_{ij}, r_{ik}, b_j, b_k>$. Let us also define an extended syntactic profile of a corpus Q.

In order to compare two corpora, we will use the following algorithm.

1. Calculate syntactic profile for both corpora and select from them top 10 most frequent pairs $T_{2,1} = \{<g_{i1}, f_{i1}>\}$, $T_{2,2} = \{<g_{i2}, f_{i2}>\}$ and top 10 most frequent triples $T_{3,1} = \{<h_{i1}, f_{i1}>\}$, $T_{3,2} = \{<h_{i2}, f_{i2}>\}$.
2. Join these sets and select frequencies for both corpora $\hat{T} = \{< \hat{d}_k, f_{k1}, f_{k2} >\}$, where $\hat{d}_k \in \{g_{k1}\} \cup \{g_{k2}\} \cup \{h_{k1}\} \cup \{h_{k2}\}$ and f_{k1}, f_{k2} are frequencies for the proper tuples of the first and the second corpora. The syntactic similarity of two corpora will be calculated as a rank correlation of these two vectors $sym = corr(<f_{k1}>, <f_{k2}>)$.

For several languages, we use the same algorithm, but we join all most frequent pairs T_2 and triples T_3 of all languages in the same list.

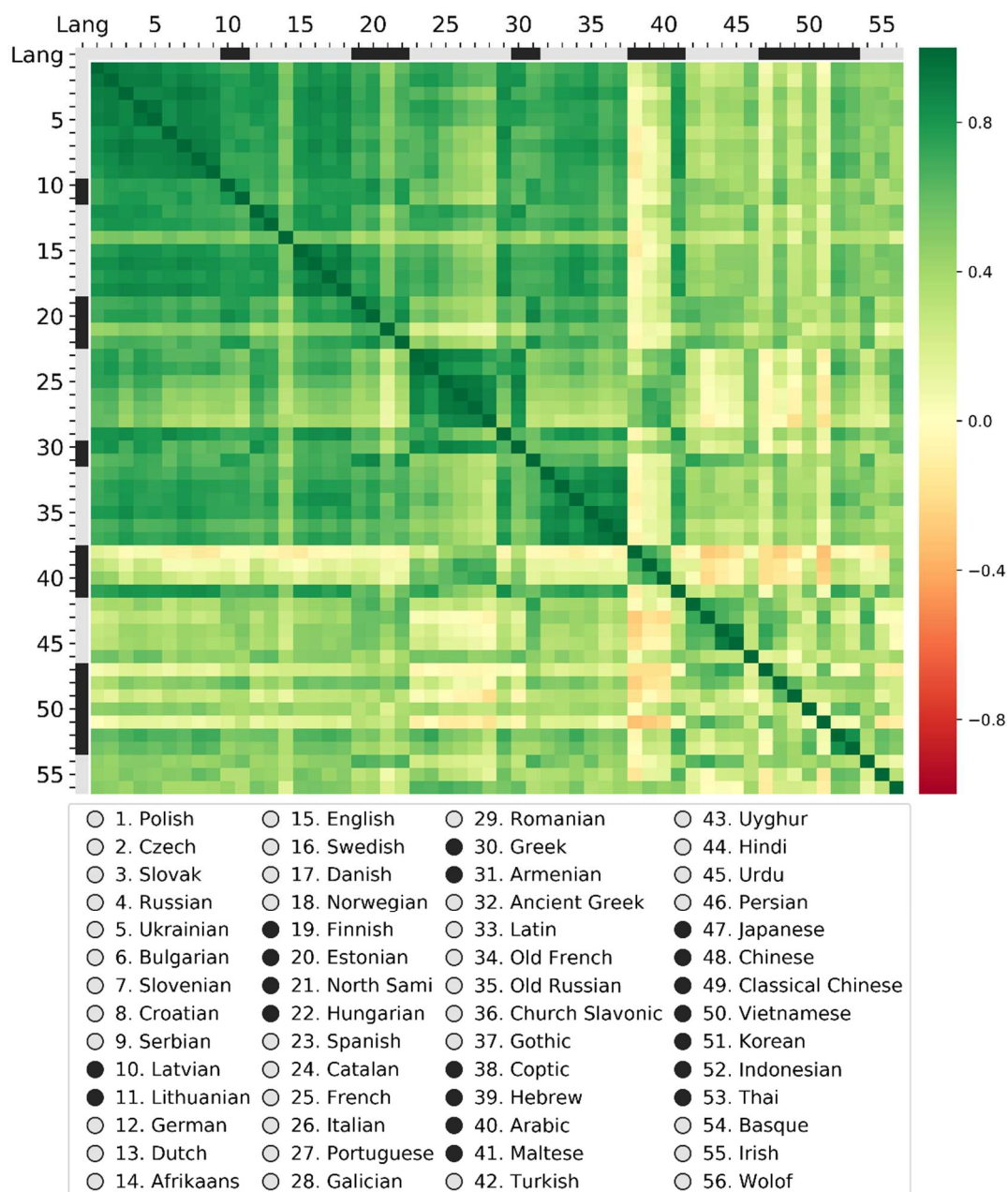|			
○ 1. Polish	○ 15. English	○ 29. Romanian	○ 43. Uyghur
○ 2. Czech	○ 16. Swedish	● 30. Greek	○ 44. Hindi
○ 3. Slovak	○ 17. Danish	● 31. Armenian	○ 45. Urdu
○ 4. Russian	○ 18. Norwegian	○ 32. Ancient Greek	○ 46. Persian
○ 5. Ukrainian	● 19. Finnish	○ 33. Latin	● 47. Japanese
○ 6. Bulgarian	● 20. Estonian	○ 34. Old French	● 48. Chinese
○ 7. Slovenian	● 21. North Sami	○ 35. Old Russian	● 49. Classical Chinese
○ 8. Croatian	● 22. Hungarian	○ 36. Church Slavonic	● 50. Vietnamese
○ 9. Serbian	○ 23. Spanish	○ 37. Gothic	● 51. Korean
● 10. Latvian	○ 24. Catalan	● 38. Coptic	● 52. Indonesian
● 11. Lithuanian	○ 25. French	● 39. Hebrew	● 53. Thai
○ 12. German	○ 26. Italian	● 40. Arabic	○ 54. Basque
○ 13. Dutch	○ 27. Portuguese	● 41. Maltese	○ 55. Irish
○ 14. Afrikaans	○ 28. Galician	○ 42. Turkish	○ 56. Wolof

Figure 2. Correlation matrix for pairs of connected words

4 EXPERIMENTAL RESULTS AND MODEL EVALUATION

For our experiments, we used the Universal Dependencies corpus [15] ver. 2.4. (accessible at http://universaldependencies.org/). We have selected 56 languages with size of corpora varying from 22 000 of word tokens for Thai up to 3.4 mln word tokens in the German corpus. All languages were divided into language groups and families: Slavic, Baltic, Germanic, Romance, Finn-Ugric, Greek-Armenian, Semitic, Turkic, Indo-Aryan, Ancient and Old. There also was a variety of languages which did not constitute a group inside the list of selected languages: Japanese, Korean, Chinese, Thai, Vietnamese, Indonesian, Basque, Irish, and

Wolof. The Coptic language do not belong to the Ancient language group but placed here because of texts similarity. Thus, we covered the world biggest language groups excluding native languages of Americas and Central Africa. Numerical data is too big and placed in supplementary materials (http://cosyco.ru/syntax/syntax_share.zip).

We calculated syntactic profiles for all these languages and used Spearman rank correlation to evaluate the similarity of languages. Correlation matrix for extended pairs of connected words is presented in Fig. 2, for extended triples of connected words at Fig. 3.
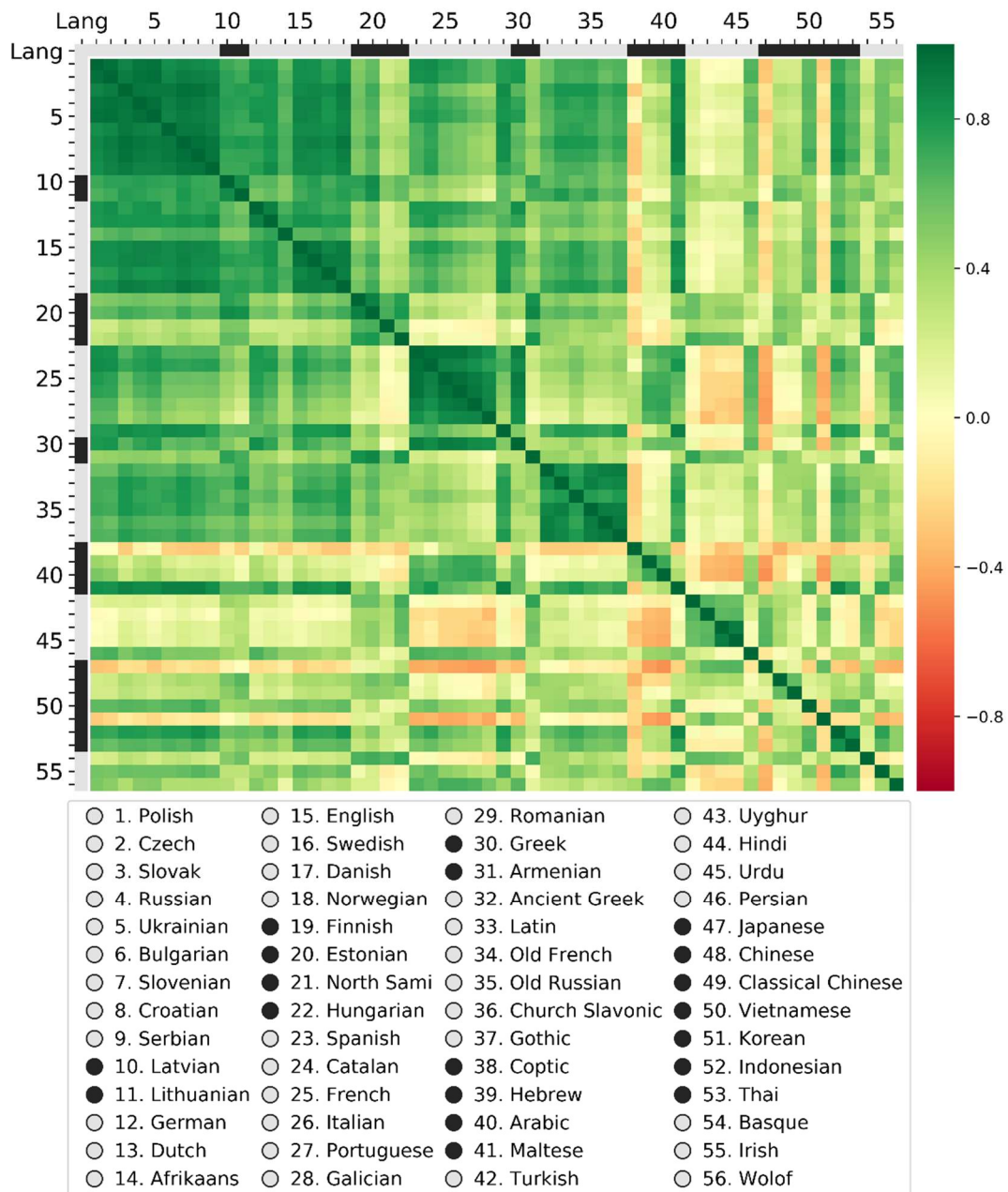

Figure 3. Correlation matrix for triples of connected words

It is easy to see that languages belonging to the same group constitute clusters on presented figures. For pairs of connected words, the most correlated language pairs are Spanish and Catalan, Polish and Czech, and Russian and Ukrainian. The most correlated language is Russian – the `average correlation is 0.64 while the average correlation for all the languages is 0.48. Coptic is the most uncorrelated language – its correlation with Arabic and Hebrew is 0.72 and 0.69 while the average correlation is equal to 0.01. Average correlations for Japanese and Korean languages are 0.03 and 0.04. The most correlated language group is Slavic – the average correlation in the group is 0.88; the second correlated group is Ancient languages (Ancient Greek, Latin, Old French, Old Russian, Church Slavonic, Gothic) – 0.86; the third group is Romance languages – 0.79 including Romanian and 0.86 excluding it.

For word triples, the situation is almost the same. One of the most correlated pairs of languages is Slovenian and Croatian. The value of correlations changes, however the qualitative image is the same. The most changed language here is Japanese; its average correlation reduces from 0.17 for word pairs to -0.11 for word triples. However, correlation keeps around zero.

The average correlation for Hindi, Urdu and Uygur reduces from 0.36, 0.34 and 0.33 for word pairs to 0.13, 0.12 and 0.11 respectively for word triples. The most tragic changes are observed for the Hungarian languages where average correlation falls from border 0.55 to neglectable 0.32.However, the average correlation among languages in the Slavic group slightly raises up to 0.91, for Ancient languages keep for 0.85, and for Romance languages keeps for 0.79 (slightly raised up to 0.89 without the Romanian language). Thus, word triples contain more language-specific information than word pairs.

To make a comparison with a common data, we have placed two extra columns on images (two right columns on all the images). The first one demonstrates the word order in a language; Subject-Verb-Object marked as dark green, Subject-Object-Verb marked as pale green, Verb-Subject-Object as beige, and languages without the preferred word order are marked as dark red (data taken from https://wals.info/). The second column demonstrates the order of a connected adjective and a noun: dark green marks adjective-first word order, beige marks noun-first word order, red marks languages without the preferred word order.

5   DATA ANALYSIS

We examined the data on the most frequent word pairs and triples for different languages and found out some differences among them. Table 1 demonstrates the most frequent words in connected pairs for Russian, Ukrainian, Polish, English, German, Swedish, Japanese, Chinese and Korean languages. In European languages, the most frequent connection is a noun in oblative case (prepositional phrase) entailed by a preposition labelling this case. European languages demonstrate more similar behavior – there are 21 types of connection for 6 languages, while Asian ones are more variable – 26 types of connection for 3 languages. This fact corresponds to the fact that Japanese and Korean languages have the lowest rate of average correlation with other languages. Note that Russian and Ukrainian languages have 8 identical combinations (correlation is 0.95), while Russian and Ukrainian have just 6 combinations coinciding with Polish (correlation 0.87 and 0.89 respectively). English and Swedish have 7 identical (correlation 0.93), English and German have 7 (correlation 0.82), German and Swedish have 6 (correlation 0.84).

Russian

head		tail	N
NOUN obl	←	ADP case	1
NOUN nmod	←	ADJ amod	2
NOUN nmod	←	ADP case	3
NOUN nmod	→	NOUN nmod	4
NOUN obl	←	ADJ amod	5
NOUN obl	→	NOUN nmod	6
VERB root	←	NOUN nsubj	7
NOUN nsubj	→	NOUN nmod	8
NOUN nsub	←	ADJ amod	9
VERB root	→	NOUN obl	10

Ukrainian

head		tail	N
NOUN obl	←	ADP case	1
NOUN nmod	←	ADJ amod	2
NOUN nmod	←	ADP case	3
NOUN nmod	→	NOUN nmod	4
NOUN obl	←	ADJ amod	5
NOUN obl	→	NOUN nmod	6
VERB conj	←	CCONJ cc	11
NOUN conj	←	CCONJ cc	12
VERB root	→	NOUN obl	10
VERB root	←	NOUN nsubj	7

Polish

head		tail	N
NOUN obl	←	ADP case	1
VERB root	→	NOUN obl	10
VERB root	←	NOUN nsubj	7
NOUN nmod	←	ADP case	3
VERB root	→	NOUN obj	13
NOUN obl	←	ADJ amod	5
NOUN obl	→	NOUN nmod	6
VERB root	←	PART advmod	14
VERB root	→	VERB conj	15
VERB root	←	NOUN obl	16

English

head		tail	N
NOUN obl	←	ADP case	1
NOUN nmod	←	ADP case	3
NOUN obl	←	DET det	17
NOUN obj	←	DET det	18
VERB root	←	PRON nsubj	19
NOUN nsubj	←	DET det	20
NOUN nmod	←	DET det	21
VERB conj	←	CCONJ cc	11
VERB root	→	NOUN obj	13
VERB root	→	NOUN obl	10

German

head		tail	N
NOUN obl	←	ADP case	1
NOUN nsubj	←	DET det	20
NOUN nmod	←	ADP case	3
NOUN nmod	←	DET det	21
NOUN obl	←	DET det	17
VERB root	←	NOUN nsubj	7
NOUN obj	←	DET det	18
VERB root	←	NOUN obl	16
NOUN obl	←	ADJ amod	5
VERB root	→	NOUN obl	10

Swedish

head		tail	N
NOUN obl	←	ADP case	1
NOUN nmod	←	ADP case	3
VERB root	→	NOUN obl	10
NOUN obl	←	ADJ amod	5
VERB root	←	NOUN nsubj	7
NOUN obl	←	DET det	17
VERB root	→	NOUN obj	13
VERB root	←	PRON nsubj	19
NOUN conj	←	CCONJ cc	12
VERB conj	←	CCONJ cc	11

Japanese

head		tail	N
NOUN nmod	→	ADP case	22 23
NOUN obl	→	ADP case	24
NOUN obj	→	ADP case	25
VERB advcl	→	SCONJ mark	26
NOUN nmod	←	NOUN compound	27
VERB root	←	VERB advcl	16
VERB root	←	NOUN obl	28
NOUN nmod	←	NOUN nmod	29 30
NOUN obl	←	NOUN nmod	
VERB advcl	←	NOUN obl	

Chinese

head		tail	N
VERB root	←	ADV advmod	31
VERB root	←	PRON nsubj	19
NOUN obl	←	ADP case	1
VERB root	→	NOUN obj	13
VERB root	←	NOUN nsubj	7
VERB root	←	NOUN obl	16
VERB acl	→	PART mark	32
VERB root	←	VERB advcl	27
NOUN obj	←	NOUN compound	33
VERB root	→	VERB ccomp	34

Korean

head		tail	N
VERB root	←	NOUN dislocated	35
VERB root	←	NOUN obj	36
VERB root	←	ADV advmod	31
VERB root	←	NOUN nsubj	7
VERB root	←	SCONJ ccomp	37
NOUN obj	←	VERB acl	38
NOUN obj	←	NOUN nmod	39
VERB acl	←	ADV advcl	40
VERB root	←	CCONJ cc	41
VERB root	←	NOUN advmod	42

Table 1. Most frequent word pairs; an arrow demonstrates left or right branching

It is easy to see that different languages demonstrate different behavior at top-10 connections. Slavic languages do not use determiners while they are a very important part in Germanic languages; the Swedish language has less determiners because they could be a postfix of a word. The Japanese language uses more adpositions because there are no grammatical cases at all while the situation with the Korean language is opposite. Thus, the method correctly demonstrates similarity and dissimilarity of world languages. However, we should check several features which could influence the achieved results.

As it was mentioned above, the Universal Dependencies (UD) corpus is a collection of corpora for a long list of languages. However, there could be several subcorpora for a language, tagged by different research groups. The tagging by different groups with different defaults could lead to corpora inconsistency. That is why we checked if different corpora for a language correlate among themselves. The correlation among Czech subcorpora is higher than 0.94, for Russian and German subcorpora is higher than 0.97.

Several languages were annotated by the same group that is responsible for UD support. They used parallel texts translated into Polish, Czech, Russian, German, English, Swedish, Finnish, Spanish, French, Italian, Portuguese, Arabic, Turkish, Hindi, Japanese, Chinese, Korean, Indonesian, and Thai languages. Using this corpus we could eliminate the influence of several factors: tagging style of a team, differences among language models created by different teams of researchers, differences among styles and genres. Using this parallel corpus has not changed the situation, the difference between correlation for the full corpus and its parallel subcorpora for the European languages stays within 0.05. However, the correlation for the Arabic and Turkish languages changes dramatically for up to ±0.25. Situation for word triples changed more than for word pairs.

We could suppose that the correlation depends on the list and number of investigated features. If we change the list of languages, then we change the number of considered features. This means that we could not correctly compare results for different lists of corpora and subcorpora. However, the proposed method allows drawing a correct sketch for the situation in similarity of syntax for different languages.

6 CONCLUSIONS

In this article, we introduced a new method for the quantitative evaluation of the syntax similarity. The experimental results demonstrate that the method draws a correct picture of similarity among world languages. Correlations between different corpora of the same language are extremely high – more than 0.95; languages belonging to the same language group have higher correlation inside the group. Slavic languages demonstrate the highest correlation inside the group. They are followed by Ancient languages. The third most similar group is Romance languages which are surprisingly weakly correlated with Latin – about 0.4.

Despite of the overall correct picture of language correlation, the method has several disadvantages. The basis of the method finds the most frequent syntactical connections for corpora of different languages and joins them into a list. Therefore, changing of the list of considered languages leads to changing of the list of the most frequent connections since there is a high probability for introduction of new connections. In this article, we use the Spearman rank correlation formula which is dependent to a feature set and incomparable for different sets. Thus, the results calculated for one set of languages are incomparable for another set. Consequently, we are not able to compare the results for different multilingual corpora directly,

as we tried to do for PUD and GSD. We are not able to compare languages pair to pair, since such comparison will be conducted on different feature sets and, consequently, will not be also comparable. Thus, the method needs some further improvement.

In spite of the mentioned drawback, the method could be successfully applied for quantitative research in such area as comparative linguistics. Here it could allow finding new connections among languages, and track language changes. It is also applicable to quantitative stylometric for finding differences among genres and styles.

REFERENCES

[1] S. Padó and M. Lapata, "Dependency-based construction of semantic space models", *Computational Linguistics*. **33** (2), 161–199 (2007).

[2] T. Mikolov, K. Chen, G. Corrado and J. Dean, "Efficient estimation of word representations in vector space" *arXiv preprint arXiv:1301.3781* (2013). https://arxiv.org/abs/1301.3781

[3] J. Pennington, R. Socher and C. Manning, "Glove: Global vectors for word representation" In *Proc. of the 2014 conference on empirical methods in natural language processing (EMNLP)*, 1532-1543 (2014).

[4] M. Nickel and D. Kiela, "Poincaré embeddings for learning hierarchical representations" *Advances in Neural Information Processing Systems*, 30, 6338–6347 (2017).

[5] B. Dhingra, C.J. Shallue, M. Norouzi, A.M. Dai and G.E. Dahl, "Embedding Text in Hyperbolic Spaces" In *Proc. of the Twelfth Workshop on Graph-Based Methods for Natural Language Processing (TextGraphs-12)*, 59–69 (2018).

[6] E. Gibson and E. Fedorenko, "The need for quantitative methods in syntax and semantics research" *Language and Cognitive Processes*, **28** (1-2), 88-124 (2013).

[7] Ö. Dahl, *The Growth and Maintenance of Linguistic Complexity*, Amsterdam: John Benjamins Publishing Company (2004).

[8] R. Köhler, *Quantitative Syntax Analysis*, Berlin; Boston: De Gruyter Mouton (2012).

[9] R. Ferrer-i-Cancho and R.V. Solé, "The small world of human language" *In Proceedings of The Royal Society of London. Series B, Biological Sciences*, **268** (1482), 2261–2265 (2001).

[10] S. Fortunato, "Community detection in graphs" *Physics Reports*, **486,** 75–174 (2010).

[11] A.P. Mikhailov, A.P. Petrov and O.G. Pronicheva, "″Power-Information-Society″ Model" *Mathematica Montisnegri*, **XLIV**, 73-83 (2019).

[12] S. Kübler, R. McDonald and J. Nivre, *Dependency Parsing*, San Rafael: Morgan & Claypool, (2009).

[13] A. Carnie, *Syntax: A generative introduction*, 3rd edition, Malden, MA: Wiley-Blackwell, (2013).

[14] V. Nastase, R. Mihalcea, D. Radev, "A survey of graphs in natural language processing" *Natural Language Engineering*, **21** (5), 665-698 (2015).

[15] J. Nivre, M.-C. de Marneffe, F. Ginter et al., "Universal Dependencies v1: A Multilingual Treebank Collection" In *Proc. of LREC-2016*, 1659-1666 (2016).

ON THE OCCASION OF THE 80TH ANNIVERSARY OF THE ACADEMICIAN OF THE RUSSIAN ACADEMY OF SCIENCES, RECTOR OF MOSCOW STATE UNIVERSITY M.V. LOMONOSOV V. A SADOVNICHY

Viktor Antonovich Sadovnichy, member of the Mathematica Montisnigri Editorial Board, celebrates its 80th anniversary this year.

Academician of the Russian Academy of Sciences, Professor V.A. Sadovnichiy is an outstanding Soviet and Russian mathematician, a major organizer of science and education, a well-known specialist in the field of computer science and applied mathematics, rector of Moscow State University, a member of many foreign Academies and Universities, including an honorary doctor of the University of Montenegro, a foreign member of the Montenegrin Academy of Sciences and arts. He authored fundamental works in mathematics and mechanics, and has a number of important applied results. The mathematical works relate to the field of theory of differential operators, the mathematical justification of a number of approaches in the relativistic theory of gravity. In works devoted to the spectral theory of non-self-adjoint operators, he proposed and developed analytical methods and ideas for studying operators with a complex occurrence of a parameter. V.A. Sadovnichy investigated the most important problem of mathematical physics - the Orr-Sommerfeld problem, which arises in the theory of hydrodynamic stability, and the boundary-value problem for the Bessel equation, and here an operator with an unbounded potential was considered for the first time in the theory of traces of the discrete operators.

The mathematicians at the University of Montenegro are grateful to Academician V.A. Sadovnichy for his mentoring, help and support provided in developing the scientific potential of the Montenegrin School of Mathematics, especially in difficult times of the blockade and isolation of Yugoslavia by Western countries.

The editorial board of the journal Mathematica Montisnigri wishes Viktor Antonovich good health, long and fruitful activities as the rector of M.V. Lomonosov Moscow State University and further successes in the development of theoretical and applied mathematics.

Mathematica Montisnigri Editorial Board

К 80-ЛЕТИЮ СО ДНЯ РОЖДЕНИЯ АКАДЕМИКА РОССИЙСКОЙ АКАДЕМИИ НАУК, РЕКТОРА МОКОВСКОГО ГОСУДАРСТВЕННОГО УНИВЕРСИТЕТА ИМ. М.В. ЛОМОНОСОВА В. А САДОВНИЧЕГО

Член Редакционной коллегии журнала Mathematica Montisnigri Виктор Антонович Садовничий в этом году отмечает 80-летний юбилей.

Академик Российской академии наук, профессор В.А. Садовничий — выдающийся советский и российский ученый-математик, крупный организатор науки и образования, известный специалист в области информатики и прикладной математики, ректор МГУ, член многих иностранных Академий и Университетов, в том числе является почетным доктором Университета Черногории, иностранным членом Черногорской Академии наук и искусств. Ему принадлежат фундаментальные труды в математике, механике, ряд важных результатов прикладного характера. Математические труды относятся к области теории дифференциальных операторов, математическому обоснованию ряда подходов в релятивистской теории гравитации. В работах, посвященных спектральной теории несамосопряженных операторов, им предложены и развиты аналитические методы и идеи изучения операторов со сложным вхождением параметра. В.А. Садовничий исследовал важнейшую задачу математической физики — задачу Орра-Зоммерфельда, возникающую в теории гидродинамической устойчивости, и краевую задачу для уравнения Бесселя, причем здесь впервые в теории следов дискретных операторов был рассмотрен оператор с неограниченным потенциалом.

Математики Университета Черногории благодарны академику В.А. Садовничему за наставничество, помощь и поддержку, оказанную в развитии научного потенциала Черногорской математической школы, особенно в трудные времена блокады и изоляции Югославии западными странами.

Редколлегия журнала Mathematica Montisnigri желает Виктору Антоновичу крепкого здоровья, долгой и плодотворной деятельности на посту ректора МГУ им. М.В. Ломоносова и дальнейших успехов в дальнейшем развитии теоретической и прикладной математики.

Редколлегия журнала Mathematica Montisnigri

INFORMATION ANALYTICAL REVIEW.
18TH INTERNATIONAL SCIENTIFIC SEMINAR "MATHEMATICAL MODELS AND MODELING IN LASER-PLASMA PROCESSES AND ADVANCED SCIENTIFIC TECHNOLOGIES" (LPPM3-2019)

V.I. MAZHUKIN*

M.V. Keldysh Institute of Applied Mathematics of RAS
Moscow, Russia
*Corresponding author. E-mail: vim@modhef.ru

Summary. The results of the Eighteenth International Scientific Seminar "Mathematical Models and Modeling in Laser-Plasma Processes & Advanced Scientific Technologies" (LPPM3-2019), which was held from September 29 to October 5, 2019 in Montenegro (Petrovac), are briefly summarized by the program committee of the seminar.

1 INTRODUCTION

The 18th International Scientific Seminar "Mathematical Models and Modeling in Laser-Plasma Processes & Advanced Scientific Technologies" (LPPM3-2019) was held from September 29 to October 5, 2019 in the city of Petrovac (Montenegro).

Figure 1 shows a photograph of the participants of the LPPM3-2019 workshop on the opening day. The Seminar organizers: M.V. Keldysh Institute of Applied Mathematics of Russian Academy of Sciences, A.M. Prokhorov Institute of General Physics of the Russian Academy of Sciences, University of Montenegro (Podgorica), Forum of Professors and Researchers of Montenegro, Scientific journal "Mathematica Montisnigri".

The seminar in 2019 coincided with the 100th anniversary of the birth of an outstanding Soviet and Russian scientist, academician of the Academy of Sciences of the USSR and the Russian Academy of Sciences Alexander Andreevich Samarskii (Fig. 2). Academician A.A. Samarskii is the founder of the Soviet and Russian schools of mathematical modeling, the creator of the fundamental general theory of difference schemes, an outstanding teacher, who brought up more than one generation of famous scientists, an active organizer and a bright propagandist of science. Scientific activity of academician A.A. Samarskii is firmly connected with the M.V. Keldysh Institute of Applied Mathematics, Academy of Sciences of the USSR and the Russian Academy of Sciences and the Institute of Mathematical Modeling of the Russian Academy of Sciences, which he headed. A brilliant scientist and an excellent organizer, he laid the potential to preserve the world level of Russian science in the most important field of mathematical modeling for our country.

The 18th International Scientific Seminar LPPM3 celebrated the 10th anniversary of its holding in Montenegro. The seminar "Mathematical models and modeling in laser-plasma processes and advanced scientific technologies" (LPPM3) was founded in 2004. The first five years, the organizers of the Seminar were two institutes of the Russian Academy of Sciences:

M.V. Keldysh Institute of Applied Mathematics and the A.M. Prokhorov Institute of General Physics. During this period, the scientific theme of the seminar was devoted to one direction "Mathematical Models and Modeling in Laser-Plasma Processes" and was constantly held in Moscow. In 2009, after joining of a group of researchers from the University of Montenegro, a new direction was formed, "Mathematical Modeling in Advanced Scientific Technologies," and the seminar site https://lppm3.ru appeared. Since that time, the seminar has been constantly held in Montenegro.

Fig. 1. The participants of the seminar LPPM3-2019 in the opening day.

Fig. 2. The opening of the seminar LPPM3-2019

2 MAIN CHARACTERISTICS OF THE SEMINAR

The representatives of more than 25 Russian and foreign scientific organizations attended the seminar in 2019. The composition of the 18th Seminar, scientific organizations and the number of participants is presented in the diagram (Fig. 3). The most numerous was the representation of the M.V. Keldysh Institute of Applied Mathematics of RAS (37%). From Russia, the scientific results were presented by researchers of eight scientific centers and institutes of the Russian Academy of Sciences, 10 universities. Montenegro was represented by researchers at the University of Montenegro. The researchers from the University of Nova Gorica (Slovenia), the University of East Sarajevo (Bosnia and Herzegovina), the University of Bangor (Bangor, Gwynedd, United Kingdom), the University of Bielefeld (Munster, Germany), Friedrich Schiller University of Jena (Germany), A*STAR Research Center (Singapore) and the University of Rochester (USA) attended the 18th LPPM3 seminar.

By tradition, the Seminar is supported by the scientific journal Mathematica Montisnigri. The journal, as before, will publish articles on the most interesting reports of 2019. The publication on the pages of the journal of innovative articles with scientific novelty and tested at the Seminar contributes to the development of mathematical science, demonstrates to the scientific community the possibilities of the methodology of mathematical modeling.

In February 2019, the 100th anniversary of the birth of Alexander Andreevich Samarskii was celebrated. He was an outstanding Soviet and Russian scientist, academician of the USSR Academy of Sciences and the Russian Academy of Sciences. The interdisciplinary focus, based on the scientific methodology of mathematical modeling, which is traditional for the LPPM3 Workshop, is a continuation and development of the ideas of A.A. Samarskii. Prof. V.I. Mazhukin (M.V. Keldysh IAM of RAS, Russia), the chairman of the program committee of the seminar devoted the plenary report "Formation of mathematical modeling. To the 100th anniversary of academician A.A. Samarskii "[1] to the prospects for the development of the methodology of mathematical modeling, first formulated by Academician A.A. Samarskii. The methodology of mathematical modeling, which is the scientific platform of the LPPM3 seminar, allows one to bring together scientists working in various subject areas: mathematics, physics, chemistry, biology, medicine, economics, history.

In three plenary and six invited reports, the main scientific directions of the seminar were formulated. Among the plenary and invited reports, one of the main areas discussed was the problem of short-pulse (nanosecond) laser action on condensed matter, which is one of the most popular subject areas of mathematical modeling. The experimental aspects were considered in plenary reports [2,3]. The prospects for the use of laser action in medicine are the subject of a plenary report [2] presented by the A.M. Prokhorov GPI of RAS, Russia. The report discussed the results of studies of laser-plasma action as an effective tool used in surgery and therapy. The plenary report [3], which was also presented by the A.M. Prokhorov GPI of RAS, was devoted to the study of phenomena arising in liquid mercury under the influence of short laser pulses. The report presented experimental results that demonstrate the behavior of pressure pulses, which may be due to the metal-insulator transition in the near-critical region of mercury. In the plenary report [4] presented by M.V. Lomonosov Moscow State University (Moscow, Russia), high-order Fano resonances and giant magnetic fields in dielectric microspheres are reported. Such resonators provide magnetic nanostructured generators with giant magnetic fields, which is attractive for many applications.
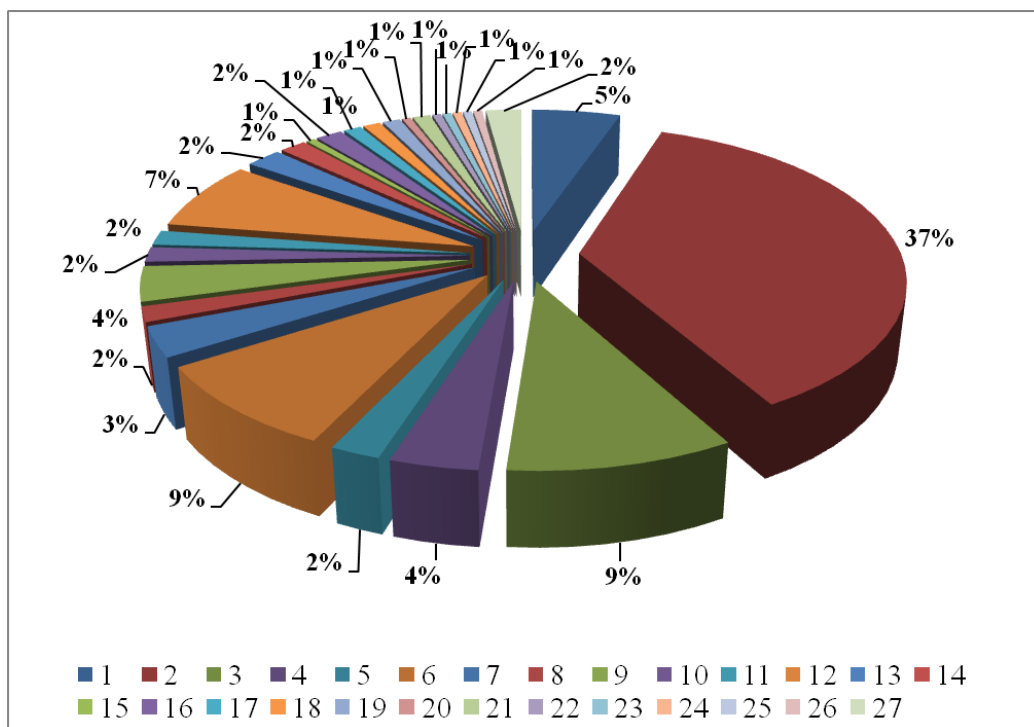
Fig. 3. The chart of the distribution of the number of speakers by scientific organizations.
Designations on the diagram:

1	National Research Nuclear University MEPhI, Moscow, Russia	15	Friedrich Schiller University of Jena, Germany
2	M.V. Keldysh Institute of Applied Mathematics of RAS, Moscow, Russia	16	Bauman Moscow State Technical University, Moscow, Russia
3	A.M. Prokhorov GPI of RAS, Moscow, Russia	17	Nova Gorica University, Slovenia
4	P. N. Lebedev Physical Institute of RAS, Moscow, Russia	18	University of Rochester, USA
5	Space Research Institute of RAS, Moscow, Russia	19	Fiber Optics Research Center of RAS, Moscow, Russia
6	ITMO University, Saint Petersburg, Russia	20	I.M. Gubkin Russian State University of Oil and Gas, Moscow, Russia
7	M.V. Lomonosov Moscow State University, Moscow, Russia	21	Ural Federal University, Yekaterinburg, Russia
8	Scientific Research Institute for System Analysis of RAS, Moscow, Russia	22	Moscow Automobile And Road Construction State Technical University, Russia
9	M.A. Lavrentyev Institute of Hydrodynamics SB of RAS, Novosibirsk, Russia	23	Bangor University, UK
10	Joint Institute of High Temperature of RAS, Moscow, Russia	24	A*STAR Research, Singapore
11	National University of Science and Technology «MISIS», Moscow, Russia	25	MIREA - Russian Technological University, Moscow, Russia
12	University of Montenegro, Podgorica, Montenegro	26	University of Bielefeld, Munster, Germany
13	University of East Sarajevo, Bosnia and Herzegovina	27	School of Mathematics and Physics № 2007, Moscow, Russia
14	Novosibirsk State University, Novosibirsk, Russia		

The experimental aspects of the problem of laser action on condensed matter were also considered in invited papers [5, 6]. The report [5], presented by the researchers from ITMO (St. Petersburg, Russia), was devoted to the urgent problem of manufacturing new optical components using compressed laser-induced microplasma (SLIMP). A new method for the experimental study of the thermophysical properties of a wide range of conductive substances at a high level of pressure temperatures was reported in an invited report [6] presented by the Joint Institute of High Temperature of RAS (Moscow, Russia).

Based on the results of the theoretical studies, the main tool of which is mathematical modeling, an invited report is presented [7]. It presents the results of mathematical modeling of the collision process of two molecular clouds (MC) in a central collision. Collisions of the MC are one of the key mechanisms for the formation of new stars (Scientific Research Institute for System Analysis of RAS, M.V. Lomonosov Moscow State University, Moscow, Russia).

The topic "Models and Algorithms for High Performance Computing" was presented by the invited reports [8,9]. The report [8] presented an effective technology for mathematical modeling of the acceleration of solids and plasma under the influence of electromagnetic forces. For mathematical modeling, the Temetos software platform was developed, which allows one to specify spatial areas of complex geometric shape and build concentrating grids in them, including unstructured ones,. The platform contains a number of service modules for preparing, launching and analyzing the results of calculations on a supercomputer, including visualization of the resulting solution. Using the modules developed for the Temetos platform, physical fields were calculated for a number of configurations of magnetic accelerators, including rail-accelerated ones, and work was done on modeling plasma acceleration under astrophysical conditions and research. The results obtained are in demand in many fundamental and applied problems. The report is presented by M.V. Keldysh IAM of RAS (Moscow, Russia).

The invited paper [9] presented by M.A. Lavrentyev Institute of Hydrodynamics of SB of RAS and Novosibirsk State University, (Novosibirsk, Russia), was devoted to the accuracy of MUSCL-type schemes when calculating shock waves. The report deals with the development of a difference scheme using the MUSCL reconstruction of numerical flows. This scheme is of particular interest because it underlies a whole class of monotone central-difference schemes of increased accuracy, the implementation of which does not use the solution of the Riemann problem at the boundary of adjacent cells of a difference grid (in contrast to standard MUSCL schemes).

The problems outlined in the plenary and invited reports were discussed during the sessions of the sections. The diagram (Fig. 4) shows the distribution of reports among the scientific organizations which submitted these reports for discussion at section meetings. According to the number of scientific reports presented at the LPPM3 seminar in 2019, the leader is the M.V. Keldysh Institute of Applied Mathematics of RAS. The share of reports of this institute in the total number of reports is 35%. In second place in the number of reports presented, the main topic of which is "Models of mathematical physics and complex analysis", is the University of Montenegro. The share of Montenegro reports in the total amount is 22%. The consequence of the fact that more than half of all reports were submitted by mathematical institutes was a change in the thematic structure (Fig. 5). The most numerous in 2019 were topics "Models and algorithms for high-performance computing" (23% of the total number of reports) and "Models of mathematical physics and complex analysis "(22%).

The following topics in the contribution are "Mathematical modeling and computational experiment in applied problems" (13%) and" Russian space "(13%), most of the reports on the later topics are also presented by M.V. Keldysh IAM of RAS.

In the reports of the subject "Mathematical modeling and computational experiment in applied problems", the methodology of molecular dynamics modeling (MDM) was discussed, and the increasing importance in the studies of the atomistic approach associated with the development of computational tools was noted.
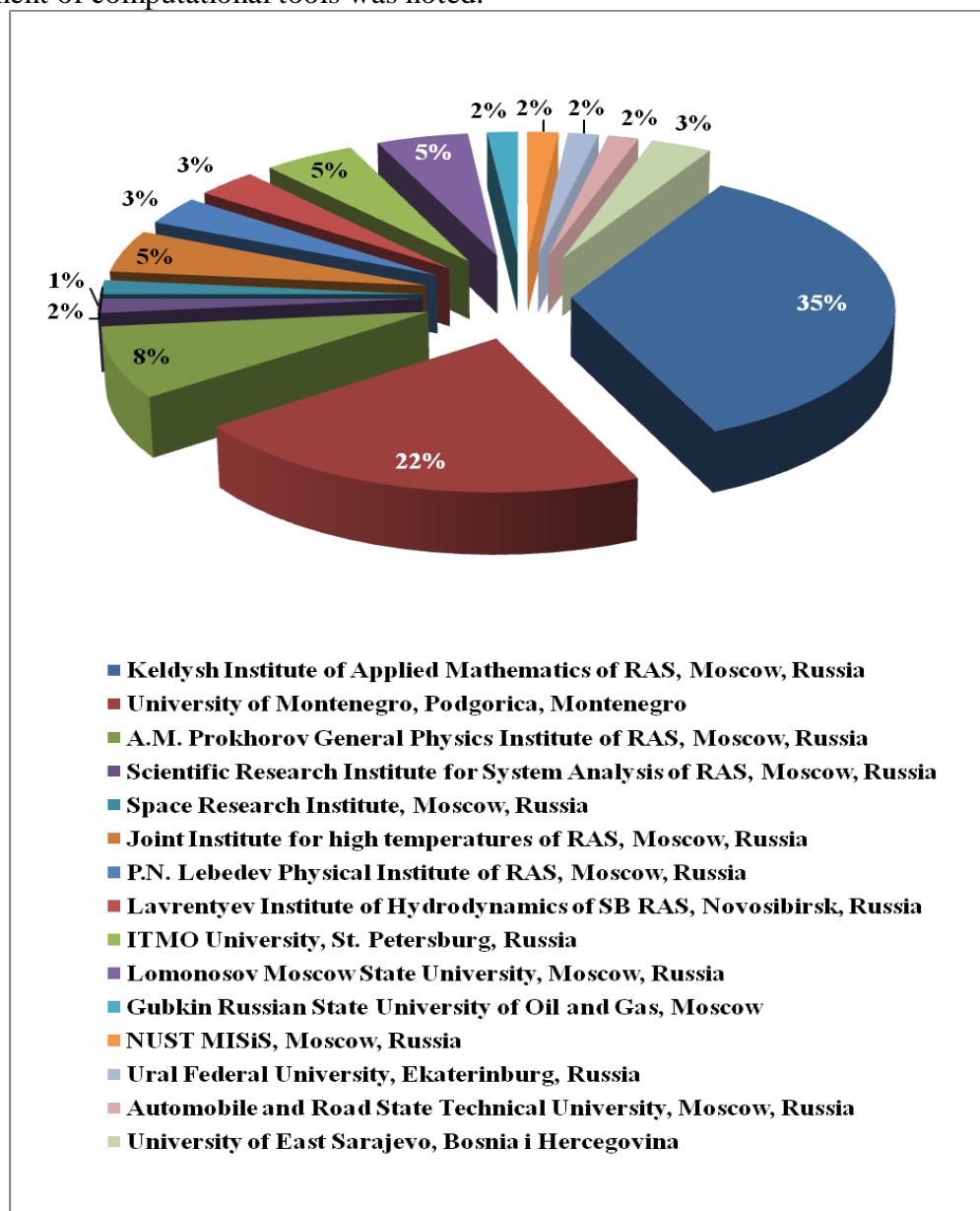
Fig. 4. Distribution chart of reports by scientific organizations of keynote speakers.

Within the framework of the molecular-dynamic methodology, the results of studies of the properties of metals [10] and semiconductors [11] in the field of melting and critical phenomena were presented (reports of M.V. Keldysh IAM of RAS). Within the topic, the

M.V. Keldysh Institute of Applied Mathematics of RAS presented a number of reports on modeling of the radiation effects in various media [12-14]. The simulation results presented in the reports are used in the design of high-tech structural materials.

The traditional topic of the seminar "Russian space" icnluded 13% of all reports. The invited report [15] presents the results of an in-depth study of physics by schoolchildren on the example of school scientific work on measuring the thermal diameter of the Sun, carried out under the guidance of the community of collectives of the A.M. Prokhorov GPI of RAS and Physics and Mathematics School No. 2007 of Moscow (Russia).

N	Scientific topics of the seminar LPPM3
1	Mathematical modeling and computational experiment in applied problems
2	Modeling of laser action on materials
3	Generation of nanoparticles and nanostructures
4	Continual and atomistic models
5	Laser ablation - experiment, theory, statements of the problems
6	Plasma theory and computational experiment
7	Models of mathematical physics and complex analysis
8	Models and algorithms for high performance computing
9	Russian space
10	Mathematical methods in biomedicine
11	Advanced scientific technology in the humanities

Table 1.
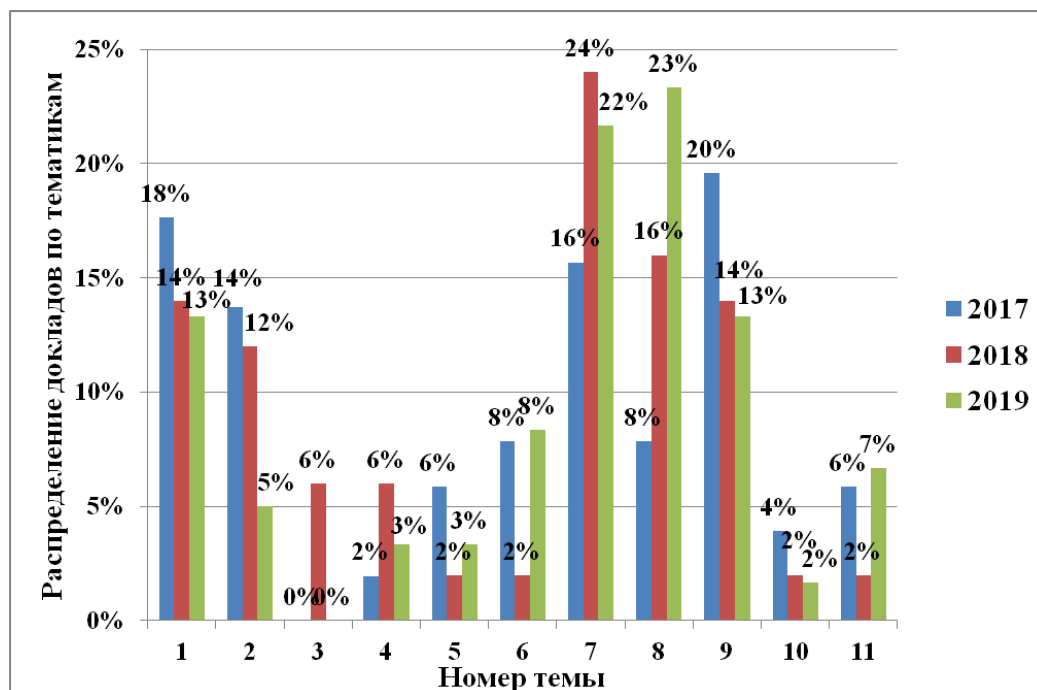
Fig. 5. Distribution of the reports over the scientific topics. The dynamics over the period from 2017 to 2019. The designations of scientific topics in the diagram are given in table 1.

In the course of section discussions, the problems of observing space objects, the development of observing systems, and the statistical processing of the obtained data were considered [16–20]. The report [21] (Institute of Space Research of RAS, Moscow, Russia) presents the results of three-dimensional numerical simulation of heat propagation in the outer layers of magnetized neutron stars. Determining the structure of the magnetic field on the surface of a neutron star is an important task of modern astrophysics. In the report [22], presented by Scientific Research Institute for System Analysis of RAS (Moscow, Russia), the actual problem of modeling operator-controlled robots was considered. The methods and approaches of automatic control of a virtual anthropomorphic robot were discussed, with the help of which the operations of capturing, holding and moving objects of a virtual environment are implemented. The proposed methods and approaches are based on the use of virtual sensors, solving the inverse kinematics problem, and synthesizing force control.

Scientists of the University of Montenegro presented reports [23-33] in the areas of complex analysis (the results of studies of various spaces of analytical and harmonic functions are presented); algebra (the results of studies of various algebraic structures, such as hypernormal rings and semisimple n-dimensional bialgebras, are presented).

The materials of the participants of the conference LPPM3-2019 can be found on the website https://lppm3.ru/en/historyeng/history-of-programmes.

3 DECISIONS OF THE SEMINAR

The following decisions were made:
- to strengthen and develop international scientific cooperation in the field of the application of mathematical modeling in every way;
- to support the basic principles of the Seminar, strengthening its interdisciplinarity, attracting for this scientists from various fields of science;
- to hold in 2020 the 19th International Scientific Seminar LPPM3 in Montenegro.

The detailed information on the preparation of the seminar, presentation materials and results of annual sessions can be found on the website: http://lppm3.ru/.

The Chair of the Program Committee, Professor V.I. Mazhukin.

4 REFERENCES

[1] V.I. Mazhukin, "The genesis of mathematical modeling. To the 100th anniversary of academician A.A. Samarskii", *XVIII International Seminar Mathematical Model & Modeling in Laser-Plasma Processes & Advanced Science Technologies. Program and Abstracts. Petrovac, Montenegro*, 48-49 (2019).

[2] D.G. Kochiev, I.A. Shcherbakov, S.V. Garnov, "Interaction of microsecond laser pulses with tissues: fundamentals and clinical applications", *XVIII International Seminar Mathematical Model & Modeling in Laser-Plasma Processes & Advanced Science Technologies. Program and Abstracts. Petrovac, Montenegro,* 50 (2019).

[3] A.A. Samokhin, E.V. Shashkov, N.S. Vorob'ev, A.E. Zubko, "Recoil pressure behavior during nanosecond laser pulse irradiation of mercury", *XVIII International Seminar Mathematical Model & Modeling in Laser-Plasma Processes & Advanced Science Technologies. Program and Abstracts. Petrovac, Montenegro,* 51-52 (2019).

[4] B. Luk'yanchuk, Z. Wang, R. Paniagua-Domínguez, A. Bekirov, A.A. Fedyanin, "High order Fano resonances and giant magnetic fields in dielectric microspheres", *XVIII International Seminar Mathematical Model & Modeling in Laser-Plasma Processes & Advanced Science Technologies. Program and Abstracts. Petrovac, Montenegro*, 53 (2019).

[5] V.P Veiko, V.A. Shkuratova, G.K. Kostyuk, M.M. Sergeev, R.A. Zakoldaev, "Compressed laser-induced microplasma (CLIMP) and its application for fabrication of new optical components", *XVIII International Seminar Mathematical Model & Modeling in Laser-Plasma Processes & Advanced Science Technologies. Program and Abstracts. Petrovac, Montenegro*, 54-55 (2019).

[6] A.G. Kaptilny. "The study of the thermophysical properties of substances at high pressures and temperatures by the method of electrical explosion of conductors", *XVIII International Seminar Mathematical Model & Modeling in Laser-Plasma Processes & Advanced Science Technologies. Program and Abstracts. Petrovac, Montenegro*, 56-57 (2019).

[7] B.P. Rybakin, "Computer simulation of the formation of clumps formed by the collision of molecular clouds", *XVIII International Seminar Mathematical Model & Modeling in Laser-Plasma Processes & Advanced Science Technologies. Program and Abstracts. Petrovac, Montenegro*, 60-61 (2019).

[8] M.P. Galanin, V.V. Lukin, A.S. Rodin, D.L. Sorokin, "Mathematical simulation of electromagnetic acceleration for solids and media with use of program platform Temetos", *XVIII International Seminar Mathematical Model & Modeling in Laser-Plasma Processes & Advanced Science Technologies. Program and Abstracts. Petrovac, Montenegro*, 64-67 (2019).

[9] O.A. Kovyrkina, V.V. Ostapenko. "On the accuracy of MUSCL type shock capturing schemes", *XVIII International Seminar Mathematical Model & Modeling in Laser-Plasma Processes & Advanced Science Technologies. Program and Abstracts. Petrovac, Montenegro*, 62-63 (2019).

[10] A.A. Aleksashkina, M.M. Demin, V.I. Mazhukin, "Determination of the phonon thermal conductivity of copper by molecular dynamics", *XVIII International Seminar Mathematical Model & Modeling in Laser-Plasma Processes & Advanced Science Technologies. Program and Abstracts. Petrovac, Montenegro*, 71-72 (2019).

[11] O.N. Koroleva, A.V. Mazhukin, M.M. Demin, P.V. Breslavskii, "Simulation of heat capacity and thermal conductivity of Si in a wide temperature range", *XVIII International Seminar Mathematical Model & Modeling in Laser-Plasma Processes & Advanced Science Technologies. Program and Abstracts. Petrovac, Montenegro*, 73-74 (2019).

[12] F.N. Voronin, V.A. Egorova, E.B. Savenkov, M.E. Zhukovskiy, "The modeling of radiation-induced thermomechanical effects in the finely dispersed medium", *XVIII International Seminar Mathematical Model & Modeling in Laser-Plasma Processes & Advanced Science Technologies. Program and Abstracts. Petrovac, Montenegro*, 112-113 (2019)

[13] S.V. Podolyako, S.A. Kazymov, M.B. Markov, S.V. Parotkin, I.A. Tarakanov, "On an algorithm of the simulating the proton transport considering the nuclear scattering", *XVIII International Seminar Mathematical Model & Modeling in Laser-Plasma Processes & Advanced Science Technologies. Program and Abstracts. Petrovac, Montenegro*, 114-115 (2019)

[14] V.A. Egorova, M.V. Alekseev, I.A. Tarakanov, R.V. Uskov, "The modeling of radiation-induced charge effects in the finely dispersed medium", *XVIII International Seminar Mathematical Model & Modeling in Laser-Plasma Processes & Advanced Science Technologies. Program and Abstracts. Petrovac, Montenegro*, 120 (2019)

[15] O.G. Tsarkova, S.N. Andreev, V.V. Belkov, P.S. Vasileva, N.E. Kondratyev, D.K. Kushnarev, "Thermal diameter of the Sun", *XVIII International Seminar Mathematical Model & Modeling in Laser-Plasma Processes & Advanced Science Technologies. Program and Abstracts. Petrovac, Montenegro*, 58-59 (2019)

[16] G.K. Borovin, A.V. Grushevskii, A.G. Tuchin, D.A. Tuchin, "Russian exploration of Venus: past and prospects", *XVIII International Seminar Mathematical Model & Modeling in Laser-Plasma*

Processes & Advanced Science Technologies. Program and Abstracts. Petrovac, Montenegro, 81-82 (2019)

[17] E.A. Pavlova, "The Features and Management system of the space industry in the Russian Federation", *XVIII International Seminar Mathematical Model & Modeling in Laser-Plasma Processes & Advanced Science Technologies. Program and Abstracts. Petrovac, Montenegro*, 83 (2019)

[18] G.K. Borovin, Yu. F. Golubev, G. S. Zaslavsky, V. A. Stepanyants, A. G. Tuchin, "E.L. Akim's huge contribution to the Russian space research", *XVIII International Seminar Mathematical Model & Modeling in Laser-Plasma Processes & Advanced Science Technologies. Program and Abstracts. Petrovac, Montenegro*, 84-85 (2019)

[19] V.A. Voropaev, G.K. Borovin, E.A. Pavlova, A.I. Streltcov, M.V. Zakhvatkin, "The safety of high-orbit satellite spaceflights", *XVIII International Seminar Mathematical Model & Modeling in Laser-Plasma Processes & Advanced Science Technologies. Program and Abstracts. Petrovac, Montenegro*, 86 (2019)

[20] G.K. Borovin, Yu. F. Golubev, A.V. Grushevskii, A. G. Tuchin, "Formation of the main methods of the scientific school of V.V. Beletsky studying the rotational motions of artificial satellites and natural celestial bodies", *XVIII International Seminar Mathematical Model & Modeling in Laser-Plasma Processes & Advanced Science Technologies. Program and Abstracts. Petrovac, Montenegro*, 87-88 (2019)

[21] S.G. Moiseenko, I.A.Kondratiev, G.S.Bisnovatyi-Kogan, M.V.Glushikhina, "3D numerical study of an anisotropic heat transfer in outer layers of magnetized neutron stars", *XVIII International Seminar Mathematical Model & Modeling in Laser-Plasma Processes & Advanced Science Technologies. Program and Abstracts. Petrovac, Montenegro*, 79-80 (2019)

[22] M.V. Mikhaylyuk, E.V. Strashnov, "Methods for space anthropomorphic robot control in virtual environment systems", ", *XVIII International Seminar Mathematical Model & Modeling in Laser-Plasma Processes & Advanced Science Technologies. Program and Abstracts. Petrovac, Montenegro*, 77-78 (2019)

[23] Ž. Pavićević, "Hyperbolic variations chord in the points Fatou of the bounded holomorphic functions", *XVIII International Seminar Mathematical Model & Modeling in Laser-Plasma Processes & Advanced Science Technologies. Program and Abstracts. Petrovac, Montenegro*, 106-107 (2019)

[24] Dušan Jokanović, "Relation between McCoy and Armendariz rings", *XVIII International Seminar Mathematical Model & Modeling in Laser-Plasma Processes & Advanced Science Technologies. Program and Abstracts. Petrovac, Montenegro*, 121 (2019)

[25] B. Zekovich, V.A. Artamonov, "Antipode in n - ary bialgebra", *XVIII International Seminar Mathematical Model & Modeling in Laser-Plasma Processes & Advanced Science Technologies. Program and Abstracts. Petrovac, Montenegro*, 122 (2019)

[26] Romeo Meštrović, Žarko Pavićević, "On some topological properties of Privalov spaces on the unit disk", *XVIII International Seminar Mathematical Model & Modeling in Laser-Plasma Processes & Advanced Science Technologies. Program and Abstracts. Petrovac, Montenegro*, 123 (2019)

[27] Kankaraš Milica, Irina Cristea, "Fuzzy reducibility in hypergroups", *XVIII International Seminar Mathematical Model & Modeling in Laser-Plasma Processes & Advanced Science Technologies. Program and Abstracts. Petrovac, Montenegro*, 124 (2019)

[28] Sanja Jancic Rasovic, Irina Cristea, Jelena Dakic, "An overview on the theory of hypernear-rings", *XVIII International Seminar Mathematical Model & Modeling in Laser-Plasma Processes & Advanced Science Technologies. Program and Abstracts. Petrovac, Montenegro*, 125 (2019)

[29] Nikola Konatar, "Behavior of the interface between two immiscible fluids in the three-dimensional case", *XVIII International Seminar Mathematical Model & Modeling in Laser-*

Plasma Processes & Advanced Science Technologies. Program and Abstracts. Petrovac, Montenegro, 126 (2019)

[30] Marijan Markovic, "Characterisation of smooth functions with given growth", *XVIII International Seminar Mathematical Model & Modeling in Laser-Plasma Processes & Advanced Science Technologies. Program and Abstracts. Petrovac, Montenegro*, 128 (2019)

[31] Dakić Jelena Momir, "An overview of known hyper-power methods for computing of outer inverses and a new general Newton method", *XVIII International Seminar Mathematical Model & Modeling in Laser-Plasma Processes & Advanced Science Technologies. Program and Abstracts. Petrovac, Montenegro*, 130 (2019)

[32] Jela Šušić, "Extreme points of multidimensional functions", *XVIII International Seminar Mathematical Model & Modeling in Laser-Plasma Processes & Advanced Science Technologies. Program and Abstracts. Petrovac, Montenegro*, 143 (2019)

[33] Milenko T. Pikula, Dragana D. Nedić, Milica Č. Bošković, "Solution of the inverse boundary problem for the Sturm-Liouville operator with delay", *XVIII International Seminar Mathematical Model & Modeling in Laser-Plasma Processes & Advanced Science Technologies. Program and Abstracts. Petrovac, Montenegro*, 145 (2019)

ВКЛАД Э.Л. АКИМА В ПРОГРАММУ КОСМИЧЕСКИХ ИССЛЕДОВАНИЙ РОССИИ

Г.К. БОРОВИН[*], Ю.Ф. ГОЛУБЕВ, Г.С. ЗАСЛАВСКИЙ, В.А. СТЕПАНЬЯНЦ, А.Г.ТУЧИН

Институт прикладной математики им. М.В. Келдыша РАН Москва, Россия
*Ответственный автор. E-mail: borovin@keldysh.ru

Ключевые слова: космический аппарат, искусственный спутник Земли, искусственный спутник Луны, искусственный спутник Марса, планета Венера, Баллистический центр, баллистико-навигационное обеспечение, бортовая система управления, гравитационный манёвр, гравитационное поле

Аннотация. 14 марта 2019 года исполнилось 90 лет со дня рождения выдающегося отечественного ученого, члена-корреспондента РАН Эфраима Лазаревича Акима (1929–2010). Вся профессиональная деятельность Э.Л. Акима была связана с Институтом прикладной математики, куда он пришел на работу сразу после окончания МГУ им.М.В.Ломоносова. Для выполнения задач, связанных с управлением космическими аппаратами, в Институте был создан отдел, который возглавил Д.Е.Охоцимский. В этот отдел пришел на работу Э.Л. Аким. Ему поручили заниматься проблемами навигации. Этот круг проблем определил дальнейшую научную судьбу Э.Л. Акима. Э.Л. Аким защитил кандидатскую и докторскую диссертации, стал лауреатом Ленинской и трижды лауреатом Государственных премий. Он возглавил Баллистический центр Института прикладной математики и руководил им до конца своей жизни. Вехи творческого пути Э.Л. Акима неразрывно связаны с программой освоения космического пространства. Важный этап освоения космического пространства был связан с исследованием Луны. Для осуществления высокоточных расчетов при проектировании орбит требовалось знать гравитационное поле Луны. Э.Л. Акиму и его ближайшим сотрудникам принадлежат пионерские результаты в построении модели гравитационного поля Луны. Под руководством Э.Л. Акима были выполнены проектные исследования, связанные с навигационным обеспечением полетов к Луне всех наших космических аппаратов (КА) («Луна 1–24»). Наряду с первой мягкой посадкой на поверхность Луны (автоматической станции «Луна-9»), следует отметить и первый искусственный спутник Луны — «Луна-10» и станцию «Луна-16», впервые осуществившую забор и доставку на Землю образцов лунного грунта.

Э.Л. Аким (вместе с Т.М. Энеевым) выполнил анализ динамики движения межпланетных КА, разработал и навигационно обосновал схему первых полетов КА к Венере и Марсу, положенная в основу всех последующих полетов наших КА к этим планетам. Под руководством Э.Л. Акима были разработаны математические модели, которые позволили получить точность навигации КА, необходимую для построения качественных изображений планеты и ее рельефа.

E. L.AKIM's CONTRIBUTION TO THE RUSSIAN SPACE RESEARCH PROGRAM

G.K. BOROVIN[*], Yu.F. GOLUBEV, G.S. ZASLAVSKY, V.A. STEPANYANTS, A.G. TUCHIN

Keldysh Institute of applied mathematics RAS Moscow, Russia
[*]*Corresponding author. E-mail: borovin@keldysh.ru

Summary. March 14, 2019 marked the 90th anniversary of the birth of the outstanding Russian scientist, corresponding member of the RAS Efraim Lazarevich Akim (1929-2010). All professional activity of E.L. Akim was connected with the Institute of applied mathematics, where he came to work immediately after graduating from Lomonosov Moscow State University. To perform tasks related to the management of spacecraft, a department was created at the Institute, which was headed by D.E. Okhotsimsky. E.L. Akim came to work in this department. He was assigned to deal with the problems of navigation. The range of issues identified for further research the fate of Akim. E.L. Akim defended his candidate's and doctoral dissertations, became a laureate of Lenin's and three times a laureate of State prizes. He headed the Ballistic center of the Institute and directed it until the end of his life. Milestones creative ways Akim is inextricably linked with the program of space exploration.

An important stage of space exploration was associated with the exploration of the moon. For the implementation of high-precision calculations in the design of orbits required to know the gravitational field of the moon. Akim and his closest employees have pioneering results in the construction of a model of the gravitational field of the moon. Under the leadership of Akim, project studies were carried out related to the navigation support of flights to the moon of all our spacecraft (SC) ("Moon 1-24"). Along with the first soft landing on the surface of the moon (automatic station "Luna-9"), it should be noted the first artificial satellite of the moon — "Luna-10" and the station "Luna-16", for the first time carried out the fence and delivery to Earth samples of lunar soil.

When the decision was made to start designing the ballistic flight of an unmanned spacecraft to Mars and Venus, the Akim (together with T.M. Eneev) was the analysis of the dynamics of interplanetary spacecraft, developed and justified navigation scheme of the first flight of the spacecraft to Venus and Mars, forming the basis for all subsequent flights of our spacecraft to these planets. 16 vehicles were sent to Venus, in the navigation support of which Akim made his irreplaceable creative contribution. Of particular note is the work on the creation of the first Atlas of Venus, built according to data obtained from the spacecrafts "Venus-15" and "Venus-16", located in the orbits of artificial satellites of Venus. Under the leadership of Akim, mathematical models were developed, which allowed to obtain the accuracy of spacecraft navigation necessary for the construction of high-quality images of the planet and its relief.

Until the end of his life, E.L. Akim kept his focus on the new, immediately guessed promising directions. Here it is worth mentioning the use of GPS and GLONASS satellite navigation systems to determine the position of spacecraft.

1 ВВЕДЕНИЕ

14 марта 2019 исполнилось 90 лет со дня рождения члена-корреспондента РАН, доктора физико-математических наук, профессора Акима Эфраима Лазаревича (14.04.1929-13.09.2010) (рис.1).

Рис.1. Эфраим Лазаревич Аким

Э.Л. Аким родился 14 марта 1929 года в г. Галич Костромской области. Его отец, Лазарь Эфраимович Аким, инженер, погиб на фронте под Москвой в 1941 году. Мать, Фаина Яковлевна работала всю жизнь библиотекарем. Старший брат, Яков Лазаревич Аким — известный детский поэт. В 1933 году семья переехала в Москву. Аким Э.Л. поступил на механико-математический факультет МГУ им.М.В. Ломоносова в 1948 году, а в 1953 году пришел на работу в Институт прикладной математики АН СССР (ныне ИПМ им. М.В. Келдыша РАН) в программистский отдел, возглавляемый Яблонским О.В. Затем он перешёл в отдел № 5, которым руководил Дмитрий Евгеньевич Охоцимский. Здесь

Аким Э.Л. активно включается в работы по баллистико-навигационному обеспечению (БНО) космических полетов.

Вся профессиональная деятельность Эфраима Лазаревича была связана с Институтом прикладной математики, куда он пришёл на работу сразу после окончания МГУ. Этот институт был организован выдающимся ученым Мстиславом Всеволодовичем Келдышем [1]. М.В. Келдыш собрал сильный коллектив для развития методов прикладной математики, с помощью которых предполагалось решить проблемы ядерной энергетики и освоения космоса. Для выполнения задач, связанных с вопросами, нарождающейся тогда ракетодинамики и управлением ракетами, в Институте был создан отдел, который возглавил Дмитрий Евгеньевич Охоцимский. Отдел Д.Е.Охоцимского был той «командой», на которую опирался М.В. Келдыш в своей многогранной деятельности в области ракетно-космической техники. Эфраим Лазаревич сразу попал в поле зрения М.В. Келдыша. М.В. Келдыш поручил Тимуру Магометовичу Энееву и Э.Л. Акиму заниматься проблемами навигации. Навигация в космическом полёте – это определение положения и скорости космического аппарата (КА), а также прогноз его движения. Этот круг проблем определил дальнейшую научную судьбу Э.Л. Акима. Он прошёл путь от стажёра-исследователя до заместителя директора института, защитил кандидатскую и докторскую диссертации, стал лауреатом Ленинской, трижды лауреатом Государственных премий. Он возглавил Баллистический центр Института прикладной математики (БЦ ИПМ), созданный в 1965 году по рекомендации М.В. Келдыша и С.П. Королёва, и руководил им до конца своей жизни.

Следует отметить, что выдающийся отечественный учёный член-корреспондент РАН Эфраим Лазаревич Аким входит в число тех лучших представителей науки и техники, чей талант и самоотдача обеспечили начало космической эры - исследование и освоение космического пространства. Важное место в его научной жизни занимали Лунные проекты и полёты к планетам. Осуществлялись проекты, которые в то время казались фантастическими: мягкая посадка на Луну, доставка грунта с Луны на Землю, получение фотографии с поверхности Венеры. Казалось, что пройдёт совсем немного времени и на Луне будет создана база, состоится пилотируемая экспедиция на Марс, отечественные космические аппараты совершат полёты в системы Юпитера и Сатурна. Однако развитие пошло по другому пути, а темпы исследований замедлились. Эфраим Лазаревич принимал, но не соглашался с этим… Он считал, что вскоре наступит время регулярных полётов на Луну, создание лунной базы, освоение природных ресурсов Луны в интересах человечества. А вслед за этим человечество начнёт осваивать и другие небесные тела. Вехи творческого пути Э.Л. Акима неразрывно связаны с российской программой освоения космического пространства.

С 1963 году начал выходить журнал Академии наук «Космические исследования». Символично, что первый номер журнала открывается фундаментальной статьёй Э.Л. Акима и его учителя Т.М. Энеева «Определение параметров движения космического летательного аппарата по данным траекторных измерений» [2]. В этой статье обобщён опыт определения орбит искусственных небесных тел, полученный ещё при первых космических полётах. На эту основополагающую статью продолжают ссылаться, хотя с тех пор прошли десятилетия и методы определения орбит совершенствовались несколькими поколениями учёных.

2 РУКОВОДИТЕЛЬ БАЛЛИСТИЧЕСКОГО ЦЕНТРА ИПМ

2.1 Лунные исследования

Важный этап освоения космического пространства был связан с исследованием Луны. Хотя Луна – это ближайшее к нам небесное тело, до недавнего времени неизвестно было, что находится на обратной стороне Луны. Тем более не было сведений о величине силы притяжения Луны над разными точками её поверхности. Для осуществления высокоточных расчётов при проектировании орбит требовалось знать гравитационное поле Луны. Только в самых первых приблизительных расчётах можно предполагать, что планета или естественный спутник – это шар. На самом деле гравитационное поле естественных небесных объектов устроено весьма причудливым образом, и если это не учитывать при расчётах, то катастрофические последствия не заставят себя ждать. Измерить гравитационное поле можно только косвенно, наблюдая за отклонениями орбит искусственных спутников. По результатам этих исследований в 1984 году была выпущена монография «Поле тяготения Луны и движение её искусственных спутников» (рис.2), в которой Э.Л. Аким - соавтор.

Э.Л. Аким внёс большой вклад в исследование и построение модели гравитационного поля Луны. Нецентральный характер гравитационного поля Луны был обнаружен по данным либрационных измерений. Однако эти косвенные измерения не могли дать качественной и количественной характеристики нецентральности. Запуск первого искусственного спутника Луны (ИСЛ) КА «Луна-10» позволил получить прямое экспериментальное подтверждение нецентральности поля тяготения Луны и определить его первые количественные характеристики. КА «Луна-10» был запущен 31 марта 1966 г. Время активного существования КА «Луна-10» составило 56 суток. Первые результаты по характеристикам нецентральности поля Луны Э.Л. Аким опубликовал в 1966г. [3]. В этой работе он всегда чувствовал внимание и поддержку академика М.В. Келдыша.

Принятая в нашей стране программа исследований гравитационного поля Луны предполагала запуски целевых спутников, выводимых на различные орбиты вокруг Луны, и организацию для них длительных систематических наземных траекторных измерений. Было предусмотрено проведение гравитационных измерений (траекторных измерений в интересах изучения поля тяготения Луны) на других спутниках Луны, для которых эти измерения не были основными. Для получения гравитационных измерений были запущены два лунных спутника: «Луна-19» и «Луна-22». Длительное активное существование этих спутников дало возможность накопить траекторные измерения на интервале более года по каждому спутнику. Траекторные измерения, выполненные по искусственным спутникам: «Луна-10-12,-14,-19,-22» позволили получить представление об эволюции в нецентральном поле лунного тяготения на значительном интервале времени орбит полярного, экваториального спутников, а также орбит спутников со

средним наклонением. Для получения более полной информации о влиянии гравитационного поля Луны на движение в нём спутников с различными наклонениями и геометрией орбит были использованы траекторные измерения по автоматическим станциям «Луна-15-18,-20,-21,-23,-24» [4]. Эти измерения были проведены на коротких интервалах времени полёта станций на орбитах ИСЛ, которые были необходимы для расчёта и проведения манёвров, обеспечивающих посадку лунных станций в заданные районы Луны. Следует отметить, что Э.Л. Аким одновременно с исследованиями поля тяготения Луны одновременно решал прикладные задачи обеспечения полётов к Луне автоматических КА. Результаты определения параметров нецентральности гравитационного поля Луны, полученные по информации КА «Луна-10», были использованы для баллистического обеспечения полёта ИСЛ «Луна-11,-12,-14». Анализ динамики движения спутников в поле тяготения был положен в основу баллистического проектирования нового поколения лунных автоматических аппаратов. Модель гравитационного поля, построенная по наблюдениям за движением ИСЛ «Луна-14» была успешно использована при управлении полётами автоматических лунных аппаратов «Луна-16 - Луна24», которые обеспечили высадку на поверхность Луны «Луноходов», забор и доставку на Землю образцов Лунного грунта». Следует также отметить, что последние траекторные измерения КА «Луна-10», использованные для оценки нецентральности поля тяготения Луны, были получены 29 мая 1966 г, в то время как первые траекторные измерения по КА НАСА «Лунар Орбитер-1» 14 августа 1966 г.

Модель гравитационного поля Луны, которую построили Э.Л. Аким и З.П.Власова, использовала траекторные измерения, полученные от 14 ИСЛ [5]. Общий объём информации оценивался величиной около 456 тысяч измерений. Построение моделей гравитационного поля Луны осуществлялось путём совместной статистической обработки траекторных измерений, полученных почти от всех отечественных ИСЛ. Было построено несколько моделей лунного поля тяготения. Сравнение построенных моделей с близкой по составу гармоник моделью поля тяготения Луны, построенной в Лаборатории реактивного движения (JPL) в США по траекторным измерениям ИСЛ серии «Лунар Орбитер», показало весьма удовлетворительное согласование наиболее крупных по величине коэффициентов этих моделей. Такое согласование моделей, построенных разными методами по независимому и различному наблюдательному материалу, явилось убедительным подтверждением их корректности.

Под руководством Э.Л. Акима были выполнены проектные исследования, связанные с навигационным обеспечением полётов к Луне всех наших космических аппаратов («Луна 1 – 24») (рис.3). За осуществление первой мягкой посадки на Луну КА «Луна-9» Э.Л. Акиму и его коллегам в 1966 г. присуждена Ленинская премия.

Мягкой посадке предшествовала подготовительная работа, в которой непосредственное участие принимал Э.Л. Аким. Примером работы из «лунного» цикла явился проект облёта и фотографирования невидимой с Земли стороны Луны. Этот проект был реализован КА «Луна-3» (рис.4). Здесь, впервые в мировой практике, был предложен и успешно реализован так называемый «гравитационный маневр» – целенаправленное изменение траектории КА в результате возмущения его движения небесным телом (в данном случае Луной). Для этого была построена общая теория и проведен анализ пространственных траекторий полёта к Луне, в том числе траекторий с облётом Луны и возвращением к Земле.
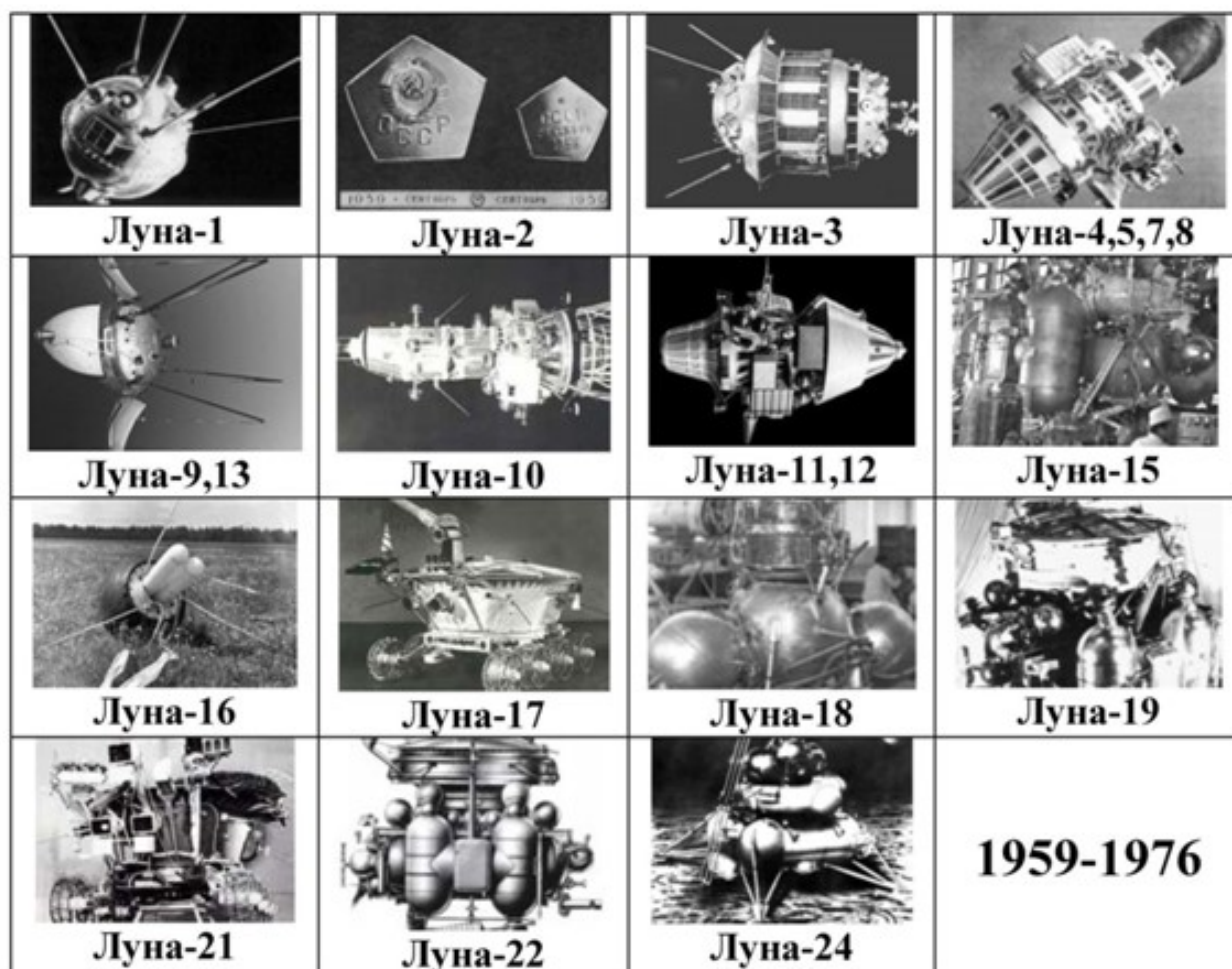
Рис.3. Советские космические аппараты, исследовавшие Луну

Попутно была разработана методика расчёта управления полётом таких аппаратов. Результаты этой работы положены в основу баллистического проектирования КА для полётов к Луне и КА серии «Зонд», предназначенных для отработки пилотируемого облёта Луны (в беспилотном варианте). Наряду с первой мягкой посадкой на поверхность Луны (автоматической станции «Луна-9»), следует отметить и первый искусственный спутник Луны «Луна-10» и станцию «Луна-16», впервые осуществившую забор и доставку на Землю образцов лунного грунта. КА Лунный грунт доставили на Землю ещё два аппарата: «Луна- 20» (рис.5) и «Луна-24».
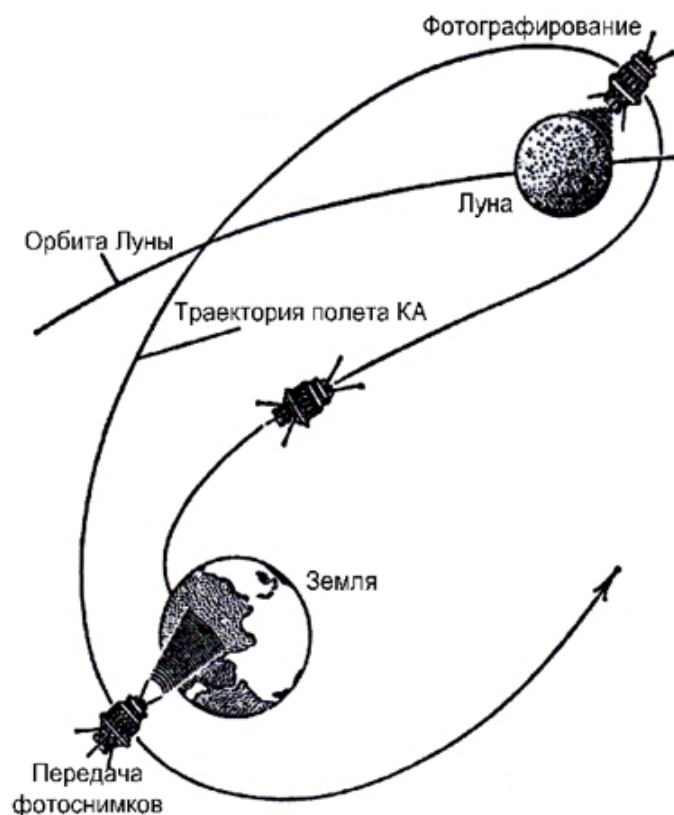
Рис.4. Проект облёта и фотографирования невидимой с Земли стороны Луны для КА «Луна-3»

Полёт КА «Луна-16» с точки зрения задач, которые приходилось решать при проектировании этих полётов, имел целый ряд особенностей. Чтобы доставить возвращаемый аппарат (ВА) с лунным грунтом на заданный полигон территории нашей страны, требовалось посадить КА на поверхность Луны в пятно радиусом 5 км вокруг выбранной точки посадки. Баллистики в то время не могли обеспечить столь высокую точность прогноза точки посадки, т.к. не имели необходимой для этого системы траекторных измерений и недостаточно точно знали лунное поле тяготения. Чтобы спрогнозировать с необходимой точностью место посадки на Земле ВА с грунтом Луны, нужно было иметь на борту ВА достаточно точную на то время дециметровую систему траекторных измерений. Но эта система имела слишком большой вес. Разместить эту систему на КА, пожертвовав научным оборудованием, было нельзя. Любой из названных причин было достаточно, чтобы отказаться от реализации проекта. Только талант, высочайшая квалификация и настойчивость Главного конструктора проекта Г.Н. Бабакина и энтузиазм команды, в которую входили и сотрудники ИПМ им.М.В. Келдыша, позволили реализовать этот проект.

Рис.5. «Луна-20». Контейнер с лунным грунтом
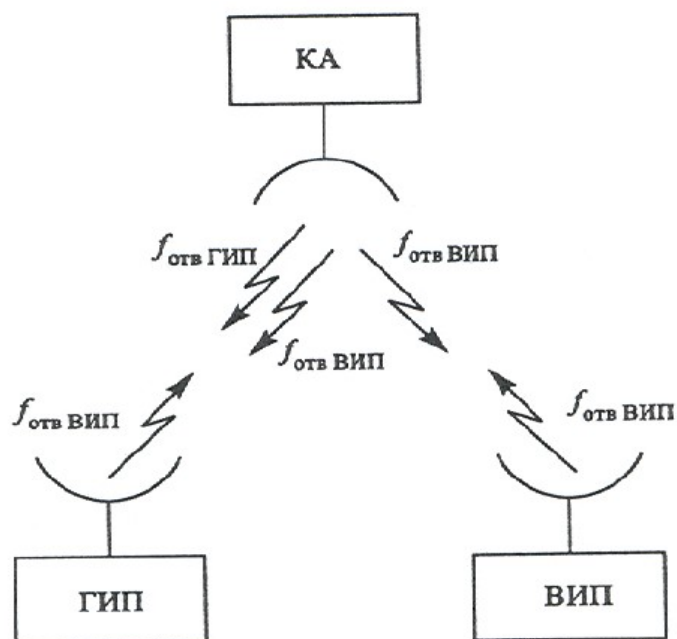
Рис.6. Высокоточная система траекторных измерений в проекте «Луна-16». (ГИП – главный измерительный пункт, ВИП – вспомогательные измерительные пункты, $f_{отв}$ - частота сигнала от измерительного пункта)

В результате была разработана и испытана новая высокоточная система траекторных измерений (рис.6). По наблюдениям за движением ИСЛ «Луна-10,11,12 и 14» была уточнена модель лунного поля тяготения. Было предложено поставить на борт ВА менее точную, но существенно более лёгкую траекторную систему метрового диапазона.

А для получения необходимой точности посадки на Землю ВА с грунтом предложили дополнительно привлечь для наблюдений за ВА оптические измерения обсерваторий Академии наук СССР. Систему траекторных измерений обычно принято дублировать. Но на борту ВА для этого не было резерва веса. Главный конструктор Г.Н.Бабакин принимает решение – обойтись без дублирования. Созданный проект оказался надёжным и позволил успешно решить задачу забора и доставки на Землю лунного грунта на всех предназначенных для этого лунных аппаратах.

2.2 Полёты к планетам Солнечной системы

Вслед за Луной пришла очередь исследования наших ближайших соседей в Солнечной системе: Венеры и Марса. Академики М.В. Келдыш и С.П.Королёв приняли совместное решение начать баллистическое проектирование беспилотных полётов к планетам Марсу и Венере. Была разработана схема управления полётом КА, которая легла в основу всех дальнейших работ, как по баллистическому проектированию, так и по практическому управлению полётами межпланетных КА. Эта схема обеспечивала достижение как максимальной точности управления в ходе полёта, так и минимальных массовых затрат, связанных с созданием самой системы управления. Коллектив Института прикладной математики участвовал по всех проектно-баллистических работах, а также работах по БНО полётов космических аппаратов, предназначенных для исследования межпланетного космического пространства, планет и малых тел солнечной системы.
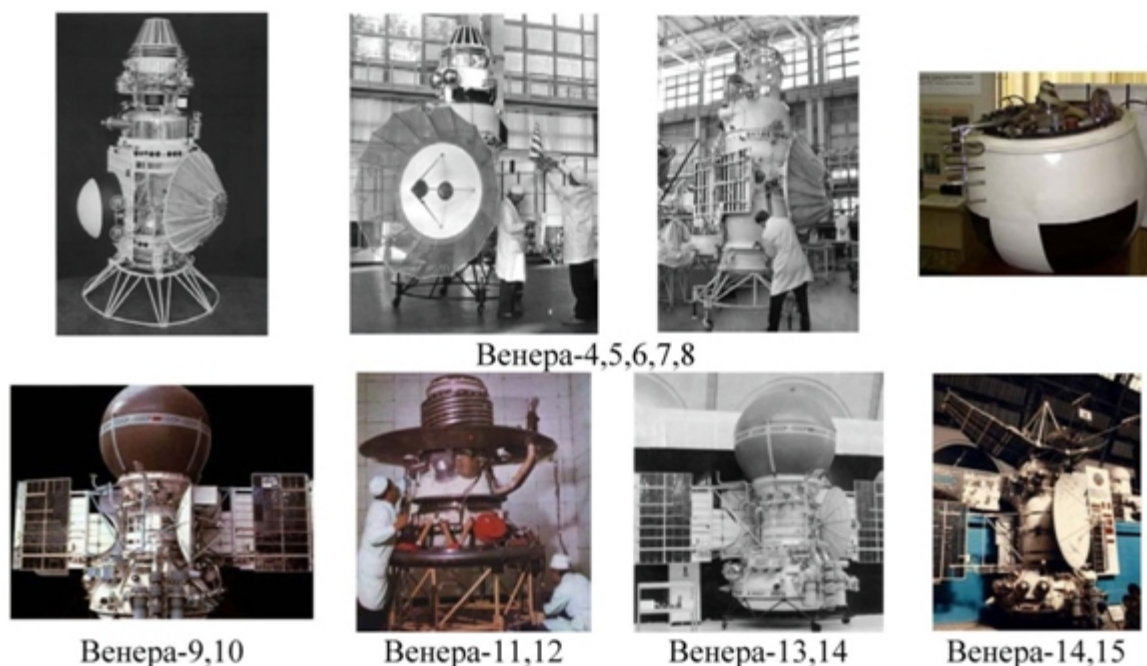

Венера-4,5,6,7,8

Венера-9,10   Венера-11,12   Венера-13,14   Венера-14,15

Рис.7. КА «Венера 4, 5, …, 16»

Э.Л. Акимом (вместе с Т.М.Энеевым) был выполнен анализ динамики движения межпланетных КА, разработана и обоснована схема первых полётов КА к Венере и Марсу, положенная в основу всех последующих полётов российских КА к этим планетам [6].

Ответственный участок полёта – сближение с планетой. При непосредственном участии Э.Л. Акима была разработана схема управления полётом КА на заключительном этапе полёта. Построена методика управления работой наземных средств слежения по измерениям доплеровского смещения частоты сигнала КА в припланетном сеансе связи Земли с КА. На Венеру было отправлено 16 аппаратов (рис.7). Отметим некоторые из космических экспедиций. КА «Венера-4» впервые осуществил передачу на Землю параметров атмосферы планеты. Первые искусственные спутники Венеры (ИСВ) «Венера-9», «Венера-10» и их посадочные аппараты передали на Землю панорамы поверхности этой планеты. ИСВ «Венера-15» и «Венера-16» позволили с помощью уникального эксперимента по радиокартографированию Венеры (рис.8) построить хорошего качества изображения планеты и её рельефа, создать первый атлас Венеры. При этом следует также отметить полёты наших КА «Вега-1» и «Вега-2» к комете Галлея с доставкой в атмосферу Венеры аэростатных зондов и выведением к ядру кометы европейской межпланетной станции «Джотто» (Международный проект «Лоцман»).

Эфраим Лазаревич внёс важный вклад в баллистико-навигационное обеспечение этих космических экспедиций.

Рис.8. Картографирование Венеры. КА «Венера-15» и «Венера-16»

2.3 Проект Союз-Апполон

Остановимся далее на некоторых, с нашей точки зрения, наиболее интересных этапах работы Э.Л. Акима.

Впечатляющий эксперимент в мире в рамках сотрудничества в космосе был проведен в июле 1975 г., когда американский корабль «Аполлон» был состыкован с советским

кораблем «Союз-19» на околоземной орбите высотой 225 км (рис.9). Полет по программе ЭПАС (экспериментальный полёт Аполлон-Союз), в ходе которого астронавты и космонавты совершали переходы с одного корабля на другой и проводили эксперименты, был полностью успешным. Э.Л. Аким, возглавляя БЦ ИПМ, внёс существенный творческий вклад в успешную реализацию проекта ЭПАС. Последовательность динамических операций, которые необходимо было выполнить космическому кораблю «Союз-19», предъявляла высокие требования к БНО управления полётом по оперативности, надёжности и точности выполнения расчётов. Все операции по выведению космического корабля «Союз-19» на орбиту и последующие манёвры выполнены с высокой точностью. На 36-м витке полёта космического корабля «Союз-19» 17 июля в 19:12 была осуществлена стыковка космических кораблей. 19 июля на 64-м витке космические корабли расстыковались, а на 66-м витке вновь состыковались. После расстыковки космических кораблей на 68-м витке их полёт проходил по самостоятельным программам. Следует отметить, что включение БЦ ИПМ в работы по пилотируемой космонавтике потребовало разработки и реализации новых методов, алгоритмов и программ.

Рис.9. Аполлон-Союз, 1975 ("Аполлон" был активен, "Союз" – пассивен)

2.3. Космические станции "Салюты"

29 сентября 1977 г. на околоземную орбиту была выведена космическая станция «Салют-6». Создание орбитального комплекса «Салют-6» – «Союз» – «Прогресс» расширило возможности исследования околоземного космического пространства. Новые возможности орбитального комплекса позволили повысить интенсивность транспортного сообщения Земля – «Салют-6» – Земля. Стыковку с орбитальной станцией «Салют-6» осуществил 31 КА, включая 4 корабля типа «Союз-Т», 12 транспортных кораблей «Прогресс» и КА «Космос-1267». На борту станции «Салют-6» работало 5 основных и 11 краткосрочных экспедиций. Всё это определило необходимость дальнейшего

совершенствования применяемых методов БНО полёта. Э.Л. Аким и здесь внёс большой творческий вклад в развитие методов БНО полёта орбитальной станции и транспортных, пилотируемых и грузовых кораблей, направляемых к ней [5]. Важнейшей задачей службы навигации является постоянное слежение за состоянием движения станции и кораблей по орбитам. Это слежение осуществлялось наземными радиотехническими средствами, выполняющими измерения наклонной дальности и радиальной скорости. В БЦ ИПМ проводилась статистическая обработка измерений и определение по ним параметров движения КА. Результаты определения параметров движения КА необходимы в первую очередь для прогнозирования движения КА. Анализ изменений параметров орбит, постоянно уточняемым по навигационным измерениям, позволяет судить о возмущениях движения, изменениях плотности верхней атмосферы и при необходимости учитывать в расчётах эти требования.

19 апреля 1982 года на орбиту была выведена орбитальная станция «Салют-7», которая обеспечила продолжение космических исследований, начатых на станции «Салют-6». 11 КА выполнили стыковку со станцией «Салют-7», включая 4 корабля «Союз», 6 КА «Прогресс» и КА «Космос-1443» [7]. На борту станции «Салют-7» проработали две основные и четыре краткосрочные экспедиции. За время управления полётом станции «Салют-7» и транспортных космических кораблей произошли две крупные нештатные ситуации, выход из которых потребовал нестандартных решений и действий от специалистов по БНО. Первая из них связана с полётом транспортного корабля «Прогресс-14», старт которого состоялся 10 июля 1982 г. в 12:57:44 по московскому времени. Средства траекторного контроля морского базирования получили траекторные измерения наклонной дальности и радиальной скорости. Баллистический центр должен был получить параметры орбиты. Однако начальное приближение, используемое в задаче определения параметров движения, оказалось столь грубым, что стандартные численные методы не обеспечивали сходимость. Поэтому пришлось применять различные ухищрения: направленный перебор вариантов начальных приближений и изменение веса измерений. Этим процессом руководил Эфраим Лазаревич. В результате напряжённой работы были получены параметры орбиты. Управление полётом вошло в штатный режим и стыковка состоялась в запланированное время 12 июля 1982 г. в 11:41. Этот случай послужил началом цикла работ по созданию методов и алгоритмов определения орбиты КА в условиях неопределённости. Сам Э.Л. Аким был автором некоторых оригинальных идей и методов решения задач подобного рода. Позже разработанные методы нашли своё воплощение в бортовой навигационной системе, работающей по сигналам навигационных спутников ГЛОНАСС и GPS [6]. Вторая нештатная ситуация произошла на станции «Салют-7» 12 февраля 1985 года. Станция со 2 октября 1984 года находилась в режиме автоматического полета [7]. Во время очередного сеанса связи обнаружилась неисправность в одном из блоков командной радиолинии станции, через который проходили радиокоманды из ЦУПа и информация со станции на Землю. Анализ состояния бортовых систем показал, что произошло автоматическое переключение на второй передатчик. С Земли выдали команду о возобновлении действия первого передатчика. Команда была принята, и станция ушла на очередной виток. Но на следующем сеансе связи информации со станции уже не было. Предстояла стыковка с не кооперируемой станцией. После нескольких месяцев тренировок космонавты В. Савиных и В. Джанибеков утром 6 июня 1985 года стартовали на корабле «Союз Т-13» [8]. Перед БЦ ИПМ стояла сложная задача. Нужно было обеспечить стыковку корабля со станцией по

разным орбитальным данным. Орбита корабля «Союз Т-13» определялась по данным траекторных измерений, а орбита станции сообщалась из Центра контроля космического пространства. При этом использовались различные модели движения КА. Разработанные в БЦ ИПМ методы согласования моделей движения обеспечили успешное выполнение расчётов по оперативному БНО управления полётом корабля «Союз Т-13» и его стыковку со станцией 8 июня 1985 г в 8:50 по московскому времени.

Следует отметить одну важную особенность оперативных работ баллистико навигационного обеспечения (БНО) полёта корабля «Союз Т-13», которая состояла в том, что БЦ ИПМ одновременно проводил работы по оперативному БНО полёта автоматических межпланетных станций «Вега-1» и «Вега-2» [9]. В момент проведения стыковки в БЦ ИПМ проводились работы к подготовке и проведению второй коррекции межпланетной станции «Вега-2». Время включения двигательных установок (ДУ): 05:45:00. В отличие от аналогичных коррекций, проведенных на станциях "Венера-11" - "Венера-14", к этой коррекции предъявлялись высокие требования по точности исполнения, т.к. она обеспечивала гравитационный маневр, необходимый для последующего полета к комете Галлея.

20 февраля 1986 года в Советском Союзе состоялся запуск ракеты-носителя "Протон-К", которая вывела на околоземную орбиту базовый блок станции "Мир", ставший основой для строительства в космосе орбитального комплекса (ОК) нового поколения. К ОК «Мир» совершили полеты и стыковались с ним 100 советских (российских) космических средств. Кроме того, с 1995 г. с ОК «Мир» проведено девять стыковок с многоразовым транспортным космическим кораблём типа «Шаттл». Работы по БНО управления полётом ОК «Мир» были возложены на ИПМ им. М.В. Келдыша Постановлениями Правительства. БЦ ИПМ под руководством Э.Л. Акима успешно выполнял работы по БНО полёта орбитальной станции «Мир» и транспортных пилотируемых космических кораблей. БЦ ИПМ оперативно и регулярно обрабатывал траекторные измерения, определял орбиты, прогнозировал движение и рассчитывал параметры манёвров каждого из этих космических кораблей. По данным бортовых измерений проводился выборочный анализ динамики движения орбитального комплекса относительно центра масс. Следует отметить, что работы со станцией «Мир» пришлись на суровый период нашей истории – девяностые годы прошлого столетия. В конце 1991 года стало ясно, что в сложившихся условиях невозможно обеспечить надёжное функционирование машин типа БЭСМ-6, АС-6, на которых был построен информационно-вычислительный комплекс БЦ ИПМ. Руководством Института прикладной математики было принято решение об ускоренном создании нового информационно-вычислительного комплекса на основе локальной сети серверов на персональных процессорах. Весной 1992 г. началась опытная эксплуатация новых аппаратно-программных средств БЦ ИПМ, а летом 1992 г. завершена эксплуатация старого вычислительного комплекса. Скорейший переход на новую платформу полностью себя оправдал. Комплекс «Мир» проработал в три раза дольше первоначально установленного срока. В конце 1990-х годов на станции начались многочисленные проблемы из-за постоянного выхода из строя различных приборов и систем. Через некоторое время Правительство РФ, ссылаясь на дороговизну дальнейшей эксплуатации, несмотря на многочисленные проекты спасения станции, приняло решение затопить «Мир». Утром 23 марта 2001 г. Орбитальный научно-исследовательский комплекс «Мир» прекратил своё существование. На последнем этапе орбитальный комплекс состоял из

базового блока, модуля «Квант», модуля «Квант-2», модуля «Кристалл», модуля «Спектр», модуля «Природа» и космического корабля «Прогресс М1-5». Работа по управлению орбитальным комплексом «Мир» на этапе его затопления имела ряд существенных отличий от выполненных ранее работ по затоплению других космических аппаратов, что определялось значительно большей массой (примерно 130 т), более сложной геометрической формой орбитального комплекса, весьма ограниченными запасами топлива на борту для управления орбитальным движением комплекса и его движением относительно центра масс. Работа по управлению орбитальным комплексом на завершающем этапе его полёта была выполнена ЦУП-М (ЦНИИмаш), РКК «Энергия», ИПМ им. М.В. Келдыша РАН, соответствующими центрами Министерства обороны и другими организациями. Работа проводилась под руководством специально созданной Росавиакосмосом Межведомственной рабочей группой по баллистико-навигационному и информационному обеспечению заключительного этапа полёта орбитального комплекса «Мир». Эфраим Лазаревич принимал активное участие в работе этой группы.

Схема затопления станции «Мир» предусматривала два этапа. Цель первого этапа – при помощи двух или трёх тормозных импульсов сформировать орбиту, обеспечивающую благоприятные условия для затопления на протяжении нескольких суток. Цель второго этапа – при заданной величине завершающего тормозного импульса, определить время его приложения, обеспечивающее затопление станции в заданном районе. В связи с тем, что солнечная активность оказывает сильное влияние на плотность атмосферы, определяющее торможение орбитального комплекса, по инициативе Эфраима Лазаревича в баллистическом центре были выполнены исследования точности прогноза индекса солнечной активности F10.7. В баллистическом центре были разработаны алгоритмы и программы, реализующие методики International Organization for Standardization ISO/CD15857. Следует отметить, что разработанные программы успешно работают по сей день. Результаты прогноза представляются на сайте [10, 11] и используются многими пользователями. Импульсы, реализовавшие сход с орбиты станции «Мир», имели такую большую длительность, что в зоне видимости станции не оставалось интервалов её пассивного движения. Поэтому Эфраим Лазаревич поставил задачу разработать специальную методику и реализовать программный комплекс для определения работы станции по наземным траекторным измерениям на фоне работы двигательных установок. Такой программный комплекс был единственным в организациях, которые обеспечивали уточнение траектории станции на заключительном этапе её полёта. Оперативная работа по БНО управления полётом станции «Мир» была завершена. Фактически это была последняя оперативная работа БЦ ИПМ по пилотируемой программе.

2.4 Развитие Методов решения задач баллистики

Большое внимание Э.Л. Аким уделял развитию методов локальной обработки траекторных измерений. В задачи локальной обработки входит выявление и удаление из дальнейшей обработки измерений, содержащих аномальные ошибки, а также сжатие информации, т.е. замена массива измерений одним или совокупностью нормальных мест. Локальная обработка позволила значительно сократить объём вычислений на этапе определения орбиты за счёт сжатия измерительной информации и уменьшения числа отбраковок измерений. Спецификой локальной обработки для искусственных спутников Земли (ИСЗ) является необходимость учёта нелинейностей в математических моделях.

Под руководством Э.Л. Акима были разработаны алгоритмы, позволяющие строить аппроксимацию измерений специальными аналитическими выражениями, зависящими от трёх параметров. Такая аппроксимация позволила идентифицировать аномальные измерения и получать статистические характеристики ошибок измерений. На разных этапах полёта станции и транспортных кораблей требования к точности знания их движения различны и это определяет необходимую частоту измерений и нужную точность определения по ним орбит. Наибольшие точности требуются при маневрировании кораблей и станций. По инициативе Э.Л. Акима и под его руководством была разработана методика и алгоритм одновременного уточнения параметров орбиты и импульса манёвра или коррекции.

Важнейшими задачами, решаемых в ходе оперативного БНО полёта станции и транспортных космических кораблей, являются задачи расчёта манёвров. Перед началом полёта корабля каждой следующей экспедиции решается задача коррекции орбиты станции. Для обеспечения наименьших затрат топлива на манёвры сближения корабля со станцией плоскость орбиты корабля должна быть близка к плоскости орбиты станции, а сама станция должна находиться в момент старта корабля на заданном угловом расстоянии впереди него. Кроме того, при проведении коррекции необходимо устранить снижение высоты орбиты станции, которое обусловлено торможением в верхних слоях атмосферы. После выведения на начальную орбиту корабль должен перейти на орбиту станции и сблизиться с ней. Для этого он должен выполнить ряд манёвров. Номинальная схема манёвров и точные значения их параметров должны уточняться с учётом данных о параметрах реальных орбит корабля и станции. Это уточнение производится последовательно по мере выполнения манёвров, поступления траекторных измерений и определения параметров движения станции и корабля. На условия сближения корабля со станцией, а также на возможные интервалы проведения манёвров накладываются ограничения, которые обусловлены требованиями системы управления кораблём, условиями освещённости корабля Солнцем, а также требованиями наблюдаемости динамических операций со станций слежения. Оптимизация схемы маневрирования и точные расчёты параметров манёвров на каждом этапе сближения корабля со станцией с учётом всех накладываемых ограничений и условий является важнейшей задачей БНО управления полётом.

Для возвращения на Землю и посадку в заданном районе корабль должен совершить манёвр схода с орбиты. Предварительные расчёты спуска производятся задолго до планируемой даты посадки. Кроме того, регулярно проводятся расчёты возможных резервных вариантов спусков для их использования в случае возникновения нештатной ситуации, требующей срочной посадки корабля. В штатном варианте окончательный расчёт манёвра схода с орбиты производится по результатам определения параметров движения, полученным за 10-12 витков до посадки. Уточнение параметров этого манёвра и прогноз координат точки посадки проводится по результатам определения параметров движения с использованием траекторных измерений за 3-4 витка до посадки. Проведение расчётов для посадки корабля, а также проведение регулярных расчётов резервных вариантов посадки является важной задачей БНО полёта космического корабля.

Современные задачи исследования Солнечной системы предъявляют высокие требования к управлению движением автоматических межпланетных станций. Успешное проектирование и реализация отечественных амбициозных проектов исследований дальнего космоса требуют единого комплекса математического моделирования, что

обеспечивает минимизацию просчетов и ошибок. Реализация проектов невозможна без создания системы управления движением нового поколения с высокой степенью автономности. В БЦ ИПМ им.М.В. Келдыша РАН выполнены работы по созданию дальнейшему развитию математических моделей управления движением космического аппарата для исследований Солнечной системы. С помощью пакета прикладных программ BalCalc, созданного в БЦ ИПМ им. М.В. Келдыша РАН, выполняются работы по баллистическому проектированию перспективных проектов исследования космического пространства [11-16].

2.5 Автономная навигационная система

До конца жизни Э.Л. Аким не терял чувство нового, сразу угадывал перспективные направления. Здесь стоит упомянуть о применении систем спутниковой навигации GPS и ГЛОНАСС для определения положения космических аппаратов. Многие уже привыкли к использованию этих систем для определения положения наземных объектов. Но Э.Л. Аким сразу увидел здесь принципиально новые возможности определения положения КА. Коллектив БЦ ИПМ совместно с промышленностью начал разработки по созданию высокоточной автономной системы навигации (АСН) ИСЗ по сигналам GPS и ГЛОНАСС (рис.10).
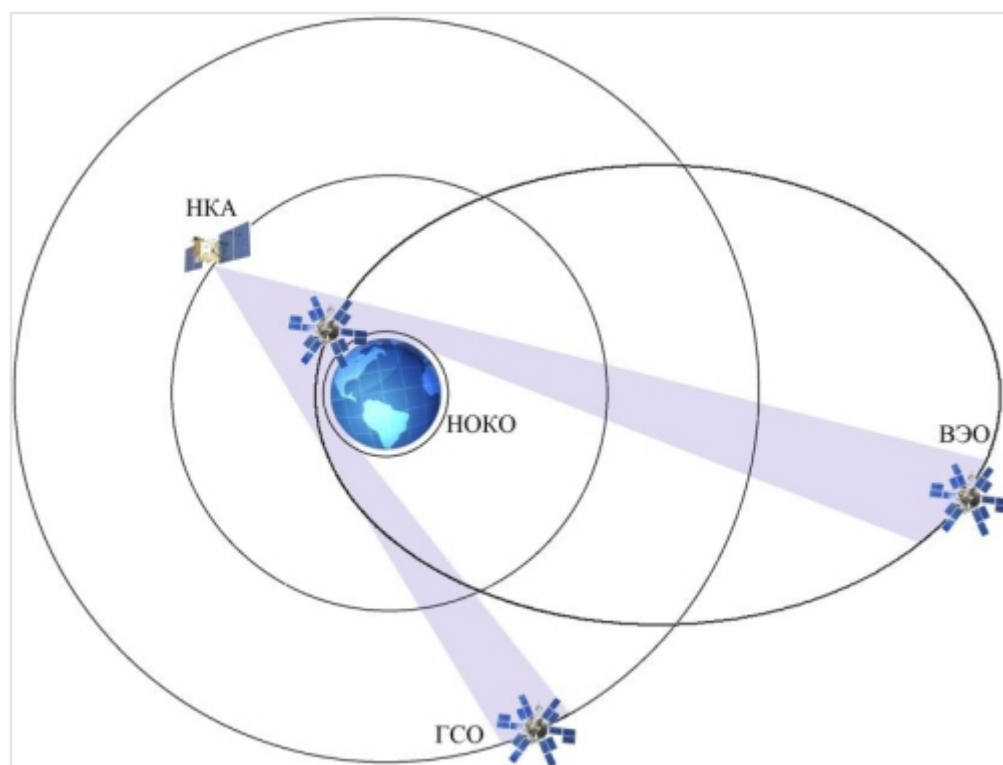
Рис.10 Взаимное расположение КА и навигационного космического аппарата (НКА) на геостационарной орбите (ГСО), высокоэллиптической орбите (ВЭО) и низкой околоземной космической орбите (НОКО)

162

Особо следует отметить, что сотрудники Э.Л. Акима решили не только традиционные для центра задачи: исследовали возможность создания высокоточной АСН, разработали для нее алгоритмы и программы на персональном компьютере, провели математическое моделирование работы систем GPS, ГЛОНАСС и АСН. Сотрудники ИПМ также участвовали в выборе бортовой вычислительной машины АСН, разработали для неё необходимое общее программное обеспечение, специальное программное обеспечение бортовых аппаратных средств: приёмника и коррелятора сигналов. И чтобы обеспечить надёжность работы АСН в космических условиях, провели её отработку на аппаратном имитаторе сигналов GPS и ГЛОНАСС. Эфраим Лазаревич был инициатором, организатором и теоретиком этой новой работы [17].

3 ЗАКЛЮЧЕНИЕ

Эфраим Лазаревич проявлял интерес к самым неожиданным и парадоксальным проектам, стремился найти в них рациональное зерно. Он старался поддержать добрым словом авторов таких проектов, говорил о том, что проект интересный, заслуживает дальнейшей проработки.

Велик вклад Э.Л. Акима в подготовку и разработку баллистико-навигационного обеспечения управления полетом КА научного назначения «Радиоастрон» и проведения на его борту высокоточных научных экспериментов. КА «Радиоастрон» проработал на орбите более 7.5 лет.

За выдающиеся заслуги Аким Э.Л. был удостоен Ленинской премии (1966), трижды лауреат Государственных премий СССР (1970, 1980, 1986), премии Правительства РФ (2005), премия им. К.Э. Циолковского РАН (2007), награждён многими государственными наградами. Э.Л. Аким – член-корреспондент РАН, заслуженный деятель науки и техники РФ. Его именем названа малая планета Солнечной системы – астероид (8321) Akim.

Вся жизнь Эфраима Лазаревича Акима – это пример беззаветного служения науке.

REFERENCES

[1] G.K. Borovin, A.V. Grushevskii, M.V. Zakhvatkin, G.S. Zaslavsky, V.A. Stepanyantz, A.G. Tuchin, D.A. Tuchin, V.S. Yaroshevsky, "Space researches in Keldysh Institute of Applied Mathematics of RAS: Past, Present, Future", *Mathematica Montisnigri*, **43**, 101-127 (2018).

[2] E.L. Akim, T.M.Eneev, "Opredelenie parametrov dvizheniyu kosmicheskogo letatelnogo apparata po dannym traektornyh izmerenii", *Kosmicheskie issledovaniy,***1**(1), 5-50 (1963). URL: ftp://ftp.kiam1.rssi.ru/pub/gps/lib/article/akim/1963_akimenee.pdf

[3] E.L. Akim, "Opredelenie gravitacionnogo polya Luny po dvizheniyu iskusstvennogo sputnika Luny "Luna-10", *Dokl. Akad. Nauk SSSR*. **170**(4), 799-802. WOS:A19668359500015 (1966).

[4] E.L. Akim, I.K. Baginov, V.P. Pavlov, V.N. Pochukaev, *Pole tyagoteniya Luny i dvizheniyum ee iskusstvennyh sputnikov*, M.: Mashinostroenie (1984).

[5] E.L. Akim, Z.P. Vlasova ,"Model gravitacionnogo polya Luny po nabluydenijam za dvizheniyum ee iskusstvennyh sputnikov "Luna-10, -12, -14, -19 I -22", *Dokl. Akad. Nauk SSSR*. **235**(1), 38-41 (1977).E.L. Akim, T.M. Eneev, "Dvizhenie iskusstvennykh sputneykov zemli. Mezhplanetnye polity", *Pricladnaia nebesnaia mehanika i upravlenie dvizheniem. Sbornik statei, posviashchenny`i` 90 letiiu so dnia rozhdeniia D.E.Ohotcimskogo. M.: IPM im. M.V.Keldysha*, 7-27 (2010). http://keldysh.ru/e-biblio/okhotsimsky/

[6] I.K. Baginov, V.P. Gavrilov, V.D. Yastrebov, E.L. Akim, R.F.Appazov, G.S. Zaslavskiy i dr., *Navigacionnoe obespechenie poleta orbitalnago kompleksa «Salyut-6»-«Soyuz»-«Progress»,* Moskva: Nauka (1985).

[7] V.P. Savinyh, *Zapiski s mertvoi stancii,* M.: ID "Sistemy Alisa" (1999).

[8] Ballistiko-navigacionnoe obespechenie proekta "Vega", Itogovyi otchet, Moskva (1986).

[9] E.L. Akim, G.S.Popov, R.V.Kalashnikov, A.N.Myamlin, Informacionno-vychislitelnaya sistema dlya ballisticheskogo obespecheniya poleta kosmicheskih apparatov, *Trudy IV nauchnyh chtenii po kosmonavtike*, Moskva (1980).

[10] http://www.kiam1.rssi.ru/~den/solar.html (Accessed October 11 2019)

[11] G.K. Borovin, I.S. Ilin, A.G. Tuchin, Quasi periodic orbits in the vicinity of the Sun-Earth L2 point and their implementation in "SPECTR-RG" & "MILLIMETRON", *Mathematica Montisnigri*, **30**, 37-45 (2014).

[12] G.K. Borovin, M.V. Zakhvatkin, V.A. Stepanyants, A.G. Tuchin, "Determination and prediction of orbital parameters of the "RADIOASTRON" mission", *Mathematica Montisnigri*, **30,** 76-98 (2014).

[13] G. Borovin, Yu. Golubev, A. Grushevskii, V. Koryanov, A. Tuchin, D. Tuchin, "Mission design in systems of outer planets within model restricted two-coupled three-body problem", *Mathematica Montisnigri*, **32,** 43-57 (2015).

[14] G.K. Borovin, I.S. Ilin, A.G. Tuchin, "Quasi periodic orbits in the vicinity of the Sun-Earth *L*1 point and their implementation in "SODA" mission", *Mathematica Montisnigri*, **37,** 5-23 (2016)

[15] G.K. Borovin, A.V. Grushevskii, A.G. Tuchin, D.A. Tuchin, "Russian exploration of Venus: Past and Prospects", *Mathematica Montisnigri*, **45,** 137-148 (2019). DOI**:** 10.20948/mathmontis-2019-45-12

[16] E.L. Akim, A.P. Astahov, R.V. Bakitko, V.P. Polshikov, V.A. Stepanyants, A.G. Tuchin, D.A. Tuchin, V.S. Yaroshevsky, "Avtonomnaya navigacionnaya sistema okolozemnogo kosmicheskogo apparata", *Izvestiya RAN. Teoriya i sistemy upravleniya,* **2,** 139-156 (2009).

SPACE IS THE DESTINY: RESEARCH OF THE SOLAR SYSTEM.

ON THE OCCASION OF THE 85-TH ANNIVERSARY OF ACADEMICIAN RAS M. Ya. MAROV

B.N. CHETVERUSHKIN[1], A.I. APTEKAREV[2], A.V.KOLESNICHENKO[3*], V.I. MAZHUKIN[4], V.P. OSIPOV[5]

[1] Scientific chief of Keldysh Institute of Applied Mathematics of RAS, Academician of RAS, Professor, Moscow, Russia

[2] Director of Keldysh Institute of Applied Mathematics of RAS, Corresponding member of RAS, Professor, Moscow, Russia

[3] Principal researcher of Keldysh Institute of Applied Mathematics of RAS Professor, Moscow, Russia

[4] Principal researcher of Keldysh Institute of Applied Mathematics of RAS, Professor, Moscow, Russia

[5] Leading researcher of Keldysh Institute of Applied Mathematics of RAS, Moscow, Russia

*Corresponding author. E-mail: kolesn@keldysh.ru

Summary. The paper is dedicated to the 85-th anniversary of the outstanding Russian scientist, full member (Academician) of the Russian Academy of Sciences Mikhail Yakovlevich Marov. Academician M.Ya. Marov is a Soviet and Russian physicist and astronomer, a leading Russian scientist in the field of theoretical and experimental study of the solar system, comparative planetology, and mathematical modeling natural and cosmic media. He owns the outstanding pioneering results of Venus and Mars research, which received widespread worldwide recognition. For the first time in the world, he carried out direct *in situ* measurements of temperature and pressure on the surfaces of Venus and Mars, conducted thorough studies of the thermal regime of Venus, peculiar dynamics of its atmosphere, and the structure and properties of clouds. He played a leading role in solving the complex problem of landing and operation of Soviet vehicles on the hot surface of Venus, which allowed us to transmit to Earth first dark and white and then color panoramas of the neighbor planet and to measure elemental composition of its rocks. He has been deeply involved is in the development and implementation of the planetary space programs «The Moon», «Venus», «Vega», «Mars», «Phobos».

The area of scientific interests of M.Ya. Marov is very broad. He is basic in mechanics and physics of space, astrophysics, planetology, mathematical modeling of space media. He made a great contribution to the advancement of our knowledge on space environment. They include the fundamentals of planetary aeronomy, mechanics of multicomponent turbulent reacting gases and heterogeneous multiphase media, non-equilibrium kinetic processes, original methods of mathematical modeling the atmospheres of planets and gas envelops of comets, migration-collisional processes of small bodies in the outer space. Thought his scientific career he nicely combined theoretical and experimental studies and took leading part in managing a few the world recognized space projects.

This biographical sketch reflects the view of many colleagues of Mikhail Yakovlevich at the Keldysh Institute of Applied Mathematics of RAS, in which he worked for about half a century – it is objective and equitable while not impartial, but imbued with admiration, respect and love.

1   THE BEGINNING OF THE CREATIVE CAREER

As fate would have it, Mikhail Yakovlevich (Fig. 1.) found himself on a stretch of space and time when humanity opened an opportunity to go into outer space, began to study and master it. He had a chance to take a direct part in this truly historic achievement in a great country - the former Soviet Union - from almost the very first steps. He was lucky enough to pursue his favorite science for many years, along with numerous colleagues and students in two excellent organizations of the Russian Academy of Sciences, where he has been working: at the Keldysh Institute of Applied Mathematics (IAM RAS) as a Head of the Department of Applied Mechanics, Space Research and Aeronomy, and currently, at the Vernadsky Institute of Geochemistry and Analytical Chemistry (GEOCHI RAS) where he occupies the position of a Head of the Department of Planetary Sciences and Cosmochemistry. He maintains a close cooperation between IAM, GEOCHI and Space Research Institute (IKI) in space projects.

Fig. 1. Academician of the Russian Academy of Sciences Mikhail Yakovlevich Marov

Mikhail Yakovlevich Marov was born in 1933 in Moscow in a middle-class family (Fig. 2.). His father, a participant in the Great Patriotic War, who was heavily injured, died early. His mother was a teacher at the Moscow Institute of Chemical Engineering. After graduating from a Moscow secondary school in 1952 with a gold medal, Mikhail Yakovlevich enrolled in the Mechanical Department of the Moscow Higher Technical School (now Moscow State Technical University) named after N. E. Bauman (MSTU) that he graduated from with honors in 1958. Mikhail Yakovlevich recalls his university and student's years with a warm feeling, although the time was hard, his mother raised him alone, laying the spiritual, moral foundations of life. He repeatedly said that he was eternally grateful to his parents, who have not only given him the gift of life, but did it very timely indeed, so he graduated from the university just in time - at the beginning of space era. Being a graduate student Mikhail Yakovlevich studied the complex section of mechanics - nonlinear oscillations. Just a few months before receiving diploma, the news of the launch of the first artificial Earth satellite in the USSR came, which shocked him to the core. For the first time he thought about outer space as a tangible entity where he would apply his knowledge, but at that time, this idea seemed an unattainable dream. The real life turned out not a plain sailing.

Fig.2. Parents, childhood, youth

The real life turned out not a plain sailing. After graduating from the university Mikhail Yakovlevich has been directed to work at the special state enterprise nearby Moscow. He paid many efforts in order to be engaged in the field close to his university training - non-linear physical processes rather than in routine engineering work. However, application area that he had to deal with was fully new - atomic physics and electronics rather than mechanics, and for two years, he combined hard study of new physical problems with the practical work. The latter was mostly carried out at the A.I. Leipunsky Physics-Energy Institute in Obninsk where Mikhail Yakovlevich spent a lot of time participating in experiments with nuclear reactors for military applications.. Later on he unexpectedly learned that these research were also related to space because in-tended for utilization in spacecraft's onboard energetics for the future interplanetary spacecraft, what Leipunsky Institute pursued following S. P. Korolev's foreseeing. It was therefore his first indirect involvement in space exploration. The second and direct one occurred after reorganization of the industry ventures integrated with the famous ОКБ-1 headed by S. P. Korolev (now the Korolev's Rocketry and Space Corporation (RSC) Energia. The laboratory where Mikhail Yakovlevich worked became a part of the unit for the development of control/orientation systems for space vehicles headed by the prominent scientist academician B.V. Rauschenbach. In the following years, they were connected with warm friendly relations. Mikhail Yakovlevich actively participated in the development of navigation systems of the first interplanetary missions - Mars and Venus

spacecraft 1MV and 2MV. Again, everything was new; many problems posed innovative solutions while imperfection of technical means often resulted in annoying errors. Nonetheless, some unique systems were set up in the short conceivable time, largely motivated by the imperatives of the Cold War, by aspiration to surpass the rival and to be the first.

Mikhail Yakovlevich worked enthusiastically, with full dedication of his knowledge and strength. Soon, however, fate drastically changed his life again. By the order of OKB -1 overheads he was nominated an assistant of one of the prominent leaders of the rocket and space industry and Deputy Minister of the State Committee for Defense Technology G.A. Tyulin. For nearly two years he has been closely engaged in the current and future problems of rocketry-space technology, including analysis of emergency rocket launches, under the direct supervision of outstanding industry specialists.

Fig. 3. M.V. Keldysh (right) and M.Ya. Marov, 1971

This period preceded the crucial turning point in his career. At one of the meetings dealing with the Lunar Race Mikhail Yakovlevich got acquaintance with Mstislav Vsevolodovich Keldysh and soon he received an invitation to join his Institute of Applied Mathematics of the USSR Academy of Sciences. Needless to say, Mikhail Yakovlevich accepted this honored invitation with a great joy. For subsequent nearly fifty years his life was tightly connected with this Institute where he really took place as a scientist and made the career from a researcher to a Head of the Department. Either way, the cosmos determined the choice of his life path. This path turned out to be not a simple indeed; there were both dramatic events of loss and finding success of discoveries culminating in recognition of the scientific community. All this was conditioned by the continuous hard work, permanent learning in different scientific disciplines during the whole his life that was driven and moti vated by his curiosity, the wish to push the frontiers of unknown and sincere dedication to science.

2 SPACE PROGRAMS AND PROJECTS

A particularly serious school that immeasurably broadened the scientific and technical horizons of Mikhail Yakovlevich and gave him invaluable experience in working with large teams and state projects was his position as the Scientific Secretary of the Interagency Scientific-Technological Council for Space Research (ISTC on SR) under USSR Academy of Sciences auspices, which was headed by M.V. Keldysh (Fig.3.). He occupied this position for about 15 years combining these responsible duties with scientific work in the Institute of Applied Mathematics. He left the position immediately after Mstislav Vsevolodovich passed away in 1978 responding negatively a call to work with other ISTC leaders.

Mikhail Yakovlevich worked in very close relations with M.V. Keldysh throughout nearly twenty years There were the most intense and saturated period of his life, his heydays as he recalls. Mikhail Yakovlevich directly participated in the development of programs of

scientific and applied space research, discussion and critical assessment of almost all proposed space projects with significant share of his time at space enterprises and rocket launch pads. He had a great opportunity to know personally, closely work together with the leaders of research institutes, and design bureaus including Chief designers of industry - members of the famous Counsel of Chief Designers headed by S.P. Korolev.

Among historical people greatly contributing to space exploration Mikhail Yakovlevich distinguish the Chief Designer of S. A. Lavochkin Scientific and Production Association (SPA) G. N. Babakin. He admired this outstanding person whom with he had especially close and friendly relationships, as well as with his deputies, and then successors. This was the venture where spacecraft for planetary exploration were designed and manufactured what stipulated our pioneering successful research of the Moon, Venus and Mars. M.V. Keldysh requested Mikhail Yakovlevich participate personally in the SPA projects development in terms of assistance in solution of fundamentally important scientific problems and related technical issues involving selection of scientific objectives and interfaces of the onboard scientific instruments with spacecraft service systems. He performed for many years the functions of Project Scientist (PS) as such person calls in the West. Mikhail Yakovlevich also undertook his own experiments with some of these spacecraft as a Principal Investigator (PI). M.V. Keldysh supported his experimental research and to facilitate the study he set up a special laboratory in the Marov's Department at IAM. The culmination of this activity became the period from the mid-1960s to the early 1980s - period of the Soviet outstanding pioneering achievements in the exploration of the Moon, Venus, and Mars (Fig. 4-7).
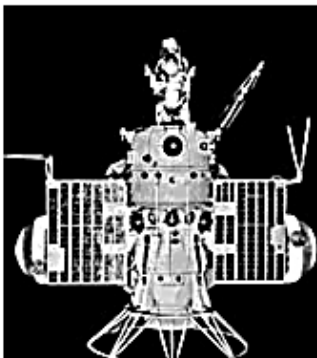
Fig. 4. 2MB – «Mars-1».
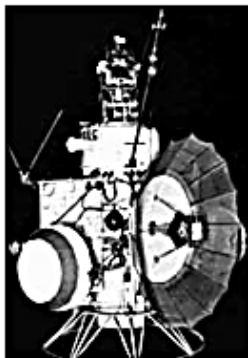
Fig. 5. 2MV – «Venus-2, -3».
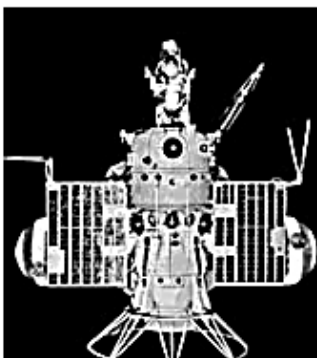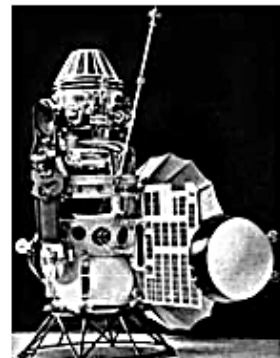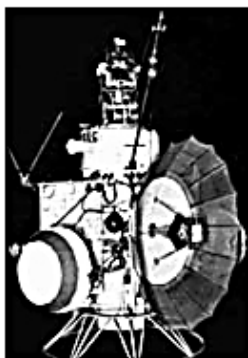

Fig. 6. 1MV – «Marsnik»

Fig. 7. 1MV – «Venus-1».

Mikhail Yakovlevich recalls with particular pride the successful multi-year research program of Venus, since the historical launch of «Venera-4» (Fig. 8-10). A lot of time and efforts have been invested to this program including his own, but that was more than rewarded with the excellent technical and scientific results. Successful entry in the Venus atmosphere and parachute descending made possible to derive the first in the world direct measurements of atmospheric parameters of this enigmatic planet. This was followed by the first landings of spacecraft on the planet's surface and their survival in harsh environmental conditions (not repeated by anyone else in the world), illumination measurements and transmission of surface panoramas, measurements of the composition of surface rocks, studying atmospheric dynamics, structure and properties of the Venus clouds, to mention a few the most important.

Fig. 8. Entrance descent in the atmosphere
(«Venus-4» - «Venus-6»)
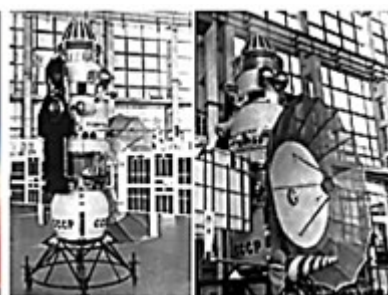
Fig. 9. Spacecraft «Venus-4» - «Venus-6»
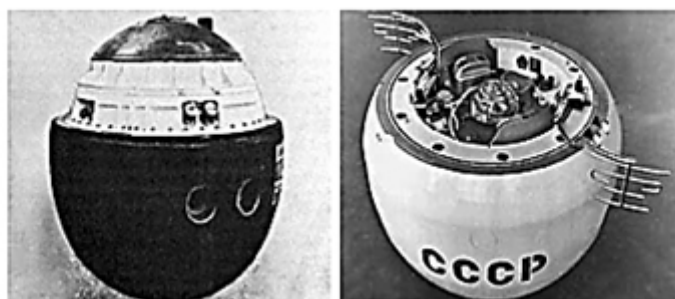
Fig. 10. The descent vehicle, «Venus-7, -8»

Russian scientists and enginners launched the first artificial satellites of Venus, studied the features of outer space around the planet. These successes were achieved by the two generations of spacecraft created under G.N. Babakin leadership. The second generation, which had a high degree of reliability, also became the technical basis of the «Vega» mission to 1P/Halley's comet and creation of the «Astron» astrophysical satellite.

Unfortunately, not all plans of Venus exploration were implemented. Especially painful to Mikhail Yakovlevich was administrative decision, not justified but adopted in 1981, to cancel the planned launch of the balloon probe for detailed study of the Venus unique clouds and related phenomena, while the project was at the final stage of manufacturing. There was the Soviet-French project led by Mikhail Marov and Jacques Blamont from the Russian and French sides, respectively. Both leaders paid to the project more than three years of their scientific career this turned out a waste of time.

Less successful was the Russian Martian program, which included artificial Mars satellites and landing vehicles. However, the first soft landing on Mars of the «Mars-3» lander and the first direct measurements of atmospheric parameters with the «Mars-6» lander became outstanding achievements. Mikhail Yakovlevich. and co-workers were proud to contribute to these projects and to obtain the scientific data, which allowed developing the first model of Martian atmosphere from the surface to ~ 70 km. As the truly epochal are the unique flights of the third generation of lunar spacecraft developed in the Babakin's venture. The automatic lunar soil sampling and return them back to Earth and long-term functioning of self-propelled vehicles (rovers) on the lunar surface were ensured (Fig.11,12). Successful implementation of these projects in the early 1970s allowed us to reduce the negative consequences of losing Lunar Race for landing a first man on the Moon. Mikhail Yakovlevich recalls his complex feelings he experienced watching Neil Armstrong stepping down the Moon surface - a mix of pride for triumph of the human genius jointly with of disappointment and bitterness that it was not Russian.
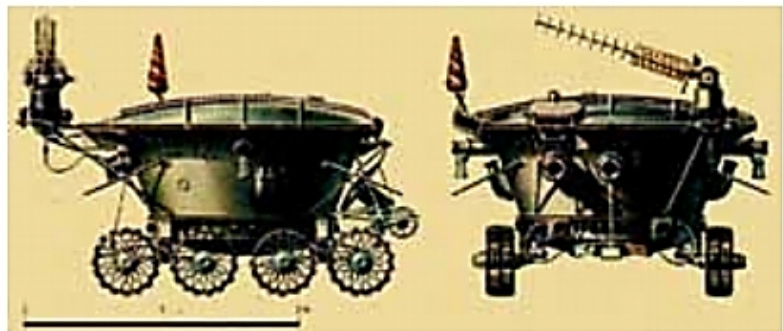
Fig. 11. «Luna 16»   Fig. 12. «Lunokhod-1»
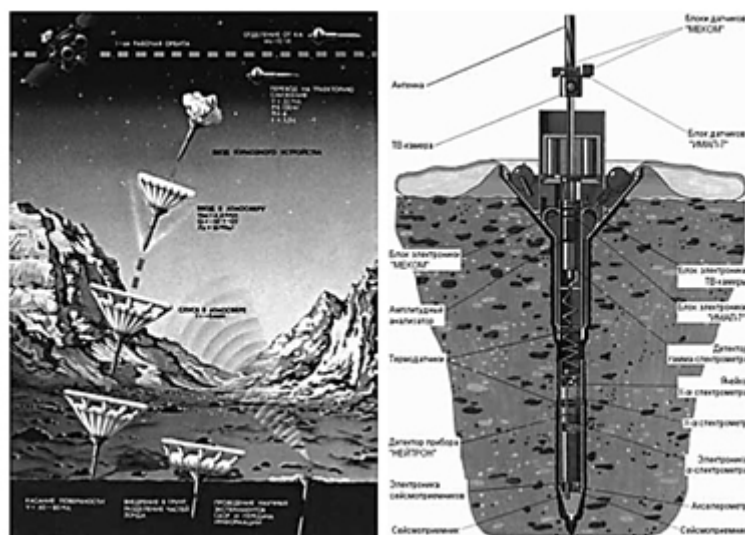
Fig. 13. Launching penetrators to the surface of Mars and the «Mecom» meteocomplex at the top of the penetrator (MARS-96 project)

It seemed possible to us only eight years after Yuri Gagarin historical flight indeed. S.P. Korolev made a lot to accomplish the goal but his premature death prevented this ambitious plan from happening. Nonetheless, the automatic lunar flights alleviated the bitter situation and kept the country's recognition as a leading space power.

The overall situation fully changed and the former recognition shacked down dramatically in the following decades. While the success of «Vega» missions predetermined the reliability of «Venera» spacecraft, the new developments years after Babakin death turned out much less perfect. This resulted in only partial program performance of the two Phobos-88 mission and the tragic failure of the Mars-96 launch (Fig. 13). Combined with the devastating effects of perestroika, this has set Russia's lunar and planetary program back decades. Of course, the absence of a leader of such magnitude as M. V. Keldysh had a huge negative impact, none of the subsequent leaders of the space program could not be compared with him, did not have such a colossal authority with the country's leadership.

At the end of the 1970s, after the death of M. V. Keldysh, Mikhail Yakovlevich voluntarily left the INTS on SR and completely switched to scientific work combining theoretical and experimental studies. In the «Vega» project Mikhail Yakovlevich was engaged in calculation of non-gravitational perturbations in the 1P/Halley comet's motion owing to sublimation of gas and dust from the nucleus surface. The goal was to increase the accuracy of rendezvous of spacecraft with the comet. In the «Phobos-88» mission project he was engaged in the modeling of remote sensing detection of ions ejected by incident laser beam from the moon surface, followed by ions measurements with by mass analyzer on-board instrument «Lima-D», in order to determine the Phobos rocks composition. In the «Mars-96» project, he was PI of the meteorological complex installed on penetrators to be jettisoned from the orbiter. The instrument developed with Finland and USA cooperation intended for long-term measurements of Mars atmospheric parameters and variations of dust abundance.

«Mars-96» disaster badly affected the Russian planetary program and aggravated the problems caused by the perestroika. Fortunately, in the late 1990s a small team of enthusiasts with Mikhail Yakovlevich involvement have undertaken heroic efforts to revive the Russian lunar-planetary program. They took into account many changes in the country and in particular in space industry dictated by the new economic interactions and marketing conditions as well as new technologies. Eventually, traditional groups of qualified specialists joined this team. Their joint efforts allowed suggesting the project of the universal planetary spacecraft. They proposed this modern vehicle to undertake «Phobos-Grunt» mission for the ambitious task to return to Earth rock samples from the Mars moon Phobos. Again, Mikhail Yakovlevich invested a lot of time and efforts in this project, which gradually received the state financial support and was included in the Federal Space Program. Its failed launch in November of 2011 literally shocked him and he long time couldn't rid of frustration.

The 20-year period of the Soviet planetary exploration and Mikhail Yakovlevich deep involvement in these historical endeavors is thoroughly reflected in the book «Soviet Robots in the Solar System. Technologies and Discoveries» (Fig. 14,15), written by M.Ya. Marov jointly with his American colleague Wesley Huntress and first published in 2011 in English by Springer-Praxis Publisher in 2011. It was translated in Russian and published by PHIZMATLIT in 2013 (Marov M. Ya., Huntress U. T. Sovetskie roboty v Solnechnoj sisteme. Tekhnologii i otkrytiya) and then in 2018 (2-nd edition). The book objectively describes successes and failures of the Soviet program of lunar-planetary research with automatic spacecraft, and analyzes the causes of unsuccessful launches in the historical

perspective. By the W. Huntress idea, the sentence: «First on the Moon, first on Venus, first on Mars» on the cover of the book pays tribute to outstanding Soviet achievements in the Moon and planets exploration. The book was awarded the prize of the International Academy of Astronautics for the best book in the fundamental sciences.

Fig. 14. Edition in Russian

Fig. 15. The book "Soviet robots in the solar systems. Mission technologies and discoveries ", published in 2011 in English by Springer-Praxis, and Diploma of the International Academy of Astronautics for the best book in basic sciences.

Despite the shroud of secrecy behind the USSR space program Mikhail Yakovlevich was known in the West as one of its leaders working closely to the head of the Soviet space program M.V. Keldysh. In addition, M.V. Keldysh assignend Mikhail Yakovlevich to participate in various international events and negotiations and hence he was in spotlight. That is why in 1971, after a successful soft landing of «Mars-3» on the Mars surface Mikhail Yakovlevich was awarded with the International Galaber Prize in Astronautics, which he called the recognition, first of all, of his colleagues from the Lavochkin enterprise. A collage of Brown University (USA), dedicated to him on occasion of 20th anniversary of the «Vernadsky-Brown» symposium, serve as appreciation an of his participation in various space program and projects respected by the foreign scientists (Fig.16).

In 2012 Mikhail Yakovlevich was awarded the NASA Diploma on the occasion of the 50th anniversary of solar system research «in recognition of the leading role in the studies of the solar system and discoveries that changed the world» (Fig. 17). In 2013, he got the famous Alvin Seiff Award «in recognition of the outstanding and unique contribution to planetary studies, including the first direct measurements in the atmospheres of Venus and Mars»(Fig.18).

The book "Soviet robots in the solar systems. Mission technologies and discoveries", published in 2011 in English by Springer-Praxis, was awarded the Diploma of the International Academy of Astronautics for the best book in the field of basic sciences. In 2013, it was released in Russian by the Publishing House of Physical and Mathematical Literature.
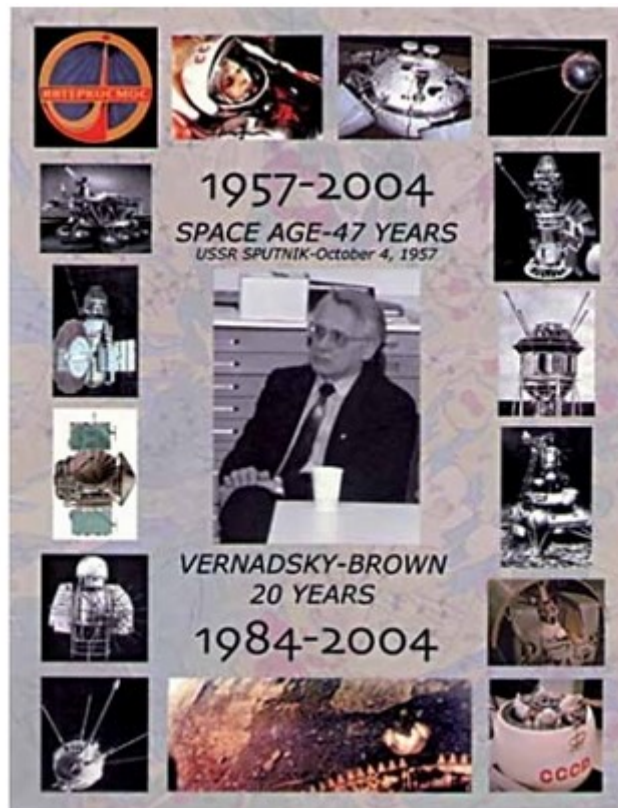
Fig. 16. Collage of Brown University (USA), awarded to the author in connection with the 20th anniversary of the symposium «Vernadsky – Brown».
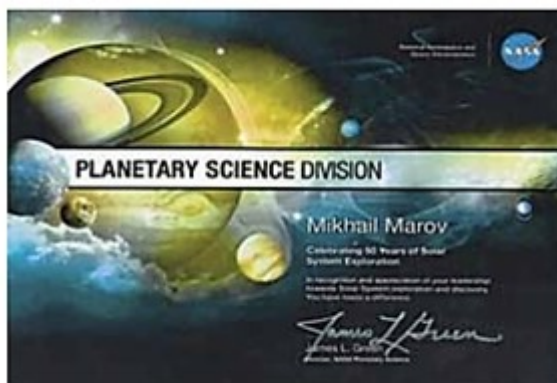

Fig. 17. A NASA diploma on the occasion of the 50th anniversary of the exploration of the solar system «in recognition of the leading role in the exploration of the solar system and the discoveries that have changed the world».

Fig. 18. Alvin Siff Award for Planetary Research.

3   SCIENTIFIC RESEARCH

In parallel with the work in STC, Mikhail Yakovlevich headed the Department of Mechanics, Planetary Research and Aeronomy at the IAM, leading theoretical and experimental studies. Integration of these duties was not a simple task and required tremendous dedication and energy concentration. Mstislav Vsevolodovich supported and directed the scientific activities of this unit, helped in solving a number of theoretical problems. In1964, Mikhail Yakovlevich defended his Ph.D., and in 1970 he received a full doctor's degree in the field of physics and mathematics sciences. In 1977, he awarded the title of Full Professor, and in 1990 elected a corresponding member of the USSR Academy of Sciences in the Division of Mechanics and Control Systems. He elected a Full Member (Academician) of the Russian Academy of Sciences in the Earth Sciences Division in 2008. These events reflected the recognition by the Academy members the importance of Mikhail Yakovlevich contribution to space and planetary sciences including their value for Earth as one of the Solar System planets.

The scientific legacy of Mikhail Yakovlevich research that he made personally and jointly with his pupils and colleagues could be divided into the following sections:

1. Physical mechanics, hydrodynamics and physical kinetics, aeronomy, mathematical modeling of space and natural environments The main colleagues and co-authors: Prof. A. V. Kolesnichenko, Corr. Member of RAS D.V. Bisikalo, Dr. V.I. Shematovich, Dr. A.M. Alferov, Dr. O.P. Krasitsky).

2. Planetary research with spacecraft, direct *in situ* measurements, development of models based on the experimental data(Principal colleagues and co-authors: Academician RAS V. S. Avduevsky, Dr. M. K. Rozhdestvensky, Prof. V. I. Polezhaev, Dr. F.S. Zavelevich, Dr. V. V. Kerzhanovich, N. F. Borodin, Dr. Yu. P. Karpeisky, Dr. B.E Moshkin, Dr. A.P., Economov, Dr. Z.P. Cheremukhina, K.K., Manuylov, Dr. V.P. Osipov, Dr. V.P. Shalimov and M.Z. Mukhoyan).

3. Planetary cosmogony and cosmochemistry, the origin and evolution of the solar system and other planetary systems (exoplanets) (The main colleagues and co-authors: Prof. A.V. Kolesnichenko, Dr. V.A. Dorofeeva, Dr. A.V. Rusol, Dr. A.B. Makalkin, Dr. S. I. Ipatov, Dr. I.M. Ziglina).

We are not going to discuss even the most significant results obtained by Mikhail Yakovlevich. in each of these sections. The detailed contents of his research can be find in his numerous papers and monographs written by himself and/or together with colleagues.

3.1 Mechanics of reacting gases, turbulence of inhomogeneous media, aeronomy, kinetics of non-equilibrium processes, mathematical modeling space environment

The section deals with specific approach of classic mechanics and gas kinetics used for specific problems of space environment modeling. This is the area where Mikhail Yakovlevich worked for almost half a century. He initiated the study of many «unknowns» with application of some basic methods of multicomponent radiative hydrodynamics, turbulence of inhomogeneous reacting media, dynamics of a rarefied gases, and physical-chemical kinetics. They paved the road to the development of the new branch of space research – planetary aeronomy, which he began to study as a postgraduate under the guidance of Professor V. I. Krasovsky. A part of these studies was inverse problems solution: deducing temperature/density of the Earth's upper atmosphere and their variations depending on the

solar and geomagnetic activity from the measured data of evolution of the artificial Earth satellites orbits. At the same time, together with his first student and then colleague A.V. Kolesnichenko, Mikhail Yakovlevich began to develop the theoretical foundations of aeronomy. The key of the problems involved in the field of rarefied gas dynamics is the direct exposure of the upper atmosphere gas to energetic solar electromagnetic and corpuscular radiation accompanied by the reactions of photolysis (dissociation, ionization, and excitation) and the numerous direct and inverse transitions - chemical reactions, together with heat and mass transfer and diffusion processes. Based on these complex studies, he developed the first models of the Earth's upper atmosphere used for accurate prediction of the lifetime of satellites and orbital stations. The results also contributed to refining CIRA - the International Reference Model compiled by the Committee on Space Research (COSPAR)). Models of ozone content variations depending on small species and turbulence were also studied in framework of the European space project GOMOS (Global Ozone Monitoring by Occultation of Stars).

Another area of aeronomy research was focused on the study of nonequilibrium kinetic processes in the rarefied gas of the upper atmospheres of Earth and other planets. These studies were started by Mikhail Yakovlevich with his other talented student V.I. Shematovich, who later successfully used the developed methods to solve the problems of astrochemistry. The basis was laid on the methods of stochastic modeling when solving the Boltzmann type equations with the right-hand side containing reaction integrals. The method made possible to take into account with a good accuracy the contribution of solar radiation and chemical sources of heating in the energy budget, as well as an efficiency of dissipation of atmospheric atoms into outer space. Original physical-probabilistic analogue of the the Boltzmann kinetic equation was constructed in the form of a random process of particle interactions/relaxations in Markov's form with the use of Monte Carlo algorithms for the numerical evaluation. Methods of statistical modeling have been successfully utilized in the study of non-equilibrium state of some Earth's upper atmosphere components with the account for ionization rate of O_2, N_2 and O, kinetic energy spectra and distribution functions of «hot» oxygen and nitrogen atoms due to photo dissociation at different heights, and spectra of kinetic energy of photoelectrons. Application of this approach to Mars allowed us to estimate the rate of water loss due to non-thermal dissipation of heavy atoms from the planet's atmosphere. The role of water in the evolution of the ancient Martian atmosphere also studied with the analysis of contribution of photolysis and chemical reactions.

This segment of Mikhail Yakovlevich scientific research also includes modeling of the structure and composition of the comet's internal coma, with a detailed study of the processes of molecular transport in the porous core, sublimation of gas and dust from the surface of the icy nucleus, and the formation and radial profiles of macro-parameters near the surface in the Knudsen layer. These models were developed jointly with V. Shematovich, D. Bisicalo, V. Strelnitsky. Together with A. V. Kolesnichenko he assessed an influence of non-gravitational perturbations on the motion of the Halley comet at different distances from the Sun. These results were used in the VEGA project for the spacecraft navigation. They also assessed the displacement of the observed «photometric» nucleus because of light scattering by dust relative to the physical one in order to point cameras and other onboard instruments correctly.

In the set works of M.Ya. Marov on the mechanics of space and natural environments, a special place occupied the studies jointly with A. V. Kolesnichenko on the complex problems of turbulence of multicomponent reacting gases. They carried out these researches including

the fundamental theoretical approaches, the respective mathematical apparatus, methods of setting and solving model problems for almost three decades and continue to develop the study successfully. The results are summarized in the numerous publications and a number of monographs published by leading Russian and foreign publishers («Nauka», «Phyzmatlit», «Binom», «Kluwer Academic Publishers» and «Springer») [1-16]. These studies focused on space applications, mostly on the problems of cosmogony, an evolution of gas-dust accretion disks. We emphasize that in the works a new direction in the studies of inhomogeneous turbulent media has emerged, involving thorough analysis of chemical reactions between gas components and dust influence in the heterogeneous medium. No less important is consideration of the hydrodynamic helicity and the efficiency of dust clusters formation in turbulent vortices because of streaming instability in the hydrodynamic flow.

3.2 Planetary space research, development of models based on the data of measurements

This large part of the Mikhail Yakovlevich scientific research is mostly related to the experimental studies with the planetary vehicles. He obtained the most important results in the study of Venus with the spacecraft «Venera-4» - «Venera-14» (1967-1981). Together with his colleagues, he had the unique chance to investigate an enigmatic Venus atmosphere and to carry out the world's first direct measurements of its parameters. «Venera-4» was the first vehicle that discovered the atmospheric properties while «Venera-7» and «Venera-8» landers reached the planet's surface and successfully operated in a very harsh environment. The second generation of more capable «Venera-9-14» landers and satellites made possible to unravel many mysteries of the Venus nature. In the height profiles of his more accurate temperature and pressure measurements, he found some inhomogeneity he associated with convection in the Venus lower atmosphere. He studied the peculiar features of the global atmospheric dynamics from the data of Doppler shift measurements of transmitters' master oscillator frequency during the landers descending, as well as by the direct wind speed measurements on the Venus surface with anemometers. As the result, the height profiles of the wind velocity from the surface to upper cloud deck were found, which confirmed an existence of atmospheric superrotation. In addition, for the first time in the world, he and his colleagues measured the solar radiation attenuation with height in several spectral ranges in the atmosphere and illumination on the surface and concluded that red rays predominate at the Venus surface giving it an orange tint. Thus, being on the Venus surface you would see orange skies over your head. These measurements made it possible to transmit first black-and-white, and then color panoramas of the surface, as well as to obtain the first data on the location and structure of the Venus clouds. Mikhail Yakovlevich studied in detail the structure and microphysical properties of the clouds with the nephelometer technique on the «Veneras-9 and 10» landers. For the first time, he discovered the three main cloud layers and transition zones in between consisting of three modes of micron-sized particles with different refractive indices. This led to the conclusion that particles of the clouds are completely different from water ice and formed by a substance of different nature, which later on was identified with concentrated sulfuric acid. In addition to the main layered cloud deck located between 49 and 68 km above the surface, he and co-workers revealed the presence of sub-cloud (at 49 to 35 km) and upper cloud (above 68 km) hazes. The state of art results of Venus study were

described in the book after M.Ya. Marov and D. Grinspoon «The Planet Venus» published by the prestigious Yale University Press.

M.Ya. Marov paid the great attention to the Venus and Mars atmospheres modeling which based, on his own measurement data. He developed the first model of the Venus atmosphere based on the temperature, pressure and chemical composition data and the detail analysis of thermodynamic properties of the atmospheric gas. He worked on the problems of radiative heat transfer and atmospheric dynamics attempting to explain the formation of runaway greenhouse responsible for the unusual Venus climate. Unfortunately, only limited data were derived from the direct measurements of altitude profiles of temperature, pressure and horizontal wind velocity from the «Mars-6» lander. Nonetheless, based on these data the Martian atmosphere he and colleagues created Mars atmosphere model that was in a good agreement with the subsequent more complete measurements on the American landers «Viking». These studies stimulated Mikhail Yakovlevich to develop meteorological complex installed on penetrators of «Mars-96» mission and later the methodology and instrument «Thermophobe» intended to measure thermal characteristics of Phobos surface with the «Phobos-Grunt» lander. This device serves as precursor of «Thermo-L» instrument for similar measurements on the lunar surface that installs on the «Luna Resource» lander.

Finally, it is worth to mention about the Mikhail Yakovlevich work on the problems of mechanics of weightlessness, in which he actively participated for several years along with V.S. Avduevsky, V.P. Osipov and their colleagues. He studied deeply enough this new advancing area of space research and published a few joint scientific papers that witness extremely broad areas of his scientific interests.

3.3 Planetary cosmogony and cosmochemistry - origin and evolution of the solar system and planetary systems around other stars (exoplanets)

The area of research, which Mikhail Yakovlevich focused on over the past two decades, is genesis of planetary systems. This branch of astrophysics known as planetary cosmogony is going back in time to middle centuries and rooted in Kant-Laplace basic ideas about an origin of the solar system. However, it took a great impetus only in the latest time when observations of circumstellar disks with the modern astronomical instruments became available, and also owing to discovery of exoplanets and relevant mathematical modeling with the use of powerful computers. Direct analysis of extrasolar matter encapsulated in its structure and composition and allowing to reconstruct the original processes of chemical reactions, phase transitions, etc. nicely complement the studies.

As the basic theory is concerned, the field combines different sections of physical mechanics from which the modern branch of mechanics of space and natural media has emerged. The modeling methods covered by planetary cosmogony involve the problems of heat and mass transfer, turbulence, and physical kinetics, to mention a few. They are closely related to aeronomy and most recently appeared cosmochemistry. The latter is the great tool allowing us to limit some constraints imposed on mathematical models when incorporating data on the structure, chemical-mineralogical composition and isotopic ratios of characteristic elements of meteorites matter. It therefore makes possible to reconstruct the processes of origin and evolution of celestial bodies and planetary systems as a whole more reliably. Vernadsky Institute is the world-recognized holder of excellent collection of meteorites including falls from the Moon and Mars, as well as lunar soil delivered by space vehicles.

This provides a synergy in the use of two approaches in the models development and in particular, it motivated Mikhail Yakovlevich to changing affiliation in order to advance the cosmogony problems through such a synergy. Currently, he and colleagues focuses on modeling the early stages of thermal and dynamical evolution of gas-dust turbulent accretion disk from a fragment of molecular cloud based on the mechanics of heterogeneous media with the account of magnetohydrodynamic (MHD) effects. They also pay significant attention to the analysis of gravitational and hydrodynamic disk instabilities resulted in disk fragmentation into fluffy clusters of fractal nature followed by their collisional interactions and growing inhabited dust particles from nanometers to pebble-boulder sizes and eventually to planetesimals.

Mikhail Yakovlevich published numerous papers and a number of monographs on the subject of stellar-planetary cosmogony that, likewise his earlier books, took national and international recognition. Among them, the monographs written with Prof. A. V. Kolesnichenko on the problems of turbulence and self-organization are to be distinguished. In these books, authors specially address the problem of turbulent accretionary discs instabilities and ordered structures formation at the originally chaotic background. In other words, following Yu. L. Klimontovich, they consider an orderly organized turbulent flow against the chaotic background. This topic is in close relation with general analysis of the behavior of chaotic systems what Mikhail Yakovlevich studied jointly with Acad. A.M. Friedman and they edited together a few published books.

Since the 1990s, Mikhail Yakovlevich studied migration processes in the solar system. In colloboration with S. Ipatov he developed the model of icy small bodies and dust particles migration from the outskirt of the solar system (Kuiper belt) involving their intermediate capture into orbits intersecting that of Jupiter followed by inward drift to orbits of the main asteroid belt and then fullfilling Amour-Apollo-Aten (NEO) group approaching the terrestrial planet orbits and thretened Earth. The corollary of the model is the conclusion that at the stage of intense bombardment by comets and asteroids of carbonaceous chondrites type with large water and other volatiles abundance (LHB) Earth could receive by the mechanism of heterogeneous accretion, an amount of water comparable to its content in the Earth's oceans. Tis could could compensate for the loss of volatiles at the Earth formation stage and is closely related also to the problem of the biosphere origin. Venus and Mars would receive comparable amounts of exogenic water, which reinforces the hypothesis of an existence of their ancient oceans lost in the course of subsequent evolution [4,6,9,11].

4 INTERNATIONAL COLLABORATION, PEDAGOGICAL AND OUTREACH ACTIVITY

The professional activity of Acad. M.Ya. Marov was tightly connected with international cooperation culminated during the period of his working at the STC. Since early 1960s he was a part of the Commission for Exploration and Use of the Outer Space (which was an open body of the secret STC) chaired by Acad. A. A. Blagonravov. In 1965, Acad M.V. Keldysh recruited Mikhail Yakovlevich to the new created Intercosmos Council responsible for the USSR international cooperation with socialist countries camp and later on with France. He continued this activity for many years. Since that time he began to travel abroad to participate in various conferences and symposia. Scientific community elected as a member and/or head of a number of commissions and working groups in the international scientific organizations

such as Committee on Space research (COSPAR), International Astronautical Federation (IAF), International Association of Geomagnetism and Aeronomy (IAGA), International Association of Meteorology and Atmospheric Physics (IAMAP). He was elected President of the Commission and then President of the Division III (Planetary Research) of the International Astronomical Union (IAU). Mikhail Yakovlevich has established friendly relations with many outstanding foreign colleagues. Among them, there were Carl Sagan, Thomas Gold, Tobias Owen, James Pollack, Gordon H. Pettengil, William Irvine, Brad Smith, Harold Masursky, Gerry Soffen, Mikhael Carr, Stiff Saunders, Jacques Blamont, James Head, Wesley Huntress and many others.

In 1971, USSR and USA signed the first Agreement on cooperation in outer space. From the Soviet side the document signed President of the USSR Academy of Sciences M.V. Keldysh and from the American side First Deputy of NASA Administrator George David Low who headed US delegation visiting Moscow. Four Joint Working Groups (JWG) were set up: Outer space, the Moon and planets; Space meteorology; Space communication; Space biology and medicine. M.Ya. Marov NASA Assistant Director Noel Hinners were nominated the co-chairs of the first JWG, which worked actively for about seven years until Reagan administration came to power. In particular, direct link (tele bridge) was established during Soviet and American Mars missions for the real time coordination of observations and scientific data exchange, with Mikhail Marov and Gery Soffen on the both sides. Mikhail Yakovlevich actively participated in international cooperation on some other space projects, including «Phobos-Grunt» and the planned «Luna» missions.

Mikhail Yakovlevich has a great experience in teaching. He gave lecture courses and served an advisor for PhD students, training above 20 candidates and doctors of science. Since 1989, he was deeply involved in educational programs of the new created International Space University (ISU) where he taught annually for 30 years serving as Head of Physical Sciences Department, Lecturer and a member of Academic Council and Board of Trustees. The university graduates future leading specialists in the field of space exploration on the international, interdisciplinary and intercultural (3I) basis using brain storming approach. Mikhail Yakovlevich contributed in the ISU activity including both permanent campus in Strasbourg (France) and summer sessions programs running over the world, and this his activity was highly appreciated. In 1994-1995, he has been teaching at the University of North Carolina working also on space projects. He is Professor of the M.V. Lomonosov Moscow University and he currently lectures at the Department of Space Research.

Throughout many years Mikhail Yakovlevich dealt with the scientific-organizing duties. Besides the above-mentioned activity in the STC and numerous international bodies, he worked and keeps working in the different commissions, committees, and councils. Currently he is a member of the Bureau of the Outer Space Council of the Russian Academy of Sciences (RAS); Chairman of the RAS Commission on K.E. Tsiolkovsky Scientific Heritage; vice-chairman of the RAS Scientific Council on Astrobiology; Member of the Expert Commission for promotion of scientific knowledge and Scientific Awards for the best works on popularization of science. He chairs the permanent workshop in the Vernadsky institute. For more than 3o years he is Editor-in-Chief of the international scientific journal «Astronomicheskij vestnik. Issledovanija Solnechnoj sistemy» (Solar System Research) issued simultaneously in Russian and English, and had been a member of Editorial boards of several international scientific journals. Since 2009, UNESCO World Heritage Committee (WHC) involved him in the astronomy-space heritage activity aimed to perpetuate the most

recognized space-rocket centers and space objects, which expanded tremendously the boundaries of our knowledge. He chaired the tentative Task Group since 2012 to initiate the process of space science and technology commemoration.

Mikhail Yakovlevich has published about 300 scientific papers in the referred journals and 18 monographs with the world-recognized domestic and foreign Publishers [1-16]. He also pursues his permanent outreach activity popularizing science through publications and TV programs. He is an author of the most recognized popular books «Planets of the solar system» (NAUKA PH, 1981 1-st and 1986 2-nd editions) and «Kosmos. From the solar system to the core of the Universe» (PHYSMATLIT, 2016 1-st and 2018 2-nd editions).

M.Ya. Marov was elected a full member of the International Academy of Astronautics, a member of the British Royal Astronomical Society. He has several distinguish state and international awards. He is laureate of the most distinguished Lenin Prize and the USSR State Prize. His Governmental awards include Order of the Labor Red Banner, Order of Honor, Order of Friendship and medals. Most recently he was awarded with the distinguish Demidov Prize and Keldysh Gold Medal of RAS for outstanding achievements in science. Among his international awards are prestigious Galabert Prize for Astronautics, Edwin Sieff Award, and COSPAR Nordberg Medal.

5. GREAT TEACHER M.V. KELDYSH

In conclusion, we would like to emphasize once again that Mikhail Yakovlevich Marov had the happy fate to be in the very core of many historical events and to share outstanding space achievements in the great country ─ Soviet Union.

He joined this enterprise when humans just only began to study space and master it. He was happy to work productively in his lovely field of science and create his scientific school. He was fortunate to know personally many wonderful people dedicated to space exploration and pioneering discoveries the world beyond the home planet. Mikhail Yakovlevich warmly reminds many of them whom with he was fortunate to be on a short stretch of space and time donated to a human by nature. He especially distinguish and esteem, however, the real leader of space breakthroughs, his Great Teacher Mstislav Vsevolodovich Keldysh. He speaks of him with a mix of infinite respect and admiration. From his teacher Mikhail Yakovlevich took many lessons learned in science and management and - most importantly – perceived his life philosophy and world attitude. He address the relationships with this amazing scientist and personality as a great gift of his fate.

Fig. 19. The great teacher M.V. Keldysh

The above biography of Mikhail Yakovlevich Marov is essentially a brief overview of what he has accomplished, and not in pursuance of official orders, but motivated by his own choice and mental capacities. Earlier telling about the main directions and issues of his scientific and scientific-organizational work, we already mentioned that many outcomes of this activity and the results of research of the scientist have been described in the numerous published

books and monographs. There is, however, one of them that he especially values. This is the unique book «Space Research» (M.V. Keldysh, M.Ya. Marov. «Kosmicheskiye Issledovaniya. M.:Nauka. 1981») based on a paper of the same title written by him jointly with his great teacher for the Proceedings «October and Science» («Oktyabr anf Nauka») and published by Nauka PH by the 60-th anniversary of October revolution in 1977.

Needless to say, Mikhail Yakovlevich feels proud of M.V. Keldysh invitation to co-author him in this work. Discussions in due course of writing the manuscript left the deep trace in his memory.

Colleagues congratulate Mikhail Yakovlevich on his remarkable anniversary and wish him many more years of active life and fruitful activity.

REFERENCES

[1]   A.D. Kuz'min, M.Ya. Marov, *Fizika planety Venera*, M.: Nauka, Gl. red. fiz.-mat. lit., (1974).
[2]   M.V. Keldysh, M.Ya. Marov, *Kosmicheskiye issledovaniya,* M.: Nauka, (1981).
[3]   M.Ya. Marov, *Planety Solnechnoy sistemy*, M.: Nauka, (1986).
[4]   M.Ya. Marov, A.V. Kolesnichenko, *Vvedeniye v planetnuyu aeronomiyu,* M.: Nauka, (1987).
[5]   M.Ya. Marov, V.I. Shematovich, D.V. Bisikalo, *Kineticheskoye modelirovaniye razrezhennogo gaza v zadachakh aeronomii*, Izd.-vo: M.: IPM im. Keldysha AN SSSR, (1990).
[6]   A.V. Kolesnichenko, M.Ya. Marov, *Turbulentnost' mnogokomponentnykh sred*, M.: MAIK «Nauka», (1998).
[7]   M.Ya. Marov, D. Grinspoon, *The Planet Venus*, Yale University Press, (1998).
[8] M.Ya. Marov, "Malyye tela colnechnoy sistemy i nekotoryye problemy kosmogonii", *UFN*, **175**(6), 668–678 (2005).
[9]   M.Ya. Marov, A.V. Kolesnichenko, *Mechanics of turbulence of multicomponent gases*, Kluwer Academic Publishers, Dordrecht, Boston, London, (2001).
[10]   *Sovremennyye problemy mekhaniki i fiziki kosmosa. K 70-letiyu so dnya rozhdeniya chl.-korr. RAN M.Ya. Marova*, (Eds. V.S. Avduyevskogo, A.V. Kolesnichenko), M.: Fizmatlit, (2003).
[11]   M.Ya. Marov, A.V. Kolesnichenko, *Turbulence and Self-Organization*, Modeling Astrophysical Objects, Springer. (2013).
[12]   W.T. Huntress, M.Ya. Marov, *Soviet Robots in the Solar System. Mission Technologies and Discoveries*, Springer –Praxis (2011).
[13]   M.Ya. Marov, W.T. Huntress, *Sovetskie roboti v Solnechnoy sisteme*, Fizmatlit, 2-oe izd., (2018).
[14]   M.Ya. Marov, *Kosmos. Ot Solnechnoy sistemy vglub' Vselennoy,* M.: Fizmatlit, 2-oe izd., (2018).
[15]   M.Ya. Marov, I.I. Shevchenko, *Ekzoplanety*, Institut komp'yuternykh issledovaniy, (2017).
[16]   V.I. Shematovich, M.Ya. Marov, "Dissipatsiya planetnykh atmosfer: fizicheskiye protsessy i chislennyye modeli", *UFN*, **188**(3), 233–265 (2018).

КОСМОС – ЭТО СУДЬБА: ИССЛЕДОВАНИЕ СОЛНЕЧНОЙ СИСТЕМЫ.

ПО СЛУЧАЮ 85-ЛЕТИЯ АКАДЕМИКА РАН М.Я. МАРОВА

Б.Н. ЧЕТВЕРУШКИН[1], А.И. АПТЕКАРЕВ[2], А.В. КОЛЕСНИЧЕНКО[3*], В.И. МАЖУКИН[4], В.П. ОСИПОВ[5]

[1] Научный руководитель ИПМ им. М.В. Келдыша РАН, академик РАН, профессор, Москва, Россия

[2] Директор ИПМ им. М.В. Келдыша РАН, член-корр. РАН, профессор, Москва, Россия

[3] Главный научный сотрудник ИПМ им. М.В. Келдыша РАН, профессор, Москва, Россия

[4] Главный научный сотрудник ИПМ им. М.В. Келдыша РАН, профессор, Москва, Россия

[5] Ведущий научный сотрудник ИПМ им. М.В. Келдыша РАН, Москва, Россия

*Ответственный автор. E-mail: kolesn@keldysh.ru

Ключевые слова: Механика сплошных сред, неравновесные кинетические процессы, исследования планет и космогония.

Аннотация. Статья посвящена 85-летию выдающегося Российского учёного, действительного члена Российской академии наук Михаила Яковлевича Марова. Академик М.Я. Маров — советский и российский физик и астроном, ведущий российский ученый в области теоретического и экспериментального изучения Солнечной системы, сравнительной планетологии, математического моделирования природных и космических сред. Ему принадлежат выдающиеся пионерские результаты исследований Венеры и Марса, которые получили широкое мировое признание. Впервые в мире им выполнены прямые измерения температуры и давления на поверхности Венеры и Марса, проведены исследования теплового режима Венеры, динамики атмосферы, структуры облаков. Он сыграл ведущую роль в решении сложной задачи посадки наших аппаратов на поверхность Венеры, благодаря чему удалось передать на Землю цветные панорамы, измерить элементный состав пород. Он непосредственный участник реализации программ «Луна», «Венера», «Вега», «Марс», «Фобос».

Область научных интересов М. Я. Марова очень широка. Она включает механику и физику космоса, астрофизику, планетологию, математическое моделирование космических сред. Он внес большой вклад в развитие наших знаний о космической среде. К ним относятся основы планетной аэрономии, механика многокомпонентных турбулентных реагирующих газов и гетерогенных многофазных сред, неравновесные кинетические процессы, оригинальные методы математического моделирования атмосфер планет и газовых оболочек комет, миграционно-коллизионные процессы малых тел в космическом пространстве. В своей научной деятельности он прекрасно сочетает теоретические и экспериментальные исследования, принимал непосредственное участие в осуществлении целого ряда наших всемирно признанных космических проектов.

Настоящий биографический очерк отражает взгляд многих коллег Михаила Яковлевича по Институту прикладной математики им. М.В. Келдыша РАН, в котором он проработал около полувека – объективный, но не беспристрастный, а проникнутый восхищением, уважением и любовью.

1. НАЧАЛО ТВОРЧЕСКОГО ПУТИ

Судьба распорядилась так, что Михаил Яковлевич Маров (рис. 1.) оказался на отрезке пространства и времени, когда человечеству открылась возможность выйти в космос, начать его изучать и освоение. Ему довелось принимать самое непосредственное участие в этом поистине историческом свершении в великой стране – Советском Союзе – практически с самых первых шагов. Ему посчастливилось заниматься любимой наукой на протяжении долгих лет вместе с многочисленными коллегами и учениками в двух великолепных организациях Российской академии наук, где ему довелось работать, – в Институте прикладной математики им. М. В. Келдыша (ИПМ им. М. В. Келдыша РАН), где он возглавлял отдел прикладной механики, космических исследований и аэрономии, и в Институте геохимии и аналитической химии им. В. И. Вернадского (ГЕОХИ РАН), в котором он возглавляет крупный отдел планетных исследований и космохимии, всемерно способствуя сотрудничеству между ИПМ, Институтом космических исследований (ИКИ) и ГЕОХИ в космических проектах.

Рис. 1. Академик Российской академии наук Михаил Яковлевич Маров

Михаил Яковлевич Маров родился в 1933 г. в Москве, в простой семье (рис. 2.). Его отец - участник Великой Отечественной войны, был тяжело ранен, рано умер. Его мать - преподаватель Московского института химического машиностроения. После окончания в 1952 г. московской средней школы с золотой медалью Михаил Яковлевич поступил на механический факультет Московского высшего технического училища (МВТУ) (ныне Московский государственный технический университет) имени Н. Э. Баумана (МГТУ) и окончил его с отличием в 1958 г. Свои школьные и студенческие годы Михаил Яковлевич вспоминает с тёплым чувством, хотя время было тяжёлое, мама, что называется, «поднимала» его одна, заложив духовные, нравственные основы жизни. Он неоднократно говорил, что бесконечно благодарен своим родителям, которые не только подарили ему жизнь, но сделали это крайне своевременно, так что он окончил университет как раз к началу космической эры. На последних курсах университета Михаил Яковлевич изучал сложный раздел механики - нелинейные колебания и был студентом-дипломником, когда пришло известие о запуске в СССР первого в мире искусственного спутника Земли. Оно потрясло его до глубины души. Тогда впервые он задумался о космосе, но мечта хоть как-то к этому приобщиться казалась тогда несбыточной.

Рис. 2. Родители, детство, юность

Его жизненный путь оказался совсем не простым. После окончания университета Михаил Яковлевич был направлен на закрытое предприятие под Москвой. Он приложил немало усилий, чтобы заниматься там исследовательской, а не рутинной инженерной работой. В течение первых двух лет он занимался нелинейными процессами в атомной физике, много времени проводил в Физико-энергетическом институте имени А. И. Лейпунского в Обнинске, участвуя в экспериментах на атомных реакторах. Как он узнал позже, эти исследования не только предназначались для оборонных проектов, но были связаны также с космосом и предназначались для использования в перспективе в бортовых энергетических установках дальних космических аппаратов (КА) и проводились по распоряжению С.П. Королева. Вскоре, однако, произошла реорганизация – предприятие, в котором Михаил Яковлевич работал, присоединили к ОКБ-1 С. П. Королёва (ныне Ракетно-космическая корпорация имени С.П. Королёва «Энергия» - РКК «Энергия»), а его лаборатория вошла в состав подразделения для разработки систем управления и ориентации космических аппаратов. Это направление возглавлял крупный учёный академик Б. В. Раушенбах, тесное общение с которым продолжалось потом долгие годы. Михаил Яковлевич принимал активное участие в разработке навигационных систем первых космических аппаратов для полётов к Марсу и Венере серий 1МВ и 2МВ. Всё тогда было внове,

многое постигалось буквально на ходу, а несовершенство технических средств часто приводило к досадным ошибкам. И, тем не менее, в кратчайшие сроки создавались совершенно уникальные системы, во многом мотивированные императивами холодной войны, стремлением превзойти соперника, быть первыми.

Вскоре, однако, судьбе было угодно вновь круто изменить жизнь Михаила Яковлевича. Неожиданно распоряжением Госкомитета по оборонной технике (ГКОТ), к которому относилось ОКБ-1, его перевели в Москву, где под непосредственным руководством выдающегося специалиста отрасли Г.А. Тюлина он вплотную занялся текущими и перспективными проблемами ракетно-космической техники, в том числе анализом аварийных пусков ракет.

А после случайной встречи с М. В. Келдышем на одном из совещаний, посвященном проблеме лунной гонки, Михаил Яковлевич получил вскоре его приглашение перейти из системы ГКОТ в Академию наук СССР, в возглавляемый им Институт прикладной математики, которое он принял с воодушевлением. Вся его последующая жизнь на протяжении более полувека связана с Академией наук, где он прошёл колоссальную школу от научного сотрудника до руководителя научного подразделения. Так или иначе, космос определил выбор его жизненного пути. Путь этот оказался достаточно сложным, было несколько крутых поворотов, были, несомненно, моменты везения, но за всем этим стояли упорный труд, непрерывная учёба, не покидавшая его любознательность, стремление к познанию нового.

2. КОСМИЧЕСКИЕ ПРОГРАММЫ И ПРОЕКТЫ

Особенно серьёзной школой, неизмеримо расширившей научно-технический кругозор и давшей бесценный опыт работы с крупными коллективами и проектами, стала его работа в течение около 15 лет Учёным секретарём Межведомственного научно-технического совета по космическим исследованиям (МНТС по КИ) при АН СССР, который возглавлял М.В. Келдыш.

Все эти годы Михаил Яковлевич работал в тесном общении с ним (рис. 3), и это был самый напряжённый и, вместе с тем, насыщенный период его жизни. Михаил Яковлевич самым непосредственным образом участвовал в разработке программ научных и прикладных космических исследований, обсуждении практически всех космических проектов, много времени проводил на предприятиях и ракетных полигонах. Ему довелось лично хорошо узнать всех главных конструкторов отрасли, руководителей и ведущих сотрудников НИИ и КБ, в том числе всех членов легендарного Совета Главных конструкторов, возглавляемого С.П. Королевым и самого Сергея Павловича. Это неизмеримо обогатило жизнь.

Рис. 3. М.В. Келдыш (справа) и М.Я. Маров, 1971 г.

Среди многих исторических личностей особенно тесные контакты установились у Михаил Яковлевич с Г.Н.

Бабакиным – Главным конструктором Научно-производственного объединения (НПО) им. С.А. Лавочкина, где создавались космические аппараты для исследований Луны и планет, его заместителями, а затем и преемниками. М.В. Келдыш поручил Михаил Яковлевич лично активно участвовать в выработке программ исследований и подготовке технических вопросов, обеспечивающих решение принципиально важных научных задач, сопряжение научной аппаратуры со служебными системами космических аппаратов для исследований Луны, Венеры, Марса, и он в течение многих лет по существу выполнял функции, которые на Западе называют Project Scientist (PS). Михаил Яковлевич проводил также собственные экспериментальные исследования на этих КА в качестве Principal Investigator (PI), чему М.В. Келдыш всячески способствовал, создав в отделе в ИПМ специальную лабораторию. Кульминационным в этой его деятельности был период с середины 1960-х до начала 1980-х гг. Именно на этот период приходятся выдающиеся пионерские достижения в исследованиях Луны, Венеры, Марса (рис. 4 -7).
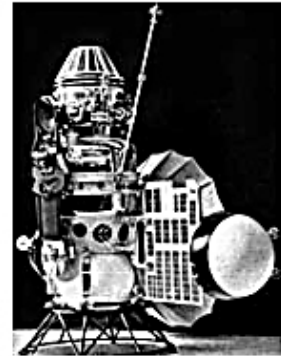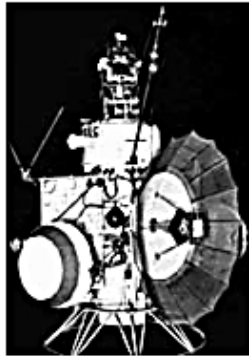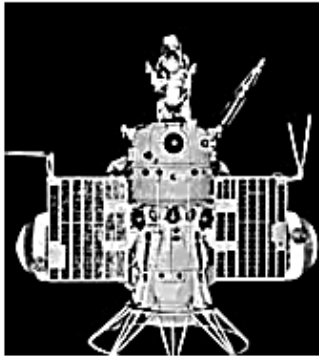
Рис.5. 2МВ – «Венера-2, -3».   Рис.5. 2МВ – «Венера-2, -3».
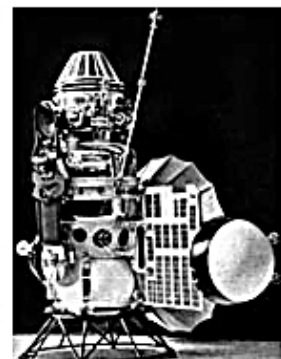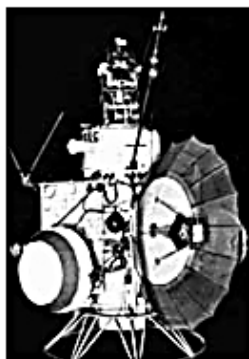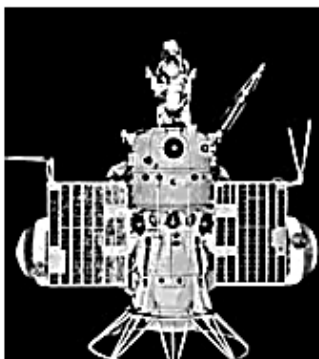
Рис.6. 1МВ – «Марсник».   Рис.7. 1МВ – «Венера-1».

С чувством особой гордости Михаил Яковлевич вспоминает об успешной многолетней программе исследований Венеры, начиная с полета «Венеры-4» (рис. 8 - 10). Осуществлению этой программы он отдал много времени и сил, но эти усилия были с лихвой вознаграждено техническими и научными результатами мирового уровня. Среди них первые прямые измерения параметров атмосферы этой загадочной планеты, первые посадки аппаратов на поверхность Венеры и их выживание в суровых условиях окружающей среды (не повторенные больше никем в мире), измерения освещённости и передача сначала черно-белых, а затем цветных панорам поверхности,

определение состава поверхностных пород, исследования атмосферной динамики, структуры и свойств венерианских облаков. Российскими учёными были, изучены особенности околопланетного космического пространства на первых искусственных спутниках Венеры. Все эти успехи были достигнуты двумя поколениями космических аппаратов, созданных Г. Н. Бабакиным, причём второе поколение, обладавшее высокой степенью надёжности, стало также технической основой программы полёта аппаратов «Вега» к комете Галлея и создания астрофизического спутника «Астрон».

Рис.8. Вход спуск в атмосфере («Венера-4» - «Венера-6»)
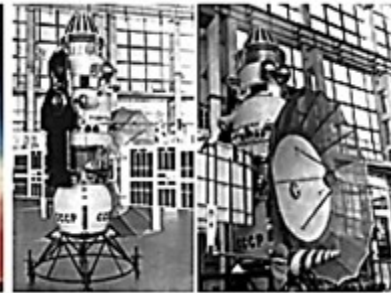
Рис. 9. КА «Венера-4» - «Венера-6»
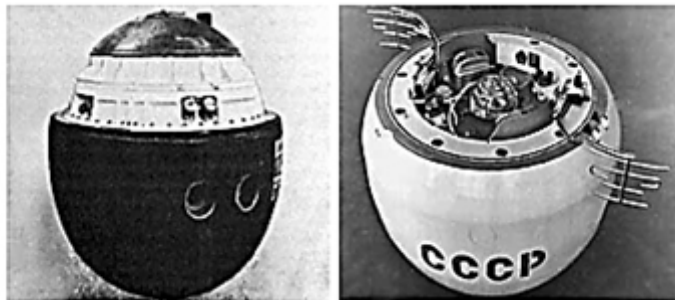
Рис. 10. Спускаемый аппарат, «Венера-7, -8»

К сожалению, не все планы исследований Венеры удалось осуществить. Для Михаила Яковлевича особенно болезненным было решение в 1981 г. об отмене запланированного запуска аэростатного зонда (баллона) для детального изучения уникальных облаков планеты. Сделано это было волевым решением, хотя этот советско-французский проект, научными руководителями которого с российской и французской стороны были, соответственно, М.Я. Маров и Жак Бламон, находился на завершающей стадии изготовления. Этому проекту было отдано около трех лет жизни, потраченными по существу впустую.

Менее успешной была российская марсианская программа, включавшая искусственные спутники Марса и посадочные аппараты. Тем не менее, выдающимися достижениями стали первая мягкая посадка на Марс КА «Марс-3» и первые прямые измерения параметров атмосферы на КА «Марс-6». На этой основе Михаилом Яковлевичем с сотрудниками была создана первая модель атмосферы Марса от поверхности до ~ 70 км.

И, конечно, поистине эпохальными стали уникальные полёты лунных космических аппаратов (рис. 11, 12), обеспечивших автоматический забор и возврат на Землю

лунного грунта и длительную работу на поверхности Луны самоходных аппаратов. Успешное осуществление этих проектов в самом начале 1970-х гг. позволило в определённой степени ослабить негативные последствия проигранной нами лунной гонки за высадку первого человека на Луну. Михаил Яковлевич неоднократно вспоминает обуревавшие его сложные чувства, когда он наблюдал выход на лунную поверхность Нейла Армстронга - сочетание гордости за триумф человеческого гения вместе с чувством досады и горечи, что это сделали не россияне. Всего лишь восемь лет назад, когда всех захлестнуло ликование от полёта Юрия Гагарина, это казалось вполне реальным. С.П. Королёв готовил даже проект пилотируемого полёта на Марс, всему этому помешала его преждевременная кончина. И, тем не менее, советские лунные автоматы позволили, что называется, сохранить лицо и получить результаты, которыми сегодня по праву гордится страна. Они закрепили за СССР признание его ведущей космической державой.
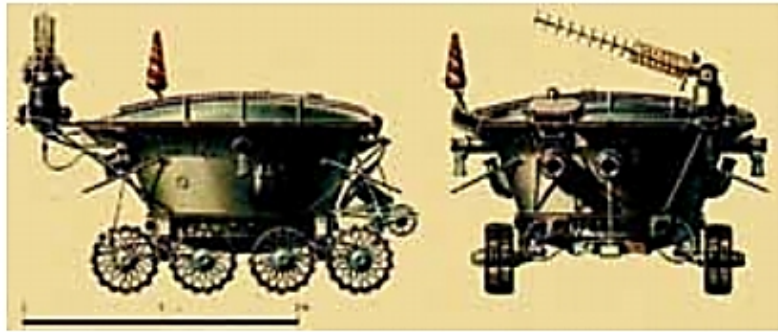
Рис.11. «Луна-16»   Рис.12. «Луноход-1»
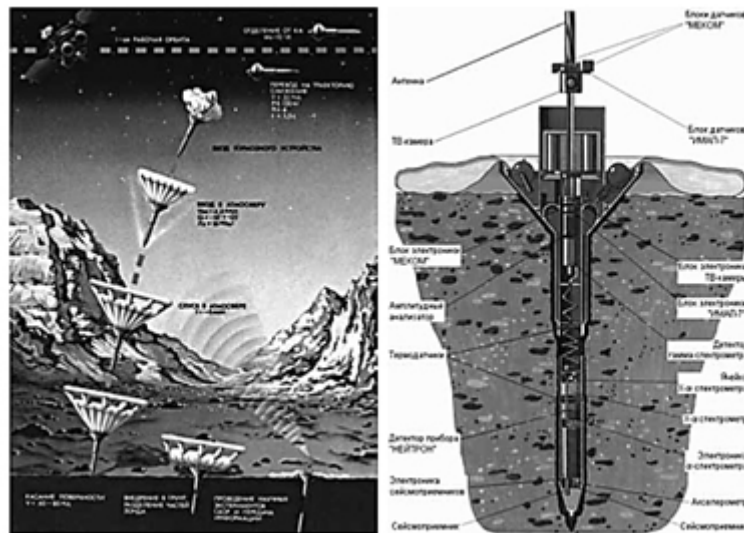
Рис.13. Спуск пенетраторов на поверхность Марса и метеокомплекс «Меком» наверху пенетратора (проект МАРС-96)

Ситуация радикально изменилась, а признание сильно пошатнулось в последующие десятилетия. Успешное завершение миссий ВЕГА было предопределено надёжностью

КА «Венера» второго поколения. Новые разработки оказались значительно менее совершенными, результатом чего стало выполнение лишь малой части программы полётов двух аппаратов к Фобосу, а вслед за тем и трагедия с запуском КА «Марс-96» (рис. 13). В совокупности с разрушительными последствиями перестройки это отбросило российскую лунно-планетную программу на десятилетия назад. Конечно, огромное негативное влияние оказало отсутствие лидера такого масштаба, как М.В. Келдыш, никто из последующих руководителей космической программы не мог с ним сравниться, не обладал таким колоссальным авторитетом у руководства страны. В конце 1970-х гг., после кончины М. В. Келдыша, Михаил Яковлевич добровольно ушёл из МНТС по КИ и целиком переключился на научную работу, совмещая теоретические и экспериментальные исследования.

В проекте «ВЕГА» Михаил Яковлевич занимался расчётами негравитационных возмущений в движении кометы Галлея вследствие сублимации газа и пыли с поверхности ледяного ядра, с целью повышения точности определения траектории на момент встречи с кометой космического аппарата. В проекте «ФОБОС-88» он занимался моделированием дистанционного определения состава поверхностных пород Фобоса с помощью разработанного в ИКИ РАН бортового прибора «Лима-Д», снабжённого лазерной пушкой и масс-анализатором эжектируемых ионов.

В проекте МАРС-96 он был научным руководителем метеокомплекса, установленного на пенетраторах, отделявшихся от орбитального аппарата и предназначавшегося для длительных измерений параметров атмосферы Марса и вариаций содержания в атмосфере пыли.

Неудача с запуском «Марса-96» оказала катастрофическое влияние на российскую планетную программу. К счастью, в конце 1990-х годов небольшая команда энтузиастов вместе с Михаилом Яковлевичем предприняла героические усилия к ее возрождению. Были учтены многие изменения в стране и, в частности, в космической отрасли, продиктованные новыми экономическими отношениями в рыночных условиях и новые технологии. Постепенно к этой команде присоединились традиционные группы квалифицированных специалистов. Их совместные усилия позволили разработать предложения по созданию универсального планетного космического аппарата. В качестве первой миссии был предложен проект «Фобос-Грунт» для выполнения амбициозной задачи по возвращению на Землю образцов пород со спутника Марса Фобос. Снова Михаил Яковлевич отдал много времени и сил этому проекту, который был, наконец, включен в Федеральную космическую программу. Тем сильнее были переживания в 2011 г. в связи с его неудачным запуском.

Насыщенный крупными событиями почти 20-летний период активной космической деятельности Михаила Яковлевича отражён в его книге «Советские роботы в Солнечной системе. Технологии и открытия» (рис. 14, 15), написанной совместно с американским коллегой Уэсли Теодором Хантрессом и изданной в 2011 г. на английском языке издательством Springer-Praxis, а 2013 г. выпущенной на русском языке редакцией физико-математической литературы издательства «Наука» (М.Я. Маров, У.Т. Хантресс, Советские роботы в Солнечной системе. Технологии и открытия/Пер.: W.T. Huntress, M.Ya. Marov, Soviet robots in the solar systems. Mission technologies and discoveries. М.: Физматлит, 2013. 612 с.).

В этой книге совершенно объективно отражены успехи и неудачи советской программы лунно-планетных исследований на автоматических КА, проанализированы их причины. На обложку книги, по предложению Уэсли Хантресса, вынесены слова: «Первые на Луне, первые на Венере, первые на Марсе», что отдаёт должное нашему выдающемуся вкладу в мировую науку. Книге была присуждена премия Международной академии астронавтики за лучшую книгу в области фундаментальных наук. Она с интересом встречена российскими читателями, в первую очередь, молодёжью, слабо знакомой с замечательным вкладом отечественной науки и техники в мировую космонавтику.

Рис. 14. Издание на русском языке
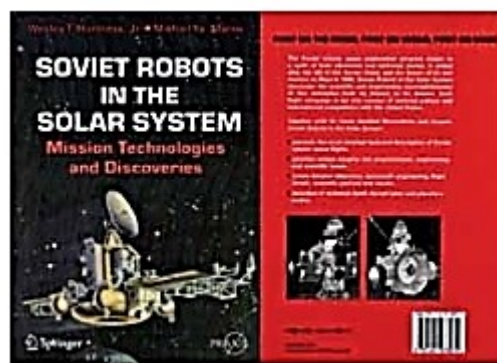
Рис. 15. Книга "Soviet robots in the solar systems. Mission technologies and discoveries", изданная в 2011 г. на английском языке издательством Springer-Praxis, и Диплом Международной академии астронавтики за лучшую книгу в области фундаментальных наук.

Несмотря на завесу секретности, в условиях которой осуществлялась в СССР космическая программа, многое на Западе было известно, в том числе, и об участии Михаила Яковлевича в этой программе. Было, в частности, известно о его позиции у М.В. Келдыша - руководителя советской космической программы. Помимо этого, М.В. Келдыш поручал Михаилу Яковлевичу участие в различных международных мероприятиях, ведение переговоров. Иными словами, Михаил Яковлевич был, что называется, на виду. Неслучайно поэтому в 1971 г., после успешной мягкой посадки на Марс КА «Марс-3», ему была присуждена Международная Галаберовская премия по астронавтике, которую при её вручении Михаил Яковлевич назвал признанием, в первую очередь, заслуг его коллег из НПО им. С.А. Лавочкина. Свидетельством оценки его участия в различных космических проектах у зарубежных учёных стал коллаж Брауновского университета (США), вручённый ему в связи с 20-летием симпозиума «Вернадский –Браун» (рис. 16).

Приятной неожиданностью стало также присуждение Михаил Яковлевич в 2012 г. Диплома НАСА в связи с 50-летием исследований Солнечной системы «в знак признания лидирующей роли в исследованиях Солнечной системы и открытий, изменивших мир» (рис. 17), а в 2013 г. - Премии Элвина Сиффа «в знак признания выдающегося и уникального вклада в планетные исследования, включая первые прямые измерения в атмосферах Венеры и Марса» (рис. 18).
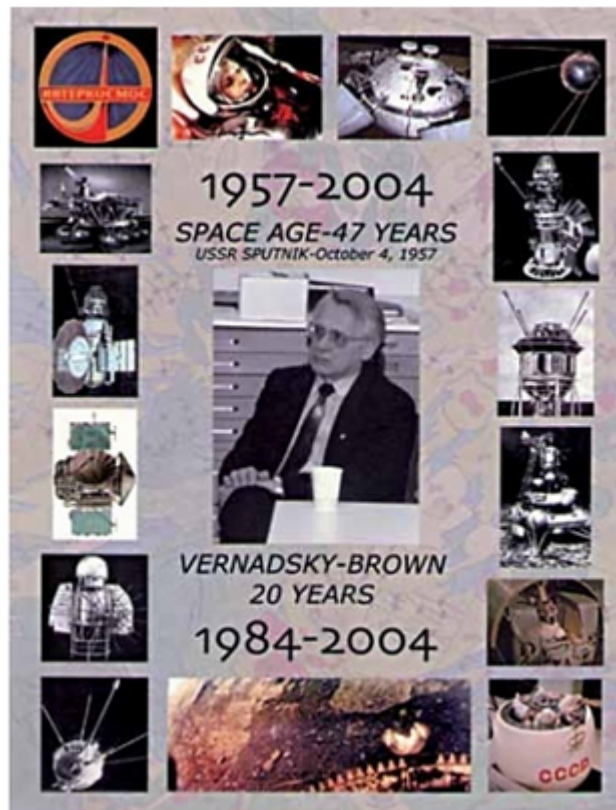
Рис. 16. Коллаж Брауновского университета (США), врученный автору в связи с 20-летием симпозиума «Вернадский - Браун».
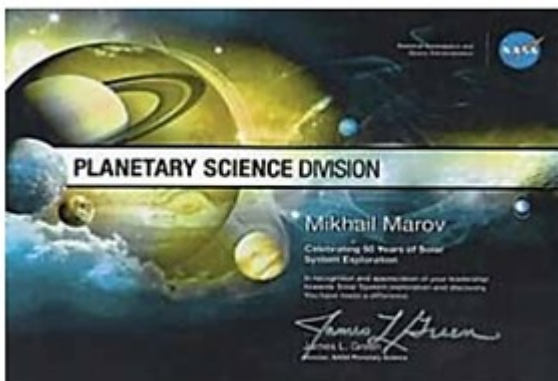

Рис. 17. Диплом НАСА в связи с 50-летием исследований Солнечной системы «в знак признания лидирующей роли в исследованиях Солнечной системы и открытий, изменивших мир».
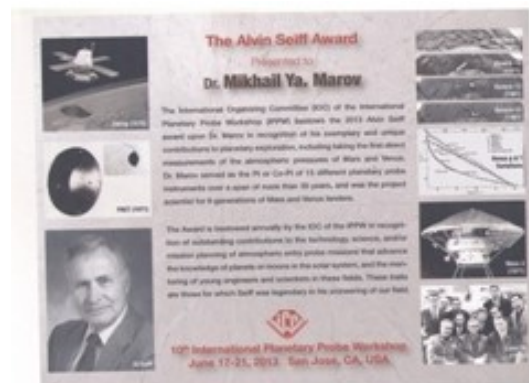

Рис. 18. Премия Элвина Сиффа за планетные исследования.

Книга «Soviet robots in the solar systems. Mission technologies and discoveries», изданная в 2011 г. на английском языке издательством Springer-Praxis была удостоена

Диплома Международной академии астронавтики за лучшую книгу в области фундаментальных наук. В 2013 г. она была выпущена на русском языке Издательством физико-математической литературы.

3. НАУЧНЫЕ ИССЛЕДОВАНИЯ

Наряду с работой в МНТС по КИ, Михаил Яковлевич возглавлял в ИПМ отдел прикладной механики, космических исследований и аэрономии, занимаясь теоретическими и экспериментальными работами. Такое совмещение было непростым и требовало колоссальной отдачи сил. Мстислав Всеволодович направлял научную деятельность этого подразделения, помогал в решении ряда теоретических проблем, которые Михаил Яковлевич с ним обсуждал, и эти уроки были бесценными. В 1962 г. Михаил Яковлевич поступил в аспирантуру, в 1964 г. защитил кандидатскую, а в 1970 г. - докторскую диссертацию по разделу физико-математических наук.

В 1977 г. ему присвоили звание профессора, в 1990 г. он был избран членом-корреспондентом АН СССР по Отделению механики и процессов управления, а в 2008 г. - академиком РАН по специальности планетные исследования Секции наук о Земле. В этом избрании нашло отражение признание членами Секции важности изучения Земли как одной из планет Солнечной системы на основе сравнительно-планетологического подхода и того вклада, который Михаилу Яковлевичу удалось внести в этот раздел современной науки.

Научные исследования, в которых лично и с коллегами/учениками ему удалось получить определённые результаты, можно разделить на следующие разделы:

1. Физическая механика, математическое моделирование космических и природных сред, аэрономия (Соавторы: проф., д.ф-м.н. А.В. Колесниченко, чл.-корр. РАН Д.В. Бисикало, д.ф.-м.н. В.И. Шематович, к.ф.-м.н. А.М. Алферов, к.ф.-м.н. О.П. Красицкий).

2. Планетные исследования на космических аппаратах, разработка моделей на основе данных измерений (Соавторы: акад. РАН В.С. Авдуевский, д.т.н. М.К. Рождественский, д.ф.-м.н. В.И. Полежаев, д.ф.-м.н., В.В. Кержанович, к.т.н. Ф.С. Завелевич, Н.Ф. Бородин, к.т.н. Ю.П. Карпейский, к.ф.-м.н. Б.Е. Мошкин, к.ф.-м.н. А.П. Экономов, к.т.н. З.П. Черемухина, К.К. Мануйлов, к.т.н. В.П. Осипов).

3. Планетная космогония и космохимия -происхождение и эволюции Солнечной системы и планетных систем у других звёзд (Соавторы: проф. А.В. Колесниченко, д.х.н. В.А. Дорофеева, к.т.н. А.В. Русол, д.ф.-м.н. С.И. Ипатов, к.ф.-м.н. А.Б. Макалкин, к.ф.-м.н. И.М. Зиглина).

Здесь нет возможности подробно изложить даже наиболее значимые результаты, полученные Михаилом Яковлевичем в каждом из этих разделов или их совокупности, к тому же приведённое деление в известном смысле условно. Поэтому мы ограничимся только очень краткими сведениями, а более подробно с содержанием его исследований можно ознакомиться в многочисленных монографиях, написанных им лично или вместе с коллегами.

3.1 Физическая механика, математическое моделирование космических и природных сред, аэрономия

Специфика космической среды и проблемы, с которыми пришлось столкнуться, предопределили разделы механики, на которых сосредоточились исследования Михаила Яковлевича на протяжении почти полувека. Это многокомпонентная радиационная гидродинамика, турбулентность неоднородных реагирующих сред, динамика разреженного газа, физико-химическая кинетика. Эти разделы составили научный базис работ в новом направлении космических исследований - аэрономии, которой Михаил Яковлевич начал заниматься ещё в аспирантуре под руководством профессора В.И. Красовского. Ему Михаил Яковлевич во многом обязан приобретёнными новыми знаниями по физике верхней атмосферы. В этих исследованиях были использованы экспериментальные данные об эволюции орбит искусственных спутников Земли, торможение которых в верхней атмосфере зависит от её состояния -температуры и плотности. Путём решения обратных задач можно определять значения этих параметров среды и их вариации в зависимости от состояния солнечной и геомагнитной активности. Одновременно, вместе со своим первым учеником и коллегой А.В. Колесниченко, Михаил Яковлевич начал заниматься разработкой теоретических основ аэрономии. Это новое научное направление, представляющее собой исследования динамики разреженного газа, подверженного прямому воздействию солнечного электромагнитного и корпускулярного излучений и сопровождаемого реакциями фотолиза (диссоциацией, ионизацией, возбуждением) и многочисленными прямыми и обратными переходами - химическими реакциями, вместе с процессами тепломассопереноса и диффузии**.** На основе комплекса этих исследований были созданы модели верхней атмосферы Земли, которые использовались для прогноза времени жизни спутников и орбитальных станций, а также при разработке международных стандартных моделей верхней атмосферы CIRA (COSPAR (Committee on Space Research International Reference Model). Были также созданы модели, на основе которых изучались причины уменьшения содержания озона в озоновом слое Земли с учётом влияния различных малых компонентов, в том числе, в рамках европейского проекта GOMOS (Global Ozone Monitoring by Occultation of Stars), и делались прогнозы его эволюции.

Другим направлением аэрономических исследований стало изучение неравновесных кинетических процессов в разреженном газе верхних атмосфер Земли и других планет. Эти исследования были начаты вместе с другим его талантливым учеником В.И. Шематовичем, который в дальнейшем успешно использовал развитые методы для решения проблем астрохимии. В основу были положены методы стохастического моделирования при решении уравнений больцмановского типа с правыми частями, содержащими интегралы реакций. Метод позволяет с хорошей точностью учесть вклад радиационных и химических источников нагрева и эффективность диссипации атмосферных атомов в космическое пространство. Основой служит построение физико-вероятностного аналога кинетического явления в виде случайного процесса и численная реализация уравнения эволюции состояния газа в марковской форме с использованием алгоритмов Монте-Карло. Методы статистического моделирования, в разработке которых принимал также участие Д.В. Бисикало, были успешно применены при изучении степени неравновесности состояния ряда компонентов верхней

атмосферы Земли с учётом скорости ионизации O2, N2 и O, спектров кинетической энергии «горячих» атомов кислорода и азота вследствие фотодиссоциации, их функций распределения на разных высотах и спектров кинетической энергии фотоэлектронов. Данный подход был использован также для оценки темпов потери воды на Марсе вследствие нетепловой диссипации тяжёлых атомов из атмосферы планеты. Помимо этого, роль воды в марсианской атмосфере изучалась на других моделях с учётом вклада фотолиза и химических реакций.

К данному разделу исследований относится также моделирование образования и эволюции внутренней комы кометы, с подробным изучением процессов молекулярного переноса в пористом ядре, сублимации газа и пыли с поверхности ледяного ядра, формирования и радиальных профилей макропараметров кнудсеновского слоя у его поверхности. Им совместно с А.В. Колесниченко были сделаны оценки вклада негравитационных возмущений в движение кометы на разных удалениях от Солнца. Помимо этого, были получены радиальные профили макропараметров разреженного газа в газовой оболочке кометы Галлея и оценено положение наблюдаемого фотометрического ядра, смещённого относительно физического ядра из-за эффектов светорассеяния пылью. Эти результаты использовались в проекте ВЕГА.

В работах М.Я. Марова по механике космических и природных сред особое место занимают исследования по проблемам турбулентности многокомпонентных реагирующих газов. Они проводились на протяжении почти трёх десятилетий и продолжают успешно развиваться в настоящее время совместно с А.В. Колесниченко. Результаты, включающие основополагающие теоретические подходы, соответствующий математический аппарат, методы постановки и решения модельных задач, отражены в многочисленных публикациях и ряде монографий авторов, выпущенных ведущими отечественными и зарубежными издательствами «Наука», «Бином. Лаборатория знаний», «Kluwer Academic Publishers» и «Springer» (см. список литературы [1-16]). Эти исследования в значительной степени ориентированы на проблемы космогонии, эволюции газопылевых аккреционных дисков. Следует подчеркнуть, что в этих работах нашло своё отражение новое направление в исследованиях неоднородных турбулентных сред, когда учитывается наличие химических реакций между газовыми компонентами, а также влияние пыли в случае гетерогенной среды. Существенной новизной отличается также рассмотрение гидродинамической спиральности и эффективности образования пылевых кластеров в турбулентных вихрях.

3.2 Планетные исследования на космических аппаратах, разработка моделей на основе данных измерений

Этот большой раздел научных исследований целиком связан с экпериментальными результатами. Наиболее крупные результаты были получены М.Я. Маровым в исследованиях Венеры на космических аппаратах «Венера-4» – «Венера-14» (1967–1981). Ему довелось вместе с коллегами осуществить первые в мире прямые измерения параметров атмосферы Венеры, измерить значения температуры и давления на ее поверхности, изучить термодинамические свойства атмосферного газа. Были изучены особенности динамики атмосферы, получены профили ветра по высоте путем допплеровских измерений при спуске космических посадочных аппаратов и измерена

скорость ветра на поверхности посредством чашечных анемометров. Эти исследования подтвердили наличие на Венере атмосферной суперротации. Также впервые в мире были проведены измерения характера уменьшения с высотой солнечного излучения в нескольких диапазонах спектра, получены значения освещённости на поверхности и сделан вывод о преобладании красных лучей, придающих поверхности оранжевый оттенок. Эти измерения позволили передать сначала чёрно-белые, а затем и цветные панорамы поверхности, а также получить первые данные о расположении и структуре облаков. Впервые была определена слоистая структура и микрофизические характеристики основных облаков - наличие трёх слоёв и переходных зон, состоящих из трёх мод частиц микронных размеров с различными показателями преломления. Это позволило сделать вывод о том, что частицы облаков совершенно отличны от водяного льда и образованы веществом другой природы, которой оказалась концентрированная серная кислота. Помимо чёткого определения расположения облачных слоёв на высоте от 49 до 68 км над поверхностью, было также выявлено наличие подоблачной (49 до35 км) и надоблачной (выше 68 км) дымки.

Большое внимание М.Я. Маров уделял разработке моделей, в основе которых лежали, в первую очередь, полученные им собственные данные измерений. Это касалось структуры атмосферы и облаков, теплового режима и атмосферной динамики Венеры. На основе прямых измерений высотных профилей температуры, давления и скорости горизонтального ветра на КА «Марс-6» была создана модель, в хорошем согласии с которой оказались последующие более полные измерения на американских посадочных аппаратах «Викинг». Эти исследования стимулировали в дальнейшем разработку методики, по которой был создан прибор «Термофоб» для измерений термических характеристик поверхности Фобоса на КА «Фобос-Грунт» и приборы «Термо-Л» для аналогичных измерений на поверхности Луны на КА «Луна-Ресурс». Наконец, следует упомянуть о работах по механике невесомости, в которых Михаил Яковлевич участвовал в течение ряда лет вместе со своими коллегами. Эти работы позволили ему достаточно глубоко вникнуть в этот перспективный раздел космических исследований и опубликовать ряд совместных научных работ.

3.3 Планетная космогония и космохимия -происхождение и эволюции Солнечной системы и планетных систем у других звёзд

Это направление исследований, на котором сосредоточены интересы Михаила Яковлевича Марова в течение последних двух десятилетий. Эта ветвь астрофизики, известная как планетная космогония, уходит своими корнями в средние века, в основополагающие идеи Канта-Лапласа о происхождении солнечной системы. Однако это направление приобрело большой импульс лишь в последнее время, когда стали доступны наблюдения околозвездных дисков с помощью современных астрономических инструментов, а также благодаря открытию экзопланет и новым возможностям математического моделирования с использованием современных компьютеров. Большой вклад вносит анализ структуры и состава внеземного вещества, позволяющий реконструировать ранние процессы химических реакций, фазовых переходов и др.

Теоретической основой создания моделей служит физическая механика, современным разделом которой является механика космических и природных сред.

Проблемы и методы моделирования, охватываемые планетной космогонией, включают задачи тепломассопереноса, турбулентности, физической кинетики, и во многом они связаны с аэрономией. В последние десятилетия к ним добавилась космохимия. Ограничениями, накладываемыми на модели, служат исследования структуры, химико-минералогического состава вещества метеоритов, специфики изотопных отношений характерных элементов, составляющие предмет космохимии и позволяющие реконструировать процессы происхождения и эволюции небесных тел и, в совокупности с развиваемыми моделями, - планетной системы в целом. В институте ГЕОХИ им. В.И. Вернадского обеспечивается необходимый синергизм этих двух подходов. Комплекс исследований включает в себя моделирование ранней эволюции газопылевого турбулентного аккреционного диска на основе механики гетерогенных сред, в том числе с учётом магнитогидродинамических (МГД) эффектов. Совместно с коллегами разработаны модели термической и динамической эволюции диска на стадии аккреции вещества из молекулярного облака на протосолнце, получены условия формирования субдиска, его фрагментации на рыхлые газопылевые сгущения вследствие гравитационной и/или гидродинамической неустойчивости и их последующего укрупнения при столкновениях, отвечающие ограничениям на сохранение углового момента.

Значительное внимание Михаил Яковлевич уделял, начиная с 1990-х гг. исследованию миграционных процессов в Солнечной системе. Совместно с С.И. Ипатовым им развита модель миграции ледяных тел и пылевых частиц из внешних областей Солнечной системы (пояса Койпера), их промежуточного захвата на орбиты, пересекающие орбиту Юпитера, и последующего дрейфа на орбиты Главного пояса астероидов и к планетам земной группы. Следствием модели является вывод о том, что на этапе интенсивной бомбардировки кометами и астероидами типа углистых хондритов Земля могла получить за счёт гетерогенной аккреции количество воды, сопоставимое с её содержанием в земных океанах, что могло компенсировать утрату летучих на стадии формирования планет земной группы при высоких температурах вблизи Солнца. Аналогичные объемы воды могли получить Венера и Марс, что подкрепляет гипотезу о существовании у них древних океанов. Это направление исследований напрямую связано также с проблемой происхождения земной биосферы. По разделу космогонии Михаил Яковлевич опубликованы многочисленные статьи и ряд монографий. Среди них монографии с проф. А.В. Колесниченко по проблемам турбулентности и самоорганизации, причём их содержание в значительной степени связано с проблемами планетной космогонии. Опубликованы сборники, посвящённые проблемам хаоса, на фоне которого возникают упорядоченные структуры в космической турбулизованной среде, и проблемам образования и эволюции астрофизических дисков [4,6,9,11].

4. МЕЖДУНАРОДНОЕ СОТРУДНИЧЕСТВО И ПЕДАГОГИЧЕСКАЯ ДЕЯТЕЛЬНОСТЬ.

В профессиональной деятельности акад. М.Я. Марова, особенно в период работы в МНТС по КИ, существенное место занимали вопросы международного сотрудничества. С начала 1960-х гг. он тесно общался с сотрудниками Комиссии по исследованию и использованию космического пространства (которая была открытым

органом МНТС по КИ) и её председателем − замечательным человеком А.А. Благонравовым. В 1965 г. М.В. Келдыш привлёк Михаила Яковлевича к работе созданного для международного сотрудничества стран социалистического лагеря Совета «Интеркосмос», к которому вскоре примкнула Франция, и эта его деятельность продолжалась в течение многих лет. С этого же времени начались его зарубежные поездки для участия в различных конференциях и симпозиумах. М.Я. Маров возглавлял ряд комиссий и рабочих групп в таких международных научных организациях как COSPAR, IAF (International Astronautical Federation), IAGA (International Association of Geomagnetism and Aeronomy), IAMAP (International Association of Meteorology and Atmospheric Physics), избирался президентом сначала Рабочей группы 16, а затем Дивизиона III (Планетные исследования) Международного астрономического союза (International Astronomical Union - IAU). Со многими зарубежными коллегами у Михаила Яковлевича сложились дружественные отношения, среди них такие выдающиеся учёные, как Карл Саган (Carl Edward Sagan), Томас Голд (Thomas Gold), Жак Бламон (Jacques Blamont), Гордон Петтенгил (Gordon H. Pettengil), Уильям Ирвайн (William Irvine), Бред Смит (Brad Smith), Тоби Оуэн (Tobias C. Owen), Гарольд Мазурский (Harold Masursky), Джерри Соффен (Gerry Soffen), Майкл Карр (Mikhael Carr), Стив Саундерс (Stiff Saunders), Джим Хэд (James Head), Нэсли Хантресс (Wesley Huntress) и др.

В 1971 г. было подписано первое Соглашение между Академией наук СССР и НАСА США о сотрудничестве в космических исследованиях. Его подписали президент АН СССР М.В. Келдыш и первый заместитель директора НАСА Джордж Дейвид Лоу (George David Low) во время визита американской делегации в Москву. Были созданы четыре совместные Рабочие группы: Космос, Луна и планеты; Космическая метеорология; Космическая связь; Космическая биология и медицина. М.Я. Маров. был назначен сопредседателем Рабочей группы по космосу, Луне и планетам, а с американской стороны им стал помощник Директора НАСА Ноэль Хиннерс (Noel Hinners). В частности, в рамках этой Рабочей группы был организован телемост для координации исследований Марса при помощи советского и американского КА, с двух сторон которого были М.Я. Маров и Джерри Соффен. Михаил Яковлевич активно участвовал в международном сотрудничестве по проекту «Фобос-Грунт».

У М.Я. Марова большой опыт педагогической работы, включая чтение лекций и руководство аспирантами. Им подготовлено свыше 20 кандидатов и докторов наук. Свыше 30 лет Михаил Яковлевич сотрудничает с Международным космическим университетом (International Space University − ISU). Он, по существу, находился у его истоков, возглавляя много лет факультет космической физики, избирался в Академический совет и Совет директоров. Начиная с 1989 г., он ежегодно читает курсы лекций в этом университете, который выпускает будущих ведущих специалистов в области освоения космоса на международной, междисциплинарной и межкультурной (3I) основе с использованием метода мозгового штурма. Михаил Яковлевич участвует в работе ISU, включая как постоянный кампус в Страсбурге (Франция), так и программы летних сессий, проходящие по всему миру, и это его деятельность получила высокую оценку. В 1994-1995 годах он преподавал в Университете Северной Каролины (США), работая также над космическими проектами. Он является профессором Московского

университета им. М.В. Ломоносова и в настоящее время читает лекции на факультете космических исследований.

На протяжении многих лет Михаил Яковлевич успешно совмещает с научной научно-организационную работу. Помимо упомянутой деятельности в МНТС по КИ и многочисленных международных органах, он работал и продолжает работать в различных комиссиях, комитетах и советах. В настоящее время является членом Бюро Совета по космосу Российской академии наук (РАН); председателем Комиссии РАН по научному наследию К.Э. Циолковского; заместителем председателя Научного совета РАН по астробиологии; членом экспертной комиссии по пропаганде научных знаний и присуждению научных премий за лучшие работы по популяризации науки. Он ведет постоянный научный семинар в институте Вернадского. Более 3 лет является главным редактором международного научного журнала «Астрономический вестник. Исследования Солнечной системы» (Solar System Research) издаваемого одновременно на русском и английском языках, а также входил в редколлегии ряда международных научных журналов.

С 2009 года Комитет всемирного наследия ЮНЕСКО (WHC) привлек Михаила Яковлевича к деятельности в области астрономии и космического наследия, направленной на увековечение наиболее признанных ракетно-космических центров и космических объектов. С 2012 года он возглавляет временную Рабочую группу по космическому наследию, призванную увековечить исторические центры по созданию и запуску ракетно-космических систем, как выдающееся культурное наследие и достояние всего человечества. С 2009 года Комитет всемирного наследия ЮНЕСКО (WHC) привлек Михаила Яковлевича к деятельности в области астрономии и космического наследия, направленной на увековечение наиболее признанных ракетно-космических центров и космических объектов. С 2012 года он возглавляет временную Рабочую группу по космическому наследию, призванную увековечить исторические центры по созданию и запуску ракетно-космических систем, как выдающееся культурное наследие и достояние всего человечества.

Михаил Яковлевич опубликовал около 300 научных работ в реферируемых журналах и 18 монографий, изданных ведущими мировыми отечественными и зарубежными издателями [1-16]. Он также ведет активную просветительскую деятельность, популяризируя науку посредством публикаций и телевизионных программ. Он является автором наиболее признанных популярных книг «Планеты Солнечной системы» (наука РН, 1981 1-й и 1986 2-й выпуски) и «Космос. От Солнечной системы до ядра Вселенной» (PHYSMATLIT, 2016 1-й и 2018 2-й выпуски).

М.Я. Маров был избран действительным членом Международной академии астронавтики, членом Британского Королевского астрономического общества. Имеет несколько отличных государственных и международных наград. Он лауреат наиболее заслуженной Ленинской премии и Государственной премии СССР. Его правительственные награды включают орден Трудового Красного Знамени, Орден Почета, Орден Дружбы и медали. Совсем недавно за выдающиеся достижения в науке он был награжден премией Демидова и золотой медалью Келдыша РАН. Среди его международных наград-престижная премия Галаберта по астронавтике, премия Эдвина Сиффа и медаль КОСПАРА Нордберга.

5. ВЕЛИКИЙ УЧИТЕЛЬ М.В. КЕЛДЫШ

В заключение хотелось бы еще раз подчеркнуть, что Михаилу Яковлевичу Марову выпала счастливая судьба быть в самом центре многих исторических событий и непосредственно участвовать в выдающихся космических свершениях в великой стране - Советском Союзе. Он пришел в эту область, когда только началось изучение и освоение космоса. Ему довелось плодотворно работать в замечательной области науки и создать свою научную школу. Ему посчастливилось лично знать многих выдающихся людей, посвятивших себя исследованию космоса и пионерским открытиям за пределами собственной планеты. Михаил Яковлевич с теплым чувством вспоминает многих из тех, с кем судьба подарила возможность сотрудничать на коротком отрезке человеческой жизни. Но из всех современников он особо выделяет своего великого учителя Мстислава Всеволодовича Келдыша (рис. 19). О нем он говорит со смесью бесконечного уважения и восхищения. Он усвоил много уроков своего учителя и в науке, и в искусстве управления, но самое главное - воспринял его жизненную философию и мировоззрение. Саму возможность узнать этого выдающегося ученого и удивительного человека, много лет с ним тесно общаться он считает настоящим подарком судьбы.

Рис. 19. Великий учитель М.В. Келдыш.

Приведенная выше биография Михаила Яковлевича Марова – это, по существу, краткий обзор того, что ему удалось совершить, во многом руководствуясь собственным житейским кредо. Ранее, рассказывая об основных направлениях его научной и научно-организационной работы, мы отмечали, что многие результаты этой деятельности и результаты исследований ученого описаны в многочисленных опубликованных книгах и монографиях. Есть, однако, среди этих книг одна, которую Михаил Яковлевич особенно выделяет и ценит. Это – уникальная книга «Космические исследования. М.: Наука. 1981»), основу которой составляет одноименная статья, написанная М.Я. Маровым совместно со своим великим учителем для сборника «Октябрь и наука», выпущенного издательством «Наука» в 1977 году к годовщине Октябрьской революции.

Излишне говорить о том, что Михаил Яковлевич с гордостью вспоминает о приглашении М.В. Келдыша стать его соавтором в этой работе. Дискуссии в процессе подготовки рукописи оставили глубокий след в его памяти.

Коллеги поздравляют Михаила Яковлевича с замечательным юбилеем и желают ему еще многих лет активной жизни и плодотворной деятельности.

REFERENCES

[1] A.D. Kuz'min, M.Ya. Marov, *Fizika planety Venera*, M.: Nauka, Gl. red. fiz.-mat. lit., (1974).
[2] M.V. Keldysh, M.Ya. Marov, *Kosmicheskiye issledovaniya,* M.: Nauka, (1981).
[3] M.Ya. Marov, *Planety Solnechnoy sistemy*, M.: Nauka, (1986).

[4] M.Ya. Marov, A.V. Kolesnichenko, *Vvedeniye v planetnuyu aeronomiyu,* M.: Nauka, (1987).

[5] M.Ya. Marov, V.I. Shematovich, D.V. Bisikalo, *Kineticheskoye modelirovaniye razrezhennogo gaza v zadachakh aeronomii*, Izd.-vo: M.: IPM im. Keldysha AN SSSR, (1990).

[6] A.V. Kolesnichenko, M.Ya. Marov, *Turbulentnost' mnogokomponentnykh sred*, M.: MAIK «Nauka», (1998).

[7] M.Ya. Marov, D. Grinspoon, *The Planet Venus*, Yale University Press, (1998).

[8] M.Ya. Marov, "Malyye tela colnechnoy sistemy i nekotoryye problemy kosmogonii", *UFN*, **175**(6), 668–678 (2005).

[9] M.Ya. Marov, A.V. Kolesnichenko, *Mechanics of turbulence of multicomponent gases*, Kluwer Academic Publishers, Dordrecht, Boston, London, (2001).

[10] *Sovremennyye problemy mekhaniki i fiziki kosmosa. K 70-letiyu so dnya rozhdeniya chl.-korr. RAN M.Ya. Marova*, (Eds. V.S. Avduyevskogo, A.V. Kolesnichenko), M.: Fizmatlit, (2003).

[11] M.Ya. Marov, A.V. Kolesnichenko, *Turbulence and Self-Organization*, Modeling Astrophysical Objects, Springer. (2013).

[12] W.T. Huntress, M.Ya. Marov, *Soviet Robots in the Solar System. Mission Technologies and Discoveries*, Springer –Praxis (2011).

[13] M.Ya. Marov, W.T. Huntress, *Sovetskie roboti v Solnechnoy sisteme*, Fizmatlit, 2-oe izd., (2018).

[14] M.Ya. Marov, *Kosmos. Ot Solnechnoy sistemy vglub' Vselennoy,* M.: Fizmatlit, 2-oe izd., (2018).

[15] M.Ya. Marov, I.I. Shevchenko, *Ekzoplanety*, Institut komp'yuternykh issledovaniy, (2017).

[16] V.I. Shematovich, M.Ya. Marov, "Dissipatsiya planetnykh atmosfer: fizicheskiye protsessy i chislennyye modeli", *UFN*, **188**(3), 233–265 (2018).